Development of a novel experimental platform for the study of Cytokinin perception and signalling pathway

Estefania Pavesi

Numéro National de Thèse : 2022ENSL0019

THESE
en vue de l'obtention du grade de Docteur, délivré par
l'ECOLE NORMALE SUPERIEURE DE LYON
en cotutelle avec
HEINRICH HEINE UNIVERSITY

Ecole Doctorale N° 340
Biologie Moléculaire, Intégrative et Cellulaire (BMIC)

Discipline : Sciences de la vie et de la santé

Soutenue publiquement le 28/09/2022, par :
Estefanía PAVESI

Development of a novel experimental platform for the study of Cytokinin perception and signalling pathway

Développement d'une nouvelle plateforme expérimentale pour l'étude de la perception et de la signalisation des cytokinines

Devant le jury composé de :

BENKOVA, Eva, Professeure, Institute of Science and Technology (Austria), Rapporteure
GROTH, Georg, Professeur, Institute of Biochemical Plant Physiology- HHU Düsseldorf (Germany), Rapporteur
CAILLAUD, Marie-Cécile, Chargée de recherche HDR, RDP ENS de Lyon, Examinatrice
INGRAM, Gwyneth, Directrice de Recherche, RDP ENS de Lyon, Examinatrice
STAHL, Yvonne, Professeure, Institute of Developmental Genetics- HHU Düsseldorf (Germany), Examinatrice
VERNOUX, Samuel Teva, Directeur de Recherche, RDP ENS de Lyon, Directeur de thèse
ZURBRIGGEN, Matias, Professeur, Institute of Synthetic Biology- HHU Düsseldorf (Germany), Co-Tuteur de thèse

Acknowledgements

First of all, I would like to thank Prof Dr Matias Zurbriggen and Dr Teva Vernoux for giving me the opportunity to do my doctoral thesis in your institutes. Thank you both for the many scientific discussions and for encouraging me to follow my own ideas. Thank you, Matias, for always having the door open when I needed to discuss a result, or ask for advice. And Teva, thank you for your constant support even in the distance. I would like also to thank my mentor Prof Rüdiger Simon for the insightful conversations.

To everyone at the AG Zurbriggen. Thank you Kun, Hannes, Uriel and Leonie, Lisa and Nicole, Cha San. Thank you for sharing your time and teaching me all the fascinating techniques I have learned in the past three years. A special thanks goes to Christoph, Amanda, Sarah, Yeliz, Josepha, Jonas and Carroll, and all students for your great predisposition and your warmth. Thank you for the shared moments inside and outside the lab. For the BBQs under the rain and the lunches under the sun. You will be missed.

Gracias Migue y Ode por sus charlas y su energía siempre positiva! Gracias Sofi, Pame, Pauli, Arantxa y Ro. Gracias por enseñarme a ser más flexible y ayudarme a adapatarme en este mundo tan lejos de casa.

To the Signal team, thank you for all the fruitful discussions and feedbacks. This PhD wouldn't have been the same without all your experienced input during the seminars and forth. Your passion for science is contagious, I wish we could have spent more time at the lab together. And Raque, por toda tu ayuda desde el comienzo de este doctorado, gracias!

Thank you Marie-Cecile for the kind conversations and career advises.

I would also like to thank to all technical assistants. Your work made this study possible. Thank you Reinhi, Michaela, Raphael, and a huge special thanks to Stefanie. Your patience with my last minutes changes was endless. Thanks!

To my friends. Jörg for the proof-reading of this thesis and your always optimistic attitude. To my soul-sisters, for your constant support and affection, thank you Caro, Flori and Anto.

Big thanks to my family, son mi todo. Your unconditional love is my motor to continue growing. Thanks for encouraging me to keep going and for believe in me.

Last, Marcos. Vos sabés que yo no sé que sería de mi sin vos. Sos mi mejor amigo, mi sostén y mi motivación. Por muchos años más de amistad y crecimiento.

Gracias a todos! Merci! Dankeschön!

Table of Contents

List of Figures

List of tables

Abbreviations

A-ARR	Type-A *Arabidopsis* Response Regulator
ABA	Abscisic Acid
AFB	Auxin signal F-box Protein
AHP	*Arabidopsis* Histidine-containing phospho-transfer Protein
AHK	*Arabidopsis* Histidine Kinase
APB	Acceptor Photo Bleaching
AP2/EREBP	Apetala 2/ Ethylene Responsive Element Binding Protein
AP2/ERF	Apetala 2/ Ethylene Response Factor
ARF	Auxin Response Factor
BA	*N*6-benzyladenine
B-ARR	Type-B *Arabidopsis* Response Regulator
BCR	B Cell Antigen Receptor
BiFC	Bimolecular Fluorescence Complementation
CaMV 35S	Cauliflower Mosaic Virus 35S
CHASE	Cyclase/ Histidine kinases Associated Sensor Extracellular
CHO	Chinese Hamster Ovary
CK	Cytokinins
CKI1	Cytokinins Independent 1
CKX	Cytokinins Oxidase
CRE	Cytokinins Response Element
CRF	Cytokinins Response Factor
CRM	Cytokinins Response Motif
cZ	*cis*-Zeatin
*c*ZRMP	*cis*-Zeatin Riboside Monophosphate
DAPI	4´, 6-diamidino-2-fenilindol
DHZ	Dihydrozeatin
DMAPP	Dimethylallyl Diphosphate
EGFP	enhanced Green Fluorescent Protein
E	Glutamate
Eapp	Apparent FRET efficiency
ECRM	extended version of Cytokinins Response Motif
ENT	Equilibrative Nucleotide Transporter

E-Protein	Eerythromycin Repressor Protein
ER	Endoplasmic Reticulum
ERF	Ethylene Response Factor
FLIM	Fluorescence Lifetime Imaging Microscopy
FLUC	Firefly Luciferase
FP	Fluorescent Protein
FRET	Förster Resonant Energy Transference
FRET FLIM	Fluorescent Lifetime Imaging Microscopy
GA	Gibberellins
H	Histidine
HEK-293T	Human Embryonic Kidney 293-T cells
HK	Histidine Kinase
HPt or HP	Histidine-containing phospho-transfer Protein
IAA	Indol-3-Acetic Acid
iP	Isopentyladenine
IPT	Isopentenyladenine Transferases
JA	Jasmonic Acid
K	Lysine
Kd	Dissociation Constant
KIN	Kinetin
KMD	Kiss Me Deadly
LOG	Lonely Guy
LUC	Luciferase
mCherry	Monomeric Cherry fluorescent protein
mIG	membrane-bound Immunoglobulin
MoClo	Modular cloning
MP	Auxin Response Factor 5/ Monopteros
MPP	6-(3-methylpyrrol-1-y1)purine
N	Asparagine
NLS	Nuclear Localization Signal
NPC	Nuclear Pore Complex
PARE	Promotor containing an Auxin Response Element
PEI	Polyethylenimine
PEG	Polyethylen glycol
PPI	Protein-Protein Interaction
PT	Post-Transfection

PTK	Protein Tyrosine Kinase
PUP	Purine Permease Family
RAM	Root Apical Meristem
REC	Receiver domain
R	Arginine
RLuc	Renilla Luciferase
ROI	Region Of Interest
RR	Response Regulator
SAM	Shoot Apical Meristem
SCF	Skp, Cullin, F-box containing complex
SL	Strigolatones
SLN1	Synthetic Lethal of N-Rule 1
SV40	Simian Virus 40 early
TAA1	Tryptophan Aminotransferase of Arabidopsis 1
TCS	Two-Component System
TDZ	Tidiazuron
tetO	Operator Motiv of Tetracycline Repressor
TetR	Tetracycline Repressor
TF	Transcription Factor
TGA 3	TGA1A-Related Gene 3
TPL	Topless
tZ	*trans*-Zeatin
tZR	*trans*-Zeatin Riboside
tZRMP	*trans* -Zeatin Riboside-5´-monophosphate sodium salt
WT	Wildtype
WUS	Wuschel protein
Y2H	Yeast Two Hybrid
YFP	Yellow Florescent Protein
2MeSiP	2-Methylthio-N^6-isopentenyladenine

Summary

Cytokinins (CK) hormones are one of the main morphogenetic signals in plants. They modulate plants growth, developmental and physiological processes. The CK signal network involves a histidine kinase receptor that after hormone perception triggers a His-to-Asp phospho-relay, a phosphotransferase protein and a response regulator that directly modulates the transcription of target genes. The study of CK canonical circuit and their function in plants has so far been addressed using classic genetic approaches such as qualitative analysis of loss-of-function mutants or transient protein expression in isolated plant cells (protoplasts), bacteria or yeast. The characterization of individual signalling components, however, has been impeded due to the high level of complexity of the pathway in terms of genetic redundancy, extensive crosstalk with other networks and shared components as well as multiple negative feedbacks.

Synthetic biology is an interdisciplinary field that provides us with tools to tackle this impediment. Implementing basic engineering principles combined with modern cell biology we dissected the *Arabidopsis thaliana* CK signalling pathway to rebuild a synthetic CK-responsive biological network in mammalian cells. The combination of quantitative approaches such as confocal microscopy, protein-protein interaction (PPI) and reporter genes expression allowed us to characterize functional CK signalling regulators. We investigated the receptor selectivity for different CK and explored the mode of action of three response regulators (RRs) acting as repressors of CK signalling. The absence of endogenous plant proteins in our platform permitted to evidence different roles for members of the same multigene family, including a novel regulatory mechanism and non-canonical activation of a type-B *Arabidopsis* response regulator (B-ARR). We further quantitatively investigated PPIs between various signalling effectors. These analyses allowed us to both explore the role of the conserved aspartate(D) residue of the B-ARRs as well as the effect of the formation of different complexes on the CK pathway activation. We also explored a proposed CK-dependent subcellular relocation of the Cytokinin response factors (CRFs) for the design of a ratiometric biosensor. Finally, validation of our observations in *Arabidopsis* protoplasts demonstrated the predictive power of our synthetic biology platform. This work reflects the potential of synthetic biology approaches for the exploration of plant signalling pathways. We believe that this platform will accelerate the generation of new knowledge by rapidly challenging new hypotheses for their posterior, and most important, validation *in planta*.

Zusammenfassung

Cytokinine (CK) Hormone gehören zu den wichtigsten morphogenetischen Signalen in Pflanzen. Sie regulieren das pflanzliche Wachstum, die Entwicklung und physiologische Prozesse. Im CK-Signal-Netzwerk löst ein Histidinkinasenrezeptor nach hormoneller Perzeption eine His-Asp Phosphorylase, ein Phosphotransferprotein und einen Antwortregulator aus, der die Transkription der betreffenden Gene steuert. Studien zu CK kanonischen Schaltungen und ihrer Funktion in Pflanzen haben bisher auf klassischen genetischen Vorgehensweisen aufgebaut, wie etwa qualitative Analysen zu Loss-of-Function-Mutationen oder transienten Proteinexpressionen in isolierten Pflanzenzellen (Protoplasten), Bakterien und Hefen. Individuelle Signalisierungskomponenten konnten dagegen nur beeinträchtigt dargestellt werden. Grund dafür ist die hohe Komplexität des Verbindungswegs in Form der genetischen Redundanz, weitreichender Überschneidung mit anderen Netzwerken und gemeinsamer Bestandteile sowie des zahlreichen negativen Feedbacks. Die Synthetische Biologie ist eine interdisziplinäre Fachrichtung, die uns Instrumente zum Angehen dieser Problematik in die Hand gibt. Durch grundlegende technische Prinzipien kombiniert mit moderner Zellbiologie konnten wir den CK-Signalweg der *Arabidopsis thaliana* (Acker-Schmalwand) zerteilen zum Bau eines synthetischen CK-responsiven biologischen Netzwerkes in Säugetierzellen. Die Verknüpfung von quantitativen Methoden, wie etwa konfokaler Mikroskopie, Protein-Protein-Interaktion (PPI) und Reportergen Expression erlaubte uns, funktionierende signalisierende CK-Regulatoren darzustellen. Wir untersuchten die Rezeptorselektivität verschiedener CK und erforschten die Wirkungsweise von drei responsiven Regulatoren (RRs), die als Repressoren der CK-Signalisierung dienten. Der Mangel an endogenen pflanzlichen Proteinen in unserer Plattform beweist verschiedene Rollen für die Angehörigen derselben Multigenfamilie, einschließlich einem neuartigen regulierenden Mechanismus und einer nicht-kanonischen Aktivierung eines Typ-B *Arabidopsis* responsiven Regulators (B-ARR). Quantitativ untersuchten wir ebenfalls PPIs zwischen mehreren signalübertragenden Effektoren. Diese Analysen befähigten uns, die Aufgabe des beibehaltenen Aspartatrests des B-ARRs sowie den Effekt der Formation der unterschiedlichen Komplexe auf die Aktivierung des CK-Verbindungswegs zu testen. Des Weiteren prüften wir eine CK-abhängige subzelluläre Verschiebung der Cytokinin responsiven Faktoren (CRFs) für den Entwurf eines ratiometrischen Biosensoren. Schlussendlich demonstrierte die Validation

unserer Beobachtungen in *Arabidopsis* Protoplasten die Prognosefähigkeit unserer Plattform der synthetischen Biologie.

Diese Arbeit zeigt das Potential von synthetisch biologischen Verfahren zur Erforschung von signalübertragenden Verbindungswegen. Wir sind davon überzeugt, dass diese Plattform eine neue Generation an Wissen hervorbringen kann, indem sie nach neuen Hypothesen verlangt und der Validation in planta.

Résumé

Les hormones végétales de la famille des cytokinines (CK) sont un des principaux signaux morphogénétiques des plantes. Elles régulent leur croissance, leur développement et divers processus physiologiques. Les cytokinines sont perçues grâce à un récepteur de type "histidine-kinase", qui une fois lié à l'hormone, déclenche un phospho-relai d'histidine-à-aspartate, qui active en cascade une protéine phospho-transférase puis un facteur de la famille des "Régulateurs de Réponse" (RR), capables à leur tour de moduler directement la transcription de gènes cibles. Cette voie canonique de signalisation CK et ses fonctions chez les plantes ont été jusqu'ici étudiées à travers des approches de génétique classiques telle que des analyses qualitatives de perte de fonction dans des lignées mutantes, ou grâce à des expressions transitoires de protéines dans des cellules isolées de plantes (protoplastes), bactéries ou levures. Jusqu'ici, ces approches n'ont pas vraiment permis d'entreprendre la caractérisation individuelle des différents composants de la voie de signalisation CK, en raison d'un haut niveau de redondance génétique, de nombreuses interférences et composants partagés avec d'autres voies de signalisation, ou encore du fait de l'existence de nombreuses rétro-actions négatives.

La biologie synthétique, domaine interdisciplinaire, offre des outils pour surmonter ces obstacles. En combinant les principes de base de l'ingénierie à la biologie moderne, nous avons disséqué la voie de signalisation des CK de la plante modèle *Arabidopsis thaliana* pour reconstruire une voie de signalisation CK synthétique dans des cellules de mammifères. La combinaison de nombreuses approches quantitatives (microscopie confocale, interaction protéine-protéine, expression de gènes rapporteurs) nous ont permis de caractériser les régulateurs fonctionnels de la signalisation CK. Nous avons en particulier étudié la sélectivité du récepteur pour différentes CK et exploré le mode de fonctionnement de trois facteurs RR agissant comme répresseurs de la signalisation CK. L'absence de protéines endogènes de plantes dans notre système expérimental hétérologue a permis de mettre en évidence des rôles différents au sein des membres d'une même famille multigénique, notamment un mécanisme inédit impliquant une activation non-canonique d'un facteur RR de type B issu de *Arabidopsis* (B-ARR). Nous avons ensuite étudié quantitativement les interactions protéine-protéine entre les différents effecteurs de signalisation de la voie des CK. Ces analyses nous ont permis d'une part d'explorer le rôle du résidu aspartate conservé des B-ARR, et d'autre part les effets de la formation de différents complexes sur l'activation de la voie. Nous avons aussi examiné l'hypothèse existante d'une relocalisation subcellulaire de protéines appelées "facteurs de

réponse aux cytokinines" (CRF), dan l'idée de concevoir un biosenseur quantitatif. Pour finir, nous avons confirmé nos observations en protoplaste d'*Arabidopsis,* démontrant le pouvoir de prédiction de notre plateforme de biologie synthétique. Ce travail reflète le potentiel des approches de biologie synthétique pour l'exploration des voies de signalisation des plantes. Nous pensons que cette plateforme peut accélérer l'acquisition de connaissances nouvelles en permettant de tester rapidement des questions et hypothèses jusqu'ici inexplorées, avant de valider les plus prometteuses dans des expériences qui restent nécessaires *in planta*.

1. Introduction

1.1 Rationale of this thesis

Due to the impossibility to escape from adverse environmental stresses, plants have developed highly efficient and sophisticated programs to respond to external stimuli in order to adapt and survive.

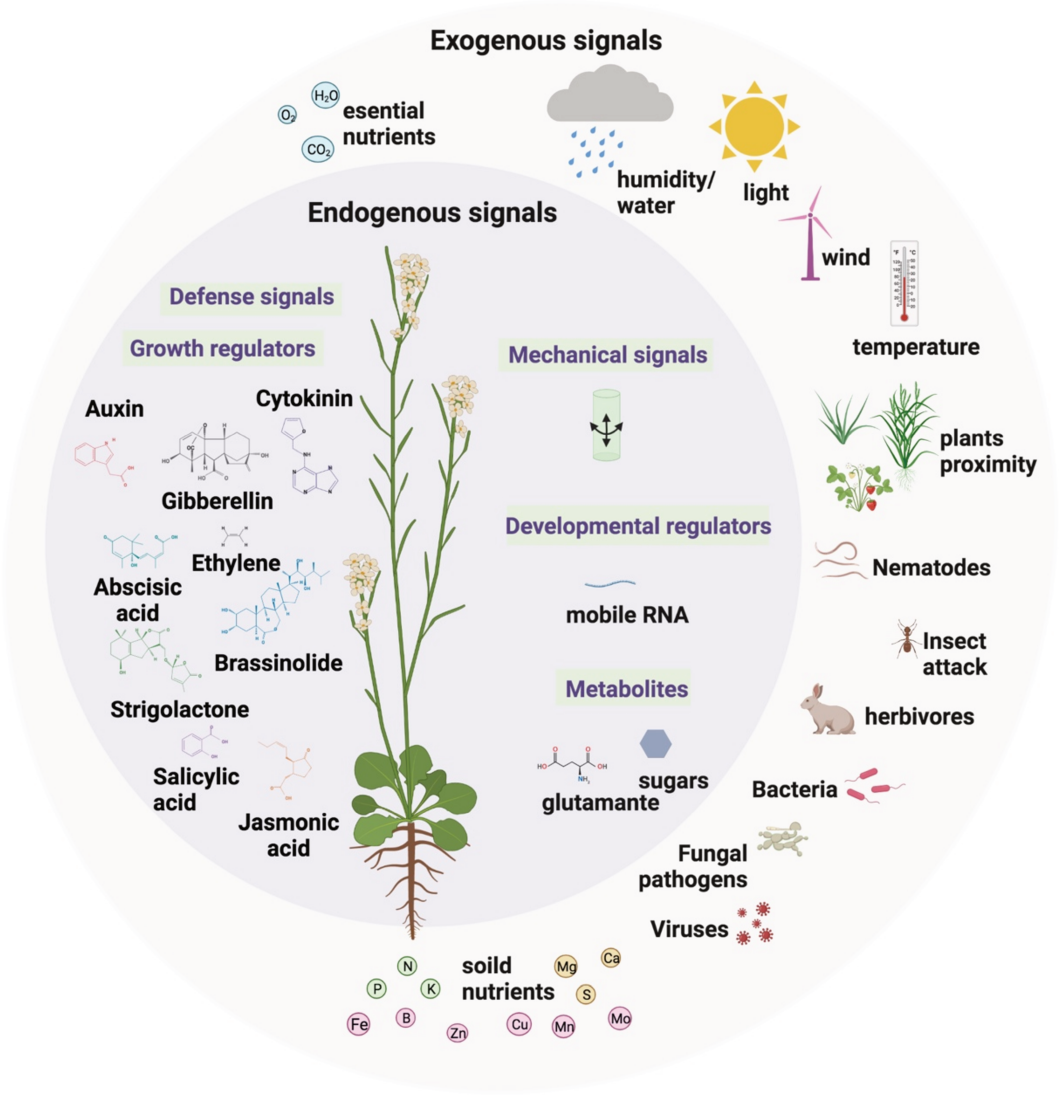

Figure 1. Plants coordinate a wide range of signals for growth and development. Plants have evolved into highly sophisticated organisms that can integrate both endogenous and environmental signals to regulate growth and developmental processes that ensure their survival.

The integration of both external and internal signals allows them to take advantage of favourable conditions to coordinate growth, development and physiological processes (**Fig. 1**)[1,2].

Among all physical and chemical stimuli plants had mastered to integrate, phytohormones are the main morphogenetic signal. These small molecules can influence several processes individually or, more commonly, as a coordinated response that involves several networks. Together with auxins, gibberellins (GA), brassinosteroids, abscisic acid (ABA) and ethylene, CK are one of the six classical hormones in plants. CK take on many roles in plant development. The ones that have placed these hormones as potential protagonists of a second "Green Revolution"[3] are: the regulation of seed yield[4,5], the participation in pathogen defense[6–8] and nutrient uptake[9,10].

Therefore, a deeper understanding on how CK (in coordination with other phytohormones) determine the architecture of plants can play an important part to address food shortage and climate change, two main contemporary issues. Therefore, unravelling the mechanistic underlying CK signal transduction is fundamental in order to achieve these goals. Towards this aim, to overcome the limitations encountered when studying signalling pathways in plants, such as the interconnectivity with other networks, the functional redundancy, and the negative feedback loops, is needed. This dissertation seeks to contribute to the generation of new knowledge by providing an experimental (orthogonal) platform for the study of CK perception and signalling networks. On the basis of a large body of literature available, we will focus this study on the CK signalling network of the model organism, *Arabidopsis thaliana*. While *Arabidopsis* is not of major agronomic significance its CK pathway is conserved in rice, maize, tomato, and poplar[11–16]. Therefore, the results presented in this study can potentially be extrapolated to other species of great ecological and economical importance.

1.2 Cytokinins

1.2.1 Discovery and function

The search for substances that pair up with auxin to stimulate cell division of cultured plant stem tissues culminated in the identification of 6-furfurylaminopurine, an N6 adenine derivate present in coconut milk (a liquid endosperm), later named Kinetin (KIN)[17,18]. Twenty-five

years later zeatin was identified in maize endosperm[19]. As KIN is presumed to be a product of oxidative DNA damage rather than a molecule synthesized *de novo,* zeatin is instead considered the first identified naturally occurrent CK. Through the years the regulation of several growth, developmental and physiological processes by these hormones have encouraged the plan to find other natural or synthetic occurring molecules with similar activity[8,20,21].

In addition to the functions in the regulation of seed size[4,5] and inmunity[6–8], CK modulate a plethora of processes in plants. Importantly, CK maintain both apical meristems by increasing cell proliferation in the shoot apical meristem (SAM), while inhibiting elongation in the root apical meristem (RAM) and lateral root formation[22,23]. They play a role in chloroplasts development, leaf expansion and seeds germination as well as flowering and fruit ripening[21,24]. Moreover, CK also influence the dynamic of the microtubular cytoskeleton in roots[25], and are linked to nodulation and light response[21] (**Fig. 2**). Altogether, from organ formation to senescence, CK regulate key processes during all of the plants´ life cycle.

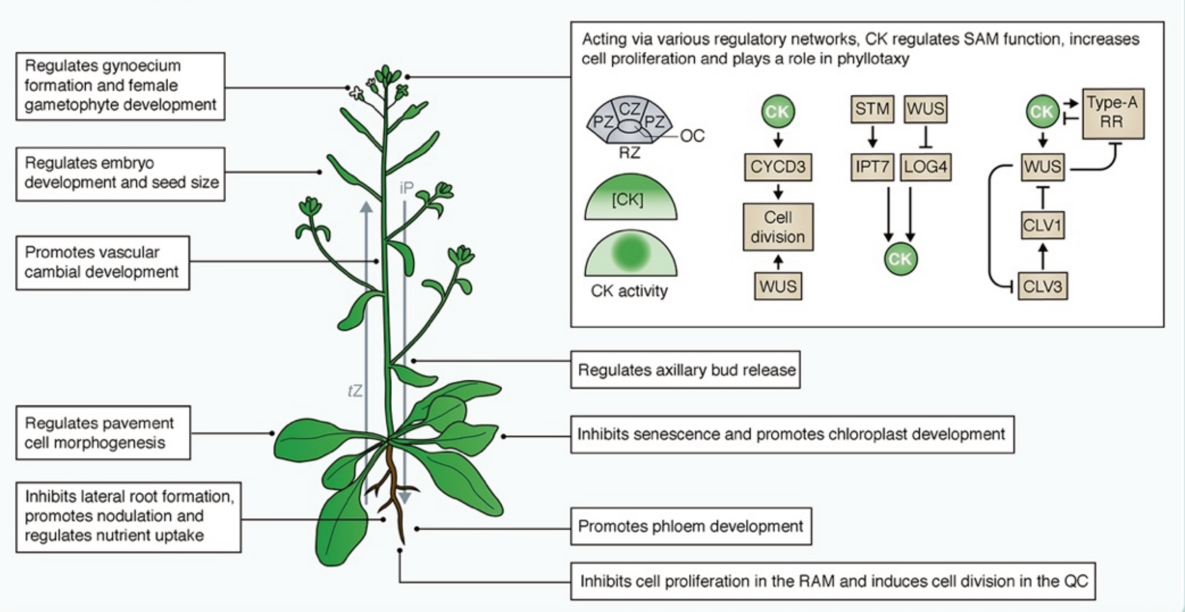

Figure 2. CK role in growth and developmental processes in plants. CK regulate a plethora of developmental processes in plants. Their role in shoot apical meristem cell proliferation is especially remarkable as it involves the regulation of morphogens as well as interaction with the auxin pathway. For this function CK are transported via the xylem as trans-zeatin (tZ). In exchange the iP-type are transporter to the root via the phloem. **Adapted from Kieber & Schaller, 2018.**

1.2.2 Metabolism and activation

CK are adenine derivatives with either an isoprenoid or aromatic side chain in the N6 position of the adenine ring. The isoprenoid derivates are the most abundant forms in plants including isopentenyladenine (iP), *cis*- and *trans*- Zeatin (*c*Z, and *t*Z), and dihydrozeatin (DHZ). Present in their nucleobase-, riboside- or ribotide- forms, as well as their inactive O-, N^7- and N^9-sugar conjugates[26]. Their biosynthesis has come a long way since the proposal of the naturally occurring cZ being mainly a product of tRNA hydrolysis and posteriorly interconverted into *t*Z[27].

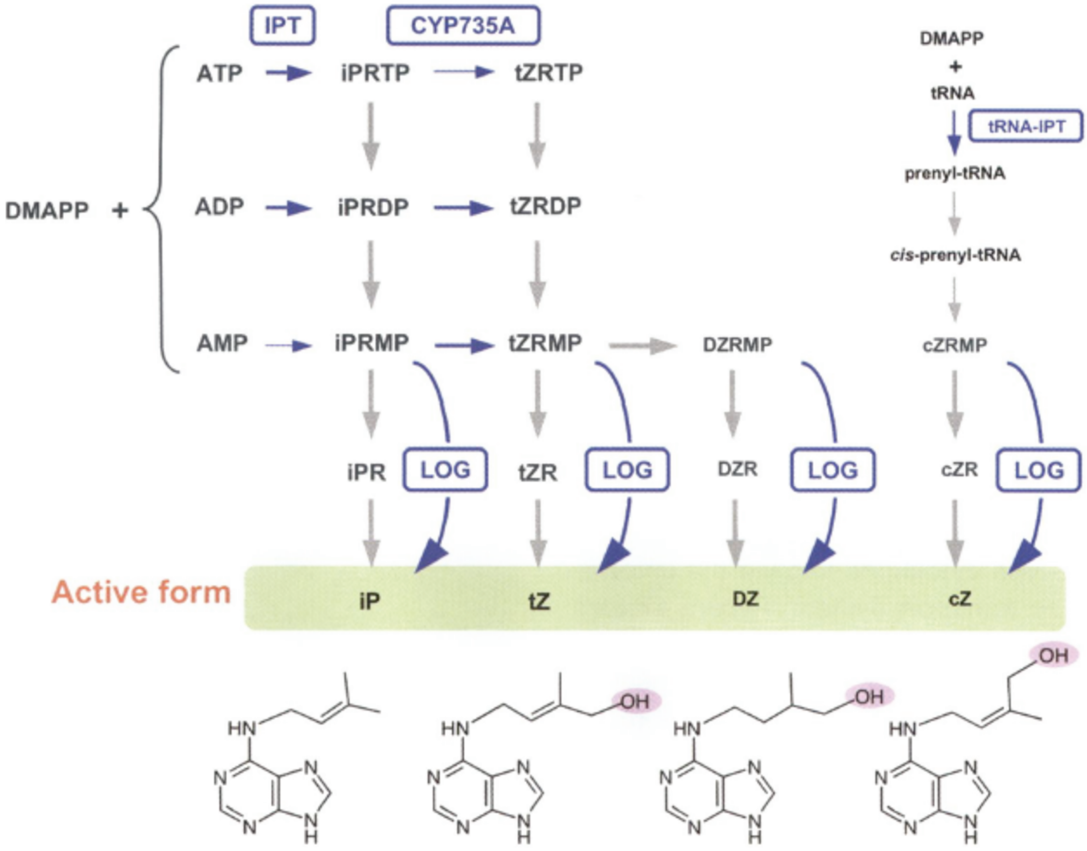

Figure 3. Overview of *de novo*, and tRNA degradation, metabolic pathways of cytokinins. AMP adenosine 5'-monophosphate, ADP adenosine 5'-diphosphate, ATP adenosine 5'-triphosphate, CKX cytokinins oxidase/dehydrogenases, cZ cis-Zeatin, cZR cZ riboside, cZRMP cZ riboside 5'-monophosphate, CYP735A cytochrome P450 monooxygenase, family 735, subfamily A (cytokinins trans-hydroxylase), DMAPP dimethylallyl diphosphate, DHZ Dihydrozeatin, DHZR DHZ riboside, DHZRMP DHZ riboside 5'-monophosphate, IPT isopentenyl transferase, iP N6-(D2 -isopentenyl)adenine, iPR iP riboside, iPRMP iP riboside 5' –monophosphate, iPRDP isopentenyladenosine- 5'-diphosphate, iPRTP isopentenyladenosine- 5'-triphosphate, NCS adenosine nucleosidase, LOG cytokinins phosphoribohydrolase 'Lonely guy', tRNA Transfer ribonucleic acid, tZ trans-Zeatin, tZR tZ riboside, tZRDP tZ riboside 5'-diphosphate, tZRMP tZ riboside 5' monophosphate, tZRTP tZ riboside 5'-triphosphate, RPH ribonucleotide phosphohydrolase. **Adapted from Hiroshe et al. 2008.**

Today we know that the initial step of isoprenoid-like CK biosynthesis is catalysed by isopentenyladenine transferases (IPT) (**Fig. 3**). These proteins add a prenyl group derived from the dimethylallyl diphosphate (DMAPP) to: 1. the N^6 position of an ADP/ATP[26,28], producing (iP)-type CK or 2. an adenine bound to tRNA, generating the *c*Z-type.
Later, the iP nucleotides will be converted into tZ-type CK by hydroxylation of the side chain induced by the cytochrome P450 enzymes, CYP735A1 and CYP73542[29]. On the other hand, the hydrolysis of the modified tRNA produces the *c*Z riboside monophosphate (*c*ZRMP). Finally, the CK nucleoside 5′- monophosphate phosphoribohydrolase LONELY GUY (LOG) catalyses the conversion of all nucleotides into their active free-bases form[30].
The reduced form of zeatin DHZ, however, is an exception. Knowledge regarding this derivate metabolism is still scarce, probably because it is excluded from most studies as it has been long considered the less active form of *tZ*[31,32].
The aromatic CK, represented by KIN, the N^6-benzyladenine (BA), its hydroxyderivates (topolin or methoxiderivates) and the 6-(3-methylpyrrol-1-y1)purine (MPP) are also an exception. The natural occurrence of these CK is reserved to fewer plants[33–35]. Their biosynthesis, in particular, is still unknown. They supposedly originate from symbiotic bacteria or nucleic acids. The ortho-topolin form 2-methylthio-derivates are believed to originate exclusively from tRNA hydrolysis. Nevertheless, both natural and synthetic aromatic CK are weak substrates for the CKX, therefore, their effect is presumed to last over time[36,37].

1.2.3 Transport and de-activation

In *Arabidopsis thaliana*, the relative abundance of CK in different tissues and developmental stages depends on the expression patterns of the genes involved in their biosynthesis[38,39] and degradation[13,40] as well as on their long-distance transport[32]. The tZ-riboside (tZR) is the main CK type found in the xylem while the phloem primary transports iP-type[41]. In addition, CK can be also transported across the plasma membrane and into the lumen of the endoplasmic reticulum (ER). CK efflux across the plasma membrane is carried out by the ABC transporters, the ABCG14, mainly expressed in the roots[42]. The decrease of the content of CK in the shoots in *atabcg14* mutant lines proposed the main role for these transporters in root-to-shoot communication[42]. This signal exchange is thus essential for coordinating CK responses in both

organs[26,43]. On the other hand, CK influx is carried out by the purine permease family (PUP)[44,45] and the nucleotide transporters (ENT)[46,47].

Together with hormone efflux (possibly into the apoplast[48,49]) the levels of CK are finely tuned by either conjugation to a sugar or cleavage by the CKX family[50]. Glycosylation of the N^6 or N^9 residue is irreversible and results in the loss of CK activity, possibly, by decreasing the ligand affinity for the receptor[51–53]. As N-glycosylation is believed to be gained later in evolution, it was proposed that this mechanism intends to reduce the toxic aldehyde product from CKX degradation[36,54]. On the contrary, O-glucosides could be considered a reservoir of CK, as this type of glycosylation can be reversed by β-glucosidases[55]. Further, CKX-mediated degradation of most naturally occurring CK involves the irreversible cleavage at the N^6-side chain of both the free-base and riboside form[50]. Exceptions are DHZ and aromatics derivates, including the synthetic CK BA used in this study, which are resistant to CKX degradation[40,56].

1.2.4 Perception and signalling pathway

CK signal transduction involves an extended version of the basic Two-component systems (TCS) found in yeast and bacteria (**Fig. 4**). In these organisms, the TCS are the major circuits to perceive and respond to environmental cues[57,58]. These simpler systems involve a sensor kinase that perceives and propagates the signal, and a RR that receives it by means of an His-to-Asp phospho-transfer. CK canonical circuit instead, similarly to other TCS found in higher organisms[59,60], includes a hybrid histidine kinase receptor that comprises both a donor and receiver domain, a phosphotransferase protein and a RR that directly modulate the transcription of target genes[61–63].

In *Arabidopsis thaliana*, binding of CK to the *Arabidopsis* Histidine Kinase (AHK) receptors triggers the phospho-relay (**Fig. 5**). The phosphate at the conserved D residue in the receiver domain of the AHK is then transferred to Histidine (H) residue of the *Arabidopsis* Histidine-containing Phosphotransferase (AHP1-5). Later, these intermediate proteins phosphorylate the RR of the pathway, the type-B *Arabidopsis* Response Regulators (B-ARRs), whose activation lead to the transcriptional regulation of the genes responsive to CK[61–63].

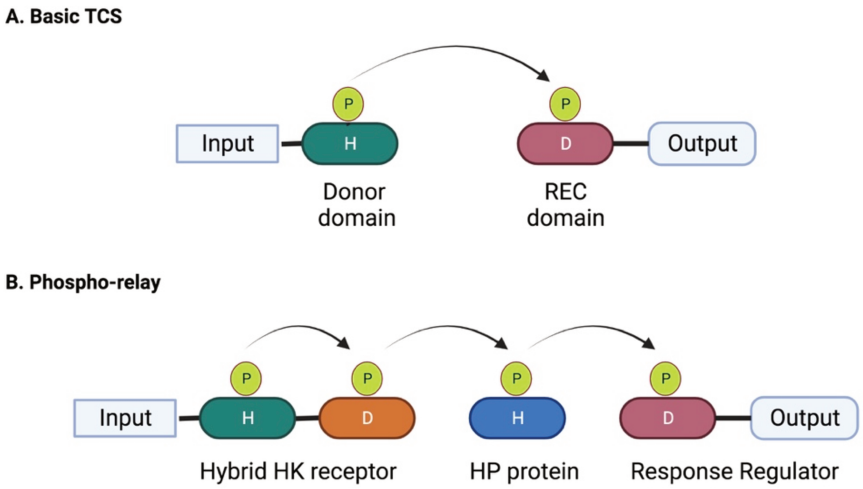

Figure 4. Representation of TCS systems. A. TCS found in yeast and bacteria. A sensor HK phosphorylates the circuit response regulator via a His-to-Asp phospho-transfer. B. Extended version of the basic TCS. A hybrid HK phosphorylated the RR via an intermediate, the HP protein. D, aspartate; H, histidine; HP, Histidine-containing phosphotransferase; REC, receiver domain; TCS; Two-component system

A second less characterized RR, the Cytokinin Response Factor (CRF) can, in turn, modulate CK signalling[64]. However, their phosphorylation by the AHPs has not yet been shown. In addition, the type-A[65] and type-C[66,67] ARRs, and the pseudo phospho-transfer protein AHP6[68,69] participate in negative-feedback loops modulating CK signal.

In plants, 65% of annotated genes belong to multigene families, probably as a consequence of tandem and segmental gene duplication. In *Arabidopsis*, 50% of multigene families have, at least, five members[70,71]. The families of proteins involved in CK signals are no exception. *Arabidopsis* genome encodes for 5 AHKs, 5 AHPs, 23 ARRs and 12 CRFs. This multiplicity of proteins within the same family proposes a high level of functional redundancy, which hinders the study of the contribution of single TCS components to the network. The second level of complexity in the study of the TCS is the non-canonical activation of CK responses, which may lead to misinterpretations of the results. Two known examples are the Cytokinin Independent 1 (CKI1) receptor, an HK that lacks the CK binding domain yet its overexpression generates CK responses[72] and the upregulation of CRF3 as a response to cold stress[73].

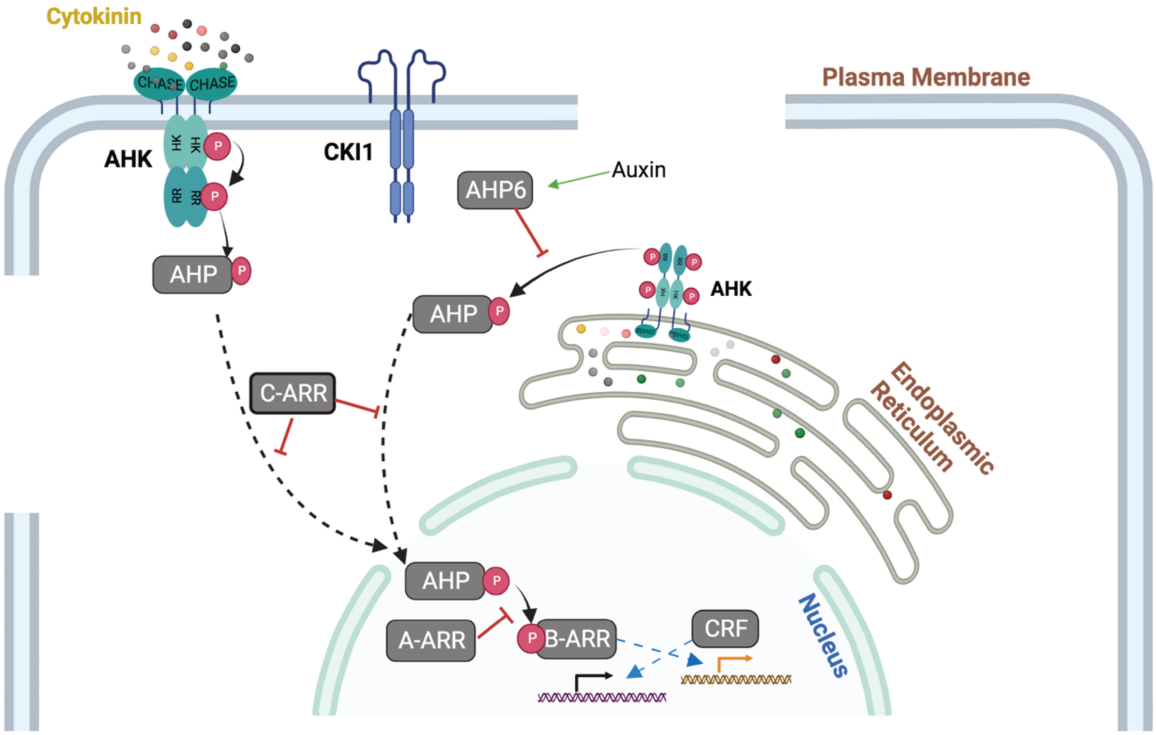

Figure 5. Representation of CK perception and signalling pathway in Arabidopsis thaliana. After hormone binding to the CHASE (Cyclase/ Histidine kinases Associated Sensor Extracellular) domain of the *Arabidopsis* Histidine Kinase receptor (AHK), the conformational change triggers the phosphor-relay. The phosphate (P) is then transferred to the *Arabidopsis* histidine-containing phosphotransferase (AHP), and finally to the type-B *Arabidopsis* response regulator (B-ARR). A second response regulator, the cytokinin response factor (CRF) also regulates CK responsive genes. The type A- and type C-ARR together with AHP6 act as repressors of CK signalling.

In addition, a large body of literature has investigated the interconnectivity among different phytohormones' networks[74–78]. This crosstalk, which leads to coordinated responses, represents the third major impediment to interrogating CK signalling *in planta*. To mention a few examples, it has been observed that jasmonates (JA) can diminish CK signalling by repressing AHK4/CRE1 while promoting AHP6 expression, positively regulating drought-induced xylem differentiation[79]. As well related to drought response, the SnRK2 protein kinases, key components of the ABA signalling pathway, were proposed to phosphorylate and activate the type-A ARR, thus downregulating CK responses[80,81]. Oppositely, auxin seems to inhibit these negative RRs in the SAM where CK signal is essential for cell division through ARF5/MONOPTEROS[69,82]. In roots, however, auxin and CK have antagonistic roles regulating RAM size by the generation of high auxin/ low CK regions where cell proliferation is favoured and areas of low auxin/ high CK in the transition/elongation zone promoting cell differentiation. This regulatory effect includes activators of the CK pathway such as the B-

ARR, ARR1 and the CRFs. The latter integrates both auxin and CK signal by the regulation of PIN1 expression[83–85]. Lastly, CK are involved in pathogen defence together with salicylic acid. Another B-ARR, ARR2, interact with the transcription factor (TF) TGA1A-RELATED GENE 3 (TGA3) to activate as a dimer the transcription of a marker gene for systemic acquired resistance[7].

1.2.4.1 *Arabidopsis* Histidine Kinase Receptors

The first HK receptor believed to be involved in CK sensing was CKI1. Not only was it overexpression in calli-induced constitutive CK responses[86], but later it was suggested to be involved in the regulation of female gametophyte development, vegetative growth and A-ARRs expression[87–89]. While CKI1 is not a genuine CK receptor, its identification suggested that CK was perceived by a TCS.

Only three years after CKI1 was identified, a second HK receptor was isolated from dehydrated *Arabidopsis* plants, the AHK1[90]. In yeast mutants for a structurally related HK receptor, the Synthetic lethal of N-rule 1 (SLN1), AHK1 was shown to respond to osmotic stress yet not to CK[90]. More recently, a recombinant AHK1 protein was successfully purified in bacteria further evidencing its phosphatase activity *in vitro*[91].

The first canonical CK receptor was discovered almost simultaneously by three different groups, finally showing to encode for the same HK. It was identified as the gene responsible for the *wooden leg* mutation and referred to as WOL[92]. Later, for inducing CK resistance in tissue culture it was named CYTOKININ RESPONSE 1 (CRE1)[62]. It was finally titled the Arabidopsis HISTIDINE KINASE 4 or AHK4 (which is what will be referred to henceforth in this work) and was revealed after in silico screening using a conserved domain of known HKs[93]. The first evidence of AHK4 activation by CK was obtained by analysing the complementation of an SLN1 lethal mutant (sln1Δ) in yeast[62]. Only when CK was added into the media, the AHK4 expressing cells bypassed the lethal phenotype. As for AHK1, this receptor also presents intrinsic phosphatase activity, which prevails in the absence of a ligand[94].

Within the 5 members of the AHK family only AHK5 lacks the extracellular domain, which is involved in the hormone binding. Instead, this receptor participates in both peroxide- and ethylene-induced stomata closure[95]. On the contrary, AHK2 and AHK3, are (as AHK4) genuine CK receptors and were characterized in the same *in silico* study previously mentioned. The three CK sensing receptors, AHK2, 3 and 4, consist of:

1. two or three transmembrane regions,
2. a conserved extracellular CHASE domain (cyclase/ histidine kinases associated sensor extracellular) involved in hormone binding[96,97],
3. a cytosolic region that contains the HK domain and
4. a receiver domain.
5. A diverse receiver domain is present in the C-terminal end as well, it is, however, unlikely to be involved in the phosphor-transfer.

The AHK 2, 3 and 4 receptors are expressed in all plant tissues (with different mRNA abundance in each of them) and they are believed to act in concert[93,98,99]. Nevertheless, some predominant roles were attributed to each of them. For example, AHK4 is predominately expressed in vascular tissues and RAM and thus it is the main regulator of primary root growth controlling of cell proliferation and elongation as well as shoot regeneration in-vitro[62,92,98]. AHK3, on the other hand, is more abundant in shoots, inducing photomorphogenesis and chlorophyll retention during dark-induced senescence, and together with AHK2, is involved in leaf formation[98]. Importantly, both *ahk3* and *ahk4* single mutants displayed particular phenotypes, while the *ahk2* mutant did not. The phenotypes of the double mutants were enhanced compared to the single mutant and the triple mutant rendered plants infertile, due to the CK effects on female gametophyte development[100,101] (**Fig. 6**).

At the cellular level, whether these receptors are present (and active) in the plasma or endoplasmic reticulum (ER) membrane was extensively debated. Evidence suggest that the AHKs localize, and initiate CK signalling, mainly at the ER[14,102–104]. However, recent studies proposing a functional activation of the HK receptors localized at the plasma membrane should not be dismissed[105,106].

Crystal structure and *in silico* analysis showed that a monomer of AHK4 binds a molecule of CK, independently of its nature (natural or synthetic) in the same site. Moreover, the binding pocket can allocate isoprenoid and aromatic CK without a major structural rearrangement. Oppositely, the larger or apolar nature of the derivates modified by N- and O-glycosylation restricts the binding, thus explaining the absence of activity of such derivates[53,107].

Different groups calculated the apparent dissociation constant (Kd) of these receptors using saturation assays with ^{3}H-CK and comparison with unlabelled competitors *in vitro*. The Kd for AHK2, 3 and 4 is now estimated to be approximately 40 nM[52]. For these assays, initially, the receptors incubated with the probes were expressed either in *Escherichia coli*[14,61,108–111] or

yeast[72]. Additionally, biochemical parameters of the hormone binding to AHKs, including pH, temperature and salt dependency were investigated, as well in these heterologous systems[14,100,110]. However, the composition of the membrane in bacteria greatly differs from that of plants[112,113], raising the question of the suitability of bacteria-based systems for the study of the AHK receptors. To overcome this difficulty isolated systems based on plant membranes were further implemented[51,52], providing a native-like environment for the receptor.

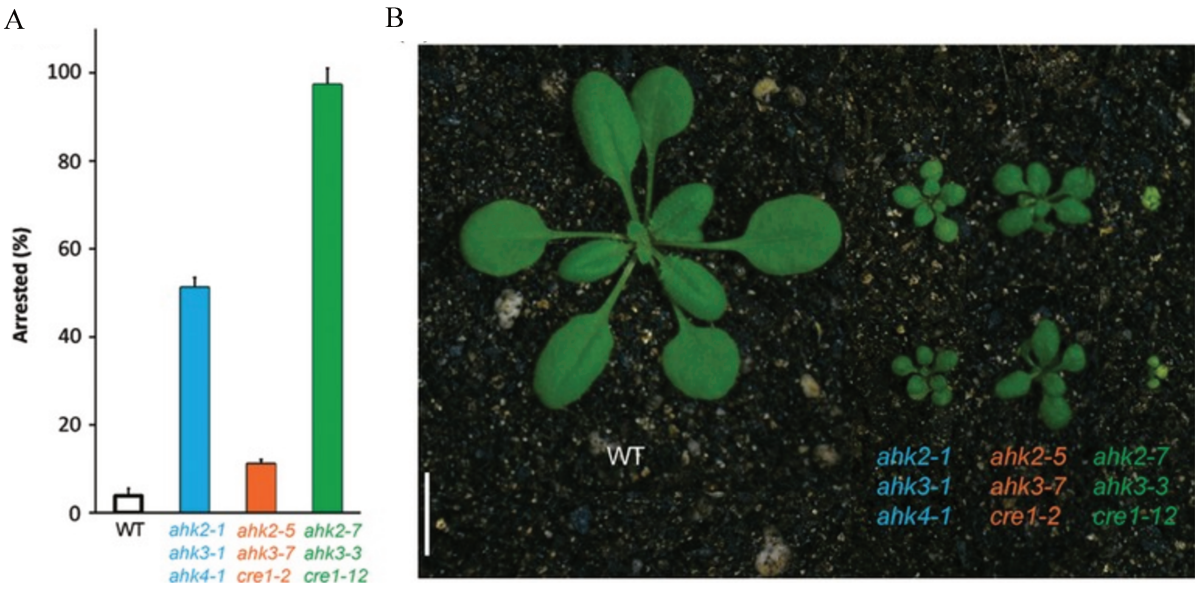

Figure 6. The ahk2, ahk3, ahk4 triple mutants severely affected gametophytes and rosettes development. A. Percentage of arrested gametophyte in wild type (wt) and triple mutants. While all lines presented fewer ovules, only the *ahk2-1, ahk3-1, ahk4-1*; and the *ahk2-2, ahk-3, cre1-12* lines were morphologically different (n>50 from at least three plants for each mutant) **B.** Aerial phenotype analysis of 4-week-old wt and triple mutants. The strongest rosette morphology was observed in the *ahk2-7, ahk3-3, cre1-12* mutant. Consistently, this line has the highest percentage of arrested gametophytes (scale bar: 1cm). **Adapted from Cheng et. al 2013.**

The following is a summary of all *in vitro* and *in vivo* outcomes. AHK3 showed higher affinity for tZ, followed by DHZ and iP, and had the lowest affinity for BA and cZ in comparison with AHK4 in all tested conditions. The latter instead showed a higher affinity to iP and tZ followed by BA and cZ. Based on the lower affinity for iP-types observed for AHK3, it was proposed that this receptor sensitivity is higher for root-derived CK (tZ-Types)[100]. A much-debated question is whether the ribosides, the main long-distance forms of CK, have genuine CK activity[36,52,53,107,114]. While the affinity of the AHKs for tZR and iPR was evidenced in the previously mentioned bacteria-based assays, no receptor activation has so far been associated with the observed hormone binding.

Further, *in vivo* analyses in *Arabidopsis* protoplast addressed the activation of reporter genes after the addition of the isoprenoid derivates tZ[61,115,116] and iP[61]; or BA[51,61]. The latter, while not focused upon the calculation of the Kd, provided evidence of the sensitivity of the receptors for different CK forms. Nevertheless, investigation of the sensitivity of the receptors, as well as the activation of CK response by different CK/AHK combinations in plants, could be impeded by CK metabolism, non-canonical activation of the pathway and negative regulators. Therefore, it will be advantageous to engineer a more suitable platform for quantitative *in vivo* analysis with reduced complexity yet conserved general mechanisms such as transport/secretion systems.

1.2.4.2 *Arabidopsi*s Histidine-containing Phosphotransferase proteins

After signal perception, five of the six HPs encoded in the genome of *Arabidopsis* (AHP1 to 5) mediate the transfer of the phosphate from the hybrid HK to the response regulators. These proteins lack catalytic activity therefore they rather act as phospho-donors for the B-ARRs. Within the cell, AHPs are localized both in the nucleus and the cytoplasm, constantly shuffling independently of the presence of the hormone[117]. AHPs interaction with several members of the HK (including CKI1), RR and CRF family was suggested, supporting their role as intermediate proteins in the pathway[61,118–121].

Protein alignment of AHP1-5 revealed that these approximately 150 amino acids long proteins have a highly conserved sequence[122]. Interestingly, as mentioned before for the AHKs, the role of the AHPs as mediators of the TCS in *A. thaliana* was first evidenced after complementation with AHP1 of a *ypd1*Δ yeast mutant line[123]. Moreover, *in vitro* studies of AHK4 kinase and phosphatase activity included AHP1,2,3 and 5, together with YPD1. Up until then, it was the only HP proven to receive the phosphate from the CK receptor[94]. Altogether these analyses demonstrate an interkingdom functionality of the TCS components.

The expression of these phosphotransferases is induced by CK coincidently with their function as pathway mediators. Down-regulation of their expression was reported in response to abiotic stress [124]. Moreover, the AHPs can be S-nitrosylated in a conserved cysteine residue by nitric acid reducing their ability to both, receive and transfer the phosphate[125].

AHP regulatory roles have been widely assayed using loss-of-function mutants and fewer overexpression assays (mainly for AHP2). Single mutants displayed an undisguisable response to CK compared to wildtype (WT)[126]. Moreover, the quintuple mutant *ahp1 ahp2 ahp3 ahp4*

ahp5 exhibit reduced shoot development, enlarged seeds and diminished fertility, similar to the *ahk2 ahk3 ahk4* triple mutant. The study of double mutant lines for *ahp2 ahp3* revealed these proteins prominent role as negative regulators of drought-tolerance[124] (**Fig. 7**). Later, the loss of central and antipodal cells fates in ovules of the triple mutant *ahp2 ahp3 ahp5* suggested they play a role in female gametophyte development[127].

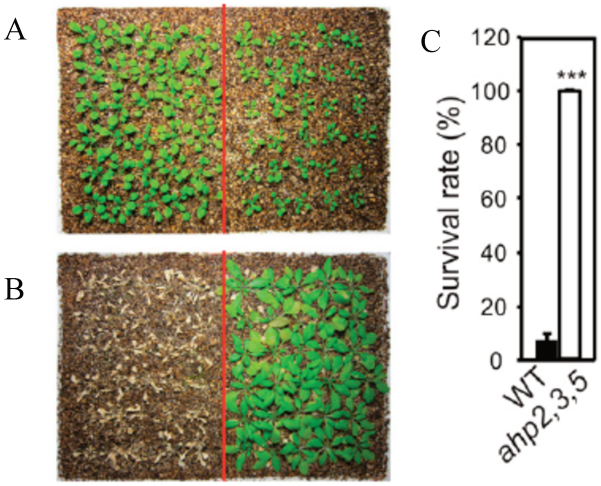

Figure 7. The *ahp2, ahp3, ahp5* triple mutant presents enhanced drought tolerance.
A. 3-week-old mutant lines presented reduce growth compared to the WT. **B.** Photography of 3-week-old plants prior rewatering and inflorescence removal, after 13d of drought stress shows increase stress tolerance in mutant lines. **C.** Survival rates showing the average of three independent experiments (n=30 plants/ line) evidence AHP negative role in drought reponse (***P<0,001). **Adapted from (Nishiyama et al. 2013)**

AHP2, 3 and 5 were proposed to be expressed ubiquitously in plants, while AHP1 was predominantly found in roots[122]. AHP4 is mainly expressed in the aerial parts of the plants and it was suggested to have a weak contribution to CK responses, proposing that it may instead interfere with the pathway, for example, by interaction with other signalling elements[122,126].
AHP6, the pseudo-HP of *Arabidopsis* thaliana, is a unique protein in the AHP family. The negative regulatory function of this AHP was first discovered in screening for suppressors of *wol* root phenotype. The *wol ahp6* double mutant evidenced a role for AHP6 in promoting protoxylem specification[68]. Interestingly, AHP6 expression is induced by auxin[128]. In shoots, where CK and auxins have an antagonist function, AHP6 seems to work in coordination with auxin to regulate developmental patterns. To this end, AHP6 can move to adjacent cells via plasmodesmata[69,128,129].
It has been proposed that the mechanism of action of AHP6 inhibition relies on an interference with the phospho-transfer between the different domains of the hybrid HK receptor, and between the AHPs and B-ARRs[94]. However, how precisely this pseudo-HP lacking a conserved phosphorytable residue affects the phospho-transfer remains unknown.

1.2.4.3 *Arabidopsis* Response Regulators

The type-B ARR family includes 11 transcription factors known as the main effectors of the CK pathway. Oppositely, the 10 type-A ARRs and the type-C ARRs act as negative regulation of CK signalling.

1.2.4.3.1 Type-A Response Regulators

The type-A response regulators family comprise 10 proteins whose sequence includes a receiver (REC) domain yet lacks the transactivation domain present in the B-ARRs. Transcription of these RRs is rapidly induced after exogenous CK application and occurs in the absence of *de novo* protein synthesis[130]. Because of this fast induction, the promoters of the A-ARRs, mainly ARR5 and ARR6, are often used to engineer reporter systems for the study of CK transcriptional responses.

Transcripts levels of many A-ARRs are regulated by other inputs as well. ARR7 and ARR15 expression is repressed by auxin in the SAM, but induced by the same hormone in the RAM[82,131]. ARR5 that is highly expressed in SAM and RAM is transcriptionally suppressed in the WUSCHEL (WUS) domain, thus controlling the spatial distribution of CK response in the SAM[132]. In addition, ARR4, which is mostly found in stems, leaves and flowers, seems to be post-transcriptionally regulated. In response to the phytochrome B action, the level of ARR4 protein but not of its mRNA will increase. In turn, ARR4 will stabilize the active form of phytochrome B both in yeast and in plants[133,134].

Two mechanisms were proposed as the mode of action of these RRs. First, as it was shown that response regulators can interact with several AHPs and their sequence contains a conserved asp residue, they could be competing for AHP interaction/phosphate with the B-ARRs[130]. A second model based on biochemical and structural studies proposes that, even when ARR-A/B interactions were not evidenced, they may be forming an inhibitory complex when both are in their phosphorylated state. Another piece of evidence that supports the latter hypothesis is the finding that the phosphomimic form of a type-A ARRs could partially rescue the *arr3 arr4 arr5 arr6* mutant phenotype[135]. This implied that, even when the A-ARRs cannot receive the phosphate (as they mimic the phosphorylated state by the point mutation) from AHP, they still exert their inhibitory role. In the same direction, a non-phosphorytable mutant of ARR7 was still localized in the nucleus and had a similar half-life as the WT, when the conserved D residue

was replaced for asparagine (N). However, this mutant failed in generating ARR7 phenotype[136].

These proteins function will be enhanced by CK, as evidenced by the increase stability of these proteins in the presence of the hormone[135]. Later, dephosphorylation and further degradation by the ubiquitin-proteasome pathway result in the turn-off of these RRs.

1.2.4.3.2 Type-B Response Regulators

The B-ARRs are transcription factors (TF), whose sequences comprise a C-terminal region of variable length and an evolutionary conserved REC in the N-terminal end. The C-terminal region includes a Myb-like DNA binding domain followed by an activation domain rich in glycine and proline and a nuclear localization signal (NLS)[137,138].

It is believed that the REC domain of the B-ARRs masks the DNA-binding domain, thus negatively regulating their function; as its deletion leads to constitutive activation of the responsive genes[139–141]. Further, phosphorylation at the REC domain seems to be key to releasing this inhibition, as phosphomimic forms ARR1(D94E)[142] and ARR2(D80E)[138] resulted in a constitutive up-regulation of CK responses. These observations agree with the phospho-transfer being the motor of the CK signalling by triggering a conformational change in the RRs. Interestingly, analysis of the CK-inducible expression of reporter systems in *Arabidopsis* protoplasts further revealed the ability to activate CK responses of the non-phosphorytable mutants of ARR2[16,61] and ARR18[143], when the conserved D residue was replaced for N. These findings suggest that other modifications at the conserve D, which presumably alter the structure of the REC domain, can activate these B-ARRs by unmasking their DNA-binding domain.

Type-B ARRs will bind their target DNA either in a core CK response motif (CRM) A/GGATC or an extended version (ECRM) AAGAT(T/C)TT, as characterized for ARR1[137,140,141]. Based on their DNA-binding domains, these TFs have been further subdivided into three subfamilies: B-I (ARR1, ARR2, ARR10, ARR11, ARR12, ARR14 and ARR18), B-II (ARR13, ARR21) and B-III (ARR19, ARR20)[144,145]. The most widely studied subfamily has been, by far, the B-I. These seven RRs are expressed in all tissues and play a predominant role in controlling CK responses. Among them, ARR1, ARR10 and ARR12 have been shown to regulate the majority of genes involved in canonical CK responses[146–148].

These three TFs are similarly expressed in roots, hypocotyl and cotyledons and localize in the cell's nucleus[149]. Studies of their mutants presented them as regulators of different division and

differentiation events. The *arr1 arr10 arr12* triple mutant was shown to have reduced apical dominance in the SAM, while abnormalities were observed in vascular development[147,149,150]. The antagonistic role of auxins and CK was also promoted by these RRs, as ARR1 and ARR12 can induce SHY2 expression, a known auxin signalling repressor[83,84]. Importantly, many phenotypes of the *b-type-arr* triple mutant were analogous to those observed in *ahk2 ahk3 ahk4* triple mutants, reinforcing the idea that these TFs have a prominent role in the CK response[147] (**Fig. 8**).

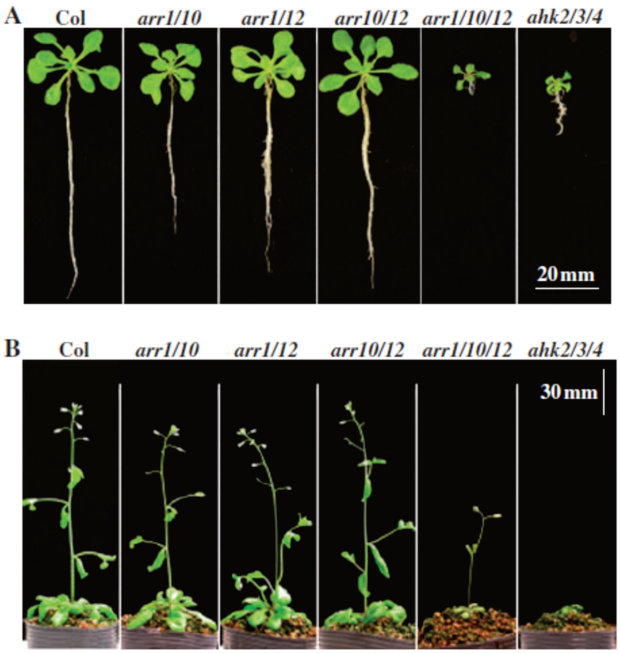

Figure 8. The *arr1, arr10, arr12* affect *Arabidopsis* aerial and root growth.
A. 18-day-old WT, double and triple mutant for *arr*, and *ahk* were grown on MS agar plates on long day conditions. Only the *arr* triple mutant exhibit a strong phenotype, comparable with the receptor triple mutant in roots. **B.** 14-day-old plants were grown in MS and then transferred to soil for another 14d. Triple mutants for the response regulators developed inflorescence later than the WT, yet produced flowers, while the receptor triple mutant was not fertile. **Adapted from (Ishida et al., 2008)**

In prokaryotes, homologous RRs involved in TCS pathways require dimerization, or even, oligomerization for their activation[151,152]. In addition, eukaryotic organisms also use TFs complex formation as a regulatory mechanism[153]. It is therefore likely that the B-ARRs can bind and activate their target genes as dimers. Homo- and heterodimerization of the B-ARRs have been proven for some of these TFs by Y2H. In these studies, ARR10 was suggested to interact with CRF6 and ARR12 with CRF1/2, and other TFs belonging to different networks[119,121]. Moreover, ARR14 was proposed in the same studies to form homodimers and heterodimers with ARR2. However, the biological relevance of these interactions needs to be further assessed. Up-to-now evidenced, activation of CK responses by homo- or heterodimers between the B-ARRs are: the activation of ARR6 promoter by ARR18 homodimer and ARR1-ARR12 transactivation of TRYPTOPHAN AMINOTRANSFERASE OF ARABIDOPSIS 1 (TAA1)[154,155].

It was also proven that the DELLAs (aspartic acid–glutamic acid–leucine–leucine–alanine) proteins enhance the transactivation ability of ARR1 and can bind as a complex to the TAA1 promoter[155]. Additional support to the TFs complex hypothesis is the evidence that more than 50% of the promoters of CK inducible genes lack the CRM or ECRM motif. Moreover, from the genes recognized by ARR1, ARR10 and ARR12, less than 15% are transcriptionally regulated by CK[141,149,156]. Therefore, suggesting the need for these TFs to interact with others that physically bind the promoter of the target genes.

In comparison with the A-ARRs, only increased stability of ARR1 was so far evidenced in the presence of the CK[157]. Finally, CK signal transduction will be regulated by the degradation of the B-ARRs as well.

This turnover involved the F-box family of proteins, the Kiss Me Deadly (KMD), that targets the B-ARRs for degradation by the ubiquitin-proteasome pathway, with particular kinetics for different members of the family[158].

1.2.4.3.3 Type-C Response Regulators

Even when the type-C ARRs structure is similar to those of the type-A ARRs, unlike them, C-ARRs expression is not regulated by CK[67,159] . Moreover, their functional receiver domain resembles those of the HKs. This family includes two proteins, ARR22 and ARR24. Both C-ARRs are expressed in the cell cytoplasm at the funiculus/chalaza junction developing seeds or pollen grains, respectively, and their loss-of-function mutants failed in displaying a particular phenotype[160]. However, ectopic overexpression of ARR22 in *Arabidopsis* induced dwarf phenotypes and general attenuation of CK responsive genes expression, as observed for the receptors and the type-B ARR triple mutants[66,67].

Surprisingly, ARR22 activity depletion occurred when the aspartate was replaced with alanine, asparagine or glutamate[161]. Therefore, unlike type-A ARRs, the role of this protein is not likely induced by phosphorylation, but rather, by the availability of a phosphor-receiver residue. This supported the finding that ARR22 could rapidly dephosphorylate AHP5 by *in vitro* assays, while no phosphorylated C-ARR could be recovered. Suggesting that ARR22 might act as a histidine phosphatase[67]. As this RR can interact as well with other AHPs (Y2H and *in planta*), it was questioned, if ARR22 may function as a histidine phosphatase to other HPs from different organisms[66,161].

Overexpression (-ox) of type-A ARRs as ARR7, ARR4 and ARR15, while partially repressed B-ARRs responses generate weaker repression in comparison with the ARR22-ox mediated

signal depletion[162]. This suggested that the down-regulation of CK signalling by the C-ARRs seems to be more efficient than the exerted by the A-ARRs.

1.2.4.4 Cytokinins Response Factors

The CRFs were first identified as CK-responsive genes that rapidly increased the levels of transcripts after hormone treatment[64]. Subsequently, binding sites for the type-B ARRs were found in the promotors of two members of this family, CRF2 and CRF5. The role of these proteins as regulators of CK responses was later evidenced by analysing the transcriptome of double mutant lines for *crf* or *b-arr*. This study revealed a substantial overlap in the transcriptional regulation exerted by these two families of TFs[64,141], proposing the CRFs as effectors of CK pathway.

As observed for the other signalling element involved in this pathway, the phenotypes were more visible in higher order loss-of-function mutants suggesting functional redundancy[64]. As an example, the *crf5 crf6* double mutant, but no other mutant combination of CRFs were embryo lethal, thus suggesting that these TFs have a role in the control of embryo development[64]. Further, CRF2, CRF3 and CRF6 have been suggested to regulate numerous stress responses (reviewe[163]). In addition to its capacity to negatively regulate senescence[164], CRF6 was proposed to regulate oxidative stress via a non-canonical TCS pathway[165].

Unlike the type-B ARRs, the CRFs belong to the B-5 subgroup of the family of the Apetala 2 (AP2) transcription factors[166].

The AP2 domain is located in the middle of the sequence of these proteins, flanked by a highly variable region in the C-terminal and an evolutionary conserved N-terminal part. The N-terminal end includes a domain that differentiates the CRF from the other AP2 TFs, the CRF domain. This sequence is crucial for their PPI. The C-terminal variable domain presents a putative phosphorylation site with an SP(T/V)SVL motif[167]. Based on the conservation of this C-terminal region, the CRFs can be further subdivided into 5 clades. Clade I (CRF1-CRF2), Clade II (CRF3-CRF4) and Clade III (CRF5-CRF6) have been so far the most, if not the only ones, under study. Each clade has been attributed a role in a specific type of stress response: Clade I to salt stress, Clade II to cold response and Clade III to oxidative stress response[163,165,168]. However, there is evidence of proteins from different clades being involved in the same type of response. For example, CRF 2 and 3 regulates lateral root formation during cold response[73]. Interestingly, the same study showed that CRF3 can be upregulated by cold

via non-canonical circuits. This evidences once more the high level of complexity and interconnectivity within different networks for the regulation of common responses. In addition, Clade IV CRFs (CRF7 and CRF8) lack the conserved C-terminal domain (thus, the putative phosphorylation site) questioning whether these TFs participate in the phospho-relay[119].

CRFs were proposed to be located mainly in the cytoplasm and relocated into the nucleus in a hormone-dependent manner, as it was also initially suggested for the AHPs[64,169]. However, later studies questioned this hypothesis, finding the CRFs in the nucleus before any CK application, in protoplasts and onion epidermal cells[170], in stable transgenic lines expressing CRF1 or CRF5[171] and in protoplasts, when analysing cold response[73].

Finally, CRF1-8 ability to form homo- and heterodimers as well as to interact with the AHP1-5, was identified using Y2H and/or Bimolecular Fluorescent Complementation (BiFC), with some exceptions [119]. Further proven interactions with the ARRs were previously mentioned.

1.3 Synthetic biology (SynBio)

The term “synthetic biology” was first used by Stéphane Leduc in 1910 in his book *Théorie physico-chimique de la vie et générations spontanées* and later in two following publications: *The mechanism of life* (1911) and *La Biologie Synthétique* (1912)[172]. Although Leduc’s use of the term (mainly referring to crystals) does not correlate with today´s usage, his philosophical conception still applies. A good example is his description of the *synthetic method* as *“reproduction by the forces of physics of biological phenomena that must contribute to give us a comprehension of life”* (Leroc 1912, page 12). Nevertheless, synthetic biologists have a more ambitious goal. Whereas they still focus on synthetically reproducing naturally occurring events to understand life, they also aim to create biological systems that do not exist in nature. Therefore, we could define SynBio as a multidisciplinary field that combines theoretical and experimental strategies for the engineering of novel biological modules and systems as well as the re-design of previously existing biological systems with new functionalities.

The iconic event that brought forth the “synthetic thinking" was the characterization of the lac operon, highlighting the existence of modules that can specifically regulate gene expression[173]. Moreover, Jacob and Monod proposed the possibility of generating new systems by recombining existing ones. Altogether, the discovery of chemical synthesis[174,175], the emergent

molecular cloning methods[176,177], the polymerase chain reaction (both for amplification and mutagenesis)[178] and the ground-breaking CRISPR/Cas application for genome editing[179] have propelled decades of design and engineering of building blocks for such systems.

The engineering of a genetic toggle switch[180], a transcriptional regulatory loop controlled by an oscillatory function[181] and an autoregulatory gene network[182] in bacteria were the start of this still-growing field. Since then, the application of SynBio has been far-reaching and encompass: biocomputing[183], design of new proteins[184], production of living materials[185,186], synthetic life[187], biotherapeutics[188,189], organoide[190], biofuel production[191], reconstruction of signalling pathways[12] and even applications in space exploration[192] (For more applications refer to[193,194]).

1.3.1 Modular reconstruction strategy for the analysis of signalling processes

The perception and transduction of endogenous and exogenous signals are essential for all living organisms to coordinate growth, differentiation, metabolism and survival. Signalling pathways present natural modularity where each building block has a distinguished role and participates in the signal transduction over a wide array of PPIs (or second messengers) with the other components. These networks comprise a multiplicity of signalling elements often presenting functional redundancy. In addition, numerous feedback control loops modulate this circuit, together with cross-interactions with other pathways. The intrinsic complexity of most signalling pathways has long-limited the detailed study of their kinetics and dynamic interactions, as well as the role of individual components and the mechanism underlying their function. To better understand (and manipulate) these complex processes, new approaches are needed[195].

To assist the classic genetic, biochemical and molecular biology approaches, the modular architecture of signalling pathways has been utilized to generate tools, which can be further implemented for SynBio strategies[193,196,197]. Among them, of main importance for the acquisition of new knowledge are the bottom-up approaches[198–200]. These methods attempt to build new experimental models combining biological and artificial building blocks. Further, partial or full reconstruction of the signalling networks after heterologous expression in orthogonal systems reduces the level of complexity of the analysis. The dissection of the pathway into their minimal components permits the quantitative analysis of the role of single

elements in the network, their subcellular location and the level of expression. Posterior addition of other elements through the bring-in-and-play approach allows them to explore their PPIs or to perform competition assays while analysing, for example, different RRs activation or repression.

This method has to this day been successfully applied for deciphering the key role of proteins in many fundamental biological processes. As an example, transient expression of mammalian proteins in cells of the evolutionary distant *Drosophila melanogaster* permitted the study of the signal transduction from the B cell antigen receptor (BCR)[201]. This complex is formed by a membrane-bound immunoglobulin (mIg) and the Igα/Igβ heterodimer. By expressing these proteins in different combinations, a model for this complex transport from the ER to the plasma membrane and assembly was proposed. The enhanced green fluorescent protein (EGFP) was used as the reporter gene to evidence the complex relocation. Moreover, combinatorial analysis of the kinase activity of the mutant form of the BCR proximal protein tyrosine kinase (PTK) Syk permitted to characterize of the role of its SH2 domain in the signal transduction.

Synthetic approaches had also been fundamental in the study of phytohormone signalling pathways. Many of these works were focused on the study of the auxin pathway. An example is the partial reconstruction of the auxin-induced degradation system in the yeast Saccharomyces cerevisiae[202]. Briefly, auxin responses required the turnover of the Auxin/Indole-3- Acetic Acids (IAAs) by interaction with the Transport Inhibitor Resistant1/Auxin signal F-box Protein (AFBs). To explore the degradation behaviour of different IAAs/AFB complexes, a yellow fluorescent protein (YPF)-IAA fusion was expressed in yeast in the presence of AFB. Posterior treatment with different concentrations of the hormone allowed us to visualize the differential degradation rate of the different complexes. Later, the same group reconstructed a minimal auxin response circuit to explore the contribution of single modules to auxin responses[203]. In this innovative study, a synthetic switch was engineered to visualize auxin-induced transcription. In this module, the expression of the GFP reporter was controlled by a promotor containing an auxin response element (PARE). In the absence of the hormone the IAAs repress the activity of the auxin response factors (ARFs) by recruiting the co-repressor TOPLESS (TPL). As expressed before, in the presence of auxin the IAAs are targets for degradation. The IAAs turnover results further in the activation of the PARE promotor, and thus in increasing signal of GFP.

1.3.2 Mammalian cells as *chassis* for plant signalling pathway reconstruction and study

A critical step during pathway reconstruction is the selection of an appropriate structure (chassis or host) that supports the synthetic network. The chassis directly affects the behaviour of the system and determinates the available tools for its analysis[199].

Yeast, as previously mentioned, and bacteria have some advantages as hosts for reconstruction. The genome of these organisms has been sequenced and is trackable, they have rapid growth and inexpensive maintenance and there is a wide range of tools available for transformation[180,181,193]On the other hand, limitations of working with bacteria are the lack of quantitative tools for PPI and the need for codon optimization for correct plant protein expression. Further, even when properly translated, correct protein folding and function cannot be ensured, as bacteria introduces reduced post-transcriptional modification. Yeast instead are evolutionarily closer to plants, yet they tend to hyper-glycosylate proteins. In addition, while we recognize the great contribution of the Y2H technique for the identification of many PPIs, this approach is not quantitative, requires nuclear localization of the partners and presents a high rate of false positives[204,205]. These organisms, moreover, present major disadvantages particularly for the study of CK signalling pathway, as pursued in this work. First, as CK signal comprise a membrane receptor, the different architecture of the membrane in prokaryotes may not alter or imped AHK function. Secondly, as mentioned in the previous section, both bacteria and yeast include multiple TCS pathways. These endogenous components are, even more, known to interact with the TCS of *Arabidopsis thaliana*, thus obscuring the analysis of the observations.

In contrast, mammalian cells as a platform for the reconstruction and study of signalling pathways offer multiple advantages. Since the development of the first inducible switch for mammalian cells, adopting the tetracycline-regulated promoter of *E. coli*, a wide range of expression vectors and analytical tools were developed to simplify the experimental set-up and provide quantitative readouts[197,199,206–208]. In addition, while several regulatory mechanisms are preserved, such as protein degradation, there is a reduced amount of mammalian homologous for most plant regulatory elements. Moreover, plant proteins are normally properly expressed and active in mammalian cells, even when the temperature of growth differs[209–211]. Therefore, mammalian cells closely mimic the natural plant environment allowing fast and systematic screening of plant signalling pathways, with tight control of the level of complexity (**Fig. 9**).

Of particular importance for this work, the membranes from plants and mammals have similar composition, while no TCS has been characterized in these organisms. Furthermore, there is a growing body of literature that recognizes the suitability of this platform for the study of plant signalling pathways.

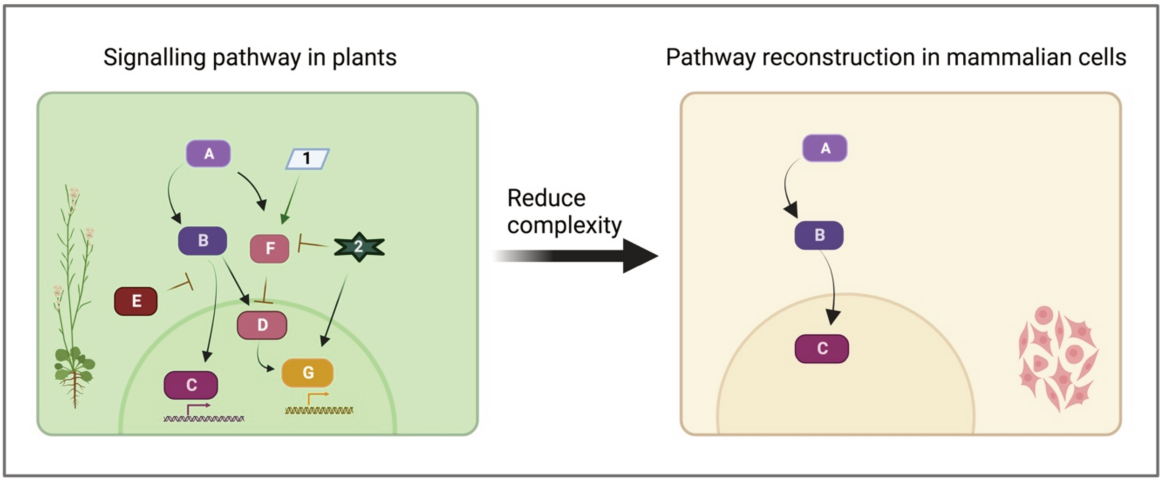

Figure 9. Illustration of the advantage of heterologous expression in orthogonal systems. Phytohormones perception and signalling is a complex mechanism that coordinate sensing of signal molecules, inter- and intrapathway interactions and extensive feedback control. Functional redundancy of the signalling elements hinder the identification of single component contribution to the pathway. Reconstruction of plan pathways in mammalian cells contribute to reduce the level of complexity of the analysis, while providing a setting that resembles plants natural environment, yet avoiding interconnectivity with other networks. The expanded tool box for quantitative studies, and genome modification in this orthogonal platform are major assets driving pathways reconstruction.

For example, in 2009 an auxin-based degron system was proven to rapidly deplete proteins in mammalian cells using the endogenous Skp, Cullin, F-box containing complex (SCF) degradation pathway[212], highlighting the importance of the conserved mechanisms between mammals and plants. Further, the possibility of optimizing synthetic tools for posterior implementation in plants is another superior advantage of the mammalian system. An example is the successful characterization in the Human Embryonic Kidney 293-T cells (HEK-293T) of a radiometric luminescent biosensor for auxin[213]. More recently, the formation of a ternary complex between COP1, SPA1 and the DELLA proteins was evidenced, and quantified in a similar system[214–216], providing evidence of the predictive power of mammalian platforms.

1.3.3 Tool-box for exploring plant signalling pathways in mammalian cells

From their perception to the transduction of the signal, phytohormone signalling networks can be interrogated and manipulated by systematic implementation of different SynBio approaches. These include (but are not limited to) the study of proteins` function and location, quantitative analysis of transcriptional regulation and PPIs as well as manipulation of protein degradation[195,217].

The control of transcriptional regulation is usually achieved through the design of genetic switches, combining natural and engineered molecular parts[217]. For interrogating hormone signalling at the transcription level, the design of these switches usually includes the introduction of multiple repeats of binding sites for the TFs of the pathway followed by a reporter gene. This was exemplified by the P_{ARE}: GFP in the previous section and it is also the rational design for the CK sensitive promotor-reporter systems. The engineering of TCS: firefly luciferase (LUC) was an important breakthrough for CK signal comprehension[61]. This synthetic reporter comprises the LUC gene under the control of concatemerized binding motif for the B-ARRs (normally, from the ARR5, or ARR5 promotors) and the 35S promotor of the cauliflower mosaic virus (CaMV). The TCS:LUC, and later its version where GFP was implemented as the reporter gene, allowed the visualization of CK signal patterns in plants with high specificity for the first time[131].

Synthetic tools such as the TCS:GFP, which allows for analyse with high spatial resolution of the perception of an analyte, are called biosensors. A biosensor should, ideally, offer a high signal-to-noise ratio, be sensitive and selective for the analyte, and be easily detected, while not perturbing the system. In addition, subcellular resolution and quantitative output are desired as well. Transcriptional fluorescent biosensors, such as the TCS:GFP, integrate both perception and signalling events. This delayed response restricts the observable processes as well as the dynamic of the measurement. Moreover, no subcellular resolution or quantitative readout can be achieved by these biosensors. Alternatives biosensors are the ratiometric biosensors, which include a normalization module that permits quantification, as the ones previously mentioned[213,218]. The latter, is specifically a degradation-based biosensor, and the same principle was implemented for the design of JA, GA and Strigolatones (SL), reviewed in[219]. In addition, relocation-, or Föster resonance energy transfer (FRET)-based biosensors offer a ratiometric measurement as well[195,213,219–222].

The relocation-based biosensor comprises two modules. The sensory module includes a protein that changes the subcellular distribution in response to a signal fused to a fluorescent protein (FP). The second module is a normalization module that includes a second FP, for example, constitutively expressed in the nucleus. After perception of the signal and relocation, the ratio between the FPs provides a quantitative read-out. Moreover, as protein relocation can occur within seconds, these biosensors allow the quantification of rapid changes *in vivo* and with subcellular resolution. However, to this day no relocation biosensors were designed for the analysis of hormone pathways yet they have many other applications reviewed in[220].

A FRET-based biosensor for hormone sensing requires the signal-dependent interaction between two proteins. Each of the two candidates for interaction is tagged to an FP from an established FRET pair. This approach relies on the energy transfer from a donor-fluorophore to an acceptor-fluorophore, and requires: 1. an overlap of the donor emission spectra with the acceptor absorption spectra, 2. proximity of both molecules (below 10nm) and, 3. a correct orientation of their dipolar moments[223] (**Fig. 10A-D**). Many FRET pairs have been optimized over the years improving their brightness, photostability, folding at 37°C, reduced sensitivity to pH, reducing interconversion, etc[204,205,224,225]. Cyan-yellow and red-green pairs are the more widely used. Particularly, the mCherry-EGFP excitation induces less autofluorescence from flavoproteins, less phototoxicity and has greater spectra separation[204,226,227]. This approach was used for the study of ABA perception as well as for GA and was reviewed in[219].

Besides being used for the detection of low abundance molecules, such as hormones, FRET-based approaches are widely implemented to quantitative interrogate PPIs. In comparison with the bi-molecular fluorescent complementation approach (BiFC), which relies upon the re-assembly of a slip FP[228,229], FRET approaches present no false positives, while still providing the subcellular definition. First, most split fragments can spontaneously reassemble. Secondly, the irreversible complementation of the split fluorescent protein fragments hinders the analysis of the interaction dynamics.

Among all FRET approaches available to explore PPIs, the FRET-Acceptor photobleaching technique (APB) measures the donor emission after photobleaching of the acceptor. During FRET, the donor fluorescence is quenched (reduced) by the energy transfer to the acceptor[230]. Therefore, disrupting the acceptor fluorophore by photobleaching results in an increase in the donor fluorescence. This event is irreversible and eliminates the quenching effect[230] (**Fig. 10**).

A major advantage of this technique is that quantification of the energy transfer can be later performed with most confocal fluorescent microscopes. However, because photobleaching is irreversible, it allows only one use per cell, limiting dynamic measurements[205]. For the latter, as well as for proteins with low expression patterns, FRET FLIM (fluorescent lifetime imaging microscopy) is a more suitable technique[204,231,232].

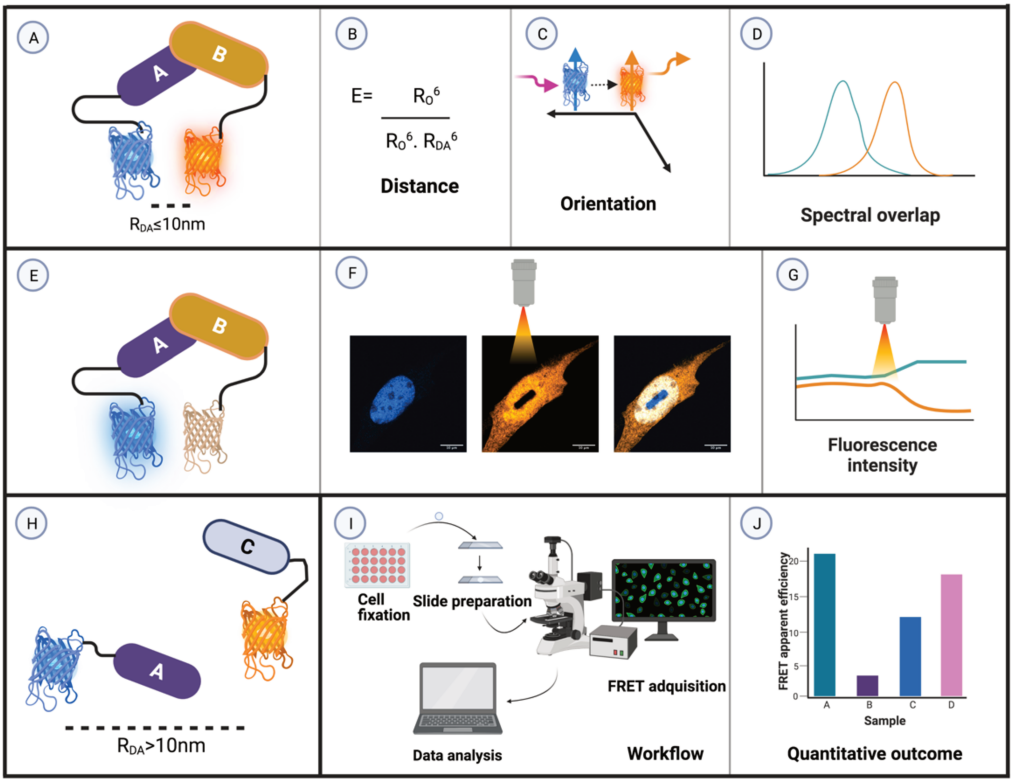

Figure 10. Föster resonance energy transfer (FRET) principle and data analysis..
A-D. The term "FRET pair" defines two fluorescent proteins (FP) with overlapping spectrum. If the donor and acceptor of this couple are fused, independently, to two proteins presumed to interact, their complex formation will bring the FP to close proximity. If the fluorophores dipoles are properly oriented, the energy transfer can take place, and the donor protein fluorescent intensity will decrease. **E-G**. If the acceptor fluorophore is bleached, its intensity will decrease (close to 0%), evidencing an increase in the donor signal. **H**. Two candidate proteins not interacting will not favor the energy transfer. **I-J.** For FRET acquisition the cell will grow on top of a microscopy glass. Samples will then be fixed and mounted in a slide for further observation in the confocal microscope. The apparent FRET efficiency is then calculated and represented as the average of 10 independent measurements. Protein A, B, and C, hypothetic proteins; E, transfer efficiency; RDA, mean distance between the dipoles of the fluorophore; R0, Föster radio.

An alternative for the rapid and quantitative screening of PPIs in mammalian cells is the use of split TF systems. The first engineered chimeric transcription factor included the DNA-binding motif of the tetracycline repressor (TetR) and the transcriptional activation domain VP16 of

the Herpes simplex virus[233]. The binding of TetR as a dimer to the operator motif for the repressor (tetO) naturally occurs in the absence of tetracycline, inhibiting the expression of tetracycline resistance genes. TetR protein fused to VP16 converted this repressor system in a tetracycline-controlled transcriptional activator of a desired gene, located downstream the tetO and a minimal promoter. Several years later, this system was transferred to yeast and mammalian cells. tetR and VP16 were then used for analysing PPIs by M2H. Replacing the dimerization domain of the TetR for either bait or prey protein, the chimeric TF TetR-prey/bait-VP16 activity was restored, in the absence of doxycycline[234]. In 2013, a more intuitive M2H design using the TetR-VP16 system was engineered[235], where TetR-PIF6 / PhyB-VP16 split TF controlled the expression of a reporter gene in a red light-dependent manner. This same principle can be further used for the analysis of any PPI, where one of the candidates for interaction is fused to TetR, and the other to VP16.

2. **Aims**

This thesis aimed to address the challenge of studying plant signalling networks in their natural environment by providing a new synthetic approach for the exploration of CK perception and signalling in mammalian cells.

The specific aims of this thesis were defined as:

1. **Design and engineering of an experimental platform for the study of CK signalling using mammalian cells.**

In the first part of this thesis, we identified the minimal components needed for the full reconstruction of the *A. thaliana* CK pathway in mammalian cells. We then established the optimal experimental setup to interrogate CK responses in the orthogonal platform and presented the workflow for the studies performed in isolated plant cells (protoplasts) as validation of the observations obtained in mammalian cells.

2. **Exploring the predictive power of the new synthetic platform**

In the second part of the thesis, we addressed the previous hypothesis concerning CK signalling using the newly established experimental platform. From the signal perception down to the transcriptional activation, we interrogate the role of specific signalling elements of the pathway. While verifying the suitability of the synthetic circuit to mirror results obtained in plants, we also explored new hypotheses and gave experimental validation to overlocked observations present in the literature.

3. **Interrogating CRFs suitability for the design of a radiometric biosensor**

The last part of the thesis aimed to design a quantitative tool with spatial and temporal resolution, for the study of CK signalling *in planta*. To address this, we first explored the suitability of the CRF1 to 12 to be implemented as sensory modules for a relocation-based biosensor, by analysing a putative CK-dependent subcellular relocation. In addition, considering the design of a FRET-based biosensor, we quantified the PPIs between the CRFs and the AHPs, using MxH approaches.

3. Results and Discussion

3.1 Chapter 1. Design and engineering of an experimental platform for the study of CK signalling using mammalian cells.

The study of phytohormone signalling in plants is highly impeded by the redundancy of function of the signalling elements, the crosstalk with other phytohormone pathways, and the extensive feedback control. This high complexity especially difficult the quantitative analysis of the contribution of single components to the transduction of hormonal signals. The SynBio toolbox offers a wide supply of approaches to (quantitatively) undertake these studies by exploration of PPIs, subcellular location, or reporter assays, after reconstruction of these signalling pathways in orthogonal "complexity-free" systems[214,236,237]. In particular, for the study of CK pathway, these alternatives have included transient expression in protoplasts and partial reconstructions in heterologous systems such as bacteria and yeast. The latter is fundamental for revealing the role of all three genuine CK receptors, the AHK2, AHK3 and AHK4 permitting the study of the phospho-relay between the different TCS components. Nevertheless, the chosen heterologous systems have their limitations. Besides their known incorrect protein folding and deficient post-transcriptional modifications, both bacteria and yeast have several conserved TCS, whose components could interfere with the CK TCS analysis. Secondly, studies of the AHKs selectivity in these organisms have been largely argued based in the different lipidic composition of their membranes. These impediments remark the need of finding a more adequate platform for the TCS reconstruction. Mammalian cells models are an emerging favourite among all available chassis for heterologous expression, and particularly for the study of plant signalling. To our knowledge, and of special importance for our work, only fewer histidine kinases and histidine phosphatases have been identified in the past in this kingdom[238,239]. Moreover, no TCS has so far when characterized in this kingdom. In addition, plants and mammals have similar membrane architecture and secretion/ transport systems overcoming the limitation of using bacteria, and yeast systems.

This chapter is (partially) based on the manuscript in preparation "Full reconstruction of *Arabidopsis* CK signalling in mammalian cells reveals new regulatory mechanisms" (Pavesi et al., in preparation 2022; Appendix 7.1) and describes the establishment of a novel experimental

approach to interrogate CK signalling. We will discuss the full reconstruction of the *Arabidopsis thaliana* CK pathway in the Chinese ovary hamster K1 (CHO) cells. We will explore the rational design of a promoter-reporter system that will allow us to visualize CK responses in platform and the posterior optimization of the experimental set-up. We will interrogate our system orthogonality and sensitivity, to conclude with the analysis of the subcellular distribution in mammalian cells of the representative members of the AHK, AHP and B-ARR families used for the pathway reconstruction.

3.1.1 Full CK pathway reconstruction in mammalian cells

3.1.1.1 Reconstruction and optimization of the experimental set-up

A key step in the reconstruction of signalling pathways in orthogonal systems is the identification of the minimal components involved in the circuit. The canonical CK pathway has been characterized and comprises an AHK receptor that will transfer a phosphate to the B-ARRs via the phosphotransferase, AHP. Phosphorylation of the receptor will lead to the activation of CK-responsive genes. We hypothesized that transient expression of a member of each multigene family will be sufficient for the activation of a responsive promotor-reporter system, similar to the previously used TCS:LUC[131,169] (**Fig. 11A**). For this purpose, we engineered vectors for mammalian expression where the full-length cDNA sequence of AHK3, AHP2, and ARR10, was cloned downstream the Simian virus 40 early (constitutive) promoter (P_{SV40}) (**Fig. 11B**). The selection of these proteins was based in the vast body of literature addressing their roles[103,109,110,147,240–242] and their joint action in drought responses[124,150]. Next, the promoter-reporter system (henceforth, TCSm) was engineered including repetitions of the core for B-type DNA binding to the ARR6 promoter, followed by the minimal human cytomegalovirus early promoter (P_{CMVmin}), and the Secreted embryonic alkaline phosphatase SEAP, as the reporter gene (**Fig. 11B**). In addition, a normalization module to monitor the effect of the CK treatment in the survival of the CHO cells was designed. This module included the Gaussia luciferase gene (GLuc) also under the control of the P_{SV40}. As every assay throughout this work consistently showed no effect of the experimental condition in the cells` survival, to avoid information overload we only included a representative example in **Fig. 12C**.

After the addition of CK into the cells medium, we expect that the hormone binding to the receptors will trigger the canonical CK phospho-relay (AHK→AHP→B-ARR) resulting in the transactivation of the TCSm and observable as an increase in SEAP expression (**Fig. 11A and C**).

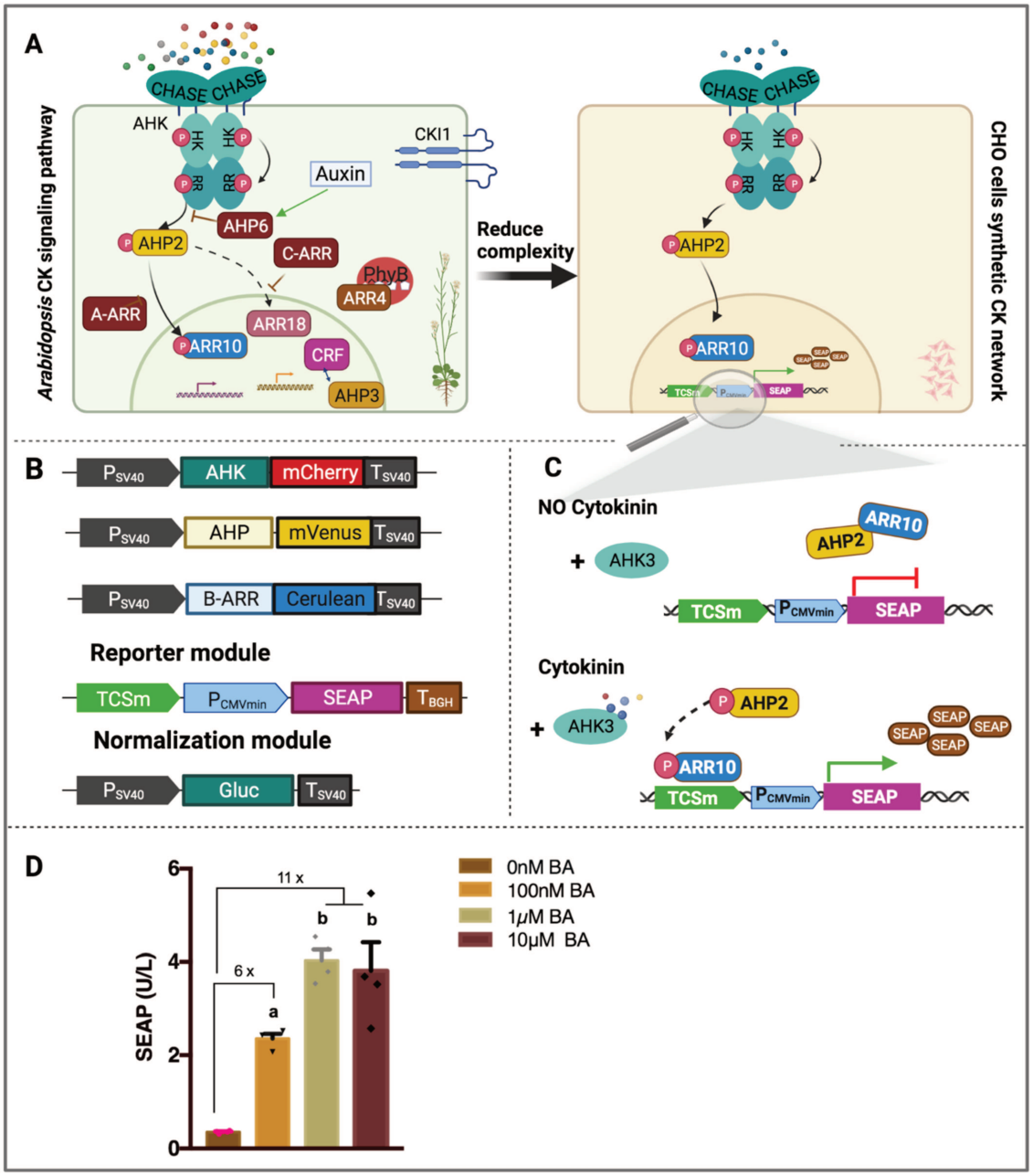

Figure 11. Synthetic reconstruction of CK pathway in CHO cells. **A.** Representation of the principle of heterologous expression in orthogonal systems applied for CK reconstruction in CHO cells. **B.** Representation of the different modules engineered for the analysis of CK responses in mammalian cells. **C.** Schematic representation of the expected behavior of the CK-responsive module used in this work. It is expected that after hormone perception ARR10 will bind the TCSm promotor and activate the reporter (SEAP) expression, in a hormone-dependent fashion. **D.** TCSm activation was quantified after addition of the indicated BA concentration in CHO cells co-expressing AHK3, AHP2, and ARR10. The system was induced for 24 h, four hours post-transfection. SEAP expression is expressed in units per litre (U/L). Data are representative of three independent experiments. Mean and S.E.M. are plotted for n= 4 mammalian samples. The statistical significance was determined using a two-way ANOVA analysis (P value < 0.001) and is indicated with bold letters. AHK, Arabidopsis histidine kinase; A-, B-, C-ARR, Arabidopsis response regulator type A, B or C; AHP, Arabidopsis histidine-containing phosphotransferase; BA, 6-bencilaminopurine; CRF, Cytokinins response factor; CHASE, Cyclase/histidine kinases associated sensor extracellular; CKI1, Cytokinins independent 1; m-Cherry, mVenus and Cerulean, fluorescent proteins; Gluc, Gaussia luciferase; P, phosphate; PCMVmin, minimal cytomegalovirus promotor; PhyB, Phytochrome B; PSV40, Simian virus 40 early promoter; SEAP, Secreted embryonic alkaline phosphatase; TCSm, CK-responsive synthetic promoter designed for this work; TBGH, Bovine growth hormone polyadenylation signal terminator; TSV40 SV40 virus terminator. This figure and the figure legend are adapted from the manuscript in preparation of Pavesi et al., Appendix 7.1.

For our initial experiment, cells were directly induced with BA 4 h post-transfection (PT), and SEAP activity was measured 24 h later. In these conditions, samples treated with 100 nM, and 1 µM BA showed a 6- and 11-fold increase in TCSm activation in comparison with the mock cells ("0nM BA"), respectively (**Fig. 11D**). Further increase in the hormone concentration did not improve the dynamic range. These results evidenced the system selectivity for CK and its sensitivity, which resembles the physiological concentration of CK in plants[52].

Next, we wondered if an increase in the period of time between the transfection and the treatment with BA could result in higher activation of the TCSm and/or increase the dynamic range. To explore this, in our following experiment we applied the hormone 24 h PT, instead of 4 h PT. Simultaneously, we induced the system with lower concentrations of BA and tested the effect of inducing the system for longer periods of time. Our results showed a significant TCSm response after 12, 24, and 48 h of BA treatment (**Fig. 12A**). After 12 h treatment approximately a 16-fold increase in the TCSm activation in comparison with the mock cell was observed at concentrations ≥ 10 nM. Due to the lack of dynamic measurement for this condition, we dismiss it. Further observation of the samples treated during 24- or 48 h with the hormone showed a good dynamic range in system response when comparing the concentration of 1 nM, 10 nM, and 100 nM of BA. However, the posterior addition of BA didn't affect the dynamic range. Therefore, we decided to treat the samples with the sampled in upcoming experiments with concentrations 1 nM, 10 nM and 100 nM of BA.

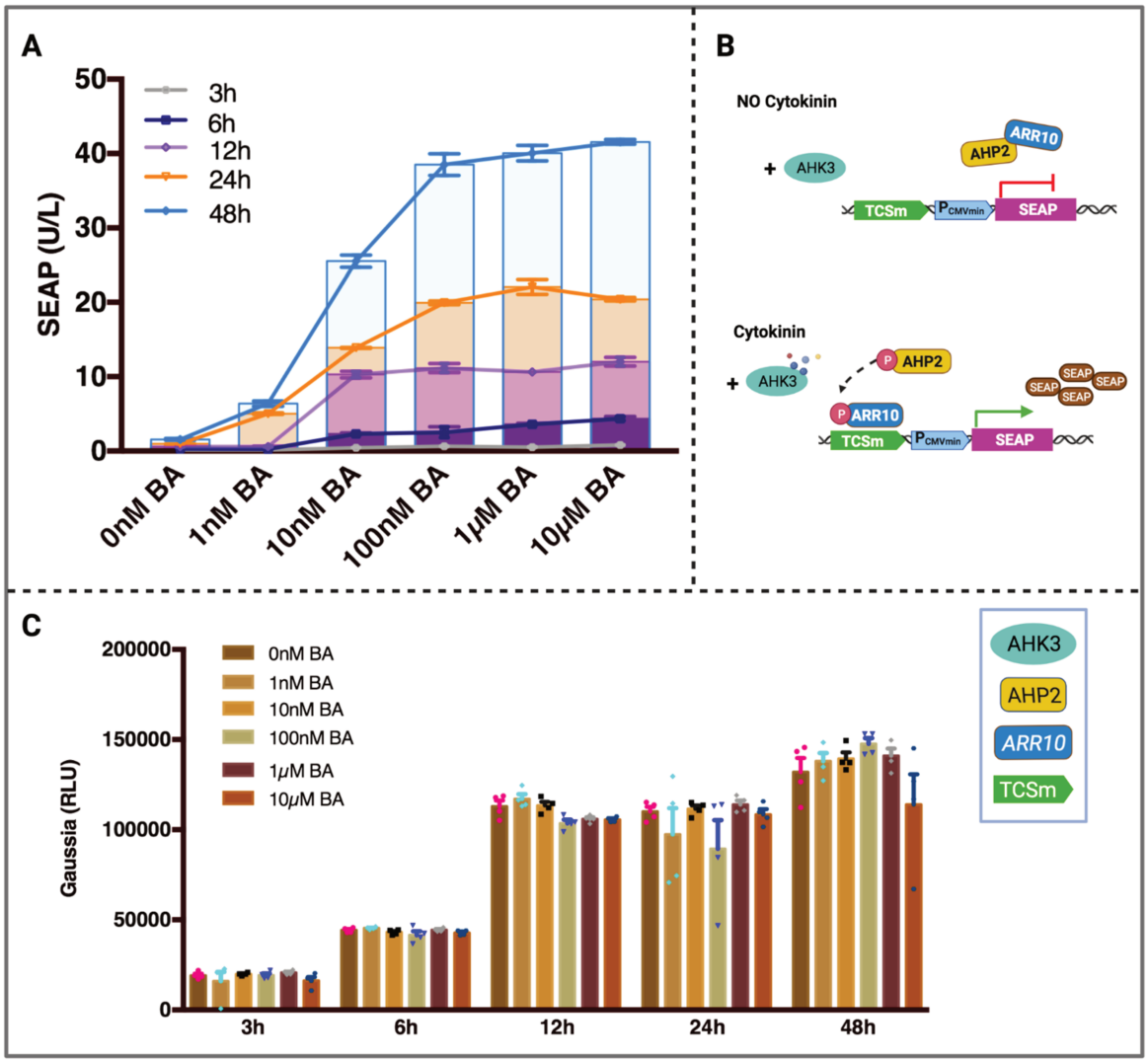

Figure 12. Optimization of the experimental set-up. A. Cells co-expressing AHK3, AHP2, and ARR10 were induced 24 h post-transfection with the indicated BA concentration during 3-, 6-, 12-, 24- or 48-additional h. SEAP expression is expressed in units per litre (U/L). **B.** Schematic representation of the expected behavior of the CK-responsive module used in this work. It is expected that after hormone perception ARR10 will bind the TCSm promotor and activate the reporter (SEAP) expression, in a hormone-dependent fashion. **C.** Gluc activity was quantified in cells expressing AHK3, AHP2, ARR10 and the TCSm, 3-, 6-, 12-, 24-, or 48 h after induction with BA in the indicated concentrations. No significant differences were observed in the survival of cells expose to CK treatment in comparison with the mock, at any time point. Gluc expression is represented in relative luminescence units (RLU). Data are representative of three independent experiments. Mean and S.E.M. are plotted for n= 4 mammalian samples. The statistical significance was determined using a two-way ANOVA analysis (P value < 0.001) and is indicated with bold letters. AHK3, Arabidopsis histidine kinase 3; ARR10, Arabidopsis response regulator 10; AHP2, Arabidopsis histidine-containing phosphotransferase 2; BA, 6-bencilaminopurine; PCMVmin, minimal cytomegalovirus promotor; SEAP, Secreted embryonic alkaline phosphatase; TCSm, CK-responsive synthetic promoter designed for this work. This figure and the figure legend are adapted from the manuscript in preparation of Pavesi et al., Appendix 7.1.

When deciding between a 24 h or a 48 h treatment we considered the dynamic range and the effect of the total length of each experimental set-up on the cells' survival. Comparing these two conditions, the systems showed a 14- and 16-fold increase after treatment with 10 nM of BA, and 21-, and 25-fold for a 100 nM concentration, after 24 h and 48 h treatment, respectively. In addition, both treatments showed a similar GLuc expression level (**Fig. 12C**). These results evidence that both treatments were equally innocuous for the cells. The diminution of the growth rate of cultured mammalian cells after 48 h treatment is normally an effect of the limiting space in the plates, and the nutrient depletion of the medium. Lastly, as extending the exposure time over 24 h presented no quantitative advantage (no increased dynamic range), we selected a 24 h treatment with BA for the following experiments.

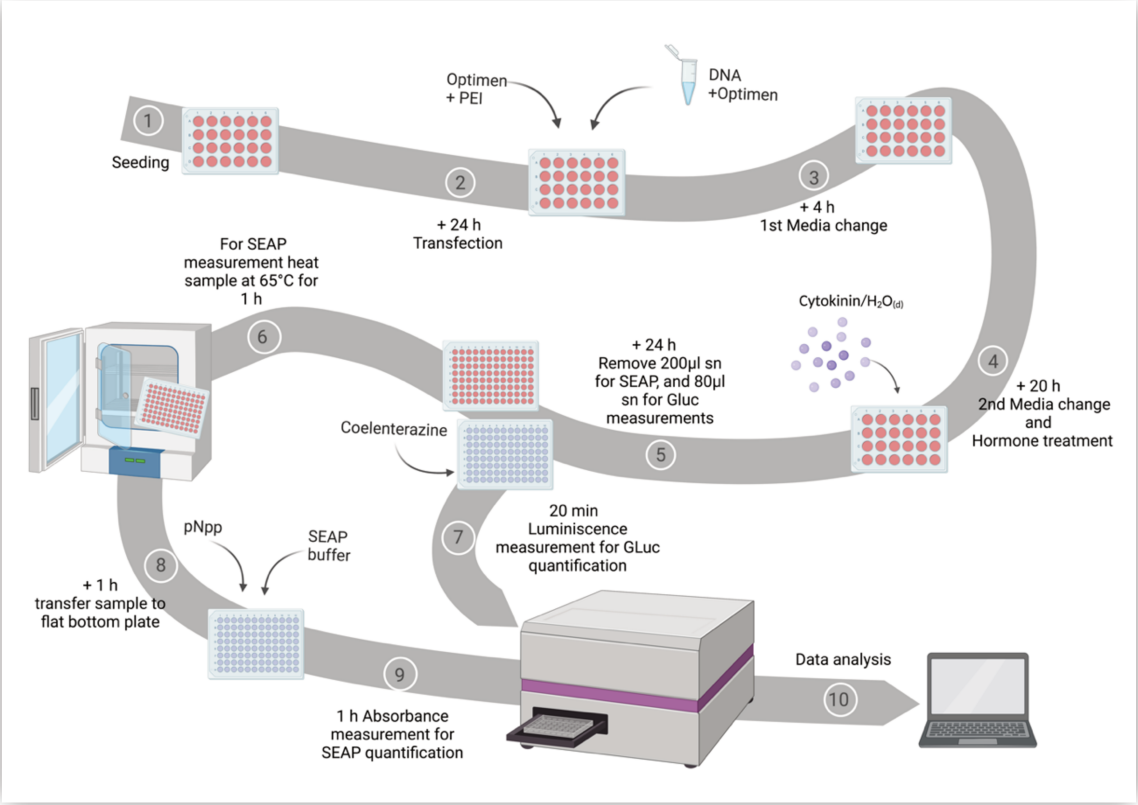

Figure 13. Schematic representation of the workflow for the analysis of CK responses in mammalian cells. 50,000 CHO cells were seeding in 24-well plates with cutltured medium and incubated for 24 h (1). The next day cells were transfected using PEI-method (2). Four h later the transfection was disrupted by changing the medium (3), and cells were incubated for another 20 h. The next day, the cells were treated with CK directl applied into the fresh medium (4). 24 h after induction 200µl of the supernatant was transferred to round-bottom plates (5) and heated at 65°C for 1 h (6), before SEAP measurement (8-9). Simultaneusly, 80µl of the supernatant were transferred to flat-bottom plates and used to measure luminiscence of GLuc (5 and 7). The data was later analysed to obtain either the activity of SEAP(U/L), or the relative luminiscence units (RLU) for GLuc. CHO, Chinese hamster ovary; GLuc, Gaussia luciferase; PEI, polyethyleneimine; pNpp, Nitrophenylphosphate; SEAP, Secreted embryonic alkaline phosphatase.

When comparing the results in **Fig. 11** where the system was induced for 24 h, with the same period of treatment as **Fig. 12**, we observed a 5- and 3-fold increase in the response in samples treated with 100 nM and 1 µM BA. These results showed the importance of permitting the system to accumulate the transiently expressed proteins before hormone induction.
Altogether, the selection of our experimental set-up considered the health of the cells and practical aspects such as days of work invested for each assay, while it searches for the best dynamic range possible. A detailed representation of the workflow can be observed in **Fig. 13**.

3.1.1.2 Analysis of the influence of the mammalian environment on the TCSm activation.

The main constraint that could impede the correct performance of the heterologous expressed pathway is the false activation (or "leakiness") of the reporter system. In the previous section, we observed no activation of the TCSm in the absence of the hormone. Moreover, there are no identified TCS in mammalian cells. However, we needed to ensure that no endogenous proteins were obscuring our observations. For this purpose, we next co-transfected either the TCSm alone or in every possible combination with the CK signalling components. Our results showed TCSm activation only when the full pathway has been reconstructed in a CK-dependent fashion (**Fig. 14A**). This evidenced orthogonality strongly suggested the suitability of our platform for assessing the CK TCS.
Next, we performed a similar assay now for AHK4-mediated responses. Whereas we didn't expect this will affect the system leakiness, we needed to assay this important CK receptor sensitivity and activation to be used in future analysis. Our results showed that the AHK4-mediated response required a concentration of 20 nM BA for the activation of the TCSm (**Fig. 14C**). In addition, AHK4 activation of the TCSm was stronger in comparison with AHK3-mediated responses.

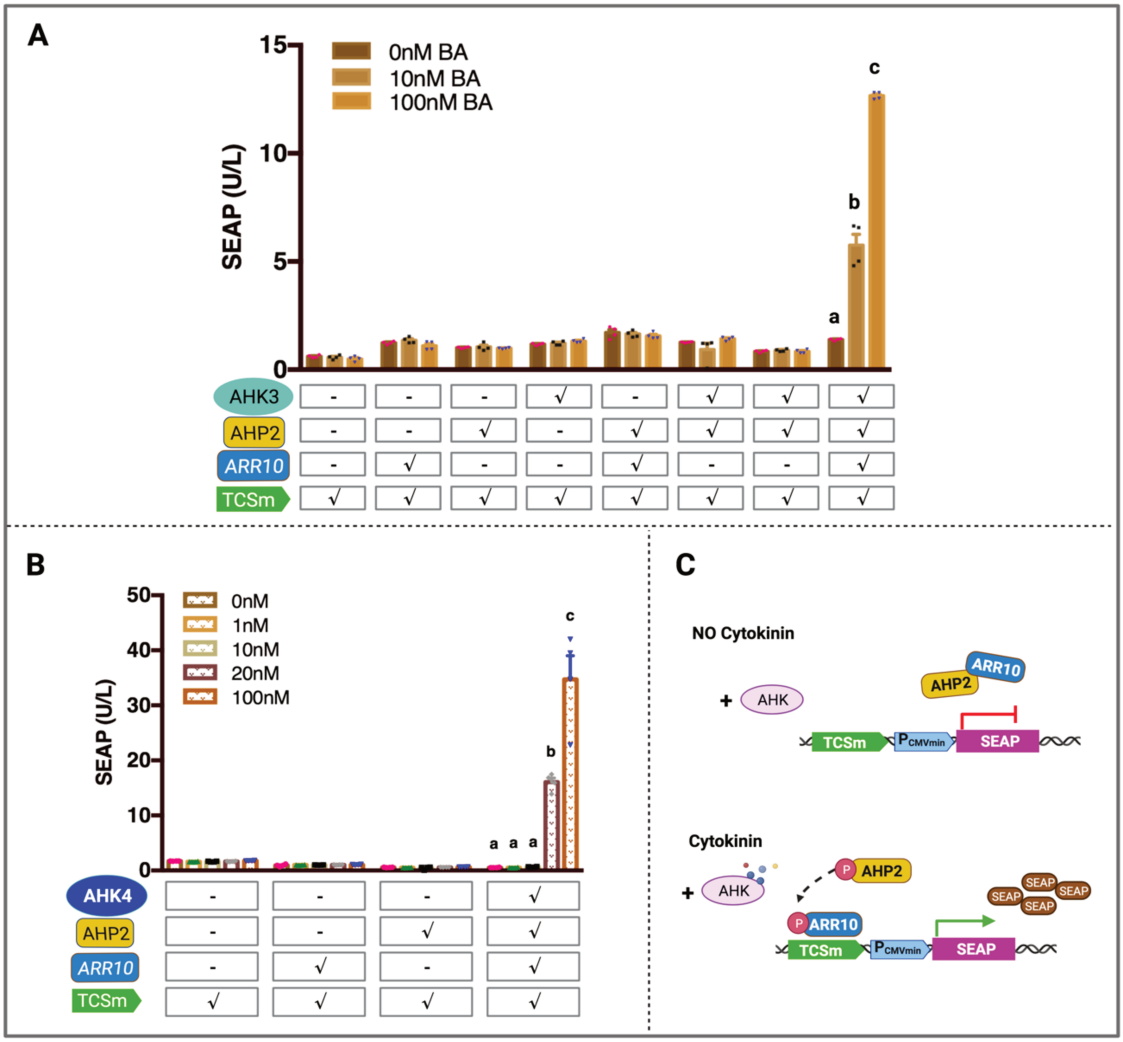

Figure 14. Analysis of the influence of endogenous mammalian proteins in the TCSm response.

A. Cells expressing TCSm either alone or with AHK3, AHP2, and ARR10; in every possible combination were induced 24 h post-transfection with the indicated BA concentration for 24 additional hours before SEAP measurement. **B.** Cells expressing TCSm either alone or with AHP2, ARR10, or both together with the AHK4 receptor were treated as described in panel A. In A and B, SEAP activity is expressed in units per litre (U/L). Data are representative of three independent experiments. Mean and S.E.M. are plotted for n= 4 mammalian samples. The statistical significance was determined using a two-way ANOVA analysis (P value < 0.0001) and is indicated with bold letters. **C.** Schematic representation of the expected behavior of the CK-responsive module used in this work. It is expected that after hormone perception ARR10 will bind the TCSm promotor and activate the TCSm, in a hormone-dependent fashion. AHK3-4, Arabidopsis histidine kinase 3 or 4; ARR10, Arabidopsis response regulator 10; AHP2, Arabidopsis histidine-containing phosphotransferase 2; BA, 6-bencilaminopurine; PCMVmin, minimal cytomegalovirus promotor; SEAP, Secreted embryonic alkaline phosphatase; TCSm, CK-responsive synthetic promoter designed for this work. This figure and the figure legend are adapted from the manuscript in preparation of Pavesi et al., Appendix 7.1.

Transient or stable gene expression in protoplasts is the most popular assays for high-throughput analysis of gene expression, protein localization and interactions [243]. These systems retain the cell identity and differentiated state of the tissue from which they are isolated and can be transformed with high efficiency.

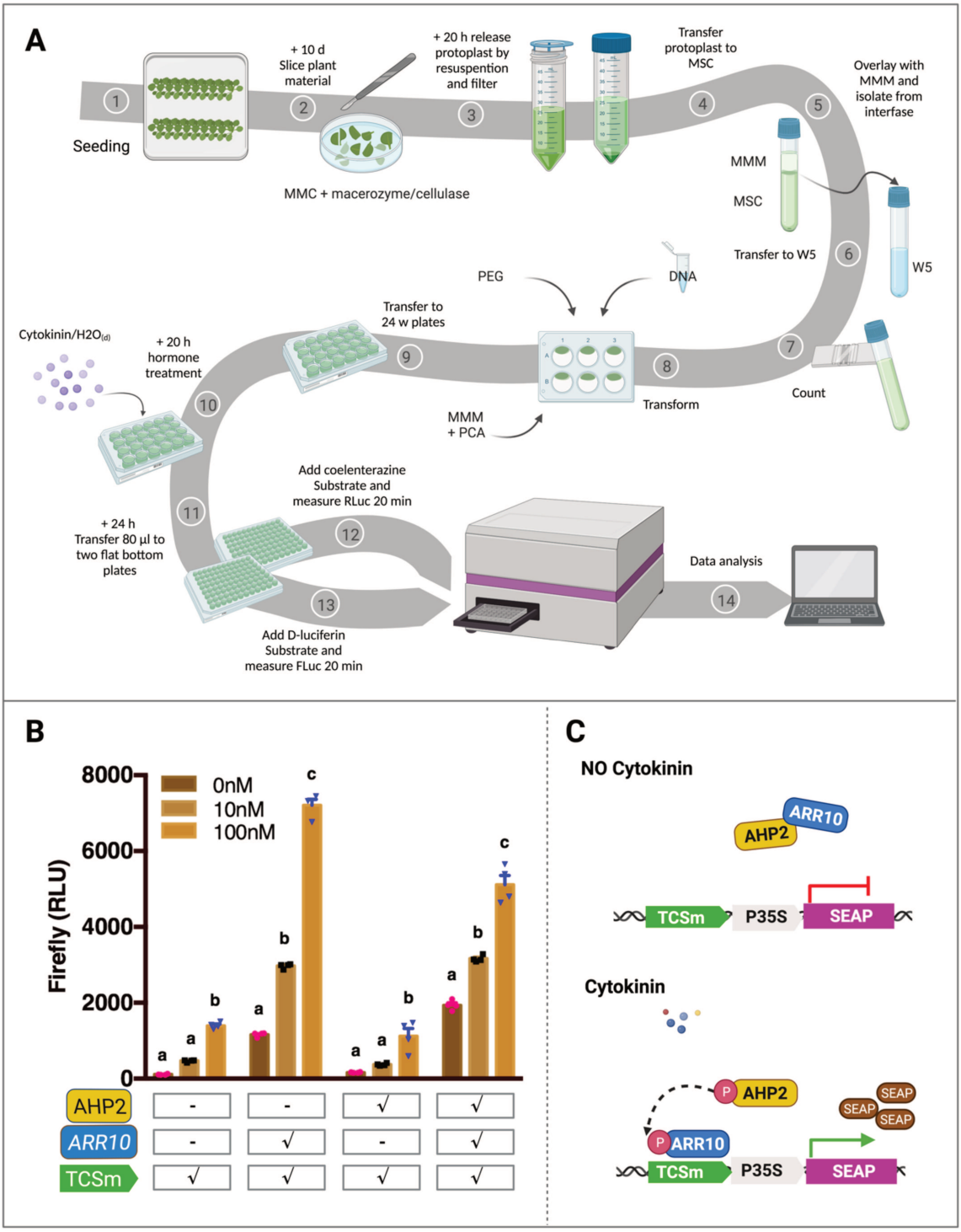

Figure 15. TCSm activation profile in *Arabidopsis* protoplasts and schematic representation of the workflow. **A**. Representation of the isolation and transformation protocol use for protoplasts experiments. Plants were grown in square SCA agar plates for 10 d (1), and later sliced in MMC buffer (2). The plant material were then digested with macerocyme for 16 h (2) before releasing the protoplasts by resuspension followed by filtration (3) into MSC buffer (4). Addition of MMM formed an interfase (5) from where the protoplasts were collected before transfer to W5 buffer (7). After counting in Rosental chamber, 500,000 were transferred into 6-well plates for PEG-transformation (8). After transfer to 24-w plates (9) the protoplasts were kept in darkness until the end of the experiment. 20 h post-transformation the system was induced by additing CK into the protoplasts suspencion (10). The following day, two flat-bottom plates with 80µl of each sample was prepare and used to measure, separately, RLuc or FLuc luminiscence. Data was analysed and the luciferases activity was expressed in relative luminiscence units (RLU). **B.** TCSm activation in protoplasts either alone, or after co-esxpression with AHP2, ARR10, or both, after addition of the indicated BA concentrations. Data are representative of three independent experiments. Mean and S.E.M. are plotted for n= 4 protoplasts samples. The statistical significance was determined using a two-way ANOVA analysis (P value < 0.0001) and is indicated with bold letters. **C.** Schematic representation of the expected behavior of the CK-responsive module used in protoplasts. It is expected that after hormone perception ARR10 will bind the TCSm promotor and activate the TCSm, in a hormone-dependent fashion. AHK, Arabidopsis histidine kinase; ARR10, Arabidopsis response regulator 10; AHP2, Arabidopsis histidine-containing phosphotransferase 2; BA, 6-bencilaminopurine; FLuc, Firefly luciferase; MMM, MMC, MSC, PCA, and W5, buffers used for protoplasts isolation described in Methods; PEG, polyethylene glycol; P35S, 35S minimal promotor; RLuc, Renilla luciferase; SEAP, Secreted embryonic alkaline phosphatase; TCSm, CK-responsive synthetic promoter designed for this work. This figure and the figure legend are adapted from the manuscript in preparation of Pavesi et al., Appendix 7.1.

Protoplasts transformation has been extensively used for the study of phytohormone pathways (auxin [244,245], GA [246], ABA [247,248], and CK [12,61,64,85,136]). Pertinently, studies have shown that a conserved two-component CK signalling pathway established in mesophyll protoplasts is also active in the root and shoot meristematic cells, the statement that could allow us to further generalize the results obtained in protoplasts to be occurring in higher plant structures [61,62]. Therefore, validation of our observations in the mammalian cells will be performed in this plant homologous system throughout this work. Therefore, next, we interrogated the performance of a TCSm system adapted for protoplast expression in *A. thaliana* leaf mesophyll protoplasts. For this, we engineered constructs for protoplast expression harbouring the full-length cDNA sequence of ARR10 and AHP2, cloned downstream of the 35S promoter (P_{35S}). As reporter, we used a previously designed plasmid containing repetitions of the B-ARRs binding site from the ARR6 promoter, followed by a P_{35Smin} and the firefly luciferase (FLuc) gene, as the reporter gene. After transformation of the promotor-reporter system alone or in very possible combination with ARR10 and/or AHP2, we quantified FLuc expression. A schematic representation of the isolation and transformation protocol in **Fig. 15A**.

This plant-based system required a concentration of 10 nM BA for its activation. Remarkably, this is the same hormone concentration needed for mammalian TCSm activation. In

comparison to the assay in the orthogonal platform, in protoplast, a higher basal level of activation of the reporter was observed at every hormone concentration. This suggests an activation of the TCSm by the TCS components present in the protoplasts` system (**Fig. 15B**). Our results also showed a 2-, 3- and 4-fold increase after treatment with concentrations of 10 nM, 100 nM, and 1 μM BA, respectively. In comparison, the dynamic range between the different measurements was significantly higher in the mammalian system. The importance of a wide dynamic range is the possibility to observe subtle changes in (for this case) CK responses. Therefore, when studying the activation of responsive promotors for less characterized B-ARRs, or the CRFs whose ability to activate CK responses is unknown, for example, a preliminary assay in the orthogonal platform could be beneficial.

3.1.2 Analysis of the subcellular localization of the CK signalling elements in CHO cells.

Once optimized the experimental set-up, and before continuing with the proof-of-principle applications of our system we thought it relevant to investigate each signalling component subcellular location in the mammalian platform. Deliberately, as showed in **Fig. 11C**, the vectors used in the previous section included a C-terminal fusion of each element to a different F: AHKs-mCherry, AHPs-mVenus, and ARRs-Cerulean. After transfection, the cells were prepared for confocal microscopy imaging. To test the effect of CK in the subcellular location of AHP2, ARR1 and ARR10, all samples were co-transfected with AHK3 (**Fig. 16**). Nevertheless, the same proteins co-transfected alone, with no other TCS components showed the same distribution as the displayed in the left panel. Our results showed both AHK receptors localized, predominantly, in the reticulum endoplasmic- but also the plasma membranes. This subcellular distribution corresponds with their location (and function) in plants[102,103,105]. However, AHK3 also showed strong accumulation in the nucleus. From the tested B-ARRs, only ARR1 was visualized in the nucleus of mammalian cells expected from the literature[149]. This RR displayed a uniform distribution yet it was also found in speckles. The latter structure was favoured when co-transfected with AHP2. Contrary, ARR10 was distributed all over the cell and unaffected by AHP2 presence. Whereas AHK3 accumulation in the nucleus or ARR10 ubiquitous distribution is an effect of the terminal fusion to the FP will be assessed in the future.

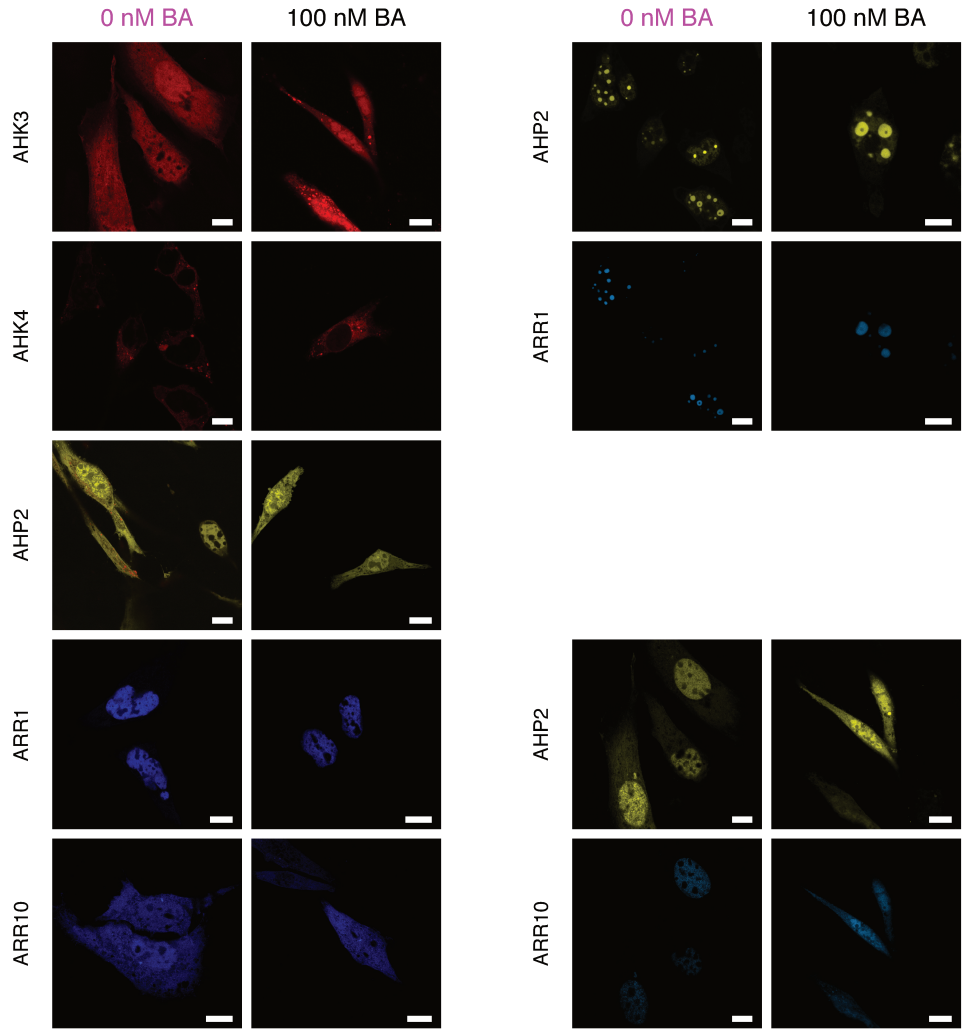

Figure 16. Confocal fluorescence imaging of subcellular location of the CK signalling elements in CHO cells. After transfection, cells were treated with either a concentration of 100 nM BA or H_2O(d) as indicated in the column title. 24 h later, samples were prepared for confocal fluorescent microscopy by fixation. Imagining was performed using 60x oil objective. mCherry, mVenus and Cerulean were visualized using excitation lasers of 561 nm, 470 nm and 405 nm respectively. Each row title indicates the protein under analysis. Images indicating AHP2, ARR1 and ARR10 also included AHK, for the analysis of the effect of CK in their subcellular location. The right upper panel shows the location of the indicated protein after ARR1 and AHP2 co-transfection. The lower right panel display the subcellular location of AHP2 or ARR10, after co-transfection. Scale bar, 10 μm. AHK, Arabidopsis histidine kinase; ARR, Arabidopsis response regulator; AHP, Arabidopsis histidine-containing phosphotransferase; BA, 6-bencilaminopurine.

AHP2 alone localized in the nucleus and the cytoplasm as previously evidenced for AHP1, 2 and 5 in protoplasts[117]. However, notably, its subcellular distribution was affected by the presence of ARR1. In these cells (upper right panel) AHP2 was found in the cell nucleus in the same location as ARR1. Altogether, as the AHPs relocate between the nucleus and the

cytoplasm, their distribution in the same compartments as the B-ARRs may be a reflection of their function. The biological significance of this observation should, however, needs to be further studied. Further, no co-transfected combination showed a hormone dependent distribution of any of the signalling elements, as previously observed for the AHPs in protoplasts and *in planta*[117].

3.1.3 Chapter discussion

To summarize, a new experimental tool for the quantitative study of CK perception and signalling by full reconstruction of the *Arabidopsis* thaliana TCS in mammalian cells has been developed. The new synthetic circuit is highly selective for the CK and responds to the physiological concentration of the hormone in plants[52] downstream the AHK3 (10 nM) and the AHK4 (20 nM) receptors. Through the optimization of the experimental setup, we have increased the TCSm response and the dynamic range. Notably, the system response is robust and showed a high signal-to-noise ratio. The lack of activation of the TCSm in the absence of any pathway component reflected the new tool orthogonality, while a similar study in *Arabidopsis* protoplasts evidenced the influence of the endogenous TCS components remarking the advantages of including orthogonal systems in the analysis of plant signalling networks. We have observed a change in AHP2 subcellular location when co-transfected with ARR1 leaving an open question of this event functionality in plants. The distinctive response and sensitivity observed for AHK4 and AHK3 propose that this new synthetic approach can be implemented for exploring the contribution of single TCS components to the pathway. Next, we will continue to explore its predictive power.

3.2 Chapter 2. Exploring the predictive power of the new synthetic mammalian platform

Studying plant signalling pathways *in planta* or homologous systems can be challenging. The functional redundancy of the signalling elements, their interconnection with components of other pathways, and multiple negative feedback loops are major limitations of these systems. In such a complex environment the contribution of single elements to the pathway is difficult (if not impossible) to interrogate. Up-to-date, to overcome these limitations partial reconstruction of plant signalling pathways in mammalian cells has been fundamental. This orthogonal platform permitted the exploration of the molecular mechanism behind the signal transduction of main phytohormones while facilitating the design of new experimental tools as biosensors. Examples are the study of the formation of a ternary complex within COP1, SPA1, and DELLA proteins driving gibberellins perception[215,216], and the characterization of a ratiometric biosensor for the analysis of auxins network[213], both performed in HEK cells.
This chapter is based on the manuscript in preparation "Full reconstruction of *Arabidopsis* CK signalling in mammalian cells reveals new regulatory mechanisms" (Pavesi et al., in preparation 2022; Appendix 7.1) and contains selected results thereof. In this section, we will investigate the predictive power of a new synthetic platform by tackling different queries so far impossible to answer in plants as well as exploring previous hypotheses. We will perform a quantitative screening of the selectivity and sensitivity of the AHK receptors for different adenine derivates. Further, through the analysis of the activation of the TCSm reporter, we will explore the contribution to CK responses of specific TCS components belonging to the same multigene families. Finally, a combined analysis of the TCSm activation and quantitative studies of PPI will facilitate the exploration of the mode of action of three negative regulators of CK network; as well as the role of the conserved aspartate of the B-ARRs in their CK responses.

3.2.1 Analysis of the sensitivity and selectivity of AHK3 and AHK4 for different CK derivates

Investigating the sensitivity of the AHK receptors for CK can help us better understand these hormones signalling while providing a new base for the manipulation of CK responses in

plants. Previous studies have approached the investigation of the sensitivity and selectivity of the AHK for different adenine derivates by studying the binding of these receptors to the hormone in isolated systems. The major impediment of studies in bacteria-based systems[43,46,99,106,92] is the inconvenience of expressing a membrane receptor in an evolutionarily distant organism with a different architecture of the membrane[104,105]. This altered environment may interfere with the receptor function, as a conformational change can disrupt its binding pocket for the hormone. On the other hand, assays performed *in vivo* in plants[42,53,107,108] need to consider the influence of endogenous TCS components that may hinder the real activation of CK response for a particular derivate, and the hormone metabolism.

The mammalian platform instead provides an orthogonal "free of complexity" environment with no TCS or other interactions, and no CK metabolism documented. While it mimics the *in planta* conditions for their conserved transport/secretion systems and membrane architecture. Moreover, we have previously shown that the TCSm activation responds to the physiological concentration of CK found in plants[52]. Therefore, to further interrogate the sensitivity and selectivity of AHK3 and AHK4 to different CK forms we co-transfected CHO cells with either AHK3 or AHK4, together with ARR10, and AHP2, and the TCSm. 24 h after hormone treatment we quantified the SEAP expression.

The adenine derivates selected for this study were representative of the most abundant and widely studied forms in plants, the isoprenoid derivates iP, the cZ, tZ, DHZ. As well as the tZR, and the nucleotide trans-Zeatin riboside-5′-monophosphate sodium salt (tZRMP), to interrogate if they play a role as genuine CK. The 2-Methylthio-N^6-isopentenyladenine (2MeSiP) has been gaining more interest for its ubiquitous presence not only in plants but other kindgdoms[249]. KIN and BA as representative of the aromatic forms of CK, and the synthetic diphenylurea Tidiazuron (TDZ)[72]. As the samples only differ in the expressed AHK, we interpreted the requirement of a lower hormone concentration for the TCSm activation, as a higher sensitivity of the receptor for the CK form. Later, the quantified SEAP expression will give us information regarding the differential activation of CK responses attributed to specific AHK-CK combinations.

Our results showed that lower concentrations of most CK forms were necessary for the AHK3-mediated activation of the TCSm, in comparison with AHK4 (**Fig. 17B-E**). This higher sensitivity of the AHK3 promotor was previously evidenced in our work for BA.

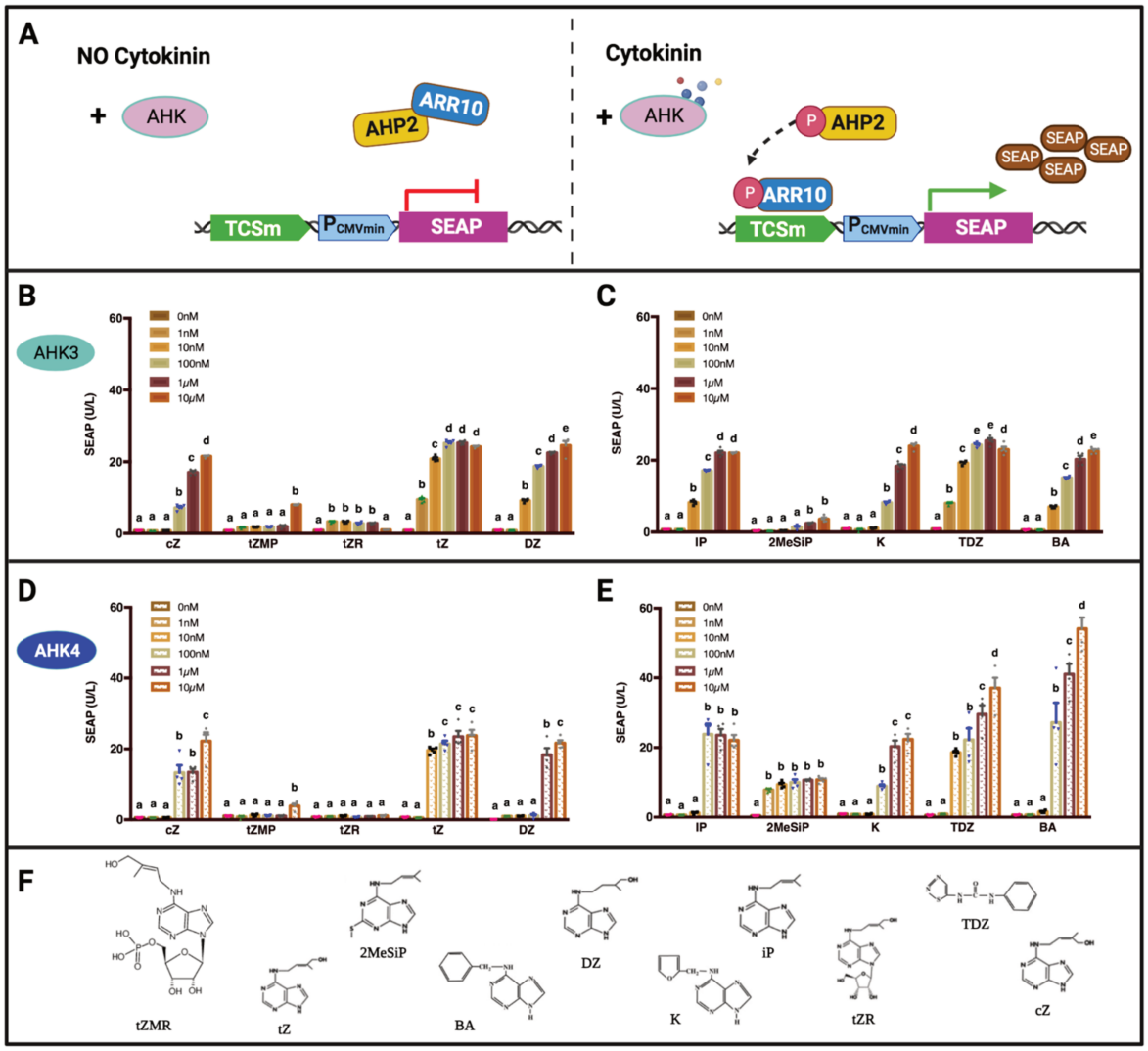

Figure 17. AHKs sensitivity and selectivity for different adenine derivates, and their downstream activation. **A.** Schematic representation of CK-responsive promotor-reporter assay used in figures B-E. It is expected that after hormone perception the B-ARRs will bind the TCSm promotor and activate the reporter, SEAP, expression. **B-C.** AHK3-mediated activation of the TCSm promotor in response to the indicated adenine derivates at different hormones concentration. **D-E.** AHK4-mediated activation of the TCSm promotor in response to the indicated adenine derivates at different hormones concentration. **F.** Representation of the chemical structure of the different CK forms use in this study. In B-E SEAP expression of samples treated with the indicated concentration of each hormone is expressed in units per litre. Data are representative of three independent experiments. Mean and S.E.M. are plotted for n= 4 mammalian samples. The statistical significance was determined using a two-way ANOVA analysis (P value < 0.001) and is indicated with bold letters. Filled bars represent AHK3-mediated responses and pattern bars AHK4-mediated responses. AHK, Arabidopsis histidine kinase; ARR, Arabidopsis response regulator; AHP, Arabidopsis histidine-containing phosphotransferase; BA, 6-bencilaminopurine; cZ, cis-Zeatin; DHZ, Dihydrozeatin; iP, isopentiladenine; K, Kinetin; PCMVmin, minimal cytomegalovirus promotor; SEAP, Secreted embryonic alkaline phosphatase; TCSm, CK-responsive synthetic promoter designed for this work; TDZ, Tidiazuron; tZ, trans-Zeatin; tZR, trans-Zeatin riboside; tZRMP, trans-Zeatin riboside-5´-monophosphate sodium salt; 2MeSiP, 2-Methylthio-N6-isopentenyladenine. This figure and the figure legend are adapted from the manuscript in preparation of Pavesi et al., Appendix 7.1.

The AHKs selectivity and sensitivity for the 10 derivates can be summarized as follows, from higher to lower sensitivity (thus, 1nM>10nM>100nM>1μM>10μM):

1. AHK3: tZR = tZ = TDZ > DZ = iP = BA > cZ = KIN > 2MeSiP > tZMP; and
2. AHK4: 2MeSiP > tZ = TDZ > cZ = iP = K = BA > DZ > tZMP.

Interestingly, cZ and KIN were perceived at 100 nM by both receptors, showing as well a similar activation of the TCSm. The nucleotide form tZMP, as well perceived by both receptors with an equal sensitivity (10 μM concentration) showed instead stronger TCSm activation downstream AHK3 (**Fig. 17B and D**). On the other hand, the riboside tZR only activated AHK3-mediated responses in a 1 nM, 10 nM, 100 nM and 1 μM concentration (**Fig. 17B**). For this derivate, an increase in the concentration did not affect the mediated TCSm activation. As the tZR is the main CK form transported into the shoot[41] where AHK3 is predominantly expressed this interaction may likely have a function in plants[62,93].

A notable exception to AHK3 higher sensitivity was with 2MeSiP. This derivate was perceived at a 1 μM concentration by AHK3, while the sensitivity for AHK4 was as low as 1nM (**Fig. 17C and E**). Moreover, posterior AHK4-mediated activation was significantly higher and was unmodified by subsequent 2MeSiP addition. Lastly, AHK4-mediated activation of the TCSm after treatment with TDZ and BA resulted in the strongest responses observed for either HK or all CK forms (**Fig. 17C and E**). Moreover, for both derivates, the reporter signal steadily increased with higher hormone concentrations, not reaching saturation in the tested conditions.

3.2.2 Study of the individual contribution of specific TCS components to CK responses

Deciphering the role of single TCS components can provide new insight into how plants modulate specific CK outputs in particular moments, in specific cells. In the previous section, we evidenced the suitability of this platform to distinguish between responses mediated by different CK forms and two AHK receptors. Because of the modularity of our system, we can reconstruct the full CK network "à la carte" by the combination of specific TCS components. This unique advantage permits (for the first time) to interrogate of single members of each multigene family involved in CK signal transduction. In chapter 1 we mentioned that the selection of ARR10 for this study was based on the evidence of is the activation of CK responses in cold stress downstream AHK3 and AHP2[150]. ARR1 together with ARR10 and ARR12 are considered main regulators of CK response in plants[65,147,148,250,251]. Therefore, there

is a broad body of literature about its biological function. Moreover, together with ARR2, ARR1 has been long studied in overexpression assays[137,139,141,242]. These previous works laid the foundations for the proposal of the activation of the B-ARRs after phosphorylation in their REC domain (as will be discussed further below). Therefore, we considered it pertinent to include ARR1 in our analysis to contrast the activation of responsive genes of these relevant B-ARRs. Exploring the differential activation of each component of the TCS is possible thanks to the quantitative nature of the synthetic approach used in this study.

Therefore, to further investigate the contribution of specific members of the B-ARR and AHP families, we generated additional constructs for mammalian expression harbouring the full-length cDNA sequence of AHP1, AHP3 to 6, and ARR1. Later, we transfected CHO cells with different customized combinations of these TCS elements together with the TCSm and measured SEAP expression 24 h after BA treatment.

The activation of the TCSm by AHP1 to 6 can be summarized from higher to lower TCSm activation as follows (**Fig. 18B-C**):

1. downstream AHK3: AHP1~AHP2>AHP3>AHP4, and
2. downstream AHK4: AHP1~AHP2>AHP3>AHP4>AHP5

From all functional AHPs, only AHP5 failed in activating CK responses in cells expressing AHK3. On the other hand, AHP4 displayed a weak activation of the TCS, independently of which receptor mediates the response. These results are in agreement with previous observations of AHP4-mediated responses *in planta*[122,126], reflecting our platform predictive power. Further, our results showed no TCSm activation in cells co-transfected with AHP6. Considering the canonical phospho-relay driving CK signal, this result was expected as this pseudo-HP lacks the phosphorytable H residue.

When analysing the B-ARRs, we observed a stronger activation of the TCSm by ARR1, in comparison with ARR10 (**Fig. 18D-E**). Due to the increased signal level of the untreated (mock) cells in ARR1, however, the dynamic range of the measurement within different BA concentrations was similar for both B-ARRs, suggesting alike CK responses. Nevertheless, a different interpretation of the activation of these B-ARRs arises when analysing the results of their co-transfection in cells expressing AHK4 (**Fig. 18E**). In comparison with samples containing only one of the RRs, at 100 nM concentrations of BA the ARR1 + ARR10 samples displayed a higher TCSm activation.

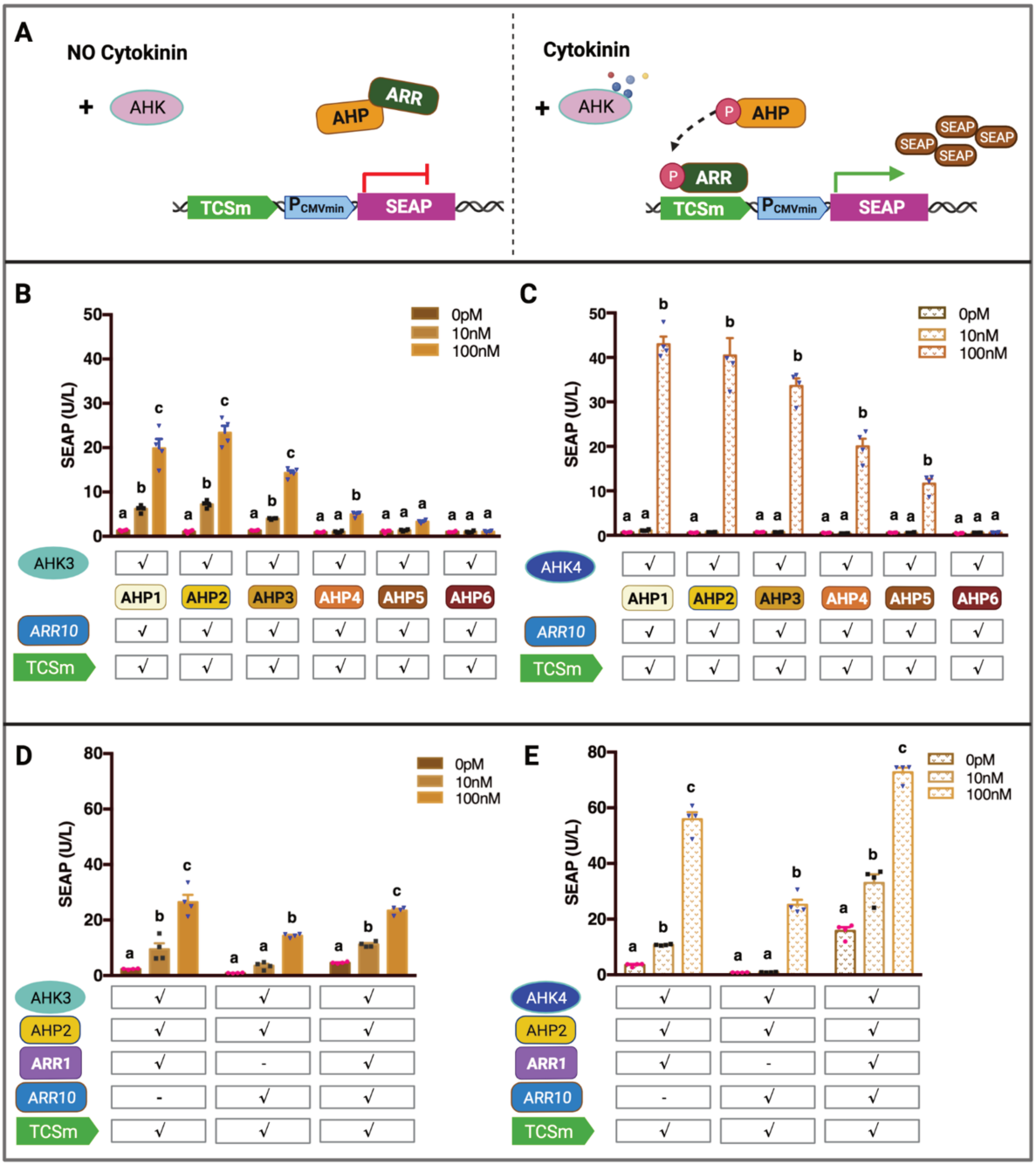

Figure 18. Contribution of specific signalling elements to CK response. **A.** Schematic representation of CK-responsive promotor-reporter assay used in figures B-E. It is expected that after hormone perception the B-ARRs will bind the TCSm promotor and activate the reporter, SEAP, expression. **B-C**. AHP1 to 6 mediated activation of the TCSm promotor. **D-E**. ARR1-, and ARR10-mediated activation of the TCSm promotor. In B-E SEAP expression of samples treated with the indicated BA concentrations is expressed in units per litre. Data are representative of three independent experiments. Mean and S.E.M. are plotted for n= 4 mammalian samples. The statistical significance was determined using a two-way ANOVA analysis (P value < 0.001) and is indicated with bold letters. Filled bars represent AHK3-mediated responses and pattern bars. P value AHK, Arabidopsis histidine kinase; ARR, Arabidopsis response regulator; AHP, Arabidopsis histidine-containing phosphotransferase; BA, 6-bencilaminopurine; PCMVmin, minimal cytomegalovirus promotor; SEAP, Secreted embryonic alkaline phosphatase; TCSm, CK-responsive synthetic promoter designed for this work. This figure and the figure legend adapted from the manuscript in preparation of Pavesi et al., Appendix 7.1

This increased TCSm level seems to be the addition of ARR1 and ARR10 individual responses. However, the significant increase of the signal both in mock cells and after the addition of 10 nM BA rather proposes a constitutive activation of the TCSm.

Lastly, while ARR10 showed the same sensitivity of response downstream AHK3, and AHK4, ARR1 activated responses at lower BA concentrations in AHK4 expressing cells. This proposes that not only the final TCSm activation but also the general sensitivity of the system depends on the receptor-CK Kd and the composition of the downstream signalling network.

3.2.3 Analysis of the mode of action of three known negative regulators of CK signal

So far in this work, we have focused the analysis on how plants can positively regulate CK signal transduction as a combinatorial effect of the different TCS components in the sample and the presence of particular CK forms (and concentrations). However, in plants, the modulation of CK responses requires both the activation and turn-off of the signal. To explore the molecular mechanism underlining the downregulation of the CK network, we co-transfected CHO cells with AHK3, AHP2 and both B-ARRs, in addition to one of the negative RRs of the pathway: ARR7 or ARR22, or with the pseudo-HP, AHP6. The results exposed below are the sum of the quantitative analyses of the TCSm activation, and PPIs performed using quantitative MxH approaches.

Comparing the effect of the addition of each RR in the TCSm activation, our results suggest that only ARR22 can block CK signalling independently of the B-ARR present (**Fig. 19C**). Similar results were previously obtained after overexpression ARR22 in *Arabidopsis* protoplasts[161,162], and from studies *in planta*[67]. These previous findings reinforce our observations, once more, supporting our experimental platform performance. Next, taking advantage of the quantitative MxH approach we tested the effect of ARR22 on the B-ARR-AHP2 interactions. While the ARR22-AHP2 interaction was formerly reported using Y2H[66], it was not detected here (**Fig. 19D**). As it has been proposed that ARR22 functions as a phospho-histidine phosphatase[67,160,161], an action that may not demand a strong PPI, we hypothesize that the transient nature of the ARR22-AHP2 interaction does not permit the

reassembly of the slip TF in mammalian cells. However, as the Y2H approach has a high rate of false positive[204] we could also suggest that the interaction may not have place.

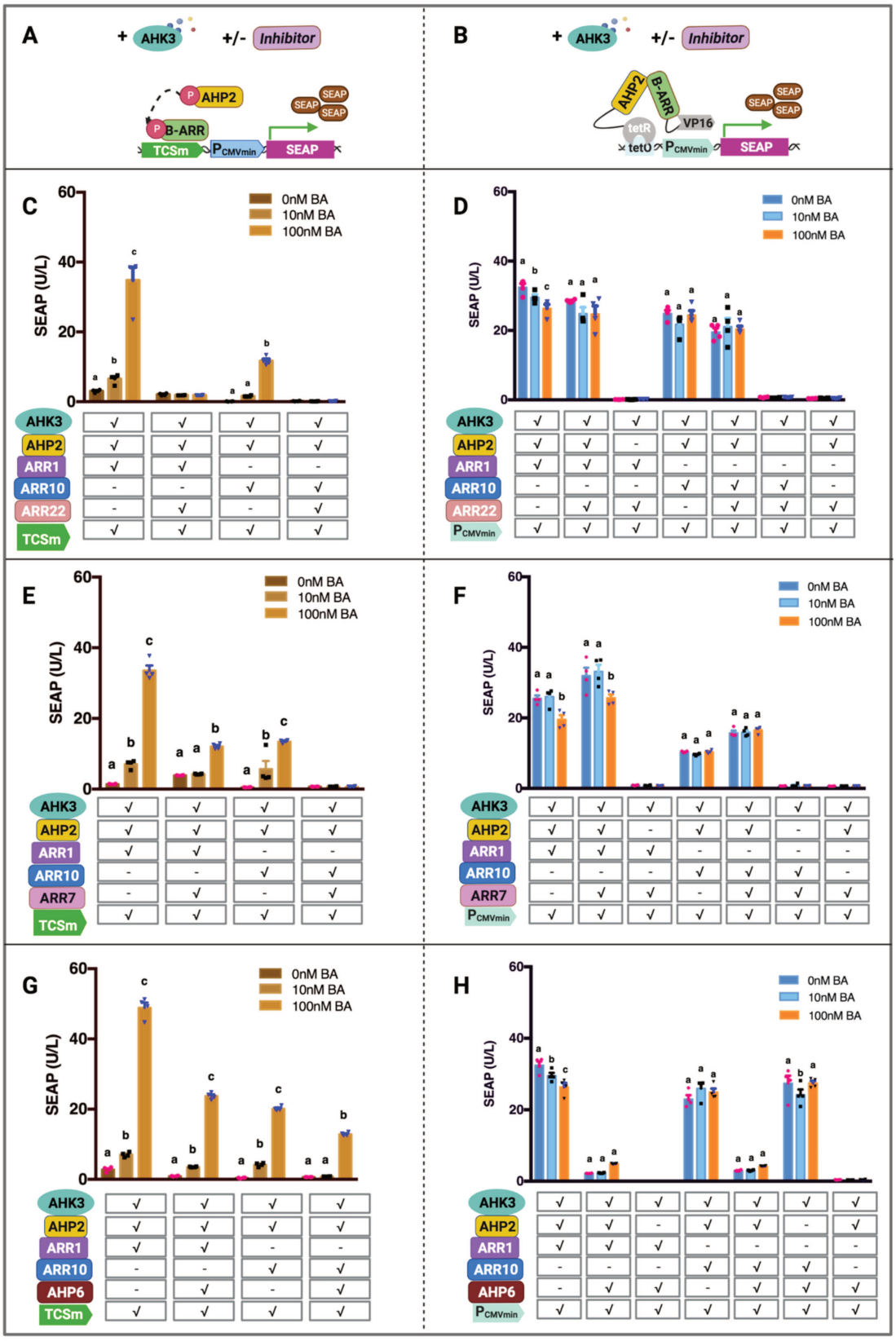

Figure 19. Analysis of the mode of action of the negative RR: ARR7, ARR22 and AHP6.

A. Schematic representation of the CK-responsive promotor-reporter assay used in figures C, E and G. It is expected that after hormone perception the B-ARRs will bind the TCSm promotor and activate the reporter, SEAP, expression. **B.** Schematic representation of the M3H and M4H assays used in figures D, F and H. tetR and VP16 conform a split transcription factor which reconstitution after interaction of their fused proteins will lead to the promotor activation. **C-D.** ARR22 effect in the TCSm activation, or B-ARRs-AHP2 interactions, respectively. Interaction between ARR22 and AHP2, or the B-ARRs were also tested. **E-F.** Analysis of ARR7 effect in the TCSm activation, or B-ARRs- AHP2 interactions, respectively. Interaction between ARR7 and AHP2, or the B-ARRs were also assayed. **G-H.** Study of AHP6 effect in the TCSm activation or the interaction between B-ARRs and AHP2, respectively. Interaction of AHP6 with AHP2 and the B-ARRs was well represented. C-H. SEAP expression of samples treated with the indicated BA concentrations is expressed in units per litre. The co-transfected proteins are indicated below the corresponding graph. Mean and S.E.M. are plotted for n= 4 mammalian samples. The statistical significance was determined using a two-way ANOVA analysis (P value < 0.001) and is indicated with bold letters. AHK, Arabidopsis histidine kinase; ARR, Arabidopsis response regulator; AHP, Arabidopsis histidine-containing phosphotransferase; BA, 6-bencilaminopurine; PCMVmin, minimal cytomegalovirus promotor; SEAP, Secreted embryonic alkaline phosphatase; TCSm, CK-responsive synthetic promoter designed for this work; tetO, operator motif for the repressor; tetR, tetracycline repressor; VP16, transcriptional activation domain of the Herpes simplex virus. This figure and the figure legend are adapted from the manuscript in preparation of Pavesi et al., Appendix 7.1..

Nevertheless, as the addition of ARR22 slightly depleted the B-ARR-AHP2 interactions, our results showed no evidence of individual ARR22-B-ARRs complexes neither, we will (in the future) test all interactions using FRET-APB. This technique requires a more laborious optimization of the experimental conditions but it is highly sensitive[204,215].

The analysis of ARR7 inhibition, on the other hand, showed a blockage of CK signalling only in cells expressing ARR10 and a reduction in the activation of the TCSm downstream ARR1 (**Fig. 19E**). Previous analysis of the role of the phosphorylation in the function of A-ARRs introduced the hypothesis that phosphorylated A-ARRs could form an inactive heterodimer with the phosphorylated B-ARRs through receiver domains[136]. To further explore this hypothesis, we next tested the ARR7 interaction with AHP2 and the B-ARRs. The MxH approach used in this study did not allow us to evidence interactions between ARR7 and AHP2, or the B-ARRs, individually (**Fig. 19F**). However, the addition of ARR7 to ARR1-AHP2, or ARR10-AHP2 couples resulted in a slight yet statistically significant increase of the measured PPI, in comparison to samples expressing no A-ARR. As the increase in the mentioned PPIs was observed as well in mock cells, we can consider this effect to be independent of the phospho-relay. We thus suggest that the molecular mechanism behind A-ARRs inhibition of CK signal may involve a ternary complex between these A-ARRs, the B-ARRs and the AHPs. In a single experiment (data not shown) we have evidenced that addition of AHP2 to the non-

interacting ARR7-ARR10 couples also significantly increases this PPI, supporting our hypothesis. However, to develop a full picture of these mechanistic will be needed to perform further competition assays by MxH and FRET-APB, supported by a Co-immunoprecipitation assay in protoplasts, for example.

Finally, analysis of the effect of AHP6 on the TCSm activation resulted in a depletion of the TCSm signal, independently of the TCS components present (**Fig. 19G**). Previous analysis had proposed that AHP6 mode of action involved disruption of the phospho-relay by interaction with other TCS elements[68]. This suggestion was based on an *in vitro* assay where the addition of AHP6 blocked the phospho-relay between AHP1 and ARR1. To test this hypothesis, we next investigated AHP6 effect on the B-ARRs-AHP2 interaction. Notably, the addition of AHP6 strongly depleted the TCSm activation in ARR1-, and ARR10-mediated responses (**Fig. 19H**). The results also showed a strong interaction between AHP6 and both B-ARRs individually, but not with AHP2. Together the results give experimental support to the hypothesis of AHP6 interfering with the phospho-relay by interaction with TCS components, and proposed the B-ARRs as the interactor partners. Therefore, we suggest that AHP6 modulates CK signalling by competing with the functional AHPs for the B-ARRs.

3.2.4 Study of the role of the conserved D of the B-ARRs in their CK response and PPI

Up to now our results have shown a CK-dependent activation of the TCSm, in agreement with the canonical TCS driving CK signalling. However, we have also evidenced an increase in the TCSm expression of untreated cells after co-transfection with both ARR1 and ARR10 (**Fig. 18D-E**). In addition, the effect of the different negative RRs, discussed in the previous section, resulted in the reduction (or blockage) of the CK responses regardless the hormone treatment. These observations cautiously suggest a non-canonical activation of the TCSm. Moreover, previous studies showed unaffected ability to activate CK responses of non-phosphorytable mutants of ARR2(D80N), and ARR18(D70N)[143,169], and the non-canonical networks involving CKI1[72]. Therefore, to explore in depth the influence of the phospho-relay in the TCSm activation, we generated non-phosphorytable mutants for the B-ARRs by replacement of the conserved D for A. We then co-transfected CHO cells and simultaneously analysed the TCSm activation and these B-ARRs PPIs.

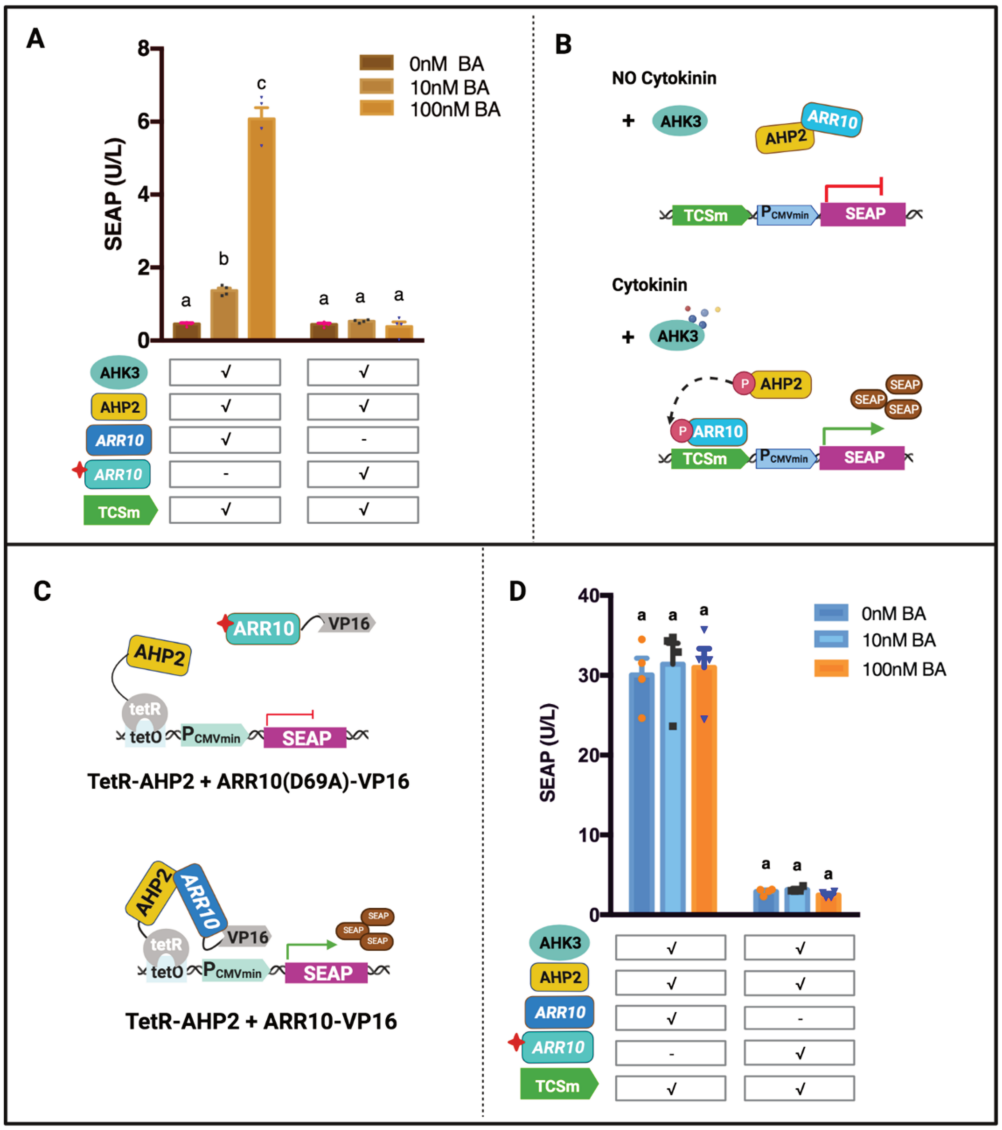

Figure 20. Role of the conserve D in ARR10 transactivation and PPIs.

A. Analysis of the TCSm activation by ARR10WT and the ARR10(D69A) non-phosphorytable mutant. **B**. Schematic representation of CK-responsive promotor-reporter assay used in figure A. It is expected that after hormone perception the B-ARRs will bind the TCSm promotor and activate the reporter, SEAP, expression. **C**. Schematic representation of the M3H and M4H assays used in figure D. tetR and VP16 conform a split transcription factor wich reconstitution after interaction of their fused proteins will lead to the promotor activation. **D.** Analysis of the effect of the D69A mutation in the PPIs of ARR10. In A and D, the star represents a mutation in the conserve D69. SEAP expression of samples treated with the indicated BA concentrations is expressed in units per litre. The co-transfected proteins are indicated below the corresponding graph. Data are representative of three independent experiments. Mean and S.E.M. are plotted for n= 4 mammalian samples. The statistical significance was determined using a two-way ANOVA analysis (P value < 0.001) and is indicated with bold letters. AHK, Arabidopsis histidine kinase; ARR, Arabidopsis response regulator; AHP, Arabidopsis histidine-containing phosphotransferase; BA, 6-bencilaminopurine; PCMVmin, minimal cytomegalovirus promotor; SEAP, Secreted embryonic alkaline phosphatase; TCSm, CK-responsive synthetic promoter designed for this work; tetO, operator motif for the repressor; tetR, tetracycline repressor; VP16, transcriptional activation domain of the Herpes simplex virus. This figure and the figure legend are adapted from the manuscript in preparation of Pavesi et al., Appendix 7.1.

Our results suggested that the B-ARRs may have the ability to generate CK responses via canonical, but also non-canonical paths. As expected for a B-ARR involved in CK canonical circuit, the mutation in the conserved D69 of ARR10 resulted in no activation of CK responses and disrupted the before evidenced interaction with AHP2 (**Fig. 20**).

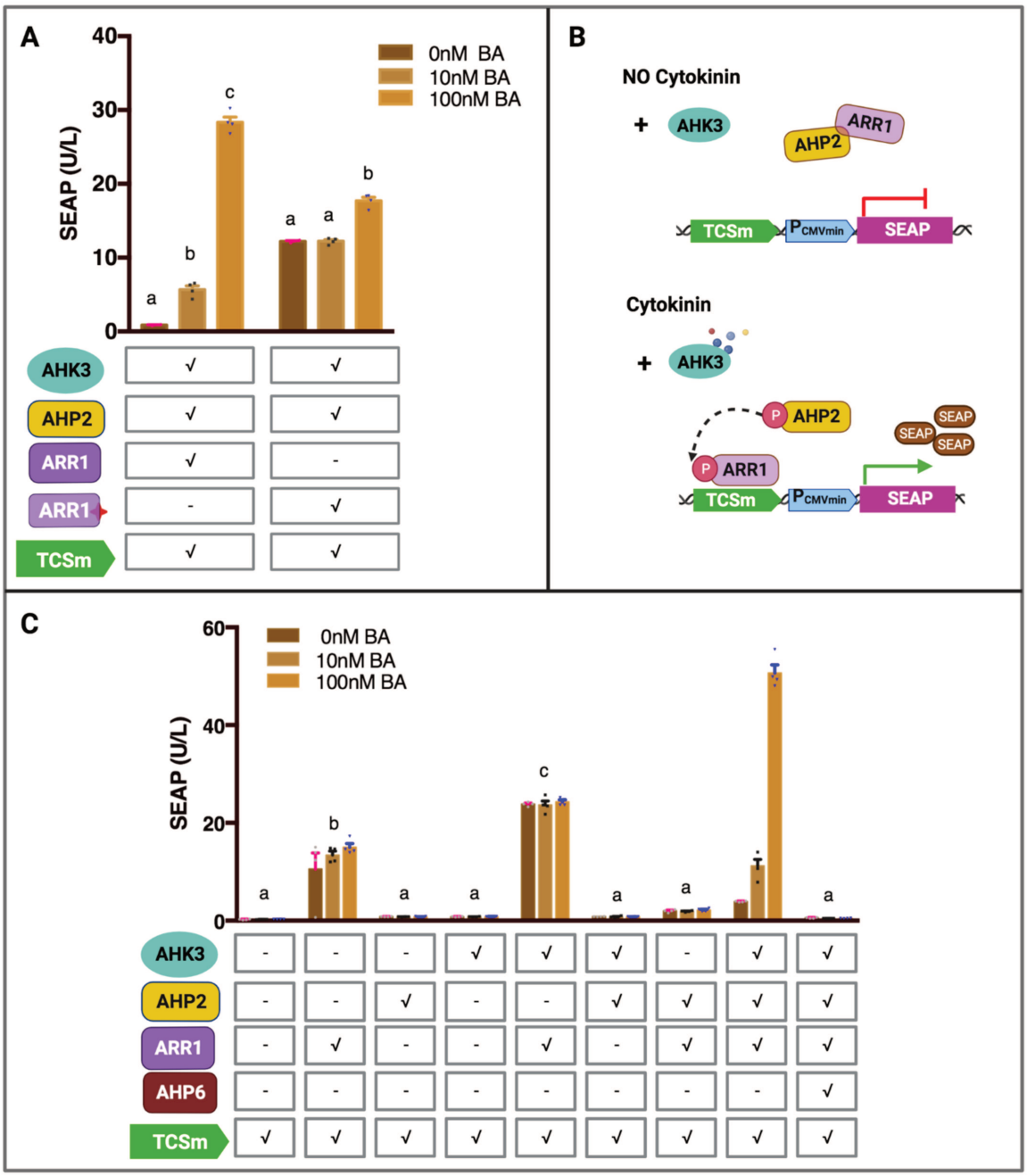

Figure 21. Study of ARR1 constitutive activation of the TCSm, and role of its D94 residue.

A. Analysis of the TCSm activation by the ARR1 WT and the ARR1(D94A) non-phosphorytable mutant. The star represents a mutation in the conserve D94. The letters indicate statistical significance of different BA concentrations within the same sample. **B.** Schematic representation of CK-responsive promotor-reporter assay used in figures A and C. It is expected that after hormone perception the B-ARRs will bind the TCSm promotor and activate the reporter, SEAP, expression. **C.** Study of the ARR1 constitutive activation of the TCSm. Letter indicate statistical significance of the level of TCSm activation between the different samples. In A and C, SEAP expression of samples treated with the indicated BA concentrations is expressed in units per litre. The co-transfected proteins are indicated below the corresponding graph. Data are representative of three independent experiments. Mean and S.E.M. are plotted for n= 4 mammalian samples. The statistical significance was determined using a two-way ANOVA analysis (P value < 0.001) and is indicated with bold letters. AHK, Arabidopsis histidine kinase; ARR, Arabidopsis response regulator; AHP, Arabidopsis histidine-containing phosphotransferase; BA, 6-bencilaminopurine; PCMVmin, minimal cytomegalovirus promotor; SEAP, Secreted embryonic alkaline phosphatase; TCSm, CK-responsive synthetic promoter designed for this work; tetO, operator motif for the repressor; tetR, tetracycline repressor; VP16, transcriptional activation domain of the Herpes simplex virus. This figure and the figure legend are adapted from the manuscript in preparation of Pavesi et al., Appendix 7.1.

Contrary, the ARR1(D94A) mutant preserved the ability to activate CK responses (**Fig. 21A**). In comparison with the ARR1 WT, our results showed weaker activation of the TCSm by the mutant after the addition of a 100 nM concentration BA. On the other hand, an increase in the TCSm activation in untreated cells and after the addition of 10 nM concentration BA was evidenced for cells expressing the ARR1(D94A), in comparison with the WT. These outcomes taken together cautiously suggest both a constitutive activation of the system by the mutant and a diminished CK response. The latter is probably an effect of the loss of an important phosphorytable residue. To further investigate our observation, the cells expressing the TCSm reporter were co-transfected with each TCS component alone, or in all possible combinations with the others. Our data showed strong activation in all experimental conditions of the TCSm in samples expressing solely ARR1, or ARR1 and AHK3 (**Fig. 21C**). Further, cells co-transfected with both ARR1 and AHP2 no longer displayed constitutive activation of the system. Constitutive CK response of ARR1 has been previously evidenced for the phosphomimic mutant ARR1(D94E)[142] and after deletion of its REC domain (ARR1ΔDDK)[137]. However, these observations were in agreement with the canonical model where the DNA binding domain of the B-ARRs is masked by the REC domain until its phosphorylation[139–141]. The results instead suggest that rather than unmasking the DNA binding domain, deletion of the REC domain, or a modification of the residue D94 may be releasing ARR1 from its inhibitor, AHP2.

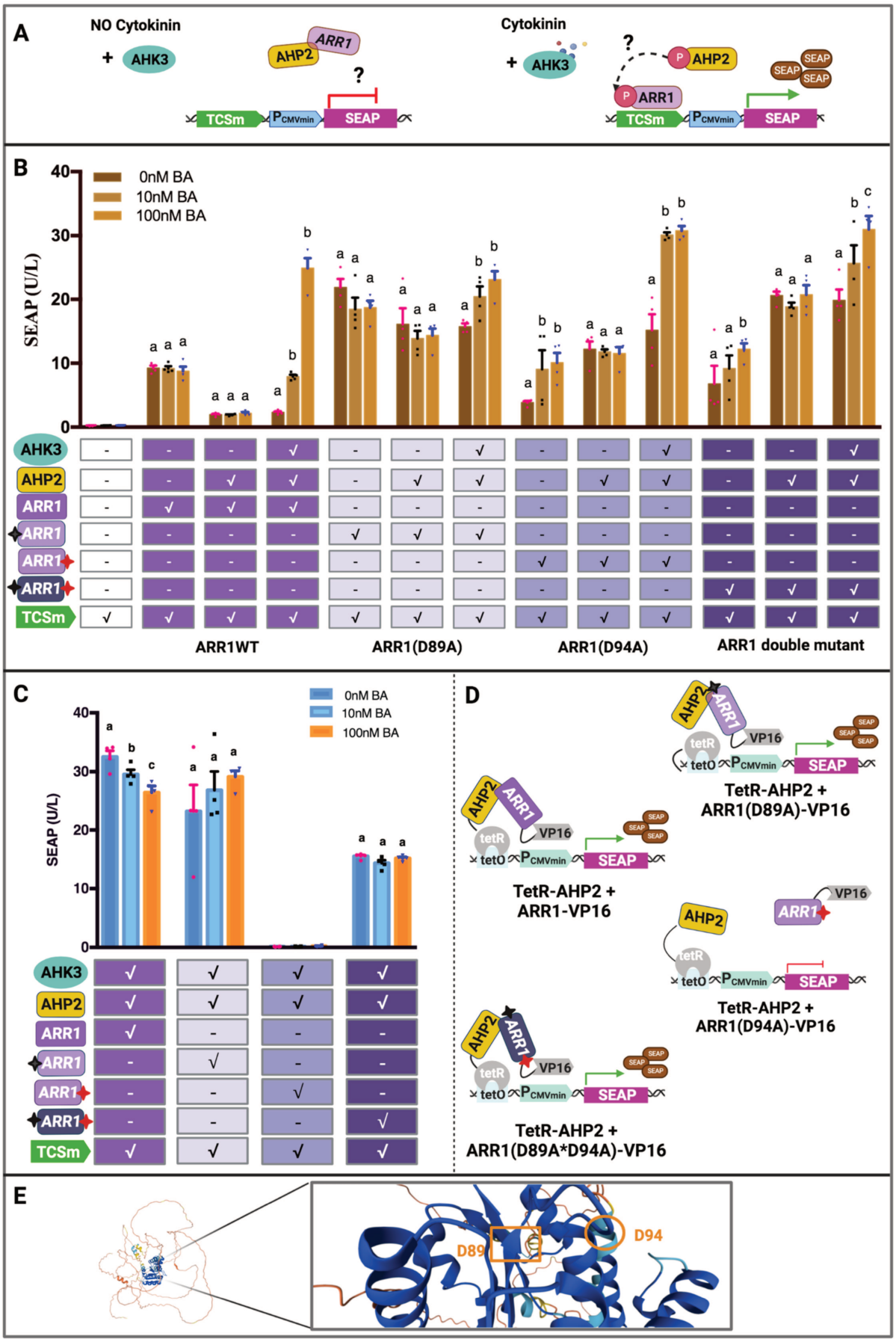
A
NO Cytokinin
AHK3
AHP2
ARR1
?
TCSm
PCMVmin
SEAP
Cytokinin
AHK3
P
AHP2
ARR1
SEAP
B
0nM BA
10nM BA
100nM BA
SEAP (U/L)
AHK3
AHP2
ARR1
ARR1
ARR1
ARR1
TCSm
ARR1WT
ARR1(D89A)
ARR1(D94A)
ARR1 double mutant
C
0nM BA
10nM BA
100nM BA
SEAP (U/L)
AHK3
AHP2
ARR1
ARR1
ARR1
ARR1
TCSm
D
tetR
tetO
VP16
TetR-AHP2 + ARR1(D89A)-VP16
TetR-AHP2 + ARR1-VP16
TetR-AHP2 + ARR1(D94A)-VP16
TetR-AHP2 + ARR1(D89A*D94A)-VP16
E
D89
D94

Figure 22. Comparison of the constitutive activation of CK responses and PPIs between ARR1WT and three mutants.

A. Schematic representation of the CK-responsive promotor-reporter assay used in figure B. It is expected that after hormone perception the B-ARRs will bind the TCSm promotor and activate the reporter, SEAP, expression. **B.** Analysis of the transactivation activity of ARR1WT and non-phosphorytable mutants ARR1(D89), ARR1(D94A) and ARR1(D89A*D94A) when transfected alone, with AHP2, or AHP2 and AHK3. **C.** Analysis of AHP2 interaction with either ARR1 WT and mutants. **D.** Schematic representation of the M3H assay used in figure C. tetR and VP16 conform a split transcription factor which reconstitution after interaction of their fused proteins will lead to the promotor activation. **E.** Ribbon representation of a section of ARR1 REC domain. The D89 and D94 residues are indicated either by a square, or a circle, respectively. In B and C, one black star (to the left), a single red star (o the right), or two stars (left and right) represents the D89A, D94A, and double mutant, respectively. SEAP expression of samples treated with the indicated BA concentrations is expressed in units per litre. The co-transfected proteins are indicated below the corresponding graph. Data are representative of three independent experiments. Mean and S.E.M. are plotted for n= 4 mammalian samples. The statistical significance was determined using a two-way ANOVA analysis (P value < 0.001) and is indicated with bold letters. AHK, Arabidopsis histidine kinase; ARR, Arabidopsis response regulator; AHP, Arabidopsis histidine-containing phosphotransferase; BA, 6-bencilaminopurine; PCMVmin, minimal cytomegalovirus promotor; SEAP, Secreted embryonic alkaline phosphatase; TCSm, CK-responsive synthetic promoter designed for this work; tetO, operator motif for the repressor; tetR, tetracycline repressor; VP16, transcriptional activation domain of the Herpes simplex virus. This figure and the figure legend are adapted from the manuscript in preparation of Pavesi et al., Appendix 7.1.

We then propose that in plants, where all TCS components are present, AHP2 inhibits the constitutive activation of target genes by ARR1 (and possibly other B-ARRs), until the concentration of the hormone is sufficient to activate CK responses.

Further support to our hypothesis of a "turn off/ turn on" model for ARR1 activation of CK responses is the slight, but significant diminution of the ARR1-AHP2 interaction observed in our MxH assay (**Fig. 22C**). The conserved CK response of the ARR1(D94A) mutant suggested the existence of a second phosphorytable residue. To further explore this, we first performed an *in silico* protein alignment using Clustal Omega[252]. The outcome of this analysis proposed the residue D89 of ARR1 as the conserved one, equivalent to the D69 in ARR10, D80 in ARR2[61], and D70 in ARR18[143]. Therefore, we decided to continue the analysis of the role of the conserved D in ARR1 activation and PPI by simultaneously testing the ARR1(D94A) mutant, the newly engineered ARR1(D89A), and the double mutant. We then investigated the TCSm activation after co-transfection with each mutant alone, in the presence of AHP2, or with AHP2 and AHP3, thus fully reconstructing the circuit. The results displayed in **Fig. 22B** suggest that mutation in the residue D89, D94, or both, does not affect ARR1 constitutive activation of the TCSm. Moreover, co-expression of each mutant with all other pathway components showed a conserved response to CK, as at higher hormone concentrations the TCSm activation increased. The influence of the phospho-relay, however, was more evident in

the D94 mutant, proposing a hierarchy among the possible phosphorytable residues, while the response to CK itself may infer the existence an additional phosphorytable residue. Future studies of the phosphorylation state of the double mutant by mass spectroscopy could help us visualize the latter hypothesis.

Notably, in comparison to the previous model of repression proposed for ARR1WT, the constitutive response of the mutants was not inhibited in the presence of the AHP2. It is therefore possible that a disruption of the interaction between ARR1 and its proposed inhibitor AHP2 is having place. To explore this hypothesis further, we analysed the interaction between the ARR1 mutants and AHP2, and compared with the ARR1WT-AHP2 complex formation. The outcome of this experiment showed that only mutation in the D94 disrupted the interaction with the AHP2 (**Fig. 22C**). Contrary, both the ARR1(D89A) and the double mutant were still capable to interact with AHP2. Hence it could be hypothesised that a reformulation of the ARR1-AHP2 complex is sufficient to hinder the suggested inhibition by AHP2.

3.2.5 Chapter discussion

In this chapter we have displayed several examples of a multitude of questions that can be investigated implementing the new synthetic approach presented in this work. The possibility to customize the reconstructed circuit allowed us to interrogate CK responses form the binding of different adenine derivates to the differential transcriptional activation of the TCSm. Overall, we have provided experimental evidence to support previous findings, while generating new hypothesis. For example, we add to the proposal of the ARR7 forming an inhibitory complex with the B-ARRs by suggesting the participation of the AHPs in this structure. Furthermore, we propose that the binding between AHP6 competes with the functional AHPs for the binding of the B-ARRs thus reducing CK responses. Moreover, we were able to visualize the suggested increased sensitivity of AHK3 for most adenine derivates in comparison with AHK4, enlarging the pool of tested CK forms. The activation of the TCSm by the tZR cautiously proposes that this adenine derivate may have genuine CK activity also *in planta*. However, further analysis on the possible metabolism of CK derivates in mammalian cells should be conducted to ensure that the observations are not an effect of the riboside interconversion to the active forms. Finally, we have raised new questions regarding the role of the TCS phospho-relay and presented preliminary evidence of a non-canonical activation of the CK responses by ARR1.

In our proposed model AHP2 plays a dual regulatory role in turning CK signalling on and off as follows (**Fig. 23**):

1. For ARR10-like B-ARRs, interaction with AHP2 is essential for their activation which occurs by means of the phospho-relay, as proposed for the canonical TCS.
2. For ARR1-like B-ARRs, interaction with AHP2 inhibits their constitutive activation of CK responses until the hormone concentration reaches a threshold. Later, either as a consequence of the phospho-transfer or still uncharacterised processes, the ARR1-like are released from their repression to further activate the target genes.

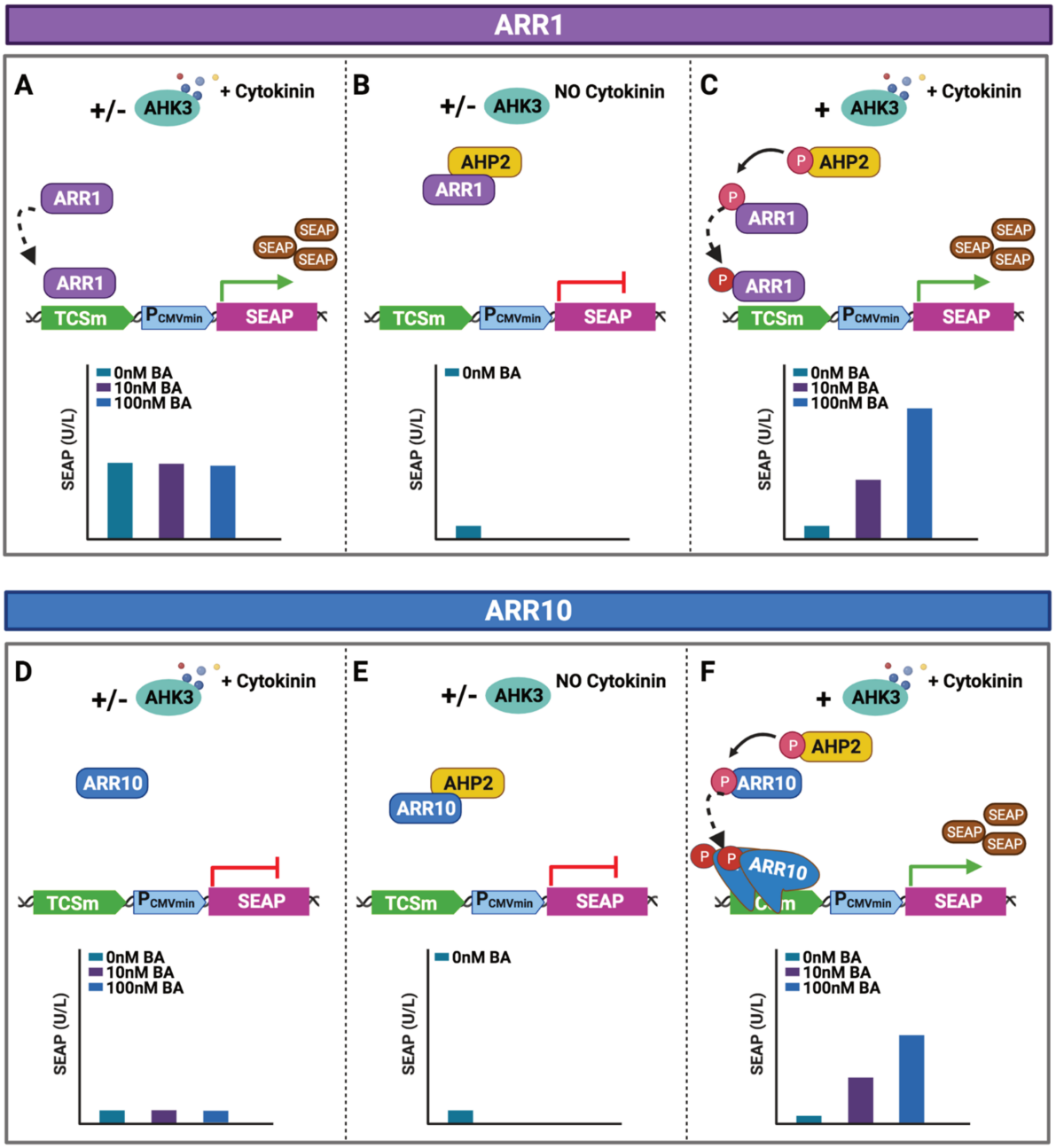

Figure 23. Schematic representation of the proposed mechanism behind ARR1- and ARR10-CK responses. ARR1 constitutively binds and activates the expression of its target genes (represented here by the TCSm) **(A).** In the presence of AHP2, ARR1 activation of the TCSm is complete repressed, probably (but not only) as a result of their PPI **(B)**, until hormone perception **(C)**. The phosphorelay triggered by CK will release ARR1 from its inhibition probably by inducing a conformational change, in a hormone dependent manner. On the other hand, ARR10 does not show constitutive activation of the TCSm **(D-E)**, and can only transactivate the CK-responsive genes after hormone perception, possibly binding as homodimers **(F)**. AHK, Arabidopsis histidine kinase; ARR, Arabidopsis response regulator; AHP, Arabidopsis histidine-containing phosphotransferase; BA, 6-bencilaminopurine; SEAP, Secreted embryonic alkaline phosphatase; TCSm, CK-responsive synthetic promoter designed for this work. The bar charts are only a representation of the expected SEAP activity in each situation, they do not show experimental data. This figure and the figure legend are adapted from the manuscript in preparation of Pavesi et al., Appendix 7.1.

3.3 Chapter 3. Interrogating CRFs suitability for the design of a new CK biosensor

In the pursuit of a complete understanding of CK function in plants, we must be able to integrate a deep knowledge of their metabolism, perception and signalling, with precise information regarding their intracellular abundance and distribution. In the previous chapters, we have shown evidence of our mammalian platform´s suitability for deciphering the contribution of single components to the network, thus providing a new experimental tool to deepen our understanding of CK perception and signalling. The spatial resolution of CK responses *in vivo*, on the other hand, was achieved thanks to the implementation of the TCSn:EGFP biosensor. However, tracking simultaneously the intracellular concentration of CK, while exploring their spatial, and temporal distribution, will require the design of a new tool. Relocation- or FRET-based biosensors are promising alternatives as they offer subcellular definition, real-time-, and quantitative-readouts[195,213,219–222]. Therefore, to design a ratiometric biosensor sensible to CK we need to identify either a subcellular location or a PPI that changes in response to the hormone.

The first evidence of the CRFs (CRF2, CRF3, and CRF6) CK-dependent relocation into the nucleus was obtained from studies in *Arabidopsis* mesophyll protoplasts, after treatment with a concentration of 2 μM BA for 10 min[64]. A few years after this proposal, three works failed in reproducing those results showing CRF[171], CRF2[73], CRF3[73] and CRF5[170,171] to be located either in the nucleus or both in the nucleus and cytoplasm of *Arabidopsis* protoplasts before CK treatment. However, up-to-date, the subcellular location of only a limited number of CRFs has been studied. Moreover, while the interaction between these TFs with the AHPs has been evidenced[119] by Y2H and BiFC, there is no information on the effect of CK upon them.

Therefore, in this chapter, we will explore the hormone-dependent relocation into the nucleus of the 12 CRFs in the search for a sensory module for a novel CK relocation biosensor. Furthermore, we will (quantitatively) investigate their PPI with the AHP family members, as well as their ability to homo-, and heterodimerise. The study of the hormone-dependency of the AHP-CRF interaction aims to design a FRET-based biosensor. Finally, we will interrogate these PPIs in *Arabidopsis* protoplasts to validate the outcome of the experiments performed in CHO cells.

3.3.1 Analysis of the CRF CK-dependent nucleus-cytoplasmatic shuttle for the design of a relocation biosensor.

In comparison to the time required for the transcription, translation and relocation of a reporter gene in a transcriptional biosensor, a nucleus-cytoplasmic shuttle of a CRF fused to an FP could reduce the visualization time of CK response from minutes to seconds. Further addition of a second module encoding a nuclear-localized FP protein would provide a quantitative read-out of the intracellular concentration of CK by the measure of the ratio between the intensity of the two FPs (**Fig. 24**). Next, to find a suitable candidate for such a biosensor, we analysed the subcellular location of the CRFs in CHO cells, and protoplasts.

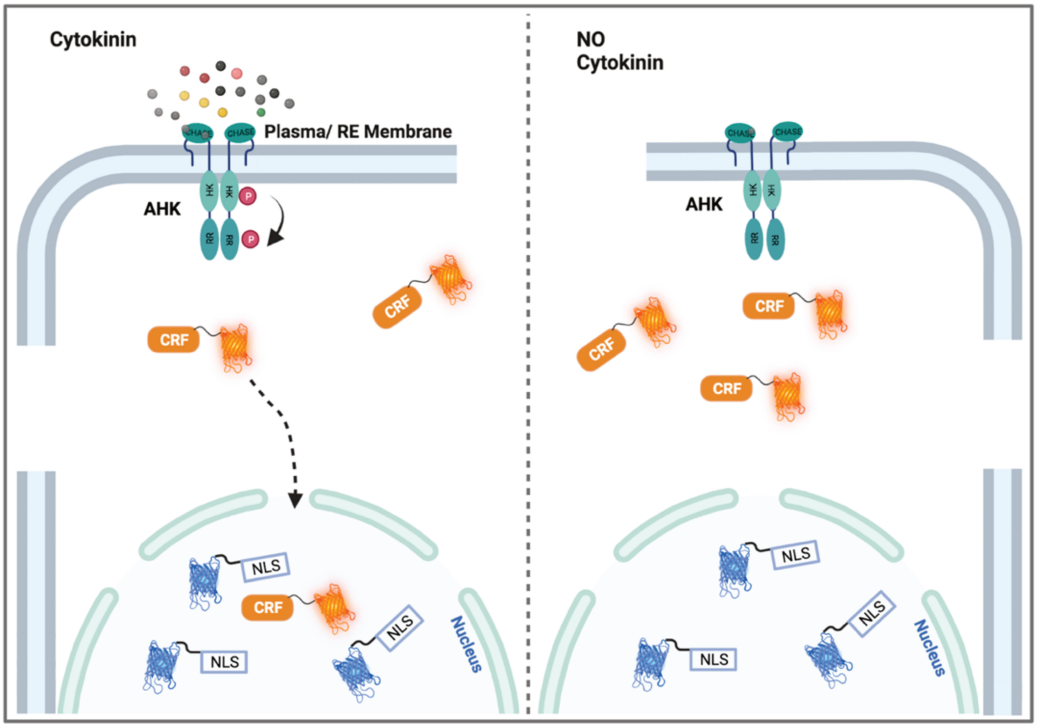

Figure 24. Schematic representation of a hypothetic CK relocation-based biosensor. The ratiometric biosensor could comprise a sensory module CRF-mVenus, which subcellular location will change in the presence of CK, and a normalization element constitutively located in the nucleus Cerulean-NLS. The ratio between mVenus and Cerulean fluorescent intensities will provide a quantitative read-out, will the change in the localization of mVenus signal will permit to visualize the spatial distribution of CK responses. To ensure equimolar amounts of both modules, they will be cloned as a same transcriptional unit. Addition of a self-cleaving peptide (as the 2A peptide) between both fusion proteins will allow their separation during translation. AHK, Arabidopsis histidine kinase; CHASE, Cyclase/histidine kinases associated sensor extracellular; CRF, Cytokinins response factor; AHP, Arabidopsis histidine-containing phosphotransferase; NLS, nuclear localization signal; RR, response regulator.

3.3.1.1 Study of the subcellular distribution of the CRFs in mammalian cells.

Taking advantage of our orthogonal platform and quantitative tools we explored CRF1 to 12 subcellular distribution in the presence or absence of CK in CHO cells. For this, we firstly engineered vectors for mammalian cell expression containing the full-length cDNA of the CRF1 to 12 with a C-terminal fusion to EGFP to avoid the disruption of the N-terminal region harbouring the nuclear localization signal (NLS). The prediction of the CRFs NLS, previously uncharacterized, was performed *in silico* using the *NLStradamus* software[253]. The results revealed a putative classic monopartite NLS sequence of variable length in the N-terminal end of most CRFs, with the exceptions of CRF3, CRF4 and CRF8 for which no NLS was detected (**Fig. 25**). In addition, to confirm these results a second *in silico* test was performed using cNLS Mapper[254]. Only putative NLS for CRF1, CRF2, CRF9 and CRF10 were predicted by this software (data not shown). The predicted NLS location as well as their core peptide enriched in arginine (R) and lysine (K) are agree with the characteristic NLS of plant transcription factors[255].

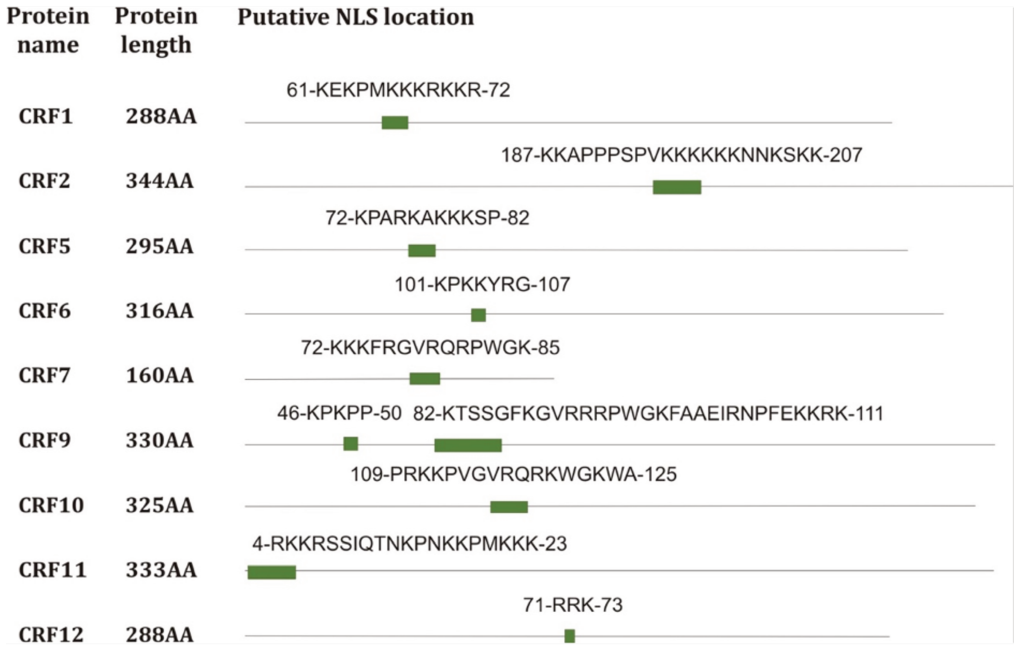

Figure 25. Sequence and location of the predicted NLS of the CRFs.

Nuclear location signals for the CRFs were determined in silico using the NLStradamus software[253], by "Posterior Prediction" with the pre-loaded models and the recommended 0,6 threshold. The green rectangles indicate the position of the NLS. The different lengths of the lines representing the full protein sequence are only an approximation to facilitate visualization of the true location of the NLS.

We next transfected CRF-EGFP fusions either alone, or in combination with AHP2 and AHK3; 24 h after hormone induction the cells were prepared for fluorescent confocal microscopy imaging (**Methods**). Our results showed most CRFs to be located in the nucleus of CHO cells or both in the nucleus and the cytoplasm (**Fig. 26**, and **Table 1**). The addition of 100 nM BA to cells where the full upstream signalling pathway was reconstructed didn't affect the subcellular location of the CRFs. Posterior analysis of the distribution of EGFP:CRFs fusions showed all proteins to localize in the cell nucleus with exception of CRF2 which was found both in the nucleus and the cytoplasm (**Table 1**). These results imply that the terminal fusion to the FP may interfere with the ability of this TF conformation and thus, with their subcellular distribution. As observed in chapter 1 for AHP2 ARR1 and ARR10, the subcellular location of the CRF was also unaffected by the presence of CK.

Table 1. Summary of the subcellular distribution of CRF1 to 12 in CHO cells and *Arabidopsis* protoplasts. Subcellular distribution of the CRF family was imaged using fluorescent confocal microscopy. Data are representative of three independent experiments. √, found in the indicated compartment; n.t. not tested.

Platform	Mammalian cells				Protoplasts			
Fusion to FP	C-terminal		N-terminal		C-terminal		N-terminal	
Subcellular compartment	Nucleus	Cytoplasm	Nucleus	Cytoplasm	Nucleus	Cytoplasm	Nucleus	Cytoplasm
CRF1	√		√		√		n.t.	
CRF2	√		√	√	√		√	
CRF3	√		√		√		√	
CRF4	√	√	√		√		n.t.	
CRF5	√	√	√		√		√	
CRF6	√	√	√		√	√	√	
CRF7	√		√		√		√	
CRF8	√		√		√		√	
CRF9	√		√		√		n.t.	
CRF10	√	√	√		√	√	√	
CRF11	√		√		√		n.t.	
CRF12	√	√	√		√		√	

Altogether, the observations obtained with our synthetic approach in the mammalian platform suggested that the CRF are in the nucleus of the CHO cells prior any hormone treatment and don not relocate after CK treatment, as observed in previous studies[73,170,171].

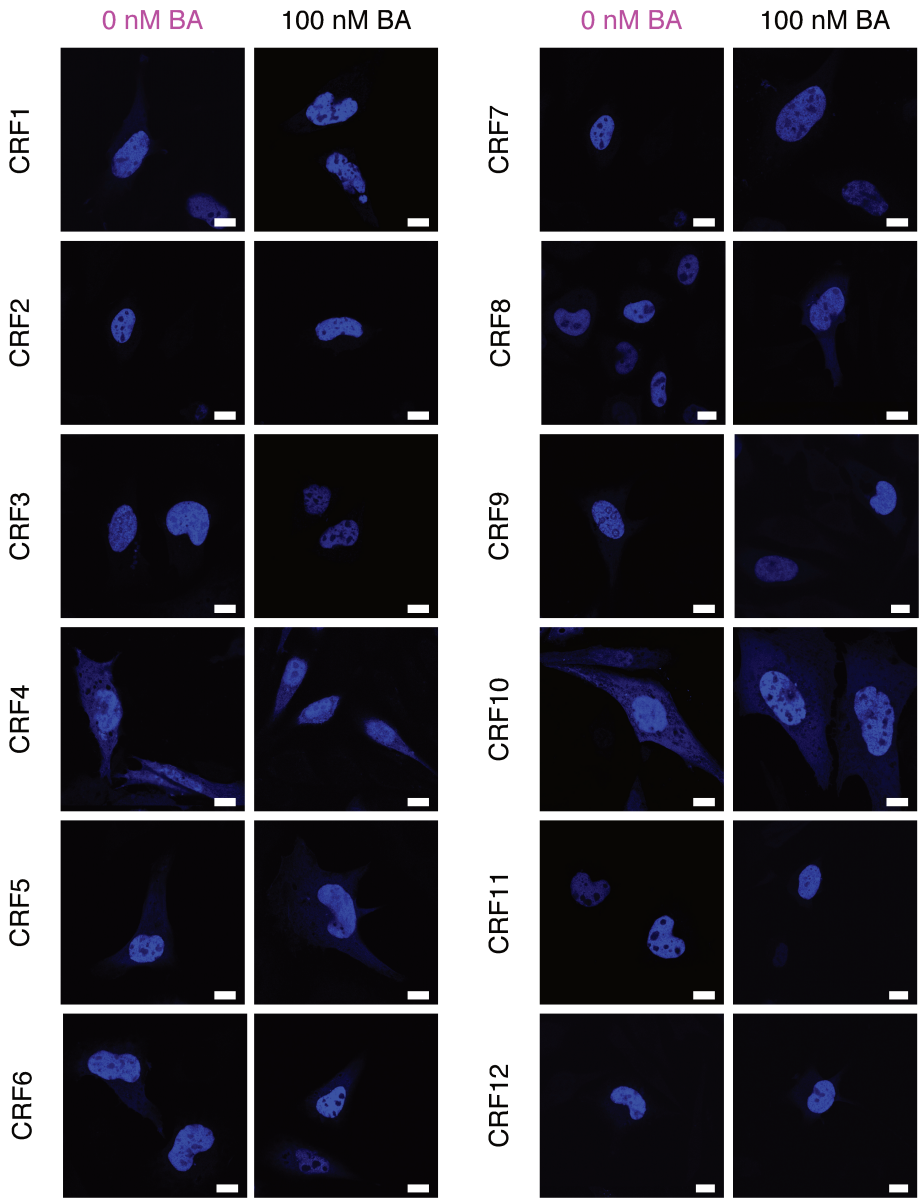

Figure 26. Confocal fluorescence imaging of subcellular location of the CRF family in CHO cells. CRFs-EGFP fusions expressed in CHO cells and examined by confocal microscopy after fixation using the 60x oil objective. EGFP was visualized using excitation laser of 488 nm and emission filters of 500–550 nm. Each column title indicates the treatment and each row title the protein tested. Scale bar, 10 µm. BA, 6-bencilaminopurine; CRF, Cytokinin response factor.

3.3.1.2 Analysis of CRF1 to 12 subcellular location in Arabidopsis protoplasts.

To further analyse the influence of CK on the subcellular distribution of the CRFs we repeated the previous analysis in *Arabidopsis* leaf mesophyll protoplasts. To this aim, we engineered constructs for the expression in protoplasts of the full-length cDNA of CRF1 to 12 under the control of a P_{35S}. C- and N-terminal fusion of the CRF to EGFP were simultaneously analysed. The protoplasts were then transformed and 24 h after hormonal treatment with a concentration of 10 μM BA, their fluorescence was observed by confocal microscopy. Our results showed that with the only exception of the C-terminal fusion to EGFP of CRF6 and CRF10, all CRFs localized in the nucleus of protoplasts prior to any hormonal treatment (**Fig. 27**). Posterior addition of BA did not affect the observations.

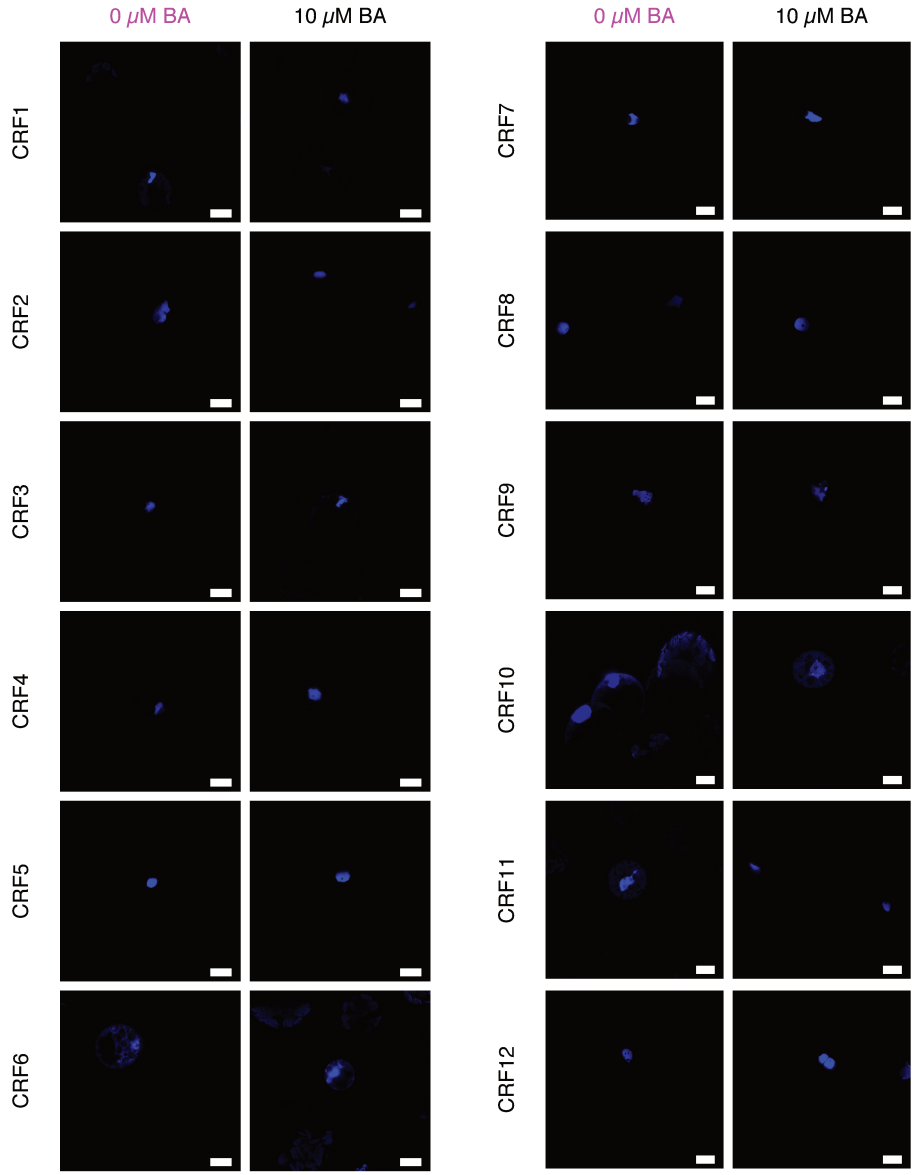

Figure 27. Confocal fluorescent imaging of the CRFs´location in Arabidopsis protoplasts.

WT *Arabidopsis* leaf mesophyll protoplasts were transformed with CRFs-EGFP fusions and confocal imaging was performed 24 h after BA induction using the 60x oil objective. EGFP was visualized using excitation lasers of 488 nm, and emission filters of 500–550 nm. Each column title indicates the treatment and each row title the protein tested. Scale bar, 10 μm. BA, 6-bencilaminopurine; CRF, Cytokinin response factor.

3.3.2 Analysis of the CRF CK-dependent PPIs for the design of a FRET-based biosensor.

Protein interaction is essential to all organisms being the driving force of nearly all cellular processes. Identification of PPIs can lead to a better understanding of multiple regulatory processes, such as signal transduction. In the CK pathway, the interaction between the TCS components along with the phospho-relay positively regulates the hormone responses. While, as shown in Chapter 2 for AHP6, complex formation with other RR of the pathway can result in signal diminution. In this work, we showed only a slight (but significant) reduction of ARR1-AHP2 interaction at increasing concentrations of BA. A previous work proposes that the CRF1 to 8 can interact with the AHP1 to 5, with exception of the CRF2-AHP2, and the CRF3-AHP2 couples[119]. However, up to now, there is no information regarding the effect of CK in the CRF-AHP interactions. Moreover, no interaction including the CRF9 to 12, or AHP6 has been assessed. The identification of any CK-dependent PPIs could impulse the design of a FRET-based biosensor. The principle behind FRET approaches was explained in the introduction of this study and a schematic representation of a hypothetic CK FRET-based biosensor can be found in **Fig**. **28**. Briefly, each protein from the two candidates for interaction will be fused to an FP from a FRET-pair. The interaction between these proteins will bring the FPs into proximity allowing the energy transfer from the donor to an acceptor. While no interaction will generate no FRET. The change in the fluorescent intensity can further be measured providing information on the intracellular concentration of CK.

Therefore, to expand the knowledge about uncharacterized CRFs in CK signalling and to search for a candidate interaction for the development of a CK FRET-based biosensor, we next focused on the quantitative study of CRFs-AHPs interactions and their CK-dependency. To this aim, we implemented MxH approaches, FRET-APB for mammalian cells studies and a split TF system for validation of our results in *Arabidopsis* protoplasts.

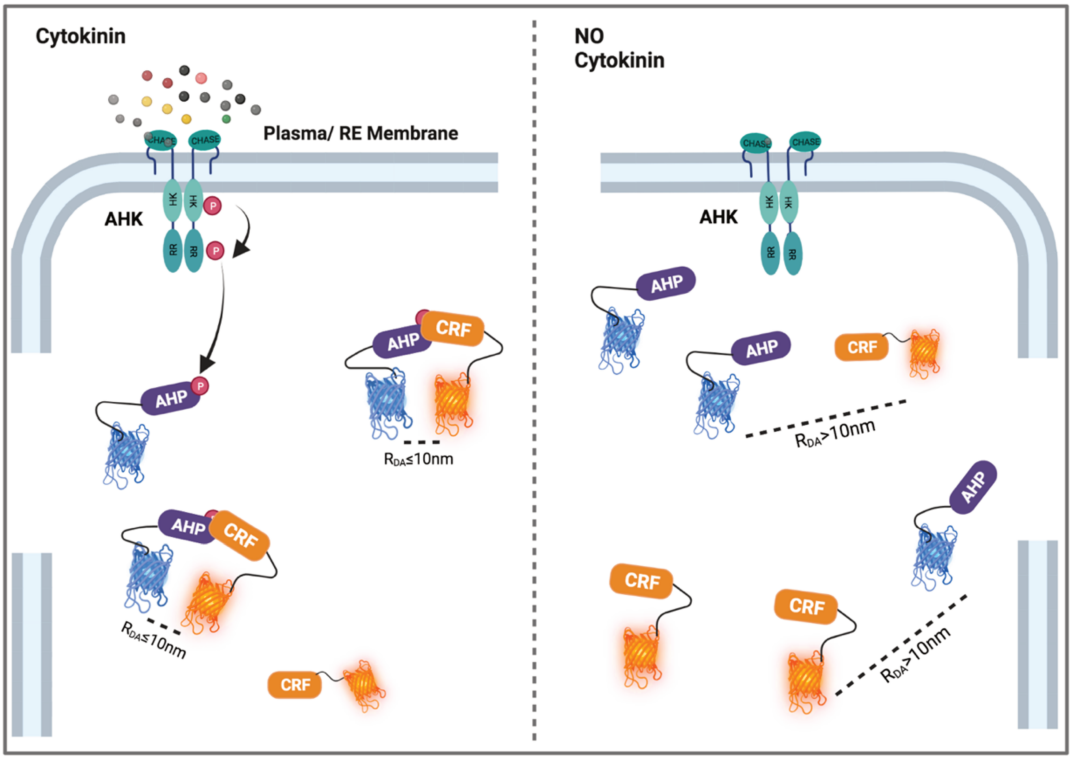

Figure 28. Schematic representation of a hypothetic CK FRET-based biosensor.
A CK sensitive FRET-based biosensor will comprise two modules: CRF-mVenus, and AHP-Cerulean. The CK dependent PPI between the CRF and the AHP will bring the FRET pair mVenus/Cerulean into close proximity allowing the energy transfer between the FP fluorophores. Quantification of FRET will allow to estimate the intracellular concentration of CK, while the merged fluorescent signal will permit to visualize CK distribution in plants. To ensure equimolar amounts of both modules, they will be cloned as a same transcriptional unit. Addition of a self-cleaving peptide (as the 2A peptide) between both fusion proteins will allow their separation during translation. AHK, Arabidopsis histidine kinase; CHASE, Cyclase/histidine kinases associated sensor extracellular; CRF, Cytokinins response factor; AHP, Arabidopsis histidine-containing phosphotransferase; NLS, nuclear localization signal; RDA, mean distance between the fluorophore's dipoles; RR, response regulator.

3.3.2.1 Analysis of CRF-AHP interactions in mammalian cells and *Arabidopsis* protoplasts.

For the study of the 72 CRF-AHP combinations in mammalian cells by MxH we first engineered plasmids containing tetR-AHPs, and CRFs-VP16 fusions and transfected them into CHO cells co-expressing the AHK3 receptor. 24 h after BA treatment SEAP expression was measured. Samples with no significant PPI were further assayed by FRET-APB. For this, we generated constructs for the expression of AHP-mCherry, in addition to the CRF-EGFP fusions used in the previous section, and co-transfected them in CHO cells. 24 h after hormone treatment the cells were fixed with paraformaldehyde (PFA) solution and mounted into

microscopy slides for observation with the fluorescent confocal microscope. The mean of the apparent FRET efficiency of 10 individual cells was then calculated. As most CRF localize exclusively in the nucleus of mammalian cells, while AHPs are distributed all over the cell, the bleaching of the acceptor fluorophore was performed in a selected stimulation region in the nucleus. Finally, 58 CRF-AHP combinations were tested in *Arabidopsis* mesophyll protoplast. For this final validation, we implemented another split transcription factor system, adapted for plant expression. As for MxH approaches, one protein was fused to the transcriptional activator VP16, while the other candidate for interaction was fused to the macrolide repressor (E protein). The E protein binding site, the erythromycin resistance operator (or etr) was cloned upstream of the 35S promoter which controls the expression of the reporter gene, FLuc. 24 h after transformation samples were treated with BA or H_2O(d), and another 24 h later FLuc luminescence was measured. The summarized data of our observations on both platforms can be found in **Table 2**.

Table 2. Summary of the quantitative analysis of CRFs-AHPs interactions in CHO cells and Arabidopsis protoplasts. For mammalian cells results represent the joint analysis by MxH and FRET-APB. PPIs in protoplasts represent the outcome of a unique x-hybrid approach. Color-filling of the table cell indicates PPI evidenced only in the corresponding platform. Data are representative of three independent experiments. n.s., $P \geq 0.1$; n.t., not tested; (*), $0{,}03 \leq P \leq 0.1$; (**), $0.1 \leq P \leq 0.002$; (***), $0.002 \leq P \leq 0.0002$; (****), $P < 0.0001$.

Platform	Mammalian cells						Protoplasts					
	AHP1	AHP2	AHP3	AHP4	AHP5	AHP6	AHP1	AHP2	AHP3	AHP4	AHP5	AHP6
CRF1	*	n.s.	n.s.	***	*	***	n.t.	n.t.	n.t.	n.t.	n.t.	n.t.
CRF2	*	****	****	****	***	****	*	****	**	**	**	**
CRF3	***	**	*	**	*	*	****	****	n.t.	**	****	***
CRF4	***	***	n.s.	n.s.	***	n.s.	n.s.	**	n.s.	n.s.	n.t.	n.s.
CRF5	***	****	***	n.s.	n.s.	**	*	**	*	n.t.	n.s.	n.t.
CRF6	***	*	***	**	**	*	****	****	****	n.s.	****	***
CRF7	*	n.s.	n.s.	**	*	n.s.	**	****	n.s.	n.t.	n.s.	***
CRF8	*	n.s.	*	n.s.	n.s.	n.s.	****	****	*	n.s.	n.s.	***
CRF9	****	****	***	*	***	*	n.t.	****	**	*	n.t.	n.s.
CRF10	****	***	**	**	**	***	**	***	**	n.s.	**	n.t.
CRF11	****	****	****	****	****	****	****	****	****	n.s.	****	n.s.
CRF12	****	n.s.	***	***	****	****	****	****	****	n.s.	****	****

Our results showed no influence of the hormone treatment in the CRF-AHP interaction, in neither of the assayed platforms. These observations may suggest that, as observed before for the ARR10-AHP2 couple in chapter 2, there is no influence of CK in these TFs interaction with

the AHPs. However, up to now, there is no evidence of the CRFs being involved in the canonical (AHK-mediated) phospho-relay. Therefore, our results rather suggest that the phosphorylation state of the AHPs does not affect their interaction with the CRFs.

Moreover, our findings provided a quantitative estimation of the strength of these RRs interaction with the AHPs, while expanding the TCS interaction map. Notably, our analysis in mammalian cells of the less characterized members of the CRF family, CRF9 to 12, showed a strong interaction with most AHPs including the pseudo-HP, AHP6. A similar interaction profile for these RRs was observed in protoplast suggesting their involvement in CK responses. Remarkably, interaction of CRF6, and CRF 10 to 12 with AHP4 was only significant in mammalian cells. This was also observed for CRF4-AHP1, CRF7-AHP5, and CRF9 and CRF10 with AHP6. Unlike Y2H and BiFC, the MxH techniques do not present false positives. Therefore, we propose that the PPIs observed in mammalian cells exclusively must be impeded in planta, for example by the formation of an inhibitory complex.

3.3.2.2 Study of CRF-CRF interactions in mammalian cells

Complete the interaction map of the TCS components could help us better understand CK signal transduction. , we next tested the ability of all 12 CRFs to form homo-, and heterodimers. For this, we used the same CRFs-VP16 fusions as before and engineered new tetR-CRFs constructs. As the CRFs are transcriptional activators in plants, we tested whether they may be able to activate transcription from the P_{CMVmin} promoter as previously observed for ARR1-mediated activation of the β-galactosidase expression when fused to GBD binding domain in yeast[108].

Table 3. Summary of the quantitative analysis of CRFs-CRFs interactions in mammalian cells by M4H and FRET-APB. Filled boxes represented assays performed exclusively by FRET-APB. Black arrows indicated the direction of reading. Data are representative of three independent experiments. n.s., $P \geq 0.1$; (*), $0{,}03 \leq P \leq 0.1$; (**), $0.1 \leq P \leq 0.002$; (***), $0.002 \leq P \leq 0.0002$; (****), $P < 0.0001$.

Platform	Mammalian cells											
	CRF1 ↓	CRF2	CRF3	CRF4	CRF5	CRF6	CRF7	CRF8	CRF9	CRF10	CRF11	CRF12
CRF1 →	****	****	ns	*	****	**	****	****	****	**	****	****
	CRF2	****	*	****	****	**	*	***	****	**	****	****
		CRF3	ns	***	ns	*	****	*	ns	***	****	ns
			CRF4	*	ns	ns	ns	*	**	***	****	**
				CRF5	****	*	****	****	****	ns	****	****
					CRF6	***	**	**	****	**	****	****
						CRF7	****	ns	ns	*	****	****
							CRF8	****	*	**	****	****
								CRF9	*	*	****	****
									CRF10	***	ns	ns
										CRF11	****	****
											CRF12	****

Therefore, we first co-transfected the tetR-CRFs fusion alone and measure SEAP expression. Remarkably, CRF10 strongly activated the mammalian promoter, followed by CRF3, and CRF4 (**Fig. 29**). Contrary, all other CRFs presented insignificant activation of the promotor. Based on these results we decided to investigate CRF3, CRF4, and CRF10 homo-, and heterodimers, exclusively by FRET-APB. The rest of the CRF-CRF interaction could be explored using the MxH approach. The summarized data of all 78 tested combinations can be found in **Table 3**. As for CRF-AHP interaction, the CRF homo-, or heterodimerization was not influenced by the hormone treatment. Our findings once more remark on the strong interaction ability of the CRF11 and CRF12. In addition, with exception of CRF3, our results proposed that all CRFs can form homodimers.

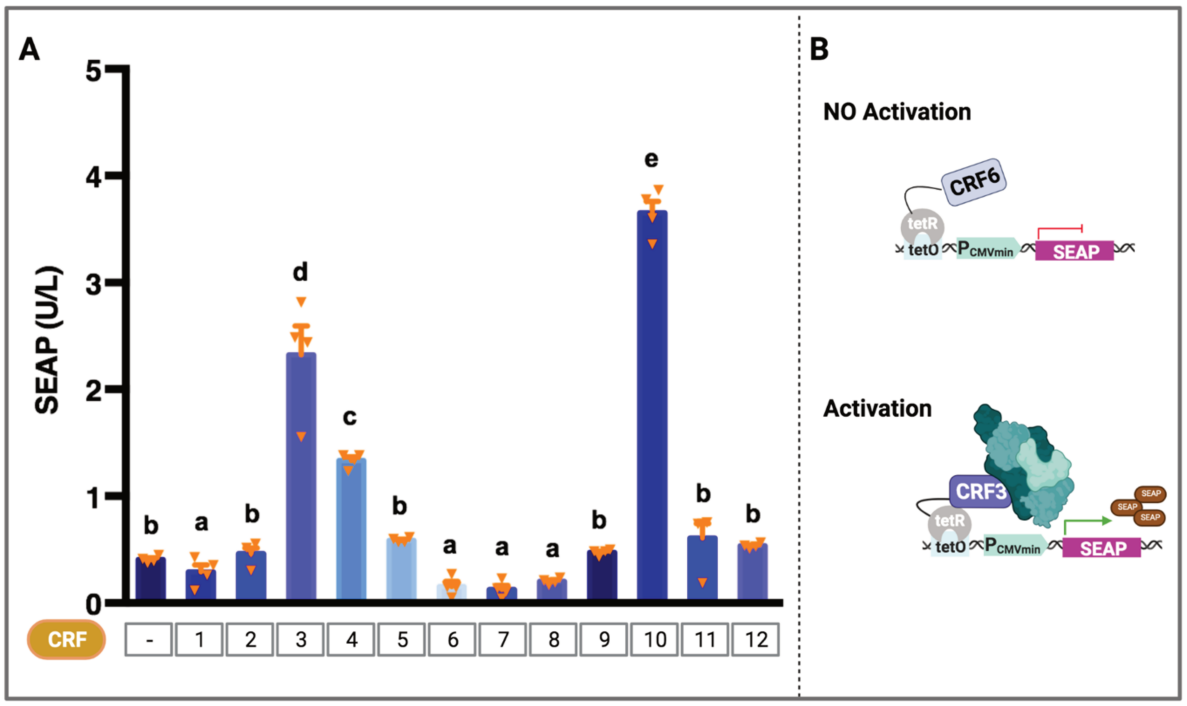

Figure 29. Analysis of the activation of the P_{CMVmin} promoter by tetR-CRFs fusion. **A.** schematic representation of the process under analysis. As transcriptional activators the CRFs may be able to recruit the mammalian transcription machinery and activate SEAP expression, when they are in the proximity of the P_{CMVmin} promoter. **B.** tetR-CRF1 to 12 fusion were independently transfected in CHO cells. SEAP activity is expressed in units per litre (U/L). Data are representative of three independent experiments. Mean and S.E.M. are plotted for n= 4 mammalian samples. The statistical significance was determined using a one-way ANOVA analysis (P value < 0.0001) and is indicated with bold letters. CRF, Cytokinins response regulator; SEAP, Secreted embryonic alkaline phosphatase; tetO, operator motif for the repressor; tetR, tetracycline repressor; VP16, transcriptional activation domain of the Herpes simplex virus.

3.3.3 Chapter Discussion

In this chapter, we showed that neither the subcellular location or the PPI of the CRFs is affected by an increase in CK concentration. Notably, this observation was evidenced with our new mammalian predictive tool and further validated in *Arabidopsi*s protoplasts. Therefore, we suggest that neither the AHP-CRF interactions nor the CRF subcellular distribution can further be used as building blocks for the sensory module of a CK relocation- or FRET-based biosensor. The evidence of the CK-independent subcellular location of the CRFs is in agreement with previous studies using in planta[65,161,162]. Moreover, we provided evidence that all 12 CRFs accumulate in the nucleus of mammalian cells and protoplasts, prior to any hormone addition. Further, the recognition of the CRF monopartite NLSs by the nuclear import machinery of the mammalian cells evidence the interkingdom functionality of these signals. Other examples of interkingdom functionality of the NLSs are the SV40 T-antigen NLS functions in the plants[256] and the single bipartite NLS from the VirD2 protein of the plant pathogen *Agrobacterium* functions in plant, *Xenopus, Drosophila*, mammalian, and yeast cells[257,258].

The analysis of the CRF interactions evidenced that each PPI has a particular strength which may be a reflection of their joint action in plants. In Chapter 2, we showed that AHP6 may negative regulate CK signalling by interacting with the B-ARRs. Therefore, we propose that the AHP6-CRFs interaction can also act as a regulatory mechanism to downregulate CK responses. On the other hand, AHP2 and AHP6 interaction with the two members of the CRF family lacking the conserved C-terminal end, the CRF7 and CFF8, was only evidenced in protoplasts. As well as the CRF12-AHP2 interaction. We thus suggest that PPIs only occurring in protoplasts are promoted by the interaction with other endogenous proteins. In addition, the ability of the CRF to homo-, and heterodimerise may suggest that the CRFs may be binding their targets genes, and activating transcription as a dimer, as previously observed for the B-ARRs[121,154]. Finally, we believe that the strong transactivation of the P_{CMVmin} observed for the tetR-CRF10 fusion could be further exploited for the design of new synthetic modules.

4. **Conclusion**

This work encompasses the design and proof-of-principle characterization of a new predictive platform for the study of CK perception and signalling pathway in orthogonal systems, taking advantage of the molecular toolbox recently expanded by the host team in Düsseeldorf[215,216]

The choice of mammalian cells as chassis for the heterologous expression of the *Arabidopsis* thaliana CK pathway proved to be advantageous for answering questions difficult or impossible to address in plants. For its evolutive proximity to plants, the mammalian model offers a comparable environment with a conserved structure of the membrane, transport/secretion systems, as well as protein folding and degradation. In comparison with bacteria and yeast, moreover, no TCS has been identified in mammalian cells, supporting the study of the CK phospho-relay in this model with low- to non-interference of endogenous kinases or phospho-donors. This assumption is also supported by the general underrepresentation of His-to-Asp phospho-cascades in mammals. Furthermore, the relevance of this platform for future studies that help decipher CK signalling is reaffirmed by the CK-dependent activation of the TCSm at the physiological concentration of the hormone found in plants. In addition, the system presents a high dynamic range of the measurements at different hormone concentrations and a high signal-to-noise ratio. This feature suggests that future exploration of weak promoters or subtle changes in their activation in response to CK can be undertaken in this system. Altogether, the CHO cells platform provided a “free of complexity” environment to trustfully interrogate different events underlying CK response from the perception of the hormone to the transcriptional activation of the target genes.

At the hormone perception level, this platform proved to be suitable for the fast and quantitative screening of the sensitivity and selectivity of the AHK receptors for structurally different CK forms. From isoprenoid- to aromatics CK including an unbound methyl derivate and a riboside as well as synthetic forms as TDZ, we interrogated in a straightforward quantitative assay the differential downstream activation, which can be interpreted as their ability to activate CK responses in plants. In the future, this experimental platform could be implemented for the analysis of new CK analogous or antagonists. However, to ensure unbiased observations, it will be necessary to perform a deep analysis of a possible metabolism of the exogenous CK inside the mammalian cells.

Furthermore, the interaction between the signalling elements acting downstream of the AHK in the signal transduction (the AHPs, the ARRs and the CRFs) was also interrogated. Using a combination of MxH and FRET-APB approaches we were able to screen 160 different TCS components interactions, proposing 50 new PPIs, for the first time with quantitative support. Highlighted is the analysis of AHP6 PPIs, which provided experimental evidence of the mechanism underlying its inhibitory function, showing that it competes with the functional AHPs for the interaction with the B-ARRs. In addition, we could also suggest that ARR7 may form a ternary inhibitory complex with AHP2 and the B-ARRs, and that these PPIs are not dependent on the phosphorylation state. The latter requires further experimental validation that could be used, for example, co-immunoprecipitation in protoplasts. MxH analysis also provided evidence of all possible CRF-AHP interactions. From the many interacting couples, the CRF9 to 12 showed (novel) strong interaction with most AHPs and CRFs, thus suggesting that these less characterized CRFs may as well be involved in CK signalling.

To support our findings in mammalian cells, PPI analysis using the split TF system in *Arabidopsis* protoplasts confirmed 55 of the 60 (re)tested interactions. These results strengthen the suitability of our platform for the interrogation of bona fide plant PPIs, establishing a quantitative framework to obtain a complete TCS interaction map. More broadly, we could aim to build a complete PPI network between the TCS components and the members of another phytohormone pathway. Remarkably, this synthetic approach permits to evidence which interactions are favoured over others by means of quantification, and at the same time provides information on the effect of CK in these interactions. In yeast and plants, the generation of non-phosphorytable mutants is inherent to the study of the role of CK in the interaction (and function) of the TCS components, as otherwise, these proteins will be phosphorylated by the endogenous TCS. Contrary, in our platform, we can simultaneously assess the phosphorylated and unphosphorylated state by merely controlling the exogenous CK added into the medium of the mammalian cells. This unique quality could be exploited to re-characterize previous observed interactions while exploring novel ones.

For example, this synthetic approach could be applied for the study of the link between the GA and CK pathways. It is known that DELLAs function as co-activators of the B-ARRs regulating the expression of TAA1[155] as well as CK response genes[259]. TAA1 is involved in auxin biosynthesis. Thus, the DELLAs-B-ARRs interactions can have a huge impact on the control of auxin responses during embryogenesis and organ formation. Nevertheless, because of

technical limitations, it remains unknown if the complex between these proteins is affected by CK. To explore this, a rapid screen using the MxH approach could provide this information to continue unravelling the intricate crosstalk between CK, GA and auxin. Moreover, it was suggested that the B-ARRs upregulate *GA2* expression. Thus, by engineering a new promoter-reporter system where the *ARR6* promotor from the TCSm is replaced by the *GA2* promotor, this synthetic platform could be used to explore the B-ARR-mediated activation of *GA* expression.

In this study, this type of combined analysis of PPIs and TCSm activation experimentally supported the novel proposal of non-canonical activation of CK responses by ARR1, and a novel regulatory role of the AHPs. Due to the absence of the plant background, we were able to observe that the same AHP providing dose-dependent CK responses after phosphorylation of ARR1 was inhibiting its basal activation in the absence of the hormone. To further nurture this hypothesis, an analysis of the non-phosphorytable AHP2 mutant will need to be conducted. We will then expect that regardless of the addition of CK, ARR1 activity remains blocked, as occurred when AHP2 was replaced by AHP6, a non-phosphorytable AHP. The next step toward understanding the biological relevance of these observations will be to analyse if other members of the AHP family exerts the same regulatory role over ARR1.

Another important contribution of this work to elucidate CK signalling was the identification of two conserved D in ARR1 (D89 and D94). Notably, the constitutive activation of the TCSm of the mutants was not inhibited by AHP2 and only the ARR1(D94A) mutant was no longer able to interact with the HP. This proposes that the conformational change of the REC domain induced by the mutations affected the configuration of the inhibitory complex. A natural progression from these observations will be to obtain and analyse in depth the structure of the AHP2-ARR1 complex. By including the mutants in the analysis, changes in the conformation could provide information on the loss of AHP2 inhibition. Moreover, using mass spectroscopy analysis we could observe the phosphorylation state of the double mutant to finally reveal the main phosphorytable residue/s. Overall this non-canonical behaviour of ARR1 leaves (at least) two open questions: ARR1 putative constitutive activation of CK response is extended to other members of the family? And what is the biological relevance of this novel regulation *in planta*?

Among the plethora of questions that can be addressed using the synthetic approach presented in this work, it will be interesting to explore the CK-dependent repression of ARR6 by WUS protein[23]. WUS function as the main regulator of stem cells fate in the SAM has been long

linked to CK signalling. The repression of A-ARRs by WUS plays a key role in increasing CK responses as part of the coordinated response that established and maintains the SAM. Therefore, testing the influence of CK in the mentioned repression can provide information about the intracellular concentration needed for WUS action in plants. Furthermore, in the same direction, ARR10, and ARR2 had been proved to activate WUS expression[150,162]. Thus, we propose that, to better understand this tight regulation in plants we could transiently express WUS from its natural promotor, instead of constitutively in the mammalian system. This approach will require some fine-tuning of each module concentration and appropriate controls, which may permit to mimic these ARR10→WUS and WUS→A-ARR regulatory cascades.

Despite its exploratory nature, this study offers new insights into the mechanism underlying CK signalling while it reflects the rapid generation of knowledge that can be achieved by the implementation of the vast SynBio toolbox in orthogonal (mammalian) systems. Looking forward, this synthetic approach in combination with a rational experimental design could be implemented as an initial explorative platform to explore a plethora of biological phenomena, for their posterior validation in plants.

5. Material and Methods

5.1 Plasmid construction.

A detailed description of the plasmid construction can be found in Table 4. DNA fragments were either amplified from cDNA or released from previous vectors by PCR with primers provided by Sigma Aldrich (Table 5), using Q5 High-Fidelity DNA Polymerase (New England Biolabs). Gel extractions were performed using NucleoSpin® Gel and PCR Clean-up kit (Macherey-Nagel). All plasmids in this work were assembled using the AQUAcloning method [210] before the transformation into chemically competent Escherichia coli strain 10-beta (NEB). The plasmids were purified using Wizard® Plus SV Minipreps DNA Purification Systems (Promega), NucleoBond® Xtra Midi kit (Macherey-Nagel). All preparations were tested by restriction enzyme digests and sequencing (GATC-biotech/SeqLab). All restriction enzymes were purchased from New England Biolabs. The TCSm promotor-reporter system consists of five direct repeats of the AAAATCTACAA- AATCTTTTTGGATTTTGTGGATTTTCTAGC sequence (core for B-type DNA binding pentamers is underlined), followed by the P_{CMVmin} and SEAP gene.

5.2 Mammalian cell culture and transfection.

Chinese hamster ovary cells (CHO-K1) were cultivated in HAM´s F12 medium (PAN, cat. no. P04-14500) supplemented with 10% fetal calf serum (FCS, PAN, cat. no. P30- 3602) and 1% penicillin/streptomycin (PAN, cat. no. P06-07100) in a 5% CO2 atmosphere at 37°C. Mammalian cells were routinely transfected as described in [260]. Briefly, 50,000 CHO-K1 cells/well were seeded in 500µl HAM cell culture medium 24h before transfection in 24 well plates (Corning). 0.75µg DNA per well was diluted in 50µL OptiMEM (Invitrogen, Thermo Fisher Scientific) and mixed with a polyethyleneimine (PEI)/OptiMEM mix [2.5µL PEI solution (1 mg/ml, Polysciences Europe GmbH cat. no. 23966-1) in 50µL OptiMEM]. After 20 min incubation at RT, 100µl of the transfection mixes were added to each well in a dropwise manner. The medium was exchanged 4h post-transfection. In co-transfections, all plasmids were transfected in equal amounts (weight-based), except stated differently in the text. For

confocal microscopy, 30,000 CHO-K1 cells were seeded onto cover glass slides placed in the 24-well cell culture dishes. Transfection proceeds as explained above.

5.3 CK treatment.

All CK derivates were purchased from OlChemim Ltd and prepared as 10mM stock solution in DMSO. When needed, the hormones were further diluted in miliQ water, with exception of 2-MeSiP which proved only soluble in DMSO. In mammalian-based assays, 24h post-transfection the cultured media was exchanged for 480µl of fresh HAMs medium and 20µl of the corresponding CK dilution for a final concentration per well of 10nM, 20nM, 100nM, 1µM, or 10µM, according to the specific assay. In protoplasts-based measurements, 20µl of the different hormone dilution was applied directly into the protoplasts' suspension. 20µl of sterile miliQ water was used as the control for both assays (0nM CK).

5.4 SEAP reporter assay.

The reporter 472 SEAP was quantified using a colourimetric assay as described previously[261]. In detail, 24h after hormone induction 200µl of the supernatant of the transfected cells was transferred into 96-well round-bottom (Costar) and incubated at 68°C for 1h, to inactivate endogenous phosphatases. Afterwards, 80µL of the heated samples were transferred into 96-well flat-bottom plates (Costar) together with 100µL of SEAP buffer (20mM homoarginine, 1mM MgCl2, 21% (v/v) diethanolamine), and 20µL of 120mM para-Nitrophenylphosphate (pNPP, Sigma-Aldrich). The absorbance of forth technical replicates was measured at 405nm for 1h using a BMG Labtech CLARIOstar multimode plate reader (Berthold Technologies, Bad Wildbad, Germany). Determination of SEAP activity [U/L] was calculated as the slope of the absorbance values [OD/min] using Lambert-Beers´s-law:

$$\frac{U}{L} = \frac{E}{\varepsilon \times d} \cdot 10^6 \cdot \frac{200}{80}$$

E= increase in optical density/para-nitrophenolate per minute; ε=18,600 M^{-1} cm^{-1}, d = length of the light path (cm), 0,6 cm; 200/80= amount of SEAP-containing supernatant (sample dilution factor).

5.5 Normalization assay in mammalian cells.

GLuc activity was quantified to visualize the effect of the hormone treatment in the mammalian cell model, as previously described[262]. Four technical replicates of 80µL of the supernatant of the mammalian cells were transferred into a 96-well white flat-bottom plates (Costar). After the addition of 20µL coelenterazine (472mM stock solution in methanol, diluted 1:1,500 in PBS; Carl Roth, Karlsruhe, Germany, no. 4094.4), the luminescence was measured for 20 min using TriStar2 LB 941 multimode plate readers (Golonka *et al*., 2019).

5.6 *Arabidopsis* leaf mesophyll protoplasts isolation and transformation.

Plants were grown for two weeks on 12cm square plates containing SCA medium (0.32% (wt/vol) Gamborg's B5 basal salt powder with vitamins (bioWORLD), 4 mM MgSO4 7H_2O, 43.8 mM sucrose and 0.8% (wt/vol) phytoagar in H_2O, pH 5.8, autoclaved, 0.1 % (vol/vol) Gamborg's B5 Vitamin Mix (bioWORLD)) a 23 °C, with a 16 h light/ 8 h dark photoperiod. Protoplasts were isolated from the plantlet leaves and transformed as described in[262]. Briefly, *Arabidopsis* leaf material was sliced with a scalpel and incubated in MMC solution (10 mM MES, 40 mM $CaCl_2 \cdot H_2O$, 467 mM mannitol, pH 5.8, sterile filtered) containing 0.5% cellulase Onozuka R10 and macerozyme R10 (SERVA Electrophoresis) and kept in darkness overnight at 23 °C. Protoplasts were then isolated by pipetting, and the suspension was transferred to a MSC solution (10 mM MES, 0.4 M sucrose, 20 mM $MgCl_2 \cdot 6H_2O$, 467 mM mannitol, pH 5.8, sterile filtered) and overlaid with MMM solution (15 mM $MgCl_2$, 5 mM MES, 467 mM mannitol, pH 5.8, sterile filtered). The interphase containing the protoplasts was collected and kept in W5 solution (2 mM MES, 154 mM NaCl, 125 mM $CaCl_2 \cdot 2H_2O$, 5 mM KCl, 5 mM glucose, pH 5.8, sterile filtered), until transformation. Meanwhile, plasmids were pre-mixed distributed in a total amount of 30 µg, and used to transform 500,000 protoplasts by dropwise addition of a polyethylene glycol (PEG) solution (4 g PEG_{4000}, 2.5 ml of 800 mM mannitol, 1 ml of 1 M $CaCl_2$ and 3 ml H_2O). The protoplasts concentration was calculated using the Rosenthal counting chamber. After 8 min incubation, 120 µl MMM and 1,240 µl PCA (0.32% (wt/vol) Gamborg's B5 basal salt powder with vitamins (bioWorld), 2 mM $MgSO_4 \cdot 7H_2O$, 3.4 mM $CaCl_2 \cdot 2H_2O$, 5 mM MES, 0.342 mM l-glutamine, 58.4 mM sucrose, 444 mM glucose, 8.4 µM calcium pantothenate, 2% (vol/vol) biotin from a biotin solution 0.02% (wt/vol) 0.1%

(vol/vol) in H_2O, pH 5.8, sterile filtered, 0.1% (vol/vol) Gamborg's B5 Vitamin Mix, 64.52 µg $µl^{-1}$ ampicillin) were added. After transformation, protoplasts were divided in 24-well plates in 800 µl aliquots (250,000 protoplasts/well).

5.7 **Luciferase assay.**

The reporter gene, FLuc, and the normalization protein RLuc were quantified as detailed previously[262]. Briefly, four replicates of 80 µl protoplasts suspension, containing approximately 25000 protoplasts, were transferred into 2 separated 96-well white flat-bottom plates (Costar) for simultaneous acquisition. 20 µl of either FLuc substrate (0.47 mM d-luciferin (Biosynth AG), 20 mM tricine, 2.67 mM $MgSO_4 \cdot 7H_2O$, 0.1 mM $EDTA \cdot 2H_2$ O,33.3 mM dithiothreitol, 0.52 mM adenosine 5′-triphosphate, 0.27 mM acetyl– coenzyme A, 5 mM NaOH, 264 µM $MgCO_3 \cdot 5H_2O$, in H_2O, pH 8) or RLuc substrate (0.472 mM coelenterazine stock solution in methanol, diluted directly before use, 1:15 in PBS) were added into each well. A 20 min measurement was performed, with integration time of 0,1 s, with either a BertholdTriStar2 S LB 942 multimode plate reader, for RLuc, or with a Berthold Centro XS3 LB 960 microplate luminometer, for FLuc.

5.8 **Fluorescent microscopy**

Transfected cells were fixated onto the microscopy cover glass cells 24 h after treatment with different concentrations of BA, or with H_2O(d). For this, the growing medium was removed and replaced for 200 µL 4% paraformaldehyde (PFA) and incubated for 10 min on ice. After another 10 min incubation, now at room temperature, the PFA was washed with PBS. The coverslips were then embedded in 8 µL of Mowiol 4-88 (Roth) supplemented with 15 mg mL-1 1,4-diazabicyclo[2.2.2]octane (DABCO, Roth) to be mounted onto microscope slides (as described by[208,214]). In order to accelerate drying, the microscope slides were incubated at 37°C for 30 min. Confocal imaging was performed using a Nikon Instruments Eclipse Ti with a C2plus confocal laser scanner, 60X oil objective, NA = 1.45). mCherry and EGFP were visualized using excitation lasers of 561 nm and 488 nm, and emission filters of 570– 1,000 nm, 500–550 nm, respectively. For Cerulean and mVenus we used the excitation lasers of 405 nm and 470 nm, and emission filters of 450-500 nm and 520-550 nm. Image acquisition,

analysis and processing (brightness and contrast) were performed with NIS-Elements Viewer (Nikon Instruments, version 4.20.00).

5.9 FRET Acceptor photobleaching

FRET–APB measurements were operated with the Nikon Instruments Eclipse Ti as mentioned above. NIS elements software (Nikon) using a laser power of 0.1 % of the 488 nm laser and 0.5% for the 561 nm laser to avoid acquisition bleaching of the fluorophores before bleaching. The frame size was kept at 512 x 512 pixels. After 30 seconds of acquisition the mCherry signal was bleached in a region of interest (ROI) with the 561 nm laser at a laser intensity of 100%. Subsequent to bleaching, the fluorescence intensity of both signals was recorded for another 30 seconds. The FRET efficiency was calculated by analysing the percentage of relative changes in EGFP intensity before and after bleaching: EFRET = $((EGFP_{after}-EGFP_{before})/(EGFP_{after})) * 100$. For each condition, 10 cells were analysed and the average EFRET was calculated.

5.10 Software.

The data was analysed using Microsoft Excel (Version 16.26 for Mac Os X) and GraphPad Prism 7 for Mac Os X version 10.13.1. Ordinary one-, and two-way ANOVAs for determination of statistical significance were performed with GraphPad Prism 7 for Mac Os X version 10.13.1. Benchling [Biology Software] (2020) was implemented for cloning, and BioRender.com was selected for graphical design.

5.11 Statistical analysis and reproducibility.

Statistical analysis was performed by using one-, or two-way ANOVA with GraphPad Prism 7.0. Outlier were determined and excluded in all experiments as described in[263]. Data are reported as mean ± SEM of $n \geq 3$ biologically independent replicates. Corresponding *P* values are indicated in the figure captions. All experiments could be reproduced with similar results.

5.12 **Plasmids**

Table 4. Plasmid designed and used in this study. All pEP plasmids were assemble using AQUA cloning[210].

Plasmid				
ID	Description and cloning procedure	Backbone	Insert	Reference
pEP001	Psv40::CRF1-EGFP::Tsv40 Insert was amplified from TAIR clone U83899 with oligos oEP060 and oEP061. Backbone was digested with NotI and CIP	pLH002	CRF1	this work
pEP002	Psv40::CRF2-EGFP::Tsv40 Insert was amplified from TAIR clone U67595 with oligos oEP062 and oEP06. Backbone was digested with NotI and CIP	pLH002	CRF2	this work
pEP003	Psv40::CRF3-EGFP::Tsv40 Insert was amplified from TAIR clone U68286 with oligos oEP064 and oEP065. Backbone was digested with NotI and CIP	pLH002	CRF3	this work
pEP004	Psv40::CRF4-EGFP::Tsv40 Insert was amplified from TAIR clone TOPO-U02-E07 with oligos oEP066 and oEP067 Backbone was digested with NotI and CIP	pLH002	CRF4	this work
pEP005	Psv40::CRF5-EGFP::Tsv40 Insert was amplified from RIKEN clone RAFL14-24-M06 with oligos oEP068 and oEP069 Backbone was digested with NotI and CIP	pLH002	CRF5	this work
pEP006	Psv40::CRF6-EGFP::Tsv40 Insert was amplified from TAIR clone TOPO-U15-D10 with oligos oEP070 and oEP071 Backbone was digested with NotI and CIP	pLH002	CRF6	this work

pEP007	Psv40::CRF7-EGFP::Tsv40 Insert was amplified from TAIR clone U16749 with oligos oEP072 and oEP073 Backbone was digested with NotI and CIP	pLH002	CRF7	this work
pEP008	Psv40::CRF8-EGFP::Tsv40 Insert was amplified from TAIR clone U83435 with oligos oEP074 and oEP075 Backbone was digested with NotI and CIP	pLH002	CRF8	this work
pEP009	Psv40::CRF9-EGFP::Tsv40 Insert was amplified from TAIR clone TOPO-U02-E04 with oligos oEP076 and oEP077 Backbone was digested with NotI and CIP	pLH002	CRF9	this work
pEP010	Psv40::CRF10-EGFP::Tsv40 Insert was amplified from TAIR clone U10932 with oligos oEP078 and oEP079. Backbone was digested with NotI and CIP	pLH002	CRF10	this work
pEP011	Psv40::CRF11-EGFP::Tsv40 Insert was amplified from TAIR clone U87062 with oligos oEP080 and oEP081. Backbone was digested with NotI and CIP	pLH002	CRF11	this work
pEP012	Psv40::CRF12-EGFP::Tsv40 Insert was amplified from TAIR clone TOPO-U04-E11 with oligos oEP082 and oEP083 Backbone was digested with NotI and CIP	pLH002	CRF12	this work
pEP013	Psv40::CRF1-mCherry::Tsv40 Insert was amplified from TAIR clone U83899 with oligos oEP060 and oEP0300 Backbone was digested with NotI and CIP	pEP037	CRF1	this work
pEP014	Psv40::CRF2-mCherry::Tsv40 Insert was amplified from TAIR clone U67595 with oligos oEP062 and oEP301 Backbone was digested with NotI and CIP	pEP037	CRF2	this work

pEP015	Psv40::CRF3-mCherry::Tsv40 Insert was amplified from TAIR clone U68286 with oligos oEP064 and oEP302 Backbone was digested with NotI and CIP	pEP037	CRF3	this work
pEP016	Psv40::CRF4-mCherry::Tsv40 Insert was amplified from TAIR clone TOPO-U02-E07 with oligos oEP066 and oEP303 Backbone was digested with NotI and CIP	pEP037	CRF4	this work
pEP017	Psv40::CRF5-mCherry::Tsv40 Insert was amplified from RIKEN clone RAFL14-24-M06 with oligos oEP068 and oEP304 Backbone was digested with NotI and CIP	pEP037	CRF5	this work
pEP018	Psv40::CRF6-mCherry::Tsv40 Insert was amplified from TAIR clone TOPO-U15-D10 with oligos oEP070 and oEP305 Backbone was digested with NotI and CIP	pEP037	CRF6	this work
pEP019	Psv40::CRF7-mCherry::Tsv40 Insert was amplified from TAIR clone U16749 with oligos oEP072 and oEP306 Backbone was digested with NotI and CIP	pEP037	CRF7	this work
pEP020	Psv40::CRF8-mCherry::Tsv40 Insert was amplified from TAIR clone U83435 with oligos oEP074 and oEP307 Backbone was digested with NotI and CIP	pEP037	CRF8	this work
pEP021	Psv40::CRF9-mCherry::Tsv40 Insert was amplified from TAIR clone TOPO-U02-E04 with oligos oEP076 and oEP308 Backbone was digested with NotI and CIP	pEP037	CRF9	this work

pEP022	Psv40::CRF10-mCherry::Tsv40 Insert was amplified from TAIR clone TOPO-U03-B11 U10932 with oligos oEP078 and oEP309 Backbone was digested with NotI and CIP	pEP037	CRF10	this work
pEP023	Psv40::CRF11-mCherry::Tsv40 Insert was amplified from TAIR clone U87062 with oligos oEP080 and oEP310 Backbone was digested with NotI and CIP	pEP037	CRF11	this work
pEP024	Psv40::CRF12-mCherry::Tsv40 Insert was amplified from TAIR clone TOPO-U04-E11 with oligos oEP082 and oEP311 Backbone was digested with NotI and CIP	pEP037	CRF12	this work
pEP026	P35s::CRF1-EGFP::Tnos Insert was amplified from pEP001 with oligos oEP174 and oEP314 Backbone was digested with AfeI and BamHI	pGEN016	CRF1	this work
pEP027	P35s::CRF2-EGFP::Tnos Insert was amplified from pEP002 with oligos oEP175 and oEP314 Backbone was digested with AfeI and BamHI	pGEN016	CRF2	this work
pEP028	P35s::CRF3-EGFP::Tnos Insert was amplified from pEP003 with oligos oEP176 and oEP314 Backbone was digested with AfeI and BamHI	pGEN016	CRF3	this work
pEP029	P35s::CRF4-EGFP::Tnos Insert was amplified from pEP004 with oligos oEP177 and oEP314 Backbone was digested with AfeI and BamHI	pGEN016	CRF4	this work
pEP030	P35s::CRF5-EGFP::Tnos Insert was amplified from pEP005 with oligos oEP178 and oEP314 Backbone was digested with AfeI and BamHI	pGEN016	CRF5	this work

pEP031	P35s::CRF6-EGFP::Tnos Insert was amplified from pEP006 with oligos oEP179 and oEP314 Backbone was digested with AfeI and BamHI	pGEN016	CRF6	this work
pEP032	P35s::CRF7-EGFP::Tnos Insert was amplified from pEP007 with oligos oEP180 and oEP314 Backbone was digested with AfeI and BamHI	pGEN016	CRF7	this work
pEP033	P35s::CRF8-EGFP::Tnos Insert was amplified from pEP008 with oligos oEP181 and oEP314 Backbone was digested with AfeI and BamHI	pGEN016	CRF8	this work
pEP034	P35s::CRF9-EGFP::Tnos Insert was amplified from pEP009 with oligos oEP182 and oEP314 Backbone was digested with AfeI and BamHI	pGEN016	CRF9	this work
pEP035	P35s::CRF10-EGFP::Tnos Insert was amplified from pEP010 with oligos oEP183 and oEP314 Backbone was digested with AfeI and BamHI	pGEN016	CRF10	this work
pEP036	P35s::CRF11-EGFP::Tnos Insert was amplified from pEP011 with oligos oEP184 and oEP314 Backbone was digested with AfeI and BamHI	pGEN016	CRF11	this work
pEP037	Psv40::mCherry::Tsv40 Insert was amplified from plasmid pEP096 Backbone was digested with NotI and XbaI	pLH002	mCherry	this work
pEP038	Psv40::AHP1-mCherry::Tsv40 Insert was amplified from TAIR clone U09679 with oligos oEP084 and oEP085 Backbone was digested with NotI and CIP	pEP037	AHP1	this work

pEP039	Psv40::AHP2-mCherry::Tsv40 Insert was amplified from TAIR clone U21117 with oligos oEP086 and oEP087 Backbone was digested with NotI and CIP	pEP037	AHP2	this work
pEP040	P35s::CRF12-EGFP::Tnos Insert was amplified from pEP012 with oligos oEP185 and oEP314 Backbone was digested with AfeI and BamHI	pGEN016	CRF12	this work
pEP041	Psv40::AHP3-mCherry::Tsv40 Insert was amplified from TAIR clone U11235 with oligos oEP088 and oEP089 Backbone was digested with NotI and CIP	pEP037	AHP3	this work
pEP042	Psv40::AHP4-mCherry::Tsv40 Insert was amplified from wt A. thaliana COL1 cDNA with oligos oEP090 and oEP091 Backbone was digested with NotI and CIP	pEP037	AHP4	this work
pEP043	Psv40::AHP5-mCherry::Tsv40 Insert was amplified from TAIR clone U89383 with oligos oEP092 and oEP093 Backbone was digested with NotI and CIP	pEP037	AHP5	this work
pEP044	Psv40::AHP6-mCherry::Tsv40 Insert was amplified from wt A. thaliana COL1 cDNA with oligos oEP094 and oEP095 Backbone was digested with NotI and CIP	pEP037	AHP6	this work
pEP046	Psv40::AHK3-mCherry::Tsv40 Insert was amplified from wt A. thaliana COL1 cDNA with oligos oEP078 and oEP079 Backbone was digested with NotI and CIP	pEP037		this work
pEP184	Psv40::CRF1-VP16-NLS(SV40)-IRES(PV)-TetR-AHP1-NLS(SV40)::Tsv40 Insert was amplified from TAIR clone U09679 with oligos oEP217 and oEP089b Backbone was digested with BsrGI and AscI	pEP166	AHP1	this work

pEP185	Psv40::CRF1-VP16-NLS(SV40)-IRES(PV)-TetR-AHP2-NLS(SV40)::Tsv40 Insert was amplified from TAIR clone U21117 with oligos oEP219 and oEP172b Backbone was digested with BsrGI and AscI	pEP166	AHP2	this work
pEP186	Psv40::CRF1-VP16-NLS(SV40)-IRES(PV)-TetR-AHP3-NLS(SV40)::Tsv40 Insert was amplified from TAIR clone U11235with oligos oEP233 and oEP173b Backbone was digested with BsrGI and AscI	pEP166	AHP3	this work
pEP187	Psv40::CRF1-VP16-NLS(SV40)-IRES(PV)-TetR-AHP4-NLS(SV40)::Tsv40 Insert was amplified from wt A. thaliana COL1 cDNA with oligos oEP235 and oEP246b Backbone was digested with BsrGI and AscI	pEP166	AHP4	this work
pEP188	Psv40::CRF1-VP16-NLS(SV40)-IRES(PV)-TetR-AHP5-NLS(SV40)::Tsv40 Insert was amplified from TAIR clone U89383 with oligos oEP237 and oEP247b Backbone was digested with BsrGI and AscI	pEP166	AHP5	this work
pEP189	Psv40::CRF1-VP16-NLS(SV40)-IRES(PV)-TetR-AHP6-NLS(SV40)::Tsv40 Insert was amplified from wt A. thaliana COL1 cDNA with oligos oEP239 and oEP248b Backbone was digested with BsrGI and AscI	pEP166	AHP6	this work
pEP190	Psv40::CRF2-VP16-NLS(SV40)-IRES(PV)-TetR-AHP1-NLS(SV40)::Tsv40 Insert was amplified from TAIR clone U09679 with oligos oEP217 and oEP089b Backbone was digested with BsrGI and AscI	pEP167	AHP1	this work

pEP191	Psv40::CRF2-VP16-NLS(SV40)-IRES(PV)-TetR-AHP2-NLS(SV40)::Tsv40 Insert was amplified from TAIR clone U21117 with oligos oEP219 and oEP172b Backbone was digested with BsrGI and AscI	pEP167	AHP2	this work
pEP192	Psv40::CRF2-VP16-NLS(SV40)-IRES(PV)-TetR-AHP3-NLS(SV40)::Tsv40 Insert was amplified from TAIR clone U11235with oligos oEP233 and oEP173b Backbone was digested with BsrGI and AscI	pEP167	AHP3	this work
pEP193	Psv40::CRF2-VP16-NLS(SV40)-IRES(PV)-TetR-AHP4-NLS(SV40)::Tsv40 Insert was amplified from wt A. thaliana COL1 cDNA with oligos oEP235 and oEP246b Backbone was digested with BsrGI and AscI	pEP167	AHP4	this work
pEP194	Psv40::CRF2-VP16-NLS(SV40)-IRES(PV)-TetR-AHP5-NLS(SV40)::Tsv40 Insert was amplified from TAIR clone U89383 with oligos oEP237 and oEP247b Backbone was digested with BsrGI and AscI	pEP167	AHP5	this work
pEP195	Psv40::CRF2-VP16-NLS(SV40)-IRES(PV)-TetR-AHP6-NLS(SV40)::Tsv40 Insert was amplified from wt A. thaliana COL1 cDNA with oligos oEP239 and oEP248b Backbone was digested with BsrGI and AscI	pEP167	AHP6	this work
pEP196	Psv40::CRF3-VP16-NLS(SV40)-IRES(PV)-TetR-AHP1-NLS(SV40)::Tsv40 Insert was amplified from TAIR clone U09679 with oligos oEP217 and oEP089b Backbone was digested with BsrGI and AscI	pEP168	AHP1	this work

pEP197	Psv40::CRF3-VP16-NLS(SV40)-IRES(PV)-TetR-AHP2-NLS(SV40)::Tsv40 Insert was amplified from TAIR clone U21117 with oligos oEP219 and oEP172b Backbone was digested with BsrGI and AscI	pEP168	AHP2	this work
pEP198	Psv40::CRF3-VP16-NLS(SV40)-IRES(PV)-TetR-AHP3-NLS(SV40)::Tsv40 Insert was amplified from TAIR clone U11235with oligos oEP233 and oEP173b Backbone was digested with BsrGI and AscI	pEP168	AHP3	this work
pEP199	Psv40::CRF3-VP16-NLS(SV40)-IRES(PV)-TetR-AHP4-NLS(SV40)::Tsv40 Insert was amplified from wt A. thaliana COL1 cDNA with oligos oEP235 and oEP246b Backbone was digested with BsrGI and AscI	pEP168	AHP4	this work
pEP200	Psv40::CRF3-VP16-NLS(SV40)-IRES(PV)-TetR-AHP5-NLS(SV40)::Tsv40 Insert was amplified from TAIR clone U89383 with oligos oEP237 and oEP247b Backbone was digested with BsrGI and AscI	pEP168	AHP5	this work
pEP201	Psv40::CRF3-VP16-NLS(SV40)-IRES(PV)-TetR-AHP6-NLS(SV40)::Tsv40 Insert was amplified from wt A. thaliana COL1 cDNA with oligos oEP239 and oEP248b Backbone was digested with BsrGI and AscI	pEP168	AHP6	this work
pEP202	Psv40::CRF4-VP16-NLS(SV40)-IRES(PV)-TetR-AHP1-NLS(SV40)::Tsv40 Insert was amplified from TAIR clone U09679 with oligos oEP217 and oEP089b Backbone was digested with BsrGI and AscI	pEP169	AHP1	this work

pEP203	Psv40::CRF4-VP16-NLS(SV40)-IRES(PV)-TetR-AHP2-NLS(SV40)::Tsv40 Insert was amplified from TAIR clone U21117 with oligos oEP219 and oEP172b Backbone was digested with BsrGI and AscI	pEP169	AHP2	this work
pEP204	Psv40::CRF4-VP16-NLS(SV40)-IRES(PV)-TetR-AHP3-NLS(SV40)::Tsv40 Insert was amplified from TAIR clone U11235with oligos oEP233 and oEP173b Backbone was digested with BsrGI and AscI	pEP169	AHP3	this work
pEP205	Psv40::CRF4-VP16-NLS(SV40)-IRES(PV)-TetR-AHP4-NLS(SV40)::Tsv40 Insert was amplified from wt A. thaliana COL1 cDNA with oligos oEP235 and oEP246b Backbone was digested with BsrGI and AscI	pEP169	AHP4	this work
pEP206	Psv40::CRF4-VP16-NLS(SV40)-IRES(PV)-TetR-AHP5-NLS(SV40)::Tsv40 Insert was amplified from TAIR clone U89383 with oligos oEP237 and oEP247b Backbone was digested with BsrGI and AscI	pEP169	AHP5	this work
pEP207	Psv40::CRF4-VP16-NLS(SV40)-IRES(PV)-TetR-AHP6-NLS(SV40)::Tsv40 Insert was amplified from wt A. thaliana COL1 cDNA with oligos oEP239 and oEP248b Backbone was digested with BsrGI and AscI	pEP169	AHP6	this work
pEP208	Psv40::CRF5-VP16-NLS(SV40)-IRES(PV)-TetR-AHP1-NLS(SV40)::Tsv40 Insert was amplified from TAIR clone U09679 with oligos oEP217 and oEP089b Backbone was digested with BsrGI and AscI	pEP170	AHP1	this work

pEP209	Psv40::CRF5-VP16-NLS(SV40)-IRES(PV)-TetR-AHP2-NLS(SV40)::Tsv40 Insert was amplified from TAIR clone U21117 with oligos oEP219 and oEP172b Backbone was digested with BsrGI and AscI	pEP170	AHP2	this work
pEP210	Psv40::CRF5-VP16-NLS(SV40)-IRES(PV)-TetR-AHP3-NLS(SV40)::Tsv40 Insert was amplified from TAIR clone U11235with oligos oEP233 and oEP173b Backbone was digested with BsrGI and AscI	pEP170	AHP3	this work
pEP211	Psv40::CRF5-VP16-NLS(SV40)-IRES(PV)-TetR-AHP4-NLS(SV40)::Tsv40 Insert was amplified from wt A. thaliana COL1 cDNA with oligos oEP235 and oEP246b Backbone was digested with BsrGI and AscI	pEP170	AHP4	this work
pEP212	Psv40::CRF5-VP16-NLS(SV40)-IRES(PV)-TetR-AHP5-NLS(SV40)::Tsv40 Insert was amplified from TAIR clone U89383 with oligos oEP237 and oEP247b Backbone was digested with BsrGI and AscI	pEP170	AHP5	this work
pEP213	Psv40::CRF5-VP16-NLS(SV40)-IRES(PV)-TetR-AHP6-NLS(SV40)::Tsv40 Insert was amplified from wt A. thaliana COL1 cDNA with oligos oEP239 and oEP248b Backbone was digested with BsrGI and AscI	pEP170	AHP6	this work
pEP214	Psv40::CRF6-VP16-NLS(SV40)-IRES(PV)-TetR-AHP1-NLS(SV40)::Tsv40 Insert was amplified from TAIR clone U09679 with oligos oEP217 and oEP089b Backbone was digested with BsrGI and AscI	pEP171	AHP1	this work

pEP215	Psv40::CRF6-VP16-NLS(SV40)-IRES(PV)-TetR-AHP2-NLS(SV40)::Tsv40 Insert was amplified from TAIR clone U21117 with oligos oEP219 and oEP172b Backbone was digested with BsrGI and AscI	pEP171	AHP2	this work
pEP216	Psv40::CRF6-VP16-NLS(SV40)-IRES(PV)-TetR-AHP3-NLS(SV40)::Tsv40 Insert was amplified from TAIR clone U11235with oligos oEP233 and oEP173b Backbone was digested with BsrGI and AscI	pEP171	AHP3	this work
pEP217	Psv40::CRF6-VP16-NLS(SV40)-IRES(PV)-TetR-AHP4-NLS(SV40)::Tsv40 Insert was amplified from wt A. thaliana COL1 cDNA with oligos oEP235 and oEP246b Backbone was digested with BsrGI and AscI	pEP171	AHP4	this work
pEP218	Psv40::CRF6-VP16-NLS(SV40)-IRES(PV)-TetR-AHP5-NLS(SV40)::Tsv40 Insert was amplified from TAIR clone U89383 with oligos oEP237 and oEP247b Backbone was digested with BsrGI and AscI	pEP171	AHP5	this work
pEP219	Psv40::CRF6-VP16-NLS(SV40)-IRES(PV)-TetR-AHP6-NLS(SV40)::Tsv40 Insert was amplified from wt A. thaliana COL1 cDNA with oligos oEP239 and oEP248b Backbone was digested with BsrGI and AscI	pEP171	AHP6	this work
pEP220	Psv40::CRF7-VP16-NLS(SV40)-IRES(PV)-TetR-AHP1-NLS(SV40)::Tsv40 Insert was amplified from TAIR clone U09679 with oligos oEP217 and oEP089b Backbone was digested with BsrGI and AscI	pEP172	AHP1	this work

pEP221	Psv40::CRF7-VP16-NLS(SV40)-IRES(PV)-TetR-AHP2-NLS(SV40)::Tsv40 Insert was amplified from TAIR clone U21117 with oligos oEP219 and oEP172b Backbone was digested with BsrGI and AscI	pEP172	AHP2	this work
pEP222	Psv40::CRF7-VP16-NLS(SV40)-IRES(PV)-TetR-AHP3-NLS(SV40)::Tsv40 Insert was amplified from TAIR clone U11235with oligos oEP233 and oEP173b Backbone was digested with BsrGI and AscI	pEP172	AHP3	this work
pEP223	Psv40::CRF7-VP16-NLS(SV40)-IRES(PV)-TetR-AHP4-NLS(SV40)::Tsv40 Insert was amplified from wt A. thaliana COL1 cDNA with oligos oEP235 and oEP246b Backbone was digested with BsrGI and AscI	pEP172	AHP4	this work
pEP224	Psv40::CRF7-VP16-NLS(SV40)-IRES(PV)-TetR-AHP5-NLS(SV40)::Tsv40 Insert was amplified from TAIR clone U89383 with oligos oEP237 and oEP247b Backbone was digested with BsrGI and AscI	pEP172	AHP5	this work
pEP225	Psv40::CRF7-VP16-NLS(SV40)-IRES(PV)-TetR-AHP6-NLS(SV40)::Tsv40 Insert was amplified from wt A. thaliana COL1 cDNA with oligos oEP239 and oEP248b Backbone was digested with BsrGI and AscI	pEP172	AHP6	this work
pEP226	Psv40::CRF8-VP16-NLS(SV40)-IRES(PV)-TetR-AHP1-NLS(SV40)::Tsv40 Insert was amplified from TAIR clone U09679 with oligos oEP217 and oEP089b Backbone was digested with BsrGI and AscI	pEP173	AHP1	this work

pEP227	Psv40::CRF8-VP16-NLS(SV40)-IRES(PV)-TetR-AHP2-NLS(SV40)::Tsv40 Insert was amplified from TAIR clone U21117 with oligos oEP219 and oEP172b Backbone was digested with BsrGI and AscI	pEP173	AHP2	this work
pEP228	Psv40::CRF8-VP16-NLS(SV40)-IRES(PV)-TetR-AHP3-NLS(SV40)::Tsv40 Insert was amplified from TAIR clone U11235with oligos oEP233 and oEP173b Backbone was digested with BsrGI and AscI	pEP173	AHP3	this work
pEP229	Psv40::CRF8-VP16-NLS(SV40)-IRES(PV)-TetR-AHP4-NLS(SV40)::Tsv40 Insert was amplified from wt A. thaliana COL1 cDNA with oligos oEP235 and oEP246b Backbone was digested with BsrGI and AscI	pEP173	AHP4	this work
pEP230	Psv40::CRF8-VP16-NLS(SV40)-IRES(PV)-TetR-AHP5-NLS(SV40)::Tsv40 Insert was amplified from TAIR clone U89383 with oligos oEP237 and oEP247b Backbone was digested with BsrGI and AscI	pEP173	AHP5	this work
pEP231	Psv40::CRF8-VP16-NLS(SV40)-IRES(PV)-TetR-AHP6-NLS(SV40)::Tsv40 Insert was amplified from wt A. thaliana COL1 cDNA with oligos oEP239 and oEP248b Backbone was digested with BsrGI and AscI	pEP173	AHP6	this work
pEP232	Psv40::CRF9-VP16-NLS(SV40)-IRES(PV)-TetR-AHP1-NLS(SV40)::Tsv40 Insert was amplified from TAIR clone U09679 with oligos oEP217 and oEP089b Backbone was digested with BsrGI and AscI	pEP174	AHP1	this work

pEP233	Psv40::CRF9-VP16-NLS(SV40)-IRES(PV)-TetR-AHP2-NLS(SV40)::Tsv40 Insert was amplified from TAIR clone U21117 with oligos oEP219 and oEP172b Backbone was digested with BsrGI and AscI	pEP174	AHP2	this work
pEP234	Psv40::CRF9-VP16-NLS(SV40)-IRES(PV)-TetR-AHP3-NLS(SV40)::Tsv40 Insert was amplified from TAIR clone U11235with oligos oEP233 and oEP173b Backbone was digested with BsrGI and AscI	pEP174	AHP3	this work
pEP235	Psv40::CRF9-VP16-NLS(SV40)-IRES(PV)-TetR-AHP4-NLS(SV40)::Tsv40 Insert was amplified from wt A. thaliana COL1 cDNA with oligos oEP235 and oEP246b Backbone was digested with BsrGI and AscI	pEP174	AHP4	this work
pEP236	Psv40::CRF9-VP16-NLS(SV40)-IRES(PV)-TetR-AHP5-NLS(SV40)::Tsv40 Insert was amplified from TAIR clone U89383 with oligos oEP237 and oEP247b Backbone was digested with BsrGI and AscI	pEP174	AHP5	this work
pEP237	Psv40::CRF9-VP16-NLS(SV40)-IRES(PV)-TetR-AHP6-NLS(SV40)::Tsv40 Insert was amplified from wt A. thaliana COL1 cDNA with oligos oEP239 and oEP248b Backbone was digested with BsrGI and AscI	pEP174	AHP6	this work
pEP238	Psv40::CRF10-VP16-NLS(SV40)-IRES(PV)-TetR-AHP1-NLS(SV40)::Tsv40 Insert was amplified from TAIR clone U09679 with oligos oEP217 and oEP089b Backbone was digested with BsrGI and AscI	pEP175	AHP1	this work

pEP239	Psv40::CRF10-VP16-NLS(SV40)-IRES(PV)-TetR-AHP2-NLS(SV40)::Tsv40 Insert was amplified from TAIR clone U21117 with oligos oEP219 and oEP172b Backbone was digested with BsrGI and AscI	pEP175	AHP2	this work
pEP240	Psv40::CRF10-VP16-NLS(SV40)-IRES(PV)-TetR-AHP3-NLS(SV40)::Tsv40 Insert was amplified from TAIR clone U11235with oligos oEP233 and oEP173b Backbone was digested with BsrGI and AscI	pEP175	AHP3	this work
pEP241	Psv40::CRF10-VP16-NLS(SV40)-IRES(PV)-TetR-AHP4-NLS(SV40)::Tsv40 Insert was amplified from wt A. thaliana COL1 cDNA with oligos oEP235 and oEP246b Backbone was digested with BsrGI and AscI	pEP175	AHP4	this work
pEP242	Psv40::CRF10-VP16-NLS(SV40)-IRES(PV)-TetR-AHP5-NLS(SV40)::Tsv40 Insert was amplified from TAIR clone U89383 with oligos oEP237 and oEP247b Backbone was digested with BsrGI and AscI	pEP175	AHP5	this work
pEP243	Psv40::CRF10-VP16-NLS(SV40)-IRES(PV)-TetR-AHP6-NLS(SV40)::Tsv40 Insert was amplified from wt A. thaliana COL1 cDNA with oligos oEP239 and oEP248b Backbone was digested with BsrGI and AscI	pEP175	AHP6	this work
pEP244	Psv40::CRF11-VP16-NLS(SV40)-IRES(PV)-TetR-AHP1-NLS(SV40)::Tsv40 Insert was amplified from TAIR clone U09679 with oligos oEP217 and oEP089b Backbone was digested with BsrGI and AscI	pEP176	AHP1	this work

pEP244	Psv40::CRF11-VP16-NLS(SV40)-IRES(PV)-TetR-AHP2-NLS(SV40)::Tsv40 Insert was amplified from TAIR clone U09679 with oligos oEP217b and oEP080b Backbone was digested with BsrGI and AscI	pEP176	AHP2	this work
pEP246	Psv40::CRF11-VP16-NLS(SV40)-IRES(PV)-TetR-AHP3-NLS(SV40)::Tsv40 Insert was amplified from TAIR clone U11235with oligos oEP233 and oEP173b Backbone was digested with BsrGI and AscI	pEP176	AHP3	this work
pEP247	Psv40::CRF11-VP16-NLS(SV40)-IRES(PV)-TetR-AHP4-NLS(SV40)::Tsv40 Insert was amplified from wt A. thaliana COL1 cDNA with oligos oEP235 and oEP246b Backbone was digested with BsrGI and AscI	pEP176	AHP4	this work
pEP248	Psv40::CRF11-VP16-NLS(SV40)-IRES(PV)-TetR-AHP5-NLS(SV40)::Tsv40 Insert was amplified from TAIR clone U89383 with oligos oEP237 and oEP247b Backbone was digested with BsrGI and AscI	pEP176	AHP5	this work
pEP249	Psv40::CRF11-VP16-NLS(SV40)-IRES(PV)-TetR-AHP6-NLS(SV40)::Tsv40 Insert was amplified from wt A. thaliana COL1 cDNA with oligos oEP239 and oEP248b Backbone was digested with BsrGI and AscI	pEP176	AHP6	this work
pEP250	Psv40::CRF12-VP16-NLS(SV40)-IRES(PV)-TetR-AHP1-NLS(SV40)::Tsv40 Insert was amplified from TAIR clone U09679 with oligos oEP217 and oEP089b Backbone was digested with BsrGI and AscI	pEP177	AHP1	this work

pEP251	Psv40::CRF12-VP16-NLS(SV40)-IRES(PV)-TetR-AHP2-NLS(SV40)::Tsv40 Insert was amplified from TAIR clone U21117 with oligos oEP219 and oEP172b Backbone was digested with BsrGI and AscI	pEP177	AHP2	this work
pEP252	Psv40::CRF12-VP16-NLS(SV40)-IRES(PV)-TetR-AHP3-NLS(SV40)::Tsv40 Insert was amplified from TAIR clone U11235with oligos oEP233 and oEP173b Backbone was digested with BsrGI and AscI	pEP177	AHP3	this work
pEP253	Psv40::CRF12-VP16-NLS(SV40)-IRES(PV)-TetR-AHP4-NLS(SV40)::Tsv40 Insert was amplified from wt A. thaliana COL1 cDNA with oligos oEP235 and oEP246b Backbone was digested with BsrGI and AscI	pEP177	AHP4	this work
pEP254	Psv40::CRF12-VP16-NLS(SV40)-IRES(PV)-TetR-AHP5-NLS(SV40)::Tsv40 Insert was amplified from TAIR clone U89383 with oligos oEP237 and oEP247b Backbone was digested with BsrGI and AscI	pEP177	AHP5	this work
pEP255	Psv40::CRF12-VP16-NLS(SV40)-IRES(PV)-TetR-AHP6-NLS(SV40)::Tsv40 Insert was amplified from wt A. thaliana COL1 cDNA with oligos oEP239 and oEP248b Backbone was digested with BsrGI and AscI	pEP177	AHP6	this work
pEP271	Psv40::CRF3-VP16-NLS(SV40)-IRES(PV)-TetR-CRF1::Tsv40 Insert was amplified from TAIR clone U83899 with oligos oEP0221 and oEP222 Backbone was digested with BsrGI and AscI	pEP168	CRF1	this work

pEP272	Psv40::CRF3-VP16-NLS(SV40)-IRES(PV)-TetR-CRF2::Tsv40 Insert was amplified from TAIR clone U67595 with oligos oEP223 and oEP224 Backbone was digested with BsrGI and AscI	pEP168	CRF2	this work
pEP275	Psv40::CRF3-VP16-NLS(SV40)-IRES(PV)-TetR-CRF5::Tsv40 Insert was amplified from RIKEN clone RAFL14-24-M06 with oligos oEP229 and oEP230 Backbone was digested with BsrGI and AscI	pEP168	CRF5	this work
pEP276	Psv40::CRF3-VP16-NLS(SV40)-IRES(PV)-TetR-CRF6::Tsv40 Insert was amplified from TAIR clone TOPO-U15-D10 with oligos oEP231 and oEP232 Backbone was digested with BsrGI and AscI	pEP168	CRF6	this work
pEP277	Psv40::CRF3-VP16-NLS(SV40)-IRES(PV)-TetR-CRF7::Tsv40 Insert was amplified from TAIR clone U16749 with oligos oEP315 and oEP316 Backbone was digested with BsrGI and AscI	pEP168	CRF7	this work
pEP278	Psv40::CRF3-VP16-NLS(SV40)-IRES(PV)-TetR-CRF8::Tsv40 Insert was amplified from TAIR clone U83435 with oligos oEP317 and oEP318 Backbone was digested with BsrGI and AscI	pEP168	CRF8	this work
pEP279	Psv40::CRF3-VP16-NLS(SV40)-IRES(PV)-TetR-CRF9::Tsv40 Insert was amplified from TAIR clone TOPO-U02-E04 with oligos oEP319 and oEP320 Backbone was digested with BsrGI and AscI	pEP168	CRF9	this work

pEP281	Psv40::CRF3-VP16-NLS(SV40)-IRES(PV)-TetR-CRF11::Tsv40 Insert was amplified from TAIR clone U87062 with oligos oEP323 and oEP324 Backbone was digested with BsrGI and AscI	pEP168	CRF11	this work
pEP282	Psv40::CRF3-VP16-NLS(SV40)-IRES(PV)-TetR-CRF12::Tsv40 Insert was amplified from TAIR clone TOPO-U04-E11 with oligos oEP325 and oEP326 Backbone was digested with BsrGI and AscI	pEP168	CRF12	this work
pEP284	Psv40::CRF5-VP16-NLS(SV40)-IRES(PV)-TetR-CRF2::Tsv40 Insert was amplified from TAIR clone U67595 with oligos oEP223 and oEP224 Backbone was digested with BsrGI and AscI	pEP170	CRF2	this work
pEP287	Psv40::CRF5-VP16-NLS(SV40)-IRES(PV)-TetR-CRF5::Tsv40 Insert was amplified from RIKEN clone RAFL14-24-M06 with oligos oEP229 and oEP230 Backbone was digested with BsrGI and AscI	pEP170	CRF5	this work
pEP288	Psv40::CRF5-VP16-NLS(SV40)-IRES(PV)-TetR-CRF6::Tsv40 Insert was amplified from TAIR clone TOPO-U15-D10 with oligos oEP231 and oEP232 Backbone was digested with BsrGI and AscI	pEP170	CRF6	this work
pEP289	Psv40::CRF6-VP16-NLS(SV40)-IRES(PV)-TetR-CRF1::Tsv40 Insert was amplified from TAIR clone U83899 with oligos oEP0221 and oEP222 Backbone was digested with BsrGI and AscI	pEP171	CRF1	this work

pEP290	Psv40::CRF6-VP16-NLS(SV40)-IRES(PV)-TetR-CRF2::Tsv40 Insert was amplified from TAIR clone U67595 with oligos oEP223 and oEP224 Backbone was digested with BsrGI and AscI	pEP171	CRF2	this work
pEP293	Psv40::CRF6-VP16-NLS(SV40)-IRES(PV)-TetR-CRF5::Tsv40 Insert was amplified from RIKEN clone RAFL14-24-M06 with oligos oEP229 and oEP230 Backbone was digested with BsrGI and AscI	pEP171	CRF5	this work
pEP294	Psv40::CRF6-VP16-NLS(SV40)-IRES(PV)-TetR-CRF6::Tsv40 Insert was amplified from TAIR clone TOPO-U15-D10 with oligos oEP231 and oEP232 Backbone was digested with BsrGI and AscI	pEP171	CRF6	this work
pEP295	Psv40::CRF6-VP16-NLS(SV40)-IRES(PV)-TetR-CRF7::Tsv40 Insert was amplified from TAIR clone U16749 with oligos oEP315 and oEP316 Backbone was digested with BsrGI and AscI	pEP171	CRF7	this work
pEP296	Psv40::CRF6-VP16-NLS(SV40)-IRES(PV)-TetR-CRF8::Tsv40 Insert was amplified from TAIR clone U83435 with oligos oEP317 and oEP318 Backbone was digested with BsrGI and AscI	pEP171	CRF8	this work
pEP297	Psv40::CRF6-VP16-NLS(SV40)-IRES(PV)-TetR-CRF9::Tsv40 Insert was amplified from TAIR clone TOPO-U02-E04 with oligos oEP319 and oEP320 Backbone was digested with BsrGI and AscI	pEP171	CRF9	this work

pEP299	Psv40::CRF6-VP16-NLS(SV40)-IRES(PV)-TetR-CRF11::Tsv40 Insert was amplified from TAIR clone U87062 with oligos oEP323 and oEP324 Backbone was digested with BsrGI and AscI	pEP171	CRF11	this work
pEP300	Psv40::CRF6-VP16-NLS(SV40)-IRES(PV)-TetR-CRF12::Tsv40 Insert was amplified from TAIR clone TOPO-U04-E11 with oligos oEP325 and oEP326 Backbone was digested with BsrGI and AscI	pEP171	CRF12	this work
pEP301	Psv40::CRF5-VP16-NLS(SV40)-IRES(PV)-TetR-CRF7::Tsv40 Insert was amplified from TAIR clone U16749 with oligos oEP315 and oEP316 Backbone was digested with BsrGI and AscI	pEP170	CRF7	this work
pEP302	Psv40::CRF5-VP16-NLS(SV40)-IRES(PV)-TetR-CRF8::Tsv40 Insert was amplified from TAIR clone U83435 with oligos oEP317 and oEP318 Backbone was digested with BsrGI and AscI	pEP170	CRF8	this work
pEP303	Psv40::CRF5-VP16-NLS(SV40)-IRES(PV)-TetR-CRF9::Tsv40 Insert was amplified from TAIR clone TOPO-U02-E04 with oligos oEP319 and oEP320 Backbone was digested with BsrGI and AscI	pEP170	CRF9	this work
pEP304	Psv40::CRF5-VP16-NLS(SV40)-IRES(PV)-TetR-CRF10::Tsv40 Insert was amplified from TAIR clone U10932 with oligos oEP321 and oEP322 Backbone was digested with BsrGI and AscI	pEP170	CRF10	this work

pEP305	Psv40::CRF5-VP16-NLS(SV40)-IRES(PV)-TetR-CRF11::Tsv40 Insert was amplified from TAIR clone U87062 with oligos oEP323 and oEP324 Backbone was digested with BsrGI and AscI	pEP170	CRF11	this work
pEP306	Psv40::CRF5-VP16-NLS(SV40)-IRES(PV)-TetR-CRF12::Tsv40 Insert was amplified from TAIR clone TOPO-U04-E11 with oligos oEP325 and oEP326 Backbone was digested with BsrGI and AscI	pEP170	CRF12	this work
pEP350	Psv40::YPD1::mVenus::Tsv40 YPD1 was amplified from S. cerevisiae strain ATCC 204508 / S288c genomic DNA with oligos oEP274 and oEP275. mVenus was amplified from pRD093 with oligos oEP288 and oEP289. Backbone was digested with NotI and XbaI	pLH002	YPD1 and mVenus	this work
pEP356	Psv40::EGFP-CRF1::Tsv40 Insert was amplified from TAIR clone U83899 with oligos oEP136 and oEP137 Backbone was digested with BsrGI and CIP	pLH002	CRF1	this work
pEP357	Psv40::EGFP-CRF2::Tsv40 Insert was amplified from TAIR clone U67595 with oligos oEP138 and oEP139 Backbone was digested with BsrGI and CIP	pLH002	CRF2	this work
pEP358	Psv40::EGFP-CRF3::Tsv40 Insert was amplified from TAIR clone U68286 with oligos oEP140 and oEP141 Backbone was digested with BsrGI and CIP	pLH002	CRF3	this work
pEP359	Psv40::EGFP-CRF4::Tsv40 Insert was amplified from TAIR clone TOPO-U02-E07 with oligos oEP142 and oEP143 Backbone was digested with BsrGI and CIP	pLH002	CRF4	this work

pEP360	Psv40::EGFP-CRF5::Tsv40 Insert was amplified from TAIR clone TOPO-U02-E07 with oligos oEP144 and oEP145 Backbone was digested with BsrGI and CIP	pLH002	CRF5	this work
pEP361	Psv40::EGFP-CRF6::Tsv40 Insert was amplified from TAIR clone TOPO-U15-D10 with oligos oEP146 and oEP147 Backbone was digested with BsrGI and CIP	pLH002	CRF6	this work
pEP362	Psv40::EGFP-CRF7::Tsv40 Insert was amplified from TAIR clone U16749 with oligos oEP148 and oEP149 Backbone was digested with BsrGI and CIP	pLH002	CRF7	this work
pEP363	Psv40::EGFP-CRF8::Tsv40 Insert was amplified from TAIR clone U83435 with oligos oEP150 and oEP151 Backbone was digested with BsrGI and CIP	pLH002	CRF8	this work
pEP364	Psv40::EGFP-CRF9::Tsv40 Insert was amplified from TAIR clone TOPO-U02-E04 with oligos oEP152 and oEP153 Backbone was digested with BsrGI and CIP	pLH002	CRF9	this work
pEP365	Psv40::EGFP-CRF10::Tsv40 Insert was amplified from TAIR clone U10932 with oligos oEP154 and oEP155 Backbone was digested with BsrGI and CIP	pLH002	CRF10	this work
pEP366	Psv40::EGFP-CRF11::Tsv40 Insert was amplified from TAIR clone U87062 with oligos oEP156 and oEP157 Backbone was digested with BsrGI and CIP	pLH002	CRF11	this work
pEP367	Psv40::EGFP-CRF12::Tsv40 Insert was amplified from TAIR clone TOPO-U04-E11 with oligos oEP158 and oEP159 Backbone was digested with BsrGI and CIP	pLH002	CRF12	this work

pEP379	Psv40::AHP2-VP16-NLS(SV40)-IRES(PV)-TetR-AHP6-NLS(SV40)::Tsv40 Insert was amplified from wt A. thaliana COL1 cDNA with oligos oEP239 and oEP248b Backbone was digested with BsrGI and AscI	pEP179	AHP6	this work
pEP380	Psv40::CRF1-VP16-NLS(SV40)-IRES(PV)-TetR-CRF1::Tsv40 Insert was amplified from TAIR clone U83899 with oligos oEP0221 and oEP222 Backbone was digested with BsrGI and AscI	pEP166	CRF1	this work
pEP381	Psv40::CRF1-VP16-NLS(SV40)-IRES(PV)-TetR-CRF2::Tsv40 Insert was amplified from TAIR clone U67595 with oligos oEP223 and oEP224 Backbone was digested with BsrGI and AscI	pEP166	CRF2	this work
pEP384	Psv40::CRF1-VP16-NLS(SV40)-IRES(PV)-TetR-CRF5::Tsv40 Insert was amplified from RIKEN clone RAFL14-24-M06 with oligos oEP229 and oEP230 Backbone was digested with BsrGI and AscI	pEP166	CRF5	this work
pEP440	Psv40::CRF1-VP16-NLS(SV40)-IRES(PV)-TetR-CRF7::Tsv40 Insert was amplified from TAIR clone U16749 with oligos oEP315 and oEP316 Backbone was digested with BsrGI and AscI	pEP166	CRF7	this work
pEP441	Psv40::CRF1-VP16-NLS(SV40)-IRES(PV)-TetR-CRF8::Tsv40 Insert was amplified from TAIR clone U83435 with oligos oEP317 and oEP318 Backbone was digested with BsrGI and AscI	pEP166	CRF8	this work

pEP442	Psv40::CRF1-VP16-NLS(SV40)-IRES(PV)-TetR-CRF9::Tsv40 Insert was amplified from TAIR clone TOPO-U02-E04 with oligos oEP319 and oEP320 Backbone was digested with BsrGI and AscI	pEP166	CRF9	this work
pEP444	Psv40::CRF1-VP16-NLS(SV40)-IRES(PV)-TetR-CRF11::Tsv40 Insert was amplified from TAIR clone U87062 with oligos oEP323 and oEP324 Backbone was digested with BsrGI and AscI	pEP166	CRF11	this work
pEP445	Psv40::CRF1-VP16-NLS(SV40)-IRES(PV)-TetR-CRF12::Tsv40 Insert was amplified from TAIR clone TOPO-U04-E11 with oligos oEP325 and oEP326 Backbone was digested with BsrGI and AscI	pEP166	CRF12	this work
pEP446	Psv40::CRF2-VP16-NLS(SV40)-IRES(PV)-TetR-CRF1::Tsv40 Insert was amplified from TAIR clone U83899 with oligos oEP0221 and oEP222 Backbone was digested with BsrGI and AscI	pEP167	CRF1	this work
pEP447	Psv40::CRF2-VP16-NLS(SV40)-IRES(PV)-TetR-CRF2::Tsv40 Insert was amplified from TAIR clone U67595 with oligos oEP223 and oEP224 Backbone was digested with BsrGI and AscI	pEP167	CRF2	this work
pEP452	Psv40::CRF2-VP16-NLS(SV40)-IRES(PV)-TetR-CRF7::Tsv40 Insert was amplified from TAIR clone U16749 with oligos oEP315 and oEP316 Backbone was digested with BsrGI and AscI	pEP167	CRF7	this work

pEP453	Psv40::CRF2-VP16-NLS(SV40)-IRES(PV)-TetR-CRF8::Tsv40 Insert was amplified from TAIR clone U83435 with oligos oEP317 and oEP318 Backbone was digested with BsrGI and AscI	pEP167	CRF8	this work
pEP454	Psv40::CRF2-VP16-NLS(SV40)-IRES(PV)-TetR-CRF9::Tsv40 Insert was amplified from TAIR clone TOPO-U02-E04 with oligos oEP319 and oEP320 Backbone was digested with BsrGI and AscI	pEP167	CRF9	this work
pEP456	Psv40::CRF2-VP16-NLS(SV40)-IRES(PV)-TetR-CRF11::Tsv40 Insert was amplified from TAIR clone U87062 with oligos oEP323 and oEP324 Backbone was digested with BsrGI and AscI	pEP167	CRF11	this work
pEP457	Psv40::CRF2-VP16-NLS(SV40)-IRES(PV)-TetR-CRF12::Tsv40 Insert was amplified from TAIR clone TOPO-U04-E11 with oligos oEP325 and oEP326 Backbone was digested with BsrGI and AscI	pEP167	CRF12	this work
pEP458	Psv40::CRF4-VP16-NLS(SV40)-IRES(PV)-TetR-CRF1::Tsv40 Insert was amplified from TAIR clone U83899 with oligos oEP0221 and oEP222 Backbone was digested with BsrGI and AscI	pEP169	CRF1	this work
pEP459	Psv40::CRF4-VP16-NLS(SV40)-IRES(PV)-TetR-CRF2::Tsv40 Insert was amplified from TAIR clone U67595 with oligos oEP223 and oEP224 Backbone was digested with BsrGI and AscI	pEP169	CRF2	this work

pEP464	Psv40::CRF4-VP16-NLS(SV40)-IRES(PV)-TetR-CRF7::Tsv40 Insert was amplified from TAIR clone U16749 with oligos oEP315 and oEP316 Backbone was digested with BsrGI and AscI	pEP169	CRF7	this work
pEP465	Psv40::CRF4-VP16-NLS(SV40)-IRES(PV)-TetR-CRF8::Tsv40 Insert was amplified from TAIR clone U83435 with oligos oEP317 and oEP318 Backbone was digested with BsrGI and AscI	pEP169	CRF8	this work
pEP466	Psv40::CRF4-VP16-NLS(SV40)-IRES(PV)-TetR-CRF9::Tsv40 Insert was amplified from TAIR clone TOPO-U02-E04 with oligos oEP319 and oEP320 Backbone was digested with BsrGI and AscI	pEP169	CRF9	this work
pEP468	Psv40::CRF4-VP16-NLS(SV40)-IRES(PV)-TetR-CRF11::Tsv40 Insert was amplified from TAIR clone U87062 with oligos oEP323 and oEP324 Backbone was digested with BsrGI and AscI	pEP169	CRF11	this work
pEP469	Psv40::CRF4-VP16-NLS(SV40)-IRES(PV)-TetR-CRF12::Tsv40 Insert was amplified from TAIR clone TOPO-U04-E11 with oligos oEP325 and oEP326 Backbone was digested with BsrGI and AscI	pEP169	CRF12	this work
pEP470	Psv40::CRF7-VP16-NLS(SV40)-IRES(PV)-TetR-CRF1::Tsv40 Insert was amplified from TAIR clone U83899 with oligos oEP0221 and oEP222 Backbone was digested with BsrGI and AscI	pEP172	CRF1	this work

pEP471	Psv40::CRF7-VP16-NLS(SV40)-IRES(PV)-TetR-CRF2::Tsv40 Insert was amplified from TAIR clone U67595 with oligos oEP223 and oEP224 Backbone was digested with BsrGI and AscI	pEP172	CRF2	this work
pEP476	Psv40::CRF7-VP16-NLS(SV40)-IRES(PV)-TetR-CRF7::Tsv40 Insert was amplified from TAIR clone U16749 with oligos oEP315 and oEP316 Backbone was digested with BsrGI and AscI	pEP172	CRF7	this work
pEP477	Psv40::CRF7-VP16-NLS(SV40)-IRES(PV)-TetR-CRF8::Tsv40 Insert was amplified from TAIR clone U83435 with oligos oEP317 and oEP318 Backbone was digested with BsrGI and AscI	pEP172	CRF8	this work
pEP478	Psv40::CRF7-VP16-NLS(SV40)-IRES(PV)-TetR-CRF9::Tsv40 Insert was amplified from TAIR clone TOPO-U02-E04 with oligos oEP319 and oEP320 Backbone was digested with BsrGI and AscI	pEP172	CRF9	this work
pEP480	Psv40::CRF7-VP16-NLS(SV40)-IRES(PV)-TetR-CRF11::Tsv40 Insert was amplified from TAIR clone U87062 with oligos oEP323 and oEP324 Backbone was digested with BsrGI and AscI	pEP172	CRF11	this work
pEP481	Psv40::CRF7-VP16-NLS(SV40)-IRES(PV)-TetR-CRF12::Tsv40 Insert was amplified from TAIR clone TOPO-U04-E11 with oligos oEP325 and oEP326 Backbone was digested with BsrGI and AscI	pEP172	CRF12	this work

pEP482	Psv40::CRF8-VP16-NLS(SV40)-IRES(PV)-TetR-CRF1::Tsv40 Insert was amplified from TAIR clone U83899 with oligos oEP0221 and oEP222 Backbone was digested with BsrGI and AscI	pEP173	CRF1	this work
pEP483	Psv40::CRF8-VP16-NLS(SV40)-IRES(PV)-TetR-CRF2::Tsv40 Insert was amplified from TAIR clone U67595 with oligos oEP223 and oEP224 Backbone was digested with BsrGI and AscI	pEP173	CRF2	this work
pEP489	Psv40::CRF8-VP16-NLS(SV40)-IRES(PV)-TetR-CRF8::Tsv40 Insert was amplified from TAIR clone U83435 with oligos oEP317 and oEP318 Backbone was digested with BsrGI and AscI	pEP173	CRF8	this work
pEP490	Psv40::CRF8-VP16-NLS(SV40)-IRES(PV)-TetR-CRF9::Tsv40 Insert was amplified from TAIR clone TOPO-U02-E04 with oligos oEP319 and oEP320 Backbone was digested with BsrGI and AscI	pEP173	CRF9	this work
pEP492	Psv40::CRF8-VP16-NLS(SV40)-IRES(PV)-TetR-CRF11::Tsv40 Insert was amplified from TAIR clone U87062 with oligos oEP323 and oEP324 Backbone was digested with BsrGI and AscI	pEP173	CRF11	this work
pEP493	Psv40::CRF8-VP16-NLS(SV40)-IRES(PV)-TetR-CRF12::Tsv40 Insert was amplified from TAIR clone TOPO-U04-E11 with oligos oEP325 and oEP326 Backbone was digested with BsrGI and AscI	pEP173	CRF12	this work

pEP494	Psv40::CRF9-VP16-NLS(SV40)-IRES(PV)-TetR-CRF1::Tsv40 Insert was amplified from TAIR clone U83899 with oligos oEP0221 and oEP222 Backbone was digested with BsrGI and AscI	pEP174	CRF1	this work
pEP495	Psv40::CRF9-VP16-NLS(SV40)-IRES(PV)-TetR-CRF2::Tsv40 Insert was amplified from TAIR clone U67595 with oligos oEP223 and oEP224 Backbone was digested with BsrGI and AscI	pEP174	CRF2	this work
pEP503	Psv40::CRF9-VP16-NLS(SV40)-IRES(PV)-TetR-CRF9::Tsv40 Insert was amplified from TAIR clone TOPO-U02-E04 with oligos oEP319 and oEP320 Backbone was digested with BsrGI and AscI	pEP174	CRF9	this work
pEP505	Psv40::CRF9-VP16-NLS(SV40)-IRES(PV)-TetR-CRF11::Tsv40 Insert was amplified from TAIR clone U87062 with oligos oEP323 and oEP324 Backbone was digested with BsrGI and AscI	pEP174	CRF11	this work
pEP506	Psv40::CRF9-VP16-NLS(SV40)-IRES(PV)-TetR-CRF12::Tsv40 Insert was amplified from TAIR clone TOPO-U04-E11 with oligos oEP325 and oEP326 Backbone was digested with BsrGI and AscI	pEP174	CRF12	this work
pEP507	Psv40::CRF10-VP16-NLS(SV40)-IRES(PV)-TetR-CRF1::Tsv40 Insert was amplified from TAIR clone U83899 with oligos oEP0221 and oEP222 Backbone was digested with BsrGI and AscI	pEP175	CRF1	this work

pEP508	Psv40::CRF10-VP16-NLS(SV40)-IRES(PV)-TetR-CRF2::Tsv40 Insert was amplified from TAIR clone U67595 with oligos oEP223 and oEP224 Backbone was digested with BsrGI and AscI	pEP175	CRF2	this work
pEP511	Psv40::CRF10-VP16-NLS(SV40)-IRES(PV)-TetR-CRF5::Tsv40 Insert was amplified from RIKEN clone RAFL14-24-M06 with oligos oEP229 and oEP230 Backbone was digested with BsrGI and AscI	pEP175	CRF5	this work
pEP512	Psv40::CRF10-VP16-NLS(SV40)-IRES(PV)-TetR-CRF6::Tsv40 Insert was amplified from TAIR clone TOPO-U15-D10 with oligos oEP231 and oEP232 Backbone was digested with BsrGI and AscI	pEP175	CRF6	this work
pEP513	Psv40::CRF10-VP16-NLS(SV40)-IRES(PV)-TetR-CRF7::Tsv40 Insert was amplified from TAIR clone U16749 with oligos oEP315 and oEP316 Backbone was digested with BsrGI and AscI	pEP175	CRF7	this work
pEP514	Psv40::CRF10-VP16-NLS(SV40)-IRES(PV)-TetR-CRF8::Tsv40 Insert was amplified from TAIR clone U83435 with oligos oEP317 and oEP318 Backbone was digested with BsrGI and AscI	pEP175	CRF8	this work
pEP515	Psv40::CRF10-VP16-NLS(SV40)-IRES(PV)-TetR-CRF9::Tsv40 Insert was amplified from TAIR clone TOPO-U02-E04 with oligos oEP319 and oEP320 Backbone was digested with BsrGI and AscI	pEP175	CRF9	this work

pEP517	Psv40::CRF10-VP16-NLS(SV40)-IRES(PV)-TetR-CRF11::Tsv40 Insert was amplified from TAIR clone U87062 with oligos oEP323 and oEP324 Backbone was digested with BsrGI and AscI	pEP175	CRF11	this work
pEP518	Psv40::CRF10-VP16-NLS(SV40)-IRES(PV)-TetR-CRF12::Tsv40 Insert was amplified from TAIR clone TOPO-U04-E11 with oligos oEP325 and oEP326 Backbone was digested with BsrGI and AscI	pEP175	CRF12	this work
pEP519	Psv40::CRF11-VP16-NLS(SV40)-IRES(PV)-TetR-CRF1::Tsv40 Insert was amplified from TAIR clone U83899 with oligos oEP0221 and oEP222 Backbone was digested with BsrGI and AscI	pEP176	CRF1	this work
pEP520	Psv40::CRF11-VP16-NLS(SV40)-IRES(PV)-TetR-CRF2::Tsv40 Insert was amplified from TAIR clone U67595 with oligos oEP223 and oEP224 Backbone was digested with BsrGI and AscI +E210	pEP176	CRF2	this work
pEP529	Psv40::CRF11-VP16-NLS(SV40)-IRES(PV)-TetR-CRF11::Tsv40 Insert was amplified from TAIR clone U87062 with oligos oEP323 and oEP324 Backbone was digested with BsrGI and AscI	pEP176	CRF11	this work
pEP530	Psv40::CRF11-VP16-NLS(SV40)-IRES(PV)-TetR-CRF12::Tsv40 Insert was amplified from TAIR clone TOPO-U04-E11 with oligos oEP325 and oEP326. Backbone was digested with BsrGI and AscI.	pEP176	CRF12	this work
pEP531	Psv40::CRF12-VP16-NLS(SV40)-IRES(PV)-TetR-CRF1::Tsv40 Insert was amplified from TAIR clone U83899 with oligos oEP0221 and oEP222. Backbone was digested with BsrGI and AscI.	pEP177	CRF1	this work

pEP532	Psv40::CRF12-VP16-NLS(SV40)-IRES(PV)-TetR-CRF2::Tsv40 Insert was amplified from TAIR clone U67595 with oligos oEP223 and oEP224. Backbone was digested with BsrGI and AscI.	pEP177	CRF2	this work
pEP542	Psv40::CRF12-VP16-NLS(SV40)-IRES(PV)-TetR-CRF12::Tsv40 Insert was amplified from TAIR clone TOPO-U04-E11 with oligos oEP325 and oEP326. Backbone was digested with BsrGI and AscI.	pEP177	CRF12	this work
pEP548	Psv40::PHYB-VP16-NLS(SV40)-IRES(PV)-TetR-CRF1::Tsv40 Insert was amplified from TAIR clone U83899 with oligos oEP0221 and oEP222. Backbone was digested with BsrGI and AscI.	pPF001	CRF1	this work
pEP549	Psv40::PHYB-VP16-NLS(SV40)-IRES(PV)-TetR-CRF2::Tsv40 Insert was amplified from TAIR clone U67595 with oligos oEP223 and oEP224. Backbone was digested with BsrGI and AscI.	pPF001	CRF2	this work
pEP550	Psv40::PHYB-VP16-NLS(SV40)-IRES(PV)-TetR-CRF3::Tsv40 Insert was amplified from TAIR clone U68286 with oligos oEP225 and oEP226. Backbone was digested with BsrGI and AscI.	pPF001	CRF3	this work
pEP551	Psv40::PHYB-VP16-NLS(SV40)-IRES(PV)-TetR-CRF4::Tsv40 Insert was amplified from TAIR clone TOPO-U02-E07 with oligos oEP227 and oEP228. Backbone was digested with BsrGI and AscI.	pPF001	CRF4	this work
pEP552	Psv40::PHYB-VP16-NLS(SV40)-IRES(PV)-TetR-CRF5::Tsv40 Insert was amplified from RIKEN clone RAFL14-24-M06 with oligos oEP229 and oEP230. Backbone was digested with BsrGI and AscI.	pPF001	CRF5	this work

pEP553	Psv40::PHYB-VP16-NLS(SV40)-IRES(PV)-TetR-CRF6::Tsv40 Insert was amplified from TAIR clone TOPO-U15-D10 with oligos oEP231 and oEP232. Backbone was digested with BsrGI and AscI.	pPF001	CRF6	this work
pEP554	Psv40::PHYB-VP16-NLS(SV40)-IRES(PV)-TetR-CRF7::Tsv40 Insert was amplified from TAIR clone U16749 with oligos oEP315 and oEP316. Backbone was digested with BsrGI and AscI.	pPF001	CRF7	this work
pEP555	Psv40::PHYB-VP16-NLS(SV40)-IRES(PV)-TetR-CRF8::Tsv40 Insert was amplified from TAIR clone U83435 with oligos oEP317 and oEP318. Backbone was digested with BsrGI and AscI.	pPF001	CRF8	this work
pEP556	Psv40::PHYB-VP16-NLS(SV40)-IRES(PV)-TetR-CRF9::Tsv40 Insert was amplified from TAIR clone TOPO-U02-E04 with oligos oEP319 and oEP320. Backbone was digested with BsrGI and AscI.	pPF001	CRF9	this work
pEP557	Psv40::PHYB-VP16-NLS(SV40)-IRES(PV)-TetR-CRF10::Tsv40 Insert was amplified from TAIR clone U10932 with oligos oEP321 and oEP322. Backbone was digested with BsrGI and AscI.	pPF001	CRF10	this work
pEP558	Psv40::PHYB-VP16-NLS(SV40)-IRES(PV)-TetR-CRF11::Tsv40 Insert was amplified from TAIR clone U87062 with oligos oEP323 and oEP324. Backbone was digested with BsrGI and AscI.	pPF001	CRF11	this work
pEP559	Psv40::PHYB-VP16-NLS(SV40)-IRES(PV)-TetR-CRF12::Tsv40 Insert was amplified from TAIR clone TOPO-U04-E11 with oligos oEP325 and oEP326. Backbone was digested with BsrGI and AscI.	pPF001	CRF12	this work

pEP602	P35s::RLUC::Tnos Insert was amplified from GB109 with oligos oEP368 and oEP369. Backbone (previously digested and religated with XhoI) was digested with SspI + CIP.	pROF052	PP35s:: RLUC::Tnos	this work
pEP701	P35s::CRF1-VP16-NLS(SV40)::Tnos Insert was amplified with oligos oEP174 and oEP521 from pEP001. Backbone was digested with AfeI amd EcoRI.	pEP708	CRF1	this work
pEP702	P35s::CRF2-VP16-NLS(SV40)::Tnos VP16NLS(SV40) was amplified fron pKT289 with oligos oEP451 and oEP476. CRF2 was amplified from pEP002 with oligos oEP175 and oEP464. Backbone was digested with AgeI and BamH1	pGEN016	VP16NLS(SV40) and CRF2	this work
pEP703	P35s::CRF3-VP16-NLS(SV40)::Tnos Insert was amplified fron pKT289 with oligos oEP451 and oEP454. Backbone was digested with EcoRI and XhoI	pEP028	VP16NLS(SV40)	this work
pEP704	P35s::CRF4-VP16-NLS(SV40)::Tnos Insert was amplified fron pKT289 with oligos oEP451 and oEP455. Backbone was digested with EcoRI and XhoI	pEP029	VP16NLS(SV40)	this work
pEP705	P35s::CRF5-VP16-NLS(SV40)::Tnos VP16NLS(SV40) was amplified fron pKT289 with oligos oEP451 and oEP476. CRF5 was amplified from pEP002 with oligos oEP178 and oEP465. Backbone was digested with AgeI and BamHI	pGEN016	VP16NLS(SV40) and CRF5	this work
pEP706	P35s::CRF6-VP16-NLS(SV40)::Tnos Insert was amplified fron pKT289 with oligos oEP451 and oEP457. Backbone was digested with EcoRI and XhoI	pEP031	VP16NLS(SV40)	this work
pEP707	P35s::CRF7-VP16-NLS(SV40)::Tnos Insert was amplified fron pKT289 with oligos oEP451 and oEP458. Backbone was digested with EcoRI and XhoI	pEP032	VP16NLS(SV40)	this work

pEP708	P35s::CRF8-VP16-NLS(SV40)::Tnos Insert was amplified fron pKT289 with oligos oEP451 and oEP459 Backbone was digested with EcoRI and XbaI	pEP033	VP16NLS(SV40)	this work
pEP709	P35s::CRF9-VP16-NLS(SV40)::Tnos VP16NLS(SV40) was amplified fron pKT289 with oligos oEP451 and oEP460; CRF9 was amplified from pEP002 with oligos oEP182 and oEP466, Backbone was digested with AgeI and BamHI	pGEN016	VP16NLS(SV40)and CRF9	this work
pEP710	P35s::CRF10-VP16-NLS(SV40)::Tnos Insert was amplified from pEP010 with oligos oEP183 and oEP520. Backbone was digested with AfeI amd EcoRI. Products were assembled into backbone using AQUA cloning	pEP708	CRF10	this work
pEP711	P35s::CRF11-VP16-NLS(SV40)::Tnos VP16NLS(SV40) was amplified fron pKT289 with oligos oEP451 and oEP462. Backbone was digested with EcoRI and XbaI	pEP036	CRF11	this work
pEP712	P35s::CRF12-VP16-NLS(SV40)::Tnos VP16NLS(SV40) was amplified fron pKT289 with oligos oEP451 and oEP476. CRF12 was amplified from pEP002 with oligos oEP470 and oEP467. Backbone was digested with AgeI and BamHI	pGEN016	VP16NLS(SV40) and CRF12	this work
pEP713	P35s::E-AHP1-NLS(SV40)::Tnos E was amplified fron pKT289 with oligos oEP468 and oEP469 AHP1:NLS(SV40) was amplified from pEP386 with oligos oEP470 and oEP476 Backbone was digested with AgeI and BamHI	pGEN016	E Protein and AHP1:NLS(SV40	this work
pEP714	P35s::E-AHP2-NLS(SV40)::Tnos E was amplified fron pKT289 with oligos oEP468 and oEP469 AHP2:NLS(SV40) was amplified from pEP386 with oligos oEP471 and oEP476 Backbone was digested with AgeI and BamHI	pGEN016	E Protein and AHP2:NLS(SV40)	this work

pEP715	P35s::E-AHP3-NLS(SV40)::Tnos E was amplified fron pKT289 with oligos oEP468 and oEP469 AHP3NLS(SV40) was amplified from pEP386 with oligos oEP472 and oEP476 Backbone was digested with AgeI and BamHI	pGEN016	E Protein and AHP3:NLS(SV40)	this work
pEP716	P35s::E-AHP4-NLS(SV40)::Tnos E was amplified fron pKT289 with oligos oEP468 and oEP469 AHP4NLS(SV40) was amplified from pEP386 with oligos oEP473 and oEP476 Backbone was digested with AgeI and BamHI	pGEN016	E Protein and AHP4:NLS(SV40)	this work
pEP717	P35s::E-AHP5-NLS(SV40)::Tnos E was amplified fron pKT289 with oligos oEP468 and oEP469 AHP5NLS(SV40) was amplified from pEP386 with oligos oEP474 and oEP476 Backbone was digested with AgeI and BamHI	pGEN016	E Protein and AHP5:NLS(SV40)	this work
pEP718	P35s::E-AHP6-NLS(SV40)::Tnos E was amplified fron pKT289 with oligos oEP468 and oEP469 AHP6NLS(SV40) was amplified from pEP386 with oligos oEP475 and oEP476 Backbone was digested with AgeI and BamHI	pGEN016	E Protein and AHP6:NLS(SV40)	this work
pEP727	Psv40::mCherry-AHK4::Tsv40 Insert was amplified fron pEP047.2 with oligos oEP497 and oEP498. Backbone was digested with BsrGI + CIP	pEP037	AHK4	this work
pEP730	(TCS)5::Pcmvmin::SEAP::Tsv40 Insert was amplified from pJA176 with oligos oEP502 and oEP503. Backbone was digested with SspI and NheI.	pPF034	(TCS)5	this work
pEP732	Psv40::AHP2-mVenus::Tsv40 Insert was amplified from pEP039 with oligos oEP086 and oEP505. mVenus was amplified from pRD093 with oligos oEP506 and oEP289. Backbone was digested with NotI and XbaI.	pLH002	AHP2	this work

pEP733	Psv40::ARR10-Cerulean::Tsv40 Insert was amplified from pEP103 with oligos oEP507 and oEP508. Backbone was digested with NotI and EcoRI	pEP351	ARR10	this work
pEP734	P35s::ARR10-VP16::Tnos Insert was amplified from pEP103 with oligos oEP511 and oEP512. Backbone was digested with AgeI and EcoRI.	pEP708	ARR10	this work
pEP754	Psv40::ARR10-VP16-NLS(SV40)-IRES(PV)-TetR-AHP2-NLS(SV40)::Tsv40 Insert was amplified from pEP733 with oligos oEP551 and oEP552. Backbone was digested withSpeI and EcoRV.	pEP387	AHP2	this work
pEP755	Psv40::ARR10-VP16-NLS(SV40)-IRES(PV)-TetR-AHP6-NLS(SV40)::Tsv40 Insert was amplified from pEP044 with oligos oEP239 and oEP248. Backbone was digested withBsrGI and AscI.	pEP754	AHP6	this work
pEP756	Psv40::ARR7-mCherry::Tsv40 Insert was amplified from pEP724 with oligos oEP579 and oEP580. Backbone was digested with NotI and EcoRI	pEP039	ARR7	this work
pEP757	Psv40::ARR1-Cerulean::Tsv40 Insert was amplified from the TAIR clone TOPO-U19-A06 with oligos oEP581 and oEP582. Backbone was digested with NotI and EcoRI	pEP733	ARR1	this work
pEP758	Psv40::ARR22-mCherry::Tsv40 Insert was amplified from TAIR clone TOPO-U11-H11 with oligos oEP583 and oEP584. Backbone was digested with NotI and EcoRI	pEP039	ARR22	this work
pEP765	Psv40::ARR10(D69A)-Cerulean::Tsv40 Baackbone was amplified with oligos oEP593 and oEP594	pEP733	ARR10(D69A)	this work
pEP767	Psv40::ARR1(D94A)-Cerulean::Tsv40 Baackbone was amplified with oligos oEP597 and oEP598 (Tm 72°C)	pEP757	ARR1(D94A)	this work

pEP768	Psv40::ARR1(D89A)-Cerulean::Tsv40 Baackbone was amplified with oligos oEP599 and oEP600 (Tm 72°C) and imner primers for backbone, oEP611 and oROF439	pEP757	ARR1(D89A)	this work
pEP769	Psv40::ARR1(D89A*D94A)-Cerulean::Tsv40 Baackbone was amplified with oligos oEP630 and oEP631, with inner primers for backbone, oEP611 and oROF439	pEP768	ARR1(D89A*D94A)	this work
pEP770	Psv40::ARR10(D69A)-VP16-NLS(SV40)-IRES(PV)-TetR-AHP2-NLS(SV40)::Tsv40 Insert was amplified from pEP765 with oligos oEP551 and oEP552. Backbone was digested withSpeI and EcoRV.	pEP387	AHP2	this work
pEP772	Psv40::ARR10-VP16-NLS(SV40)-IRES(PV)-TetR-ARR7-NLS(SV40)::Tsv40 Insert was amplified from pEP756 with oligos oEP613 and oEP614. Backbone was digested with BsrGI and AscI.	pEP754	ARR7	this work
pEP773	Psv40::ARR10-VP16-NLS(SV40)-IRES(PV)-TetR-ARR22-NLS(SV40)::Tsv40 Insert was amplified from pEP758 with oligos oEP615 and oEP616. Backbone was digested with BsrGI and AscI.	pEP754	ARR22	this work
pEP775	Psv40::ARR10(D69A)-VP16-NLS(SV40)-IRES(PV)-TetR-AHP6-NLS(SV40)::Tsv40 Insert was amplified from pEP044 with oligos oEP239 and oEP248. Backbone was digested withBsrGI and AscI.	pEP774	AHP6	this work
pEP776	Psv40::ARR1-VP16-NLS(SV40)-IRES(PV)-TetR-AHP2-NLS(SV40)::Tsv40 Insert was amplified from pEP757 with oligos oEP617 and oEP618. Backbone was digested withSpeI and EcoRV.	pEP387	ARR1	this work
pEP777	Psv40::ARR10(D89A)-VP16-NLS(SV40)-IRES(PV)-TetR-AHP2-NLS(SV40)::Tsv40 Insert was amplified from pEP768 with oligos oEP617 and oEP618. Backbone was digested withSpeI and EcoRV.	pEP387	ARR1(D89A)	this work

pEP778	Psv40::ARR10(D94A)-VP16-NLS(SV40)-IRES(PV)-TetR-AHP2-NLS(SV40)::Tsv40 Insert was amplified from pEP767 with oligos oEP617 and oEP618. Backbone was digested withSpeI and EcoRV.	pEP387	ARR1(D94A)	this work
pEP779	Psv40::ARR10(D89A*D94A)-VP16-NLS(SV40)-IRES(PV)-TetR-AHP2-NLS(SV40)::Tsv40 Insert wsa amplified from pEP769 with oligos oEO617 and oEP618. Backbone was digested withSpeI and EcoRV.	pEP387	ARR1(D89A*D94A)	this work
pEP781	Psv40::ARR1-VP16-NLS(SV40)-IRES(PV)-TetR-ARR7-NLS(SV40)::Tsv40 Insert was amplified from pEP756 with oligos oEP613 and oEP614. Backbone was digested with BsrGI and AscI.	pEP776	ARR7	this work
pEP782	Psv40::ARR7-VP16-NLS(SV40)-IRES(PV)-TetR-AHP2-NLS(SV40)::Tsv40 Insert was amplified from pEP756 with oligos oEP622 and oEP623. Backbone was digested withSpeI and EcoRV.	pEP387	ARR7	this work
pEP784	Psv40::ARR22-VP16-NLS(SV40)-IRES(PV)-TetR-AHP2-NLS(SV40)::Tsv40 Insert was amplified from pEP756 with oligos oEP622 and oEP623. Backbone was digested withSpeI and EcoRV.	pEP387	ARR7	this work
pEP788	Psv40::ARR1-VP16-NLS(SV40)-IRES(PV)-TetR-ARR2-NLS(SV40)::Tsv40 Insert was amplified from pEP758 with oligos oEP615 and oEP616. Backbone was digested with BsrGI and AscI.	pEP776	ARR22	this work
pEP793	Psv40::ARR1-VP16-NLS(SV40)-IRES(PV)-TetR-AHP6-NLS(SV40)::Tsv40 Insert was amplified from pEP044 with oligos oEP239 and oEP248. Backbone was digested withBsrGI and AscI.	pEP776	AHP6	this work

pEP795	Psv40::ARR10:VP16-NLS::IRES::TetR::ARR10::nls::Tsv40pa Insert was amplified from pEP754 with oligos oEP637 and oEP638 Backbone was digested withBsrGI and AscI	pEP754	ARR10	this work
pEP796	Psv40::ARR10(D94A):VP16-NLS::IRES::TetR::ARR10::nls::Tsv40pa Insert was amplified from pEP754 with oligos oEP637 and oEP638 Backbone was digested withBsrGI and AscI	pEP770	ARR10	this work
pJA176	(TCS)5-P35s::FLUC::Tnos			Jennifer Andress
pPF034	(tetO)13-Pcmvmin::SEAP::Tbgh||Psv40::GLUC::Tsv40pA			Patrick Fischbach
pRSET	Pt7-driven bacterial expression vector			Novagen

5.13 **Oligonucleotides**

Table 5. Oligonucleotides used for cloning in this work

Oligonucleotide ID	Sequence 5´-> 3´
oEP001	TTCAGGTCCCGGATCGGAATTGCGCGGCCGCATGGTGAGCAAGGGC
oEP002	GAAGCTTGGGCTGCAGGTCGACTTCTAGATTAAGCCTTGTACAGCTCG
oEP060	TTTCAGGTCCCGGATCGGAATTGCGCGGCCGCATGGAGACAGAGAAGAAAGTTTC
oEP061	CCGGTGAACAGCTCCTCGCCCTTGCTCACCATACTGCCACTGCCGGCGAATTCAACAGTTAAGACAGGATCCG
oEP062	TTTCAGGTCCCGGATCGGAATTGCGCGGCCGCATGGAAGCGGAGAAGAAAATG
oEP063	CCGGTGAACAGCTCCTCGCCCTTGCTCACCATACTGCCACTGCCGGCACCGGTAACAGCTAAAAGAG
oEP064	TTTCAGGTCCCGGATCGGAATTGCGCGGCCGCATGGACGAATATATTGATTTCCG
oEP065	CCGGTGAACAGCTCCTCGCCCTTGCTCACCATACTGCCACTGCCGGCGAATTCAGCAACTAATAGATCTGATATCAATG
oEP066	TTTCAGGTCCCGGATCGGAATTGCGCGGCCGCATGATGATGGATGAGTTTATGG
oEP067	CCGGTGAACAGCTCCTCGCCCTTGCTCACCATACTGCCACTGCCGGCGAATTCCACAAGTAAGAGATCGGATATC

oEP068	TTTCAGGTCCCGGATCGGAATTGCGCGGCCGCATGAAAAGCCGAGTGAGAAAATC
oEP069	CCCGGTGAACAGCTCCTCGCCCTTGCTCACCATACTGCCACTGCCGGCACCGGTCTTATCCAACAAATG
oEP070	TTTCAGGTCCCGGATCGGAATTGCGCGGCCGCATGGAGAGACGAACGAGAC
oEP071	CCGGTGAACAGCTCCTCGCCCTTGCTCACCATACTGCCACTGCCGGCGAATTCATCGAAAGAGTGATGATGATGG
oEP072	TTTCAGGTCCCGGATCGGAATTGCGCGGCCGCATGAAACGAATTGTTCGAATTTC
oEP073	CCGGTGAACAGCTCCTCGCCCTTGCTCACCATACTGCCACTGCCGGCGAATTCAACAACTTCTTCAGAAGCAC
oEP074	TCAGGTCCCGGATCGGAATTGCGCGGCCGCATGAAGCGTATTATCAGAATCTCATTC
oEP075	CCGGTGAACAGCTCCTCGCCCTTGCTCACCATACTGCCACTGCCGGCGAATTCCGCGCCTCTAGCAAC
oEP076	ATTTCAGGTCCCGGATCGGAATTGCGCGGCCGCATGTCTATAACTTGTGAGCTCTTG
oEP077	GCTCACCATACTGCCACTGCCGGCGAATTCACAAGGTTCAAAGAATCTTGCTAC
oEP078	TTTATTTCAGGTCCCGGATCGGAATTGCGCATGAGTCTGTTCCATGTGC
oEP079	GCTCACCATACTGCCACTGCCGGCGAATTCTGATTCTGTATCTGAAGGCG
oEP080	TTTATTTCAGGTCCCGGATCGGAATTGCGCGGCCGCATGAACTGGGCACTCAAC
oEP081	ATCCTCCTCGCCCTTGCTCACCATGCGGCCACTAGTGCCACTGCCACTGCCACTGCCACTGCCGGCCGACGAAGGTGAGATAGG
oEP082	TACCCATACGATGTTCCAGATTACGCTTAGTCTAGAAGTCGACCTGCAGC
oEP083	CTAAGCGTAATCTGGAACATCGTATGGGTAACTAGTGCCACTGCCAC
oEP084	TTTCAGGTCCCGGATCGGAATTGCGCGGCCGCATGGATTTGGTTCAGAAGCAG
oEP085	GCCATGTTATCCTCCTCGCCCTTGCTCACCATACTGCCACTGCCGGCGAATTCAAATCCGAGTTCGACGG
oEP086	TTTCAGGTCCCGGATCGGAATTGCGCGGCCGCATGGACGCTCTCATTGC
oEP087	GCCATGTTATCCTCCTCGCCCTTGCTCACCATACTGCCACTGCCGGCGAATTCGTTAATATCCACTTGAGGAACTATAC
oEP088	TTTCAGGTCCCGGATCGGAATTGCGCGGCCGCATGAGCTTTTCCACCATAAATAGC
oEP089	ATCATGTCTGGATCGAAGCTTTTAGGCGCGCCTTACACCTTCCGCTTTTTCTTGGGAAATCCGAGTTCGACGG
oEP090	TTTCAGGTCCCGGATCGGAATTGCGCGGCCGCATGGACACACTCATTGCTC
oEP091	GCCATGTTATCCTCCTCGCCCTTGCTCACCATACTGCCACTGCCGGCGAATTCTATATCCACTTGAGGGATTCTACC
oEP092	TTTCAGGTCCCGGATCGGAATTGCGCGGCCGCATGCAGAGGCAAGTGG
oEP093	GCCATGTTATCCTCCTCGCCCTTGCTCACCATACTGCCACTGCCGGCGAATTCCTTGGGCCTACGTGC

oEP094	TTTCAGGTCCCGGATCGGAATTGCGCGGCCGCATGAACACCATCGTCGTTG
oEP095	GCCATGTTATCCTCCTCGCCCTTGCTCACCATACTGCCACTGCCGGCGAATTCATTTATATCCACTTGAGGAATTGTACC
oEP096	TTTCAGGTCCCGGATCGGAATTGCGCGGCCGCATGTTGGGGTTGGGTG
oEP097	GCCATGTTATCCTCCTCGCCCTTGCTCACCATACTGCCACTGCCGGCGAATTCCATTGGATATCTGACTCCTGC
oEP137	GCTGCAGGTCGACTTCTAGATTACTTGTACTTAAACAGTTAAGACAGGATCCG
oEP138	CGCCGGGATCACTCTCGGCATGGACGAGCTGTACAAGACCGGTGCCGGCAGTAGTGGCGGCAGTATGGAAGCGGAGAAGAAAATG
oEP139	GCTGCAGGTCGACTTCTAGATTACTTGTACTTAAACAGCTAAAAGAGGATCCG
oEP140	CGCCGGGATCACTCTCGGCATGGACGAGCTGTACAAGACCGGTGCCGGCAGTAGTGGCGGCAGTATGGACGAATATATTGATTTCCGAC
oEP141	GCTGCAGGTCGACTTCTAGATTACTTGTACTTAAGCAACTAATAGATCTGATATCAATGAATC
oEP142	CGCCGGGATCACTCTCGGCATGGACGAGCTGTACAAGACCGGTGCCGGCAGTAGTGGCGGCAGTATGATGATGGATGAGTTTATGGATC
oEP143	GCTGCAGGTCGACTTCTAGATTACTTGTACTCACACAAGTAAGAGATCGGATATC
oEP146	CGCCGGGATCACTCTCGGCATGGACGAGCTGTACAAGACCGGTGCCGGCAGTAGTGGCGGCAGTATGGAGAGACGAACGAGAC
oEP147	GCTGCAGGTCGACTTCTAGATTACTTGTACTTAATCGAAAGAGTGATGATGATGG
oEP148	CGCCGGGATCACTCTCGGCATGGACGAGCTGTACAAGACCGGTGCCGGCAGTAGTGGCGGCAGTATGAAACGAATTGTTCGAATTTCATTC
oEP149	GCTGCAGGTCGACTTCTAGATTACTTGTACTCAAACAACTTCTTCAGAAGCAC
oEP150	CGCCGGGATCACTCTCGGCATGGACGAGCTGTACAAGACCGGTGCCGGCAGTAGTGGCGGCAGTATGAAGCGTATTATCAGAATCTCATTC
oEP151	GCTGCAGGTCGACTTCTAGATTACTTGTACTCACGCGCCTCTAGC
oEP152	CGCCGGGATCACTCTCGGCATGGACGAGCTGTACAAGACCGGTGCCGGCAGTAGTGGCGGCAGTATGATCAGTTTCAGAGAAGAGAAC
oEP153	GCTGCAGGTCGACTTCTAGATTACTTGTACTCATAAAAACTTATCGATCCAATCAGTAG
oEP154	CGCCGGGATCACTCTCGGCATGGACGAGCTGTACAAGACCGGTGCCGGCAGTAGTGGCGGCAGTATGGTTGCGATTAGAAAGGAAC
oEP155	GCTGCAGGTCGACTTCTAGATTACTTGTACCTATGAAGCTGCAAAACTTTTTAATG
oEP156	CGCCGGGATCACTCTCGGCATGGACGAGCTGTACAAGACCGGTGCCGGCAGTAGTGGCGGCAGTATGGCTGAACGAAAGAAACG
oEP157	GCTGCAGGTCGACTTCTAGATTACTTGTACTTATGGGCACGCGATATTAAG
oEP158	CGCCGGGATCACTCTCGGCATGGACGAGCTGTACAAGACCGGTGCCGGCAGTAGTGGCGGCAGTATGAAGTCCTTTGTGAAACCTG

oEP159	GCTGCAGGTCGACTTCTAGATTACTTGTACTTAAACCAAACCGAGAGGC
oEP172	ATCATGTCTGGATCGAAGCTTTTAGGCGCGCCTTACACCTTCCGCTTTTTCTTGGGGTTAATATCCACTTGAGGAACTATACC
oEP173	ATCATGTCTGGATCGAAGCTTTTAGGCGCGCCTTACACCTTCCGCTTTTTCTTGGGTATATCCACTTGAGGGATTCTACC
oEP174	TTTGGAGAGAACACGGGGACTCTAGCGCTACCGGTATGGAGACAGAGAAGAAAGTTTC
oEP175	TTTGGAGAGAACACGGGGACTCTAGCGCTACCGGTATGGAAGCGGAGAAGAAAATG
oEP176	TTTGGAGAGAACACGGGGACTCTAGCGCTACCGGTATGGACGAATATATTGATTTCCGAC
oEP177	TTTGGAGAGAACACGGGGACTCTAGCGCTACCGGTATGATGATGGATGAGTTTATGGATC
oEP178	TTTGGAGAGAACACGGGGACTCTAGCGCTACCGGTATGAAAAGCCGAGTGAGAAAATC
oEP179	TTTGGAGAGAACACGGGGACTCTAGCGCTACCGGTATGGAGAGACGAACGAGAC
oEP180	TTTGGAGAGAACACGGGGACTCTAGCGCTACCGGTATGAAGCGTATTATCAGAATCTCATTC
oEP181	TTTGGAGAGAACACGGGGACTCTAGCGCTACCGGTATGAAACGAATTGTTCGAATTTCATTC
oEP182	TTTGGAGAGAACACGGGGACTCTAGCGCTACCGGTATGATCAGTTTCAGAGAAGAGAAC
oEP183	TTTGGAGAGAACACGGGGACTCTAGCGCTACCGGTATGGTTGCGATTAGAAAGGAAC
oEP184	TTTGGAGAGAACACGGGGACTCTAGCGCTACCGGTATGGCTGAACGAAAGAAACG
oEP185	TTTGGAGAGAACACGGGGACTCTAGCGCTACCGGTATGAAGTCCTTTGTGAAACCTG
oEP188	TTTGGAGAGAACACGGGGACTCTAGCGCTAATGGACGCTCTCATTGC
oEP193	GGGAAATTCGCCTCGAGATCAGTTATCTAGTTAAGCCTTGTACAGCTCG
oEP217	GGAAGTGGTGGCGGAGGTAGCGATTGTACAATGGATTTGGTTCAGAAGCAG
oEP219	GGAAGTGGTGGCGGAGGTAGCGATTGTACAATGGATTTGGTTCAGAAGCAG
oEP221	GGAAGTGGTGGCGGAGGTAGCGATTGTACAATGGAGACAGAGAAGAAAGTTTC
oEP222	CATGTCTGGATCGAAGCTTTTAGGCGCGCCTTAAACAGTTAAGACAGGATCCG
oEP223	GGAAGTGGTGGCGGAGGTAGCGATTGTACAATGGAAGCGGAGAAGAAAATG
oEP224	CATGTCTGGATCGAAGCTTTTAGGCGCGCCTTAAACAGCTAAAAGAGGATCCG
oEP227	GGAAGTGGTGGCGGAGGTAGCGATTGTACAATGATGATGGATGAGTTTATGGATC
oEP228	CATGTCTGGATCGAAGCTTTTAGGCGCGCCTCACACAAGTAAGAGATCGGATATC
oEP229	GGAAGTGGTGGCGGAGGTAGCGATTGTACAATGAAAAGCCGAGTGAGAAAATC

oEP230	CATGTCTGGATCGAAGCTTTTAGGCGCGCCTTACTTATCCAACAAATGATCTTGGAAAAAC
oEP231	GGAAGTGGTGGCGGAGGTAGCGATTGTACAATGGAGAGACGAACGAGAC
oEP232	CATGTCTGGATCGAAGCTTTTAGGCGCGCCTTAATCGAAAGAGTGATGATGATGG
oEP233	GGAAGTGGTGGCGGAGGTAGCGATTGTACAATGGACACACTCATTGCTC
oEP235	GGAAGTGGTGGCGGAGGTAGCGATTGTACAATGCAGAGGCAAGTGG
oEP237	GGAAGTGGTGGCGGAGGTAGCGATTGTACAATGAACACCATCGTCGTTG
oEP239	GGAAGTGGTGGCGGAGGTAGCGATTGTACAATGTTGGGGTTGGGTG
oEP246	ATCATGTCTGGATCGAAGCTTTTAGGCGCGCCTTACACCTTCCGCTTTTTCTTGGGCTTGGGCCTACGTG
oEP247	ATCATGTCTGGATCGAAGCTTTTAGGCGCGCCTTACACCTTCCGCTTTTTCTTGGGATTTATATCCACTTGAGGAATTGTACC
oEP248	ATCATGTCTGGATCGAAGCTTTTAGGCGCGCCTTACACCTTCCGCTTTTTCTTGGGCATTGGATATCTGACTCCT
oEP274	TTTCAGGTCCCGGATCGGAATTGCGCGGCCGCATGTCTACTATTCCCTCAGAAATC
oEP275	GGTGAACAGCTCCTCGCCCTTGCTCACCATACTGCCACTGCCGGCGAATTCTAGGTTTGTGTTGTAATATTTAGATAACTC
oEP288	TTTGGAGAGAACACGGGGACTCTAGCGCTACCGGTATGAGCTTTTCCACCATAAATAGC
oEP289	CGAAGCTTGGGCTGCAGGTCGACTTCTAGATTACTTGTACAGCTCGTCC
oEP300	GGTCCCGGATCGGAATTGACTAGTCCCACCATGTTGGGGTTGGGTG
oEP301	AGCACTACCAGCACTATCGAATTCGATATCCATTGGATATCTGACTCCTGC
oEP302	GCCATGTTATCCTCCTCGCCCTTGCTCACCATACTGCCACTGCCGGCGAATTCAGCAACTAATAGATCTGATATCAATG
oEP303	GCCATGTTATCCTCCTCGCCCTTGCTCACCATACTGCCACTGCCGGCGAATTCCACAAGTAAGAGATCGGATATC
oEP304	GCCATGTTATCCTCCTCGCCCTTGCTCACCATACTGCCACTGCCGGCGAATTCACCGGTCTTATCCAACAAATG
oEP305	GCCATGTTATCCTCCTCGCCCTTGCTCACCATACTGCCACTGCCGGCGAATTCATCGAAAGAGTGATGATGATGG
oEP306	GCCATGTTATCCTCCTCGCCCTTGCTCACCATACTGCCACTGCCGGCGAATTCAACAACTTCTTCAGAAGCAC
oEP307	GCCATGTTATCCTCCTCGCCCTTGCTCACCATACTGCCACTGCCGGCGAATTCCGCGCCTCTAGCAAC
oEP308	GCCATGTTATCCTCCTCGCCCTTGCTCACCATACTGCCACTGCCGGCGAATTCTAAAAACTTATCGATCCAATCAGTAGTAC
oEP309	GCCATGTTATCCTCCTCGCCCTTGCTCACCATACTGCCACTGCCGGCGAATTCTGAAGCTGCAAAACTTTTTAATGG

oEP310	GCCATGTTATCCTCCTCGCCCTTGCTCACCATACTGCCACTGCCGGCGAATTCTGGGCACGCGATATTAAG
oEP311	GCCATGTTATCCTCCTCGCCCTTGCTCACCATACTGCCACTGCCGGCGAATTCAACCAAACCGAGAGGC
oEP314	CGAGATCAGTTATCTAGATCCGGTGGATCCTTACTTGTACAGCTCGTCCATG
oEP315	GGAAGTGGTGGCGGAGGTAGCGATTGTACAATGAAACGAATTGTTCGAATTTCATTC
oEP316	CATGTCTGGATCGAAGCTTTTAGGCGCGCCTCAAACAACTTCTTCAGAAGCAC
oEP317	GGAAGTGGTGGCGGAGGTAGCGATTGTACAATGAAGCGTATTATCAGAATCTCATTC
oEP318	CATGTCTGGATCGAAGCTTTTAGGCGCGCCTCACGCGCCTCTAG
oEP319	GGAAGTGGTGGCGGAGGTAGCGATTGTACAATGATCAGTTTCAGAGAAGAGAAC
oEP320	CATGTCTGGATCGAAGCTTTTAGGCGCGCCTCATAAAAACTTATCGATCCAATCAGTAG
oEP321	GGAAGTGGTGGCGGAGGTAGCGATTGTACAATGGTTGCGATTAGAAAGGAAC
oEP322	CATGTCTGGATCGAAGCTTTTAGGCGCGCCCTATGAAGCTGCAAAACTTTTTAATGG
oEP323	GGAAGTGGTGGCGGAGGTAGCGATTGTACAATGGCTGAACGAAAGAAACG
oEP324	CATGTCTGGATCGAAGCTTTTAGGCGCGCCTTATGGGCACGCGATATTAAG
oEP325	GGAAGTGGTGGCGGAGGTAGCGATTGTACAATGAAGTCCTTTGTGAAACCTG
oEP326	CATGTCTGGATCGAAGCTTTTAGGCGCGCCTTAAACCAAACCGAGAGGC
oEP368	GTTGAATACTCATACTATTAATTTTTCAATATTCGAGTCGGTCCCATTATTG
oEP369	GACAATAACCCTGATAAATGCTTCAATAATACCGGTACTAGAGCCAAGCTGATCTC
oEP451	GGGAAATTCGCCTCGAGATCAGTTATCTAGACACCTTCCGCTTTTTCTTG
oEP454	ATTCATTGATATCAGATCTATTAGTTGCTGAATTCGCCGGCAGTGGCAGTTCCGCGTACAGCC
oEP455	ATTCTTTGATATCCGATCTCTTACTTGTGGAATTCGCCGGCAGTGGCAGTTCCGCGTACAGCC
oEP457	TCTTCGACCATCATCATCACTCTTTCGATGAATTCGCCGGCAGTGGCAGTTCCGCGTACAGCC
oEP458	CTAGTGGTGGTGCTTCTGAAGAAGTTGTTGAATTCGCCGGCAGTGGCAGTTCCGCGTACAGCC
oEP459	TTGGAGCTTCTGAGGTTGCTAGAGGCGCGGAATTCGCCGGCAGTGGCAGTTCCGCGTACAGCC
oEP460	TAAGTTTTTAGAATTCGCCGGCAGTGGCAGTTCCGCGTACAGCC
oEP462	CTCCCACTCCTCTTAATATCGCGTGCCCAGAATTCGCCGGCAGTGGCAGTTCCGCGTACAGCC

oEP464	GGCTGTACGCGGAACTGCCACTGCCGGCGAATTCAACAGCTAAAAGAGGATCCGACCCGAATA
oEP465	GGCTGTACGCGGAACTGCCACTGCCGGCGAATTCCTTATCCAACAAATGATCTTGGAAAAACT
oEP467	GGCTGTACGCGGAACTGCCACTGCCGGCGAATTCAACCAAACCGAGAGGCGGTGTTGTCAGAT
oEP468	TTTGGAGAGAACACGGGGACTCTAGCGCTACCGGTCGCCACCATGCCC
oEP469	TCAGGTCCCGGATCGGAATTGCGCGGCCGCATGCTCAATTCTGCGTTACTG
oEP470	GCGGTGGAAGTGGTGGCGGAGGTAGCGATTGTACAATGGATTTGGTTCAGAAGCAG
oEP471	GCGGTGGAAGTGGTGGCGGAGGTAGCGATTGTACAATGGACGCTCTCATTGC
oEP472	GCGGTGGAAGTGGTGGCGGAGGTAGCGATTGTACAATGGACACACTCATTGCTC
oEP473	GCGGTGGAAGTGGTGGCGGAGGTAGCGATTGTACAATGCAGAGGCAAGTGG
oEP474	GCGGTGGAAGTGGTGGCGGAGGTAGCGATTGTACAATGAACACCATCGTCGTTG
oEP475	GCGGTGGAAGTGGTGGCGGAGGTAGCGATTGTACAATGTTGGGGTTGGGTG
oEP476	TCGAGATCAGTTATCTAGATCCGGTGGATCCTCACACCTTCCGCTTTTTCTTG
oEP497	CCGCCACTCCACCGGCGGCATGGACGAGCTGTACAAGGCTGGATCCAGTGGCAGTGGCAGTGGCAGTGGCATGAACTGGGCACTCAAC
oEP498	GCAGGTCGACTTCTAGATTAAGCCTTGTACTTACGACGAAGGTGAGATAGGATTAG
oEP502	GTTGAATACTCATACTCTTCCTTTTTCAATATTGCTAGCAAAATCTACAAAATCTTTTTG
oEP503	CACTAAACGAGCTCTGCTTATATAGGGCTAGCGGTCTTGGCTAGAAAATCCAC
oEP505	TGCTCACCATACTGCCACTGCCGGCGAATTCGTTAATATCCACTTGAGGAACTATAC
oEP506	ATTAACGAATTCGCCGGCAGTGGCAGTATGGTGAGCAAGGGC
oEP507	TTTATTTCAGGTCCCGGATCGGAATTGCGCGGCCGCATGACTATGGAGCAAGAAATTGAAG
oEP508	TGCTCACCATACTGCCACTGCCGGCGAATTCAGCTGACAAAGAAAAGGGAAAATG
oEP511	TTTGGAGAGAACACGGGGACTCTAGCGCTATGTACAATGACTATGGAGCAAGAAATTGAAG
oEP512	TGTACGCGGAACTGCCACTGCCGGCGAATTGGACGTCAGCTGACAAAGAAAAGGGAAAATG
oEP520	TGTACGCGGAACTGCCACTGCCGGCGAATTGGACGTCTGAAGCTGCAAAACTTTTTAATGG
oEP521	TGTACGCGGAACTGCCACTGCCGGCGAATTGGACGTCAACAGTTAAGACAGGATCCG

oEP551	CTTTTATTTCAGGTCCCGGATCGGAATTGACTAGTCCCACCATGACTATGGAGCAAGAAATTGAAG
oEP552	ACCAGCACTACCAGCACTATCGAATTCGATATCAGCTGACAAAGAAAAGGGAAAATG
oEP567	GTCGTGAAAACTACCCCAAGCTGGCCTCTGAGGCCATGAACTGGGCACTCAAC
oEP568	CTCTAGAGAATTGATCCCCAAGCTTGGCCTGACAGGCCTTACGACGAAGGTGAGATAGG
oEP579	TTTATTTCAGGTCCCGGATCGGAATTGCGCGGCCGCATGGCGGTTGGTGAG
oEP580	CCCTTGCTCACCATACTGCCACTGCCGGCGAATTCAAGTAGAGAAAAAAGGTTTTCAGATTCTG
oEP581	TTTATTTCAGGTCCCGGATCGGAATTGCGCGGCCGCATGATGAATCCGAGTCACG
oEP582	TGCTCACCATACTGCCACTGCCGGCGAATTCAACCGGAATGTTATCGATGG
oEP583	TTTATTTCAGGTCCCGGATCGGAATTGCGCGGCCGCATGGCAACAAAATCCACC
oEP584	CCCTTGCTCACCATACTGCCACTGCCGGCGAATTCAGCATCGAAGAGGTGG
oEP593	GTTTGATCTTGTTATTAGCGCTGTCGACATGCCAGACATG
oEP594	CATGTCTGGCATGTCGACAGCGCTAATAACAAGATCAAAC
oEP597	GTTCATATGCCTGCCATGGACGGTTTC
oEP598	GAAACCGTCCATGGCAGGCATATGAAC
oEP599	CGATATAGTAATCAGTGCTGTTCATATGCCTGAC
oEP600	GTCAGGCATATGAACAGCACTGATTACTATATCG
oEP611	GGTGAACAGCTCCTCGCCCTTGCTCACCATACTGCCACTGCCGGCGAATTCTGATAGCTGGTTTTCTTGAAGTG
oEP613	GCGGTGGAAGTGGTGGCGGAGGTAGCGATTGTACAATGGCGGTTGGTGAG
oEP614	GTCTGGATCGAAGCTTTTAGGCGCGCCTTAAAGTAGAGAAAAAAGGTTTTCAGATTCTG
oEP615	GCGGTGGAAGTGGTGGCGGAGGTAGCGATTGTACAATGGCAACAAAATCCACC
oEP616	ATCATGTCTGGATCGAAGCTTTTAGGCGCGCCTTAAGCATCGAAGAGGTGG
oEP617	CTTTTATTTCAGGTCCCGGATCGGAATTGACTAGTCCCACCATGATGAATCCGAGTCACG
oEP618	AGCACTACCAGCACTATCGAATTCGATATCAACCGGAATGTTATCGATGG
oEP622	CTTTTATTTCAGGTCCCGGATCGGAATTGACTAGTATGGCGGTTGGTGAG
oEP623	ACCAGCACTACCAGCACTATCGAATTCGATATCAAGTAGAGAAAAAAGGTTTTCAGATTCTG
oEP630	GCTCTTGAGCATGTTGCCCTAGAGATGGACTTAC
oEP631	GTAAGTCCATCTCTAGGGCAACATGCTCAAGAGC
oEP637	GCGGTGGAAGTGGTGGCGGAGGTAGCGATTGTACAATGACTATGGAGCAAGAAATTGAAG
oEP638	GTCTGGATCGAAGCTTTTAGGCGCGCCTTAAGCTGACAAAGAAAAGGGAAAATG

6. **References**

1. Bowman, J. L., Floyd, S. K. & Sakakibara, K. Green Genes-Comparative Genomics of the Green Branch of Life. *Cell* **129**, 229–234 (2007).
2. Sparks, T. & Menzel, A. *Plant Phenology Changes and Climate Change*. *Encyclopedia of Biodiversity: Second Edition* (Elsevier Ltd., 2013). doi:10.1016/B978-0-12-384719-5.00229-X.
3. Jameson, P. E. & Song, J. Will cytokinins underpin the second 'Green Revolution'? *J. Exp. Bot.* **71**, 6872–6875 (2020).
4. Bartrina, I., Otto, E., Strnad, M., Werner, T. & Schmülling, T. Cytokinin regulates the activity of reproductive meristems, flower organ size, ovule formation, and thus seed yield in Arabidopsis thaliana. *Plant Cell* **23**, 69–80 (2011).
5. Motoyuki, A. *et al.* Cytokinin Oxidase Regulates Rice Grain Production. *Science (80-.).* **309**, 741–745 (2005).
6. Babosha, A. V. Regulation of resistance and susceptibility in wheat-powdery mildew pathosystem with exogenous cytokinins. *J. Plant Physiol.* **166**, 1892–1903 (2009).
7. Choi, J. *et al.* The cytokinin-activated transcription factor ARR2 promotes plant immunity via TGA3/NPR1-dependent salicylic acid signaling in arabidopsis. *Dev. Cell* **19**, 284–295 (2010).
8. Argueso, C. T. *et al.* Two-component elements mediate interactions between cytokinin and salicylic acid in plant immunity. *PLoS Genet.* **8**, (2012).
9. Maruyama-Nakashita, A., Nakamura, Y., Yamaya, T. & Takahashi, H. A novel regulatory pathway of sulfate uptake in Arabidopsis roots: Implication of CRE1/WOL/AHK4-mediated cytokinin-dependent regulation. *Plant J.* **38**, 779–789 (2004).
10. Franco-Zorrilla, J. M. *et al.* Mutations at CRE1 impair cytokinin-induced repression of phosphate starvation responses in Arabidopsis. *Plant J.* **32**, 353–360 (2002).
11. Jaworek, P. *et al.* Characterization of five CHASE-containing histidine kinase receptors from Populus × canadensis cv. Robusta sensing isoprenoid and aromatic cytokinins. *Planta* **251**, 1–15 (2020).
12. Ga, E. *et al.* Reconstitution of cytokinin signaling in rice protoplasts. *Int. J. Mol. Sci.* **22**,

(2021).

13. Schmülling, T., Werner, T., Riefler, M., Krupková, E. & Bartrina Y Manns, I. Structure and function of cytokinin oxidase/dehydrogenase genes of maize, rice, Arabidopsis and other species. *J. Plant Res.* **116**, 241–252 (2003).
14. Lomin, S. N., Yonekura-Sakakibara, K., Romanov, G. A. & Sakakibara, H. Ligand-binding properties and subcellular localization of maize cytokinin receptors. *J. Exp. Bot.* **62**, 5149–5159 (2011).
15. Pils, B. & Heyl, A. Unraveling the evolution of cytokinin signaling. *Plant Physiol.* **151**, 782–791 (2009).
16. Kim, H. J. *et al.* Cytokinin-mediated control of leaf longevity by AHK3 through phosphorylation of ARR2 in Arabidopsis. *Proc. Natl. Acad. Sci. U. S. A.* **103**, 814–819 (2006).
17. Caplin, S. M. & Steward, F. C. Effect of coconut milk on the growth of explants from carrot root. *Science (80-.).* **108**, 655–657 (1948).
18. Miller, C. O., Skoog, F., Von Saltza, M. H. & Strong, F. M. Kinetin, a Cell Division Factor from Deoxyribonucleic Acid. *J. Am. Chem. Soc.* **77**, 1392 (1955).
19. Letham, D. S. Cytokinins from Zea mays. *Phytochemistry* **12**, 2445–2455 (1973).
20. Mok, M. C., Martin, R. C. & Mok, D. W. S. Cytokinins: Biosynthesis, metabolism and perception. *Vitr. Cell. Dev. Biol. - Plant* **36**, 102–107 (2000).
21. Hwang, I., Sheen, J. & Müller, B. Cytokinin Signaling Networks. *Annu. Rev. Plant Biol.* **63**, 353–380 (2012).
22. Giulini, A., Wang, J. & Jackson, D. Control of phyllotaxy by the cytokinin-inducible response regulator homologue ABPHYL1. *Nature* **430**, 1031–1034 (2004).
23. Leibfried, A. *et al.* WUSCHEL controls meristem function by direct regulation of cytokinin-inducible response regulators. *Nature* **438**, 1172–1175 (2005).
24. Checker V.G, et al. Role of Phytohormones in Plant Defense: Signaling and Cross Talk. in *Molecular Aspects of Plant-Pathogen Interaction.* (Springer, Singapore, 2018).
25. Montesinos, J. C. *et al.* Phytohormone cytokinin guides microtubule dynamics during cell progression from proliferative to differentiated stage. *EMBO J.* **39**, 1–22 (2020).
26. Sakakibara, H. Cytokinins: Activity, biosynthesis, and translocation. *Annu. Rev. Plant Biol.* **57**, 431–449 (2006).
27. Vreman, H. J., Skoog, F., Frihart, C. R. & Leonard, N. J. Cytokinins in Pisum Transfer

Ribonucleic Acid . *Plant Physiol.* **49**, 848–851 (1972).

28. Takei, K., Sakakibara, H. & Sugiyama, T. Identification of Genes Encoding Adenylate Isopentenyltransferase, a Cytokinin Biosynthesis Enzyme, in Arabidopsis thaliana. *J. Biol. Chem.* **276**, 26405–26410 (2001).
29. Takei, K., Yamaya, T. & Sakakibara, H. Arabidopsis CYP735A1 and CYP735A2 encode cytokinin hydroxylases that catalyse the biosynthesis of trans-Zeatin. *J. Biol. Chem.* **279**, 41866–41872 (2004).
30. Kurakawa, T. *et al.* Direct control of shoot meristem activity by a cytokinin-activating enzyme. *Nature* **445**, 652–655 (2007).
31. Kasahara, H. *et al.* Distinct Isoprenoid Origins of cis- and trans-Zeatin Biosyntheses in Arabidopsis. *J. Biol. Chem.* **279**, 14049–14054 (2004).
32. Miyawaki, K. *et al.* Roles of Arabidopsis ATP/ADP isopentenyltransferases and tRNA isopentenyltransferases in cytokinin biosynthesis. *Proc. Natl. Acad. Sci. U. S. A.* **103**, 16598–16603 (2006).
33. Stirk, W. A. *et al.* Comparison of endogenous cytokinins and cytokinin oxidase/dehydrogenase activity in germinating and thermoinhibited Tagetes minuta achenes. *J. Plant Physiol.* **169**, 696–703 (2012).
34. Jaworek, P. *et al.* Occurrence and biosynthesis of cytokinins in poplar. *Planta* **250**, 229–244 (2019).
35. Strnad, M. The aromatic cytokinins. *Physiol. Plant.* **101**, 674–688 (1997).
36. Hluska, T., Hlusková, L. & Emery, R. J. N. The hulks and the deadpools of the cytokinin universe: A dual strategy for cytokinin production, translocation, and signal transduction. *Biomolecules* **11**, 1–40 (2021).
37. Hluska, T. *et al.* Cytokinin metabolism in maize: Novel evidence of cytokinin abundance, interconversions and formation of a new trans-zeatin metabolic product with a weak anticytokinin activity. *Plant Sci.* **247**, 127–137 (2016).
38. Chickarmane, V. S., Gordon, S. P., Tarr, P. T., Heisler, M. G. & Meyerowitz, E. M. Cytokinin signaling as a positional cue for patterning the apical-basal axis of the growing Arabidopsis shoot meristem. *Proc. Natl. Acad. Sci. U. S. A.* **109**, 4002–4007 (2012).
39. Kuroha, T. *et al.* Functional analyses of LONELY GUY cytokinin-activating enzymes reveal the importance of the direct activation pathway in Arabidopsis. *Plant Cell* **21**, 3152–3169 (2009).

40. Galuszka, P. *et al.* Biochemical characterization of cytokinin oxidases/dehydrogenases from Arabidopsis thaliana expressed in Nicotiana tabacum L. *J. Plant Growth Regul.* **26**, 255–267 (2007).
41. Kudo, T., Kiba, T. & Sakakibara, H. Metabolism and long-distance translocation of cytokinins. *J. Integr. Plant Biol.* **52**, 53–60 (2010).
42. Ko, D. *et al.* Arabidopsis ABCG14 is essential for the root-to-shoot translocation of cytokinin. *Proc. Natl. Acad. Sci. U. S. A.* **111**, 7150–7155 (2014).
43. Kiba, T., Takei, K., Kojima, M. & Sakakibara, H. Side-Chain Modification of Cytokinins Controls Shoot Growth in Arabidopsis. *Dev. Cell* **27**, 452–461 (2013).
44. Gillissen, B. *et al.* A new family of high-affinity transporters for adenine, cytosine, and purine derivatives in Arabidopsis. *Plant Cell* **12**, 291–300 (2000).
45. Bürkle, L. *et al.* Transport of cytokinins mediated by purine transporters of the PUP family expressed in phloem, hydathodes, and pollen of Arabidopsis. *Plant J.* **34**, 13–26 (2003).
46. Hirose, N., Makita, N., Yamaya, T. & Sakakibara, H. Functional characterization and expression analysis of a gene, OsENT2, encoding an equilibrative nucleoside transporter in rice suggest a function in cytokinin transport. *Plant Physiol.* **138**, 196–206 (2005).
47. WORMIT, A., TRAUB, M., FLÖRCHINGER, M., NEUHAUS, H. E. & MÖHLMANN, T. Characterization of three novel members of the Arabidopsis thaliana equilibrative nucleoside transporter (ENT) family. *Biochem. J.* **383**, 19–26 (2004).
48. Jiskrová, E. *et al.* Extra- and intracellular distribution of cytokinins in the leaves of monocots and dicots. *N. Biotechnol.* **33**, 735–742 (2016).
49. Hirose, N. *et al.* Regulation of cytokinin biosynthesis, compartmentalization and translocation. *J. Exp. Bot.* **59**, 75–83 (2008).
50. T. Werner et al. New Insights into the Biology of Cytokinin Degradation. (2008) doi:https://doi.org/10.1055/s-2006-923928.
51. Savelieva, E. M. *et al.* Cytokinin activity of N6-benzyladenine derivatives assayed by interaction with the receptors in planta, in vitro, and in silico. *Phytochemistry* **149**, 161–177 (2018).
52. Lomin, S. N. *et al.* Plant membrane assays with cytokinin receptors underpin the unique role of free cytokinin bases as biologically active ligands. *J. Exp. Bot.* **66**, 1851–1863 (2015).

53. Hothorn, M., Dabi, T. & Chory, J. Structural basis for cytokinin recognition by Arabidopsis thaliana histidine kinase 4. *Nat. Chem. Biol.* **7**, 766–768 (2011).
54. Samanovic, M. I. *et al.* Proteasomal Control of Cytokinin Synthesis Protects Mycobacterium tuberculosis against Nitric Oxide. *Mol. Cell* **57**, 984–994 (2015).
55. Břetislav, B. *et al.* Release of Active Cytokinin by a β-Glucosidase Localized to the Maize Root Meristem . *Science (80-.).* **262**, 1051–1054 (1993).
56. Zalabák, D. *et al.* Biochemical characterization of the maize cytokinin dehydrogenase family and cytokinin profiling in developing maize plantlets in relation to the expression of cytokinin dehydrogenase genes. *Plant Physiol. Biochem.* **74**, 283–293 (2014).
57. Stock, J. B., Ninfa, A. J. & Stock, A. M. *Protein phosphorylation and regulation of adaptive responses in bacteria*. *Microbiological Reviews* vol. 53 (1989).
58. West, A. H. & Stock, A. M. Histidine kinases and response regulator proteins in two-component signaling systems. *Trends Biochem. Sci.* **26**, 369–376 (2001).
59. Appleby, J. L., Parkinson, J. S. & Bourret, R. B. Signal transduction via the multi-step phosphorelay: Not necessarily a road less traveled. *Cell* **86**, 845–848 (1996).
60. Schaller, G. E., Shiu, S. H. & Armitage, J. P. Two-component systems and their co-option for eukaryotic signal transduction. *Current Biology* vol. 21 (2011).
61. Hwang, I. & Sheen, J. Two-component circuitry in Arabidopsis cytokinin signal transduction. *Nature* **413**, 383–389 (2001).
62. Inoue, T. *et al.* Identification of CRE1 as a cytokinin receptor from Arabidopsis. *Nature* **409**, 1060–1063 (2001).
63. Schaller, G. E., Kieber, J. J. & Shiu, S.-H. Two-Component Signaling Elements and Histidyl-Aspartyl Phosphorelays † . *Arab. B.* **6**, e0112 (2008).
64. Rashotte, A. M. *et al.* A subset of Arabidopsis AP2 transcription factors mediates cytokinin responses in concert with a two-component pathway. *Proc. Natl. Acad. Sci. U. S. A.* (2006) doi:10.1073/pnas.0602038103.
65. Xie, M. *et al.* A B-ARR-mediated cytokinin transcriptional network directs hormone cross-regulation and shoot development. *Nat. Commun.* **9**, 1–13 (2018).
66. Horák, J. *et al.* The Arabidopsis thaliana response regulator ARR22 is a putative AHP phospho-histidine phosphatase expressed in the chalaza of developing seeds. *BMC Plant Biol.* **8**, 1–18 (2008).
67. Kiba, T., Aoki, K., Sakakibara, H. & Mizuno, T. Arabidopsis response regulator,

ARR22, ectopic expression of which results in phenotypes similar to the wol cytokinin-receptor mutant. *Plant Cell Physiol.* **45**, 1063–1077 (2004).

68. Mähönen, A. P. *et al.* Cytokinin signaling and its inhibitor AHP6 regulate cell fate during vascular development. *Science (80-.).* **311**, 94–98 (2006).
69. Besnard, F., Rozier, F. & Vernoux, T. The AHP6 cytokinin signaling inhibitor mediates an auxin-cytokinin crosstalk that regulates the timing of organ initiation at the shoot apical meristem. *Plant Signal. Behav.* **9**, 4–7 (2014).
70. Panchy, N., Lehti-Shiu, M. & Shiu, S. H. Evolution of gene duplication in plants. *Plant Physiol.* **171**, 2294–2316 (2016).
71. Wortman, J. R. *et al.* Annotation of the Arabidopsis Genome. *Plant Physiol.* **132**, 461–468 (2003).
72. Yamada, H. *et al.* The arabidopsis AHK4 histidine kinase is a cytokinin-binding receptor that transduces cytokinin signals across the membrane. *Plant Cell Physiol.* **42**, 1017–1023 (2001).
73. Jeon, J., Cho, C., Lee, M. R., Van Binh, N. & Kim, J. CYTOKININ RESPONSE FACTOR2 (CRF2) and CRF3 regulate lateral root development in response to cold stress in arabidopsis. *Plant Cell* **28**, 1828–1843 (2016).
74. Werner, T. & Schmülling, T. Cytokinin action in plant development. *Curr. Opin. Plant Biol.* **12**, 527–538 (2009).
75. Kieber, J. J. & Schaller, G. E. Cytokinins. *Arab. B.* **12**, e0168 (2014).
76. Pavlů, J. *et al.* Cytokinin at the crossroads of abiotic stress signalling pathways. *Int. J. Mol. Sci.* **19**, 1–36 (2018).
77. Wybouw, B. & De Rybel, B. Cytokinin – A Developing Story. *Trends Plant Sci.* **24**, 177–185 (2019).
78. Leuendorf, J. E. & Schmülling, T. Meeting at the dna: Specifying cytokinin responses through transcription factor complex formation. *Plants* **10**, (2021).
79. Jang, G. & Choi, Y. Do. Drought stress promotes xylem differentiation by modulating the interaction between cytokinin and jasmonic acid. *Plant Signal. Behav.* **13**, e1451707 (2018).
80. Rivero, R. M. *et al.* Delayed leaf senescence induces extreme drought tolerance in a flowering plant. *Proc. Natl. Acad. Sci. U. S. A.* **104**, 19631–19636 (2007).
81. Huang, X. *et al.* The Antagonistic Action of Abscisic Acid and Cytokinin Signaling

Mediates Drought Stress Response in Arabidopsis. *Mol. Plant* **11**, 970–982 (2018).

82. Zhao, Z. *et al.* Hormonal control of the shoot stem-cell niche. *Nature* **465**, 1089–1092 (2010).
83. Moubayidin, L. *et al.* The rate of cell differentiation controls the arabidopsis root meristem growth phase. *Curr. Biol.* **20**, 1138–1143 (2010).
84. Dello Ioio, R. *et al.* Cytokinins Determine Arabidopsis Root-Meristem Size by Controlling Cell Differentiation. *Curr. Biol.* **17**, 678–682 (2007).
85. Šimášková, M. *et al.* Cytokinin response factors regulate PIN-FORMED auxin transporters. *Nat. Commun.* **6**, (2015).
86. Tatsuo, K. CKI1, a Histidine Kinase Homolog Implicated in Cytokinin Signal Transduction. *Science (80-.).* **274**, 982–985 (1996).
87. Pischke, M. S. *et al.* An Arabidopsis histidine kinase is essential for megagametogenesis. *Proc. Natl. Acad. Sci. U. S. A.* **99**, 15800–15805 (2002).
88. Deng, Y. *et al.* Arabidopsis histidine kinase CKI1 acts upstream of histidine phosphotransfer proteins to regulate female gametophyte development and vegetative growth. *Plant Cell* **22**, 1232–1248 (2010).
89. Hejátko, J. *et al.* The Histidine kinases cytokinin-independent1 and arabidopsis histidine kinase2 and 3 regulate vascular tissue development in arabidopsis shoots. *Plant Cell* **21**, 2008–2021 (2009).
90. Urao, T. *et al.* A transmembrane hybrid-type histidine kinase in Arabidopsis functions as an osmosensor. *Plant Cell* **11**, 1743–1754 (1999).
91. Hofmann, A. *et al.* High-level expression, purification and initial characterization of recombinant Arabidopsis histidine kinase AHK1. *Plants* **9**, (2020).
92. Mähönen, A. P. *et al.* A novel two-component hybrid molecule regulates vascular morphogenesis of the Arabidopsis root. *Genes Dev.* **14**, 2938–2943 (2000).
93. Ueguchi, C., Koizumi, H., Suzuki, T. & Mizuno, T. Novel family of sensor histidine kinase genes in Arabidopsis thaliana. *Plant Cell Physiol.* **42**, 231–235 (2001).
94. Mähönen, A. P. *et al.* Cytokinins Regulate a Bidirectional Phosphorelay Network in Arabidopsis. *Curr. Biol.* **16**, 1116–1122 (2006).
95. Desikan, R. *et al.* The histidine kinase AHK5 integrates endogenous and environmental signals in Arabidopsis guard cells. *PLoS One* **3**, (2008).
96. Anantharaman, V. & Aravind, L. The CHASE domain: A predicted ligand-binding

module in plant cytokinin receptors and other eukaryotic and bacterial receptors. *Trends Biochem. Sci.* **26**, 579–582 (2001).

97. Heyl, A. *et al.* Evolutionary proteomics identifies amino acids essential for ligand-binding of the cytokinin receptor CHASE domain. *BMC Evol. Biol.* **7**, 1–8 (2007).
98. Higuchi, M. *et al.* In planta functions of the Arabidopsis cytokinin receptor family. *Proc. Natl. Acad. Sci. U. S. A.* **101**, 8821–8826 (2004).
99. Riefler, M., Novak, O., Strnad, M. & Schmülling, T. Hospital Uses EMR to Improve Handoff Process and Create Electronic 'Hall Pass'. *Plant Cell* **18**, 40–54 (2006).
100. Stolz, A. *et al.* The specificity of cytokinin signalling in Arabidopsis thaliana is mediated by differing ligand affinities and expression profiles of the receptors. *Plant J.* **67**, 157–168 (2011).
101. Cheng, C. Y., Mathews, D. E., Schaller, G. E. & Kieber, J. J. Cytokinin-dependent specification of the functional megaspore in the Arabidopsis female gametophyte. *Plant J.* **73**, 929–940 (2013).
102. Wulfetange, K. *et al.* The cytokinin receptors of arabidopsis are located mainly to the endoplasmic reticulum. *Plant Physiol.* **156**, 1808–1818 (2011).
103. Caesar, K. *et al.* Evidence for the localization of the Arabidopsis cytokinin receptors AHK3 and AHK4 in the endoplasmic reticulum. *J. Exp. Bot.* **62**, 5571–5580 (2011).
104. Lomin, S. N. *et al.* Studies of cytokinin receptor–phosphotransmitter interaction provide evidences for the initiation of cytokinin signalling in the endoplasmic reticulum. *Funct. Plant Biol.* **45**, 192–202 (2018).
105. Kubiasová, K. *et al.* Cytokinin fluoroprobe reveals multiple sites of cytokinin perception at plasma membrane and endoplasmic reticulum. *Nat. Commun.* **11**, 1–11 (2020).
106. Antoniadi, I. *et al.* Cell-surface receptors enable perception of extracellular cytokinins. *Nat. Commun.* **11**, (2020).
107. Romanov, G. A. & Schmülling, T. On the biological activity of cytokinin free bases and their ribosides. *Planta* **255**, 1–6 (2022).
108. Suzuki, T., Sakurai, K., Ueguchi, C. & Mizuno, T. Two types of putative nuclear factors that physically interact with histidine-containing phosphotransfer (Hpt) domains, signaling mediators in His-to-Asp phosphorelay, in Arabidopsis thaliana. *Plant Cell Physiol.* **42**, 37–45 (2001).
109. Spíchal, L. *et al.* Two cytokinin receptors of Arabidopsis thaliana, CRE1/AHK4 and

AHK3, differ in their ligand specificity in a bacterial assay. *Plant Cell Physiol.* **45**, 1299–1305 (2004).

110. Romanov, G. A., Lomin, S. N. & Schmülling, T. Biochemical characteristics and ligand-binding properties of Arabidopsis cytokinin receptor AHK3 compared to CRE1/AHK4 as revealed by a direct binding assay. *J. Exp. Bot.* **57**, 4051–4058 (2006).
111. Romanov, G. A., Spíchal, L., Lomin, S. N., Strnad, M. & Schmülling, T. A live cell hormone-binding assay on transgenic bacteria expressing a eukaryotic receptor protein. *Anal. Biochem.* **347**, 129–134 (2005).
112. Opekarová, M. & Tanner, W. Specific lipid requirements of membrane proteins—a putative bottleneck in heterologous expression. *Biochim. Biophys. Acta - Biomembr.* **1610**, 11–22 (2003).
113. Steklov, M. Y., Lomin, S. N., Osolodkin, D. I. & Romanov, G. A. Structural basis for cytokinin receptor signaling: An evolutionary approach. *Plant Cell Rep.* **32**, 781–793 (2013).
114. Nguyen, H. N., Nguyen, T. Q., Kisiala, A. B. & Emery, R. J. N. Beyond transport: cytokinin ribosides are translocated and active in regulating the development and environmental responses of plants. *Planta* **254**, 1–17 (2021).
115. Zürcher, E. *et al.* A robust and sensitive synthetic sensor to monitor the transcriptional output of the cytokinin signaling network in planta. *Plant Physiol.* **161**, 1066–1075 (2013).
116. Müller, B. & Sheen, J. Cytokinin and auxin interaction in root stem-cell specification during early embryogenesis. *Nature* **453**, 1094–1097 (2008).
117. Punwani, J. A., Hutchison, C. E., Schaller, G. E. & Kieber, J. J. The subcellular distribution of the Arabidopsis histidine phosphotransfer proteins is independent of cytokinin signaling. *Plant J.* **62**, 473–482 (2010).
118. Kakimoto, T. P Erception and S Ignal T Ransduction of C Ytokinins . *Annu. Rev. Plant Biol.* **54**, 605–627 (2003).
119. Cutcliffe, J. W., Hellmann, E., Heyl, A. & Rashotte, A. M. CRFs form protein-protein interactions with each other and with members of the cytokinin signalling pathway in Arabidopsis via the CRF domain. *J. Exp. Bot.* **62**, 4995–5002 (2011).
120. Pekárová, B. *et al.* Structure and binding specificity of the receiver domain of sensor histidine kinase CKI1 from Arabidopsis thaliana. *Plant J.* **67**, 827–839 (2011).

121. Dortay, H., Mehnert, N., Bürkle, L., Schmülling, T. & Heyl, A. Analysis of protein interactions within the cytokinin-signaling pathway of Arabidopsis thaliana. *FEBS J.* **273**, 4631–4644 (2006).

122. Tanaka, Y., Suzuki, T., Yamashino, T. & Mizuno, T. Comparative studies of the AHP histidine-containing phosphotransmitters implicated in His-to-Asp phosphorelay in Arabidopsis thaliana. *Biosci. Biotechnol. Biochem.* **68**, 462–465 (2004).

123. Suzuki, T., Imamura, A., Ueguchi, C. & Mizuno, T. Histidine-containing phosphotransfer (HPt) signal transducers implicated in His-to-Asp phosphorelay in Arabidopsis. *Plant Cell Physiol.* **39**, 1258–1268 (1998).

124. Nishiyama, R. *et al.* Arabidopsis AHP2, AHP3, and AHP5 histidine phosphotransfer proteins function as redundant negative regulators of drought stress response. *Proc. Natl. Acad. Sci. U. S. A.* **110**, 4840–4845 (2013).

125. Feng, J. *et al.* S-nitrosylation of phosphotransfer proteins represses cytokinin signaling. *Nat. Commun.* **4**, (2013).

126. Hutchison, C. E. *et al.* The Arabidopsis histidine phosphotransfer proteins are redundant positive regulators of cytokinin signaling. *Plant Cell* **18**, 3073–3087 (2006).

127. Liu, Z., Yuan, L., Song, X., Yu, X. & Sundaresan, V. AHP2, AHP3, and AHP5 act downstream of CKI1 in Arabidopsis female gametophyte development. *J. Exp. Bot.* **68**, 3365–3373 (2017).

128. Bishopp, A. *et al.* A mutually inhibitory interaction between auxin and cytokinin specifies vascular pattern in roots. *Curr. Biol.* **21**, 917–926 (2011).

129. Besnard, F. *et al.* Cytokinin signalling inhibitory fields provide robustness to phyllotaxis. *Nature* **505**, 417–421 (2014).

130. D'Agostino, I. B., Deruère, J. & Kieber, J. J. Characterization of the response of the Arabidopsis response regulator gene family to cytokinin. *Plant Physiol.* **124**, 1706–1717 (2000).

131. Müller & Sheen. Cytokinin and auxin interplay in root stem-cell specification during early embryogenesis. *Nature* **4**, 1094–1097 (2008).

132. Gordon, S. P., Chickarmane, V. S., Ohno, C. & Meyerowitz, E. M. Multiple feedback loops through cytokinin signaling control stem cell number within the Arabidopsis shoot meristem. *Proc. Natl. Acad. Sci. U. S. A.* **106**, 16529–16534 (2009).

133. Mira-Rodado, V. *et al.* Functional cross-talk between two-component and phytochrome

B signal transduction in Arabidopsis. *J. Exp. Bot.* **58**, 2595–2607 (2007).

134. Sweere, U. *et al.* Interaction of the response regulator ARR4 with phytochrome B in modulating red light signaling. *Science (80-.).* **294**, 1108–1111 (2001).
135. To, J. P. C. *et al.* Cytokinin regulates type-A Arabidopsis response regulator activity and protein stability via two-component phosphorelay. *Plant Cell* **19**, 3901–3914 (2007).
136. Lee, D. J., Kim, S., Ha, Y. M. & Kim, J. Phosphorylation of Arabidopsis response regulator 7 (ARR7) at the putative phospho-accepting site is required for ARR7 to act as a negative regulator of cytokinin signaling. *Planta* **227**, 577–587 (2008).
137. Sakai, H. *et al.* ARR1, a transcription factor for genes immediately responsive to cytokinins. *Science (80-.).* **294**, 1519–1521 (2001).
138. Lohrmann, J. *et al.* The response regulator ARR2: A pollen-specific transcription factor involved in the expression of nuclear genes for components of mitochondrial complex I in Arabidopsis. *Mol. Gen. Genet.* **265**, 2–13 (2001).
139. Sakai, H., Aoyama, T. & Oka, A. Arabidopsis ARR1 and ARR2 response regulators operate as transcriptional activators. *Plant J.* **24**, 703–711 (2000).
140. Imamura, A., Kiba, T., Tajima, Y., Yamashino, T. & Mizuno, T. In vivo and in vitro characterization of the ARR11 response regulator implicated in the His-to-Asp phosphorelay signal transduction in Arabidopsis thaliana. *Plant Cell Physiol.* **44**, 122–131 (2003).
141. Taniguchi, M., Sasaki, N., Tsuge, T., Aoyama, T. & Oka, A. ARR1 directly activates cytokinin response genes that encode proteins with diverse regulatory functions. *Plant Cell Physiol.* **48**, 263–277 (2007).
142. Kurepa, J., Li, Y., Perry, S. E. & Smalle, J. A. Ectopic expression of the phosphomimic mutant version of Arabidopsis response regulator 1 promotes a constitutive cytokinin response phenotype. *BMC Plant Biol.* **14**, 28 (2014).
143. Veerabagu, M. *et al.* The Arabidopsis B-type response regulator 18 homomerizes and positively regulates cytokinin responses. *Plant J.* **72**, 721–731 (2012).
144. Tajima, Y. *et al.* Comparative Studies on the Type-B Response Regulators Revealing their Distinctive Properties in the His-to-Asp Phosphorelay Signal Transduction of Arabidopsis thaliana. *Plant Cell Physiol.* **45**, 28–39 (2004).
145. Mason, M. G., Li, J., Mathews, D. E., Kieber, J. J. & Schaller, G. E. Type-B response regulators display overlapping expression patterns in Arabidopsis. *Plant Physiol.* **135**,

927–937 (2004).

146. Mason, M. G. *et al.* Type-B response regulators ARR1 and ARR12 regulate expression of AtHKT1;1 and accumulation of sodium in Arabidopsis shoots. *Plant J.* **64**, 753–763 (2010).
147. Ishida, K., Yamashino, T., Yokoyama, A. & Mizuno, T. Three type-B response regulators, ARR1, ARR10 and ARR12, play essential but redundant roles in cytokinin signal transduction throughout the life cycle of Arabidopsis thaliana. *Plant Cell Physiol.* **49**, 47–57 (2008).
148. Argyros, R. D. *et al.* Type B response regulators of Arabidopsis play key roles in cytokinin signaling and plant development. *Plant Cell* **20**, 2102–2116 (2008).
149. Xie, M. *et al.* A B-ARR-mediated cytokinin transcriptional network directs hormone cross-regulation and shoot development. *Nat. Commun.* **9**, 1–13 (2018).
150. Zubo, Y. O. *et al.* Cytokinin induces genome-wide binding of the type-B response regulator ARR10 to regulate growth and development in Arabidopsis. *Proc. Natl. Acad. Sci. U. S. A.* **114**, E5995–E6004 (2017).
151. Stock, J. & Da Re, S. Signal transduction: Response regulators on and off. *Curr. Biol.* **10**, 420–424 (2000).
152. Jeon, Y., Lee, Y. S., Han, J. S., Kim, J. B. & Hwang, D. S. Multimerization of Phosphorylated and Non-phosphorylated ArcA Is Necessary for the Response Regulator Function of the Arc Two-component Signal Transduction System. *J. Biol. Chem.* **276**, 40873–40879 (2001).
153. Morgunova, E. & Taipale, J. Structural perspective of cooperative transcription factor binding. *Curr. Opin. Struct. Biol.* **47**, 1–8 (2017).
154. Veerabagu, M. *et al.* The interaction of the arabidopsis response regulator ARR18 with bZIP63 mediates the regulation of PROLINE DEHYDROGENASE expression. *Mol. Plant* **7**, 1560–1577 (2014).
155. Yan, Z. *et al.* Type B response regulators act as central integrators in transcriptional control of the auxin biosynthesis enzyme TAA1. *Plant Physiol.* **175**, 1438–1454 (2017).
156. Zubo, Y. O. & Schaller, G. E. Role of the cytokinin-activated type-B response regulators in hormone crosstalk. *Plants* **9**, (2020).
157. Kurepa, J., Li, Y. & Smalle, J. A. Cytokinin signaling stabilizes the response activator ARR1. *Plant J.* **78**, 157–168 (2014).

158. Kim, H. J., Chiang, Y. H., Kieber, J. J. & Schaller, G. E. SCFKMD controls cytokinin signaling by regulating the degradation of type-B response regulators. *Proc. Natl. Acad. Sci. U. S. A.* **110**, 10028–10033 (2013).

159. Zhang, W., To, J. P. C., Cheng, C. Y., Eric Schaller, G. & Kieber, J. J. Type-A response regulators are required for proper root apical meristem function through post-transcriptional regulation of PIN auxin efflux carriers. *Plant J.* **68**, 1–10 (2011).

160. Gattolin, S. *et al.* Spatial and temporal expression of the response regulators ARR22 and ARR24 in Arabidopsis thaliana. *J. Exp. Bot.* **57**, 4225–4233 (2006).

161. Wallmeroth, N., Anastasia, A. K., Harter, K., Berendzen, K. W. & Mira-Rodado, V. Arabidopsis response regulator 22 inhibits cytokinin-regulated gene transcription in vivo. *Protoplasma* **254**, 597–601 (2017).

162. Wallmeroth, N. *et al. ARR22 overexpression can suppress plant two-component regulatory systems*. *PLoS ONE* vol. 14 (2019).

163. Hallmark, H. T. & Rashotte, A. M. Review – Cytokinin Response Factors: Responding to more than cytokinin. *Plant Sci.* **289**, 110251 (2019).

164. Zwack, P. J., Robinson, B. R., Risley, M. G. & Rashotte, A. M. Cytokinin response factor 6 negatively regulates leaf senescence and is induced in response to cytokinin and numerous abiotic stresses. *Plant Cell Physiol.* **54**, 971–981 (2013).

165. Zwack, P. J. *et al.* Cytokinin response factor 6 represses cytokinin-associated genes during oxidative stress. *Plant Physiol.* **172**, 1249–1258 (2016).

166. Sakuma, Y. *et al.* DNA-binding specificity of the ERF/AP2 domain of Arabidopsis DREBs, transcription factors involved in dehydration- and cold-inducible gene expression. *Biochem. Biophys. Res. Commun.* **290**, 998–1009 (2002).

167. Rashotte, A. M. & Goertzen, L. R. The CRF domain defines Cytokinin Response Factor proteins in plants. *BMC Plant Biol.* **10**, (2010).

168. Shi, X., Gupta, S. & Rashotte, A. M. Solanum lycopersicum cytokinin response factor (SlCRF) genes: Characterization of CRF domain-containing ERF genes in tomato. *J. Exp. Bot.* **63**, 973–982 (2012).

169. Hwang, I. & Sheen, J. Two-component circuitry in Arabidopsis cytokinin signal transduction. *Nature* **413**, 383–389 (2001).

170. Ketelsen, B. Characterization of a Cytokinin Response Factor in Arabidopsis thaliana. (University of Tromso. FACULTY OF BIOSCIENCES, FISHERIES AND

ECONOMICS DEPARTMENT OF ARCTIC AND MARINE BIOLOGY, 2012).

171. Raines, T. *et al.* The cytokinin response factors modulate root and shoot growth and promote leaf senescence in Arabidopsis. *Plant J.* **85**, 134–147 (2016).
172. S., T. Stéphane Leduc (1853-1939), de la médecine à la biologie synthétique , ,. *Hist. Sci. Med.* **43**, 67–72. (2009).
173. Jacob, F. & Monod, J. Genetic regulatory mechanisms in the synthesis of proteins. *J. Mol. Biol.* **3**, 318–356 (1961).
174. Garegg, P. J. *et al.* Nucleoside H-phosphonates. III. Chemical synthesis of oligodeoxyribonucleotides by the hydrogenphosphonate approach. *Tetrahedron Lett.* **27**, 4051–4054 (1986).
175. Froehler, B. C., Ng, P. G. & Matteucci, M. D. Synthesis of DNA via deoxynucleoside H-phosphonate intermediates. *Nucleic Acids Res.* **14**, 5399–5407 (1986).
176. Sands, B. & Brent, R. Overview of post Cohen-Boyer methods for single segment cloning and for multisegment DNA assembly. *Physiol. Behav.* **176**, 139–148 (2016).
177. Cohen, S. N., Chang, A. C. Y., Boyer, H. W. & Helling, R. B. Construction of biologically functional bacterial plasmids in vitro. *Proc. Natl. Acad. Sci. U. S. A.* **70**, 3240–3244 (1973).
178. K., S. R. *et al.* Primer-Directed Enzymatic Amplification of DNA with a Thermostable DNA Polymerase. *Science (80-.).* **239**, 487–491 (1988).
179. Jinek, M. *et al.* A programmable dual-RNA-guided DNA endonuclease in adaptive bacterial immunity. *Science* **337**, 816–821 (2012).
180. Gardner, T. S., Cantor, C. R. & Collins, J. J. Construction of a genetic toggle switch in Escherichia coli. *Nature* **403**, 339–342 (2000).
181. Elowitz. A synthetic oscillatory network repressilator. *Nature* **403**, 335–338 (2000).
182. Becskei, A. & Serrano, L. Engineering stability in gene networks by autoregulation. *Nature* **405**, 590–593 (2000).
183. Grozinger, L. *et al.* Pathways to cellular supremacy in biocomputing. *Nat. Commun.* **10**, 5250 (2019).
184. Koder, R. L. *et al.* Design and engineering of an O(2) transport protein. *Nature* **458**, 305–309 (2009).
185. Gilbert, C. & Ellis, T. Biological Engineered Living Materials: Growing Functional Materials with Genetically Programmable Properties. *ACS Synth. Biol.* **8**, 1–15 (2019).

186. Foong, C. P. *et al.* A marine photosynthetic microbial cell factory as a platform for spider silk production. *Commun. Biol.* **3**, 357 (2020).
187. Fredens, J. *et al.* Total synthesis of Escherichia coli with a recoded genome. *Nature* **569**, 514–518 (2019).
188. Anderson, J. C., Clarke, E. J., Arkin, A. P. & Voigt, C. A. Environmentally controlled invasion of cancer cells by engineered bacteria. *J. Mol. Biol.* **355**, 619–627 (2006).
189. Charbonneau, M. R., Isabella, V. M., Li, N. & Kurtz, C. B. Developing a new class of engineered live bacterial therapeutics to treat human diseases. *Nat. Commun.* **11**, 1738 (2020).
190. Hofer, M. & Lutolf, M. P. Engineering organoids. *Nat. Rev. Mater.* **6**, 402–420 (2021).
191. Atsumi, S., Hanai, T. & Liao, J. C. Non-fermentative pathways for synthesis of branched-chain higher alcohols as biofuels. *Nature* **451**, 86–89 (2008).
192. Verseux, C. N., Paulino-Lima, I. G., Baqué, M., Billi, D. & Rothschild, L. J. Synthetic Biology for Space Exploration: Promises and Societal Implications BT - Ambivalences of Creating Life: Societal and Philosophical Dimensions of Synthetic Biology. in (eds. Hagen, K., Engelhard, M. & Toepfer, G.) 73–100 (Springer International Publishing, 2016). doi:10.1007/978-3-319-21088-9_4.
193. Khalil, A. S. & Collins, J. J. Synthetic biology: Applications come of age. *Nat. Rev. Genet.* **11**, 367–379 (2010).
194. Brooks, S. M. & Alper, H. S. Applications, challenges, and needs for employing synthetic biology beyond the lab. *Nat. Commun.* **12**, 1390 (2021).
195. Samodelov, S. L. & Zurbriggen, M. D. *Quantitatively Understanding Plant Signaling: Novel Theoretical–Experimental Approaches*. *Trends in Plant Science* vol. 22 (Elsevier Ltd, 2017).
196. Weber, E., Engler, C., Gruetzner, R., Werner, S. & Marillonnet, S. A modular cloning system for standardized assembly of multigene constructs. *PLoS One* **6**, (2011).
197. Weber, W. & Fussenegger, M. Synthetic gene networks in mammalian cells. *Curr. Opin. Biotechnol.* **21**, 690–696 (2010).
198. Guido, N. J. *et al.* A bottom-up approach to gene regulation. *Nature* **439**, 856–860 (2006).
199. Kelwick, R., MacDonald, J. T., Webb, A. J. & Freemont, P. Developments in the tools and methodologies of synthetic biology. *Front. Bioeng. Biotechnol.* **2**, 1–23 (2014).

200. Lakhani, C. M., O'connor & Teeple E, Collins J, Shrestha S, Dennerlein J, et al. 乳鼠心肌提取 HHS Public Access. *Physiol. Behav.* **176**, 139–148 (2016).
201. Wossning, T. & Reth, M. B cell antigen receptor assembly and Syk activation in the S2 cell reconstitution system. *Immunol. Lett.* **92**, 67–73 (2004).
202. Havens, K. A. *et al.* A synthetic approach reveals extensive tunability of auxin signaling. *Plant Physiol.* **160**, 135–142 (2012).
203. Pierre-Jerome, E., Jang, S. S., Havens, K. A., Nemhauser, J. L. & Klavins, E. Recapitulation of the forward nuclear auxin response pathway in yeast. *Proc. Natl. Acad. Sci. U. S. A.* **111**, 9407–9412 (2014).
204. Lalonde, S. *et al.* Molecular and cellular approaches for the detection of protein-protein interactions: Latest techniques and current limitations. *Plant J.* **53**, 610–635 (2008).
205. Xing, S., Wallmeroth, N., Berendzen, K. W. & Grefen, C. Techniques for the analysis of protein-protein interactions in vivo. *Plant Physiol.* **171**, 727–758 (2016).
206. Lienert, F., Lohmueller, J., Garg, A. & Silver, P. Synthetic Biology in Mammalian Cells. *Nat Rev Mol Cell Biol* **15**, 95–107 (2014).
207. Weber, W. & Fussenegger, M. Engineering of Synthetic Mammalian Gene Networks. *Chem. Biol.* **16**, 287–297 (2009).
208. Beyer, H. M. *et al.* Red Light-Regulated Reversible Nuclear Localization of Proteins in Mammalian Cells and Zebrafish. *ACS Synth. Biol.* **4**, 951–958 (2015).
209. Beyer, H. M. *et al.* Red Light-Regulated Reversible Nuclear Localization of Proteins in Mammalian Cells and Zebrafish. *ACS Synth. Biol.* **4**, 951–958 (2015).
210. Beyer, H. M. *et al.* AQUA cloning: A versatile and simple enzyme-free cloning approach. *PLoS One* **10**, 1–20 (2015).
211. Braguy, J. & Zurbriggen, M. D. Synthetic strategies for plant signalling studies: molecular toolbox and orthogonal platforms. *Plant J.* **87**, 118–138 (2016).
212. Nishimura, K., Fukagawa, T., Takisawa, H., Kakimoto, T. & Kanemaki, M. An auxin-based degron system for the rapid depletion of proteins in nonplant cells. *Nat. Methods* **6**, 917–922 (2009).
213. Wend, S. *et al.* A quantitative ratiometric sensor for time-resolved analysis of auxin dynamics. *Sci. Rep.* **3**, 1–7 (2013).
214. Blanco-Touriñán, N. *et al.* COP1 destabilizes DELLA proteins in Arabidopsis. *Proc. Natl. Acad. Sci. U. S. A.* **117**, 13792–13799 (2020).

215. Blomeier, T. Quantitative understanding of complex light-dependent and phytohormone triggered plant signaling pathways in the orthogonal system of mammalian cells. (Heinrich-Heine University Düsseldorf, 2021).
216. Andres, J. Reconstruction and study of plant hormone signaling pathways in plant and mammalian systems. (Heinrich-Heine university Düsseldorf, 2019).
217. Andres, J., Blomeier, T. & Zurbriggen, M. D. Synthetic switches and regulatory circuits in plants. *Plant Physiol.* **179**, 862–884 (2019).
218. Brunoud, G. *et al.* A novel sensor to map auxin response and distribution at high spatio-temporal resolution. *Nature* **482**, 103–106 (2012).
219. Martin-Arevalillo, R. & Vernoux, T. Shining light on plant hormones with genetically encoded biosensors. *Biol. Chem.* **400**, 477–486 (2019).
220. Wosika, V. & Pelet, S. Relocation sensors to quantify signaling dynamics in live single cells. *Curr. Opin. Biotechnol.* **45**, 51–58 (2017).
221. Uslu, V. V. & Grossmann, G. The biosensor toolbox for plant developmental biology. *Curr. Opin. Plant Biol.* **29**, 138–147 (2016).
222. Cho, H. *et al.* A secreted peptide acts on BIN2-mediated phosphorylation of ARFs to potentiate auxin response during lateral root development. *Nat. Cell Biol.* **16**, 66–76 (2014).
223. Föster. Zwischenmolekulare Energiewanderung und Fluoreszenz. *Ann Phys* **437**, 55–75 (1948).
224. Piston, D. W. & Kremers, G. J. Fluorescent protein FRET: the good, the bad and the ugly. *Trends Biochem. Sci.* **32**, 407–414 (2007).
225. Shaner, N. C., Steinbach, P. A. & Tsien, R. Y. A guide to choosing fluorescent proteins. *Nat. Methods* **2**, 905–909 (2005).
226. Albertazzi, L., Arosio, D., Marchetti, L., Ricci, F. & Beltram, F. Quantitative FRET analysis with the E0GFP-mCherry fluorescent protein pair. *Photochem. Photobiol.* **85**, 287–297 (2009).
227. Tsutsui, H., Karasawa, S., Okamura, Y. & Miyawaki, A. Improving membrane voltage measurements using FRET with new fluorescent proteins. *Nat. Methods* **5**, 683–685 (2008).
228. Berendzen, K. W. *et al.* Screening for in planta protein-protein interactions combining bimolecular fluorescence complementation with flow cytometry. *Plant Methods* **8**, 1–

17 (2012).

229. Ohashi, K., Kiuchi, T., Shoji, K., Sampei, K. & Mizuno, K. Visualization of cofilin-actin and Ras-Raf interactions by bimolecular fluorescence complementation assays using a new pair of split Venus fragments. *Biotechniques* **52**, 45–50 (2012).
230. Skruzny, M., Pohl, E. & Abella, M. FRET microscopy in yeast. *Biosensors* **9**, 1–17 (2019).
231. Lam, A. J. *et al.* Improving FRET dynamic range with bright green and red fluorescent proteins. *Nat. Methods* **9**, 1005–1012 (2012).
232. Sun, Y., Day, R. & Periasamy, A. Investigating protein-protein interactions in living cells using FLIM. *Nat. Protoc.* **6**, 1324–1340 (2012).
233. Gossen, M. & Bujard, H. Tight control of gene expression in mammalian cells by tetracycline-responsive promoters. *Proc. Natl. Acad. Sci. U. S. A.* **89**, 5547–5551 (1992).
234. Thibodeaux, G. N., Cowmeadow, R., Umeda, A. & Zhang, Z. A tetracycline repressor-based mammalian two-hybrid system to detect protein-protein interactions in vivo. *Anal. Biochem.* **386**, 129–131 (2009).
235. Müller, K. *et al.* A red/far-red light-responsive bi-stable toggle switch to control gene expression in mammalian cells. *Nucleic Acids Res.* **41**, (2013).
236. Beyer, H. M. *et al.* Red light-regulated reversible nuclear localization of proteins in mammalian cells and zebrafish of Biology , University of Freiburg , Schänzlestrasse 1 , 79104 Freiburg , Germany - Centre for Biological Signalling Studies , University of Freiburg , Schän. *Suppl. data* 1–13.
237. Gratz, R. *et al.* Phospho-mutant activity assays provide evidence for alternative phospho-regulation pathways of the transcription factor FER-LIKE IRON DEFICIENCY-INDUCED TRANSCRIPTION FACTOR. *New Phytol.* **225**, 250–267 (2020).
238. Besant, P. G., Tan, E. & Attwood, P. V. Mammalian protein histidine kinases. *Int. J. Biochem. Cell Biol.* **35**, 297–309 (2003).
239. Steeg, P. S., Palmieri, D., Ouatas, T. & Salerno, M. Histidine kinases and histidine phosphorylated proteins in mammalian cell biology, signal transduction and cancer. *Cancer Lett.* **190**, 1–12 (2003).
240. Kumar, M. N. & Verslues, P. E. Stress physiology functions of the Arabidopsis histidine kinase cytokinin receptors. *Physiol. Plant.* **154**, 369–380 (2015).

241. Hwang, I., Chen, H. & Sheen, J. Two-Component Signal Transduction Pathways in. **129**, 500–515 (2002).
242. Imamura, A. *et al.* Compilation and characterization of Arabiopsis thaliana response regulators implicated in His-Asp phosphorelay signal transduction. *Plant Cell Physiol.* **40**, 733–742 (1999).
243. Zhang, Y. *et al.* A highly efficient rice green tissue protoplast system for transient gene expression and studying light/chloroplast-related processes. *Plant Methods* **7**, 30 (2011).
244. Abel, S. & Theologis, A. Early genes and auxin action. *Plant Physiol.* **111**, 9–17 (1996).
245. Yamagami, M., Haga, K., Napier, R. M. & Iino, M. Two Distinct Signaling Pathways Participate in Auxin-Induced Swelling of Pea Epidermal Protoplasts. *Plant Physiol.* **134**, 735–747 (2004).
246. Gubler, F., Chandler, P. M., White, R. G., Llewellyn, D. J. & Jacobsen, J. V. Gibberellin signaling in barley aleurone cells. Control of SLN1 and GAMYB expression. *Plant Physiol.* **129**, 191–200 (2002).
247. Uno, Y. *et al.* Arabidopsis basic leucine zipper transcription factors involved in an abscisic acid-dependent signal transduction pathway under drought and high-salinity conditions. *Proc. Natl. Acad. Sci. U. S. A.* **97**, 11632–11637 (2000).
248. Kim, N. *et al.* Functional characterization and reconstitution of ABA signaling components using transient gene expression in rice protoplasts. *Front. Plant Sci.* **6**, 1–11 (2015).
249. Gibb, M., Kisiala, A. B., Morrison, E. N. & Emery, R. J. N. The Origins and Roles of Methylthiolated Cytokinins: Evidence From Among Life Kingdoms. *Front. Cell Dev. Biol.* **8**, 1–14 (2020).
250. Yan, Z. *et al.* MPK3/6-induced degradation of ARR1/10/12 promotes salt tolerance in Arabidopsis . *EMBO Rep.* **22**, 1–20 (2021).
251. Mason, M. G. *et al.* Multiple type-B response regulators mediate cytokinin signal transduction in Arabidopsis. *Plant Cell* **17**, 3007–3018 (2005).
252. Goujon, M. *et al.* A new bioinformatics analysis tools framework at EMBL-EBI. *Nucleic Acids Res.* **38**, 695–699 (2010).
253. Nguyen Ba AN, Pogoutse A, Provart N, M. A. NLStradamus: a simple Hidden Markov Model for nuclear localization signal prediction. *BMC Bioinformatics.* **10**, 202 (2009).
254. Kosugi, S., Hasebe, M., Tomita, M. & Yanagawa, H. Systematic identification of cell

cycle-dependent yeast nucleocytoplasmic shuttling proteins by prediction of composite motifs. *Proc. Natl. Acad. Sci. U. S. A.* **106**, 10171–10176 (2009).

255. Liu, L., White, M. J. & Macrae, T. H. Transcription factors and their genes in higher plants. Functional domains, evolution and regulation. *Eur. j. Biochem* **257**, 247–257 (1999).
256. Van Der Krol, A. R. & Chua, N. H. The basic domain of plant B-ZIP proteins facilitates import of a reporter protein into plant nuclei. *Plant Cell* **3**, 667–675 (1991).
257. Guralnick, B., Thomsen, G. & Citovsky, V. Transport of DNA into the nuclei of xenopus oocytes by a modified VirE2 protein of agrobacterium. *Plant Cell* **8**, 363–373 (1996).
258. Relić, B., Andjelković, M., Rossi, L., Nagamine, Y. & Hohn, B. Interaction of the DNA modifying proteins VirD1 and VirD2 of Agrobacterium tumefaciens: Analysis by subcellular localization in mammalian cells. *Proc. Natl. Acad. Sci. U. S. A.* **95**, 9105–9110 (1998).
259. Marín-de la Rosa, N. *et al.* Genome Wide Binding Site Analysis Reveals Transcriptional Coactivation of Cytokinin-Responsive Genes by DELLA Proteins. *PLoS Genet.* **11**, 1–20 (2015).
260. Müller, K. & Weber, W. Optogenetic tools for mammalian systems. *Mol. Biosyst.* **9**, 596–608 (2013).
261. Müller, K., Zurbriggen, M. D. & Weber, W. Control of gene expression using a red- and far-red light-responsive bi-stable toggle switch. *Nat. Protoc.* **9**, 622–632 (2014).
262. Ochoa-Fernandez, R. Optogenetics: Methods and Protocols. in (ed. Kianianmomeni, A.) 125–139 (Humana Press, 2016).
263. Jacobs, J. L. & Dinman, J. D. Systematic analysis of bicistronic reporter assay data. *Nucleic Acids Res.* **32**, e160–e160 (2004).
264. Steiner, E. *et al.* Characterization of the cytokinin sensor TCSv2 in arabidopsis and tomato. *Plant Methods* **16**, 1–13 (2020).
265. Tao, J. *et al.* A sensitive synthetic reporter for visualizing cytokinin signaling output in rice. *Plant Methods* **13**, 1–9 (2017).
266. Mok, M. C. *et al.* Cytokinin activity of N-phenyl-N′-1, 2,3-thiadiazol-5-ylurea (thidiazuron). *Phytochemistry* **21**, 1509–1511 (1982).
267. Müller, K. *et al.* Multi-chromatic control of mammalian gene expression and signaling. *Nucleic Acids Res.* **41**, (2013).

7. Appendix

7.1 Full reconstruction of *Arabidopsis* CK signalling in mammalian cells reveals new regulatory mechanisms (Manuscript in preparation)

Estefania Pavesi[1,2], (nn), Teva Vernoux[1*], Matias D. Zurbriggen[2,3*]

1 Laboratoire de Reproduction et Développement des Plantes, Université de Lyon, ENS de Lyon, Lyon, France
2 Institute of Synthetic Biology, Heinrich-Heine Universität of Düsseldorf, Düsseldorf, Germany.
3 CEPLAS - Cluster of Excellence on Plant Sciences, Düsseldorf, Germany.

*Corresponding authors:
Matias Zurbriggen, Institute of Synthetic Biology, Heinrich-Heine Universität of Düsseldorf, and, CEPLAS - Cluster of Excellence on Plant Sciences, Düsseldorf, Germany.
E-Mail: matias.zurbriggen@uni-duesseldorf.de
Teva Vernoux, Laboratoire de Reproduction et Développement des Plantes, CNRS, INRA, ENS Lyon, UCBL, Université de Lyon, Lyon, France.
E-Mail: teva.vernoux@ens-lyon.fr

Abstract

Cytokinin (CK) hormones canonical signalling pathway involves a phospho-transfer triggered by the hormone binding to the histidine kinase receptor. Far from being linear, CK response includes multiple negative feedbacks and genetic redundancy but also can be set off by non-canonical circuits. This scenario has thwarted the understanding of the molecular mechanism behind CK's crucial role in plant growth and development. Here, we describe the design and engineering of a new platform by reconstructing the full CK signalling pathway from *Arabidopsis thaliana* in mammalian cells. Our synthetic pathway response to physiological concentrations of CK encouraged us to investigate the receptor selectivity to different adenine derivates. We quantitatively explored the contribution of individual members of each multigene family involved in CK signalling, as well as the mode of action of three negative response regulators. Further we interrogated the role of the conserved aspartate residues in response regulator's (RRs) transactivation. Finally, we quantitatively explored the interaction between different signalling elements proposing new regulatory mechanisms.

Introduction

As sessile organisms, plants cannot escape adverse environmental stressors, therefore they have developed highly sophisticated programs to respond to external stimuli to adapt, and survive. Among all physical and chemical stimuli plants have mastered to integrate, plant (Phyto)hormones are the main morphogenetic signals. Phytohormone signalling involves highly efficient and complex mechanisms, the understanding of which has challenged the scientific community for decades. The main constraints of studying hormone signalling in their natural environment include the extensive interconnectivity among them and with other networks, the high level of redundancy, and the multiple regulatory mechanisms present in plants.

CK are one of the six major hormones in plants. Since their discovery, they have captivated the attention of the scientific community, as they are involved in many growth, developmental and physiological processes; presenting a potential target for plant optimization. The canonical circuit driving CK perception and signalling resemble the two-component systems (TCS) found in bacteria and yeast. The main components of this pathway in *Arabidopsis thaliana* are the histidine kinase receptors (AHKs), the histidine-containing phosphotransferases (AHPs), and the type-B response regulators (B-ARRs). The hormone binding to the AHKs is the crucial event that will trigger the phospho-relay. After the AHKs autophosphorylation, the phosphate will be transferred to the AHPs, and finally to the receiver domain (REC) of the RRs. The binding of the B-ARRs to their consensus sequence will result in the modulation of gene expression. The primary response genes of this pathway, the type-A ARRs (A-ARRs)[130], together with the type-C ARRs (C-ARRs) and the pseudo-phosphotransferase AHP6, act as negative regulators. In addition to this extensive feedback control, all components involved in CK pathway belong to multigene families of up to 12 members. This high level of functional redundancy has demanded the generation of high order loss-of-function mutants to obtain a particular phenotype; while the knock-out of multiple genes has often led to lethal embryos. Moreover, unlike other phytohormones, CK responses can be also turned on by non-canonical circuits such as the directed by Cytokinin-independent1 (CKI1) HK receptor[86], and the Cytokinin response factors (CRF) 3, a member of a second family of RRs of the pathway, not yet linked to the canonical phospho-relay.

The field of Synthetic biology (SynBio) offers a plethora of applications which rely on the possibility of recombining existing or newly engineered building blocks for the construction

of artificial biological systems[195,213]. The study of the CK pathway has already benefited from this modularity through the design of the Two-component signalling sensor (TCS):green fluorescent protein (GFP)[115,264,265]. The TCS:GFP combines repetitions of the DNA consensus sequence recognized by the B-ARRs, with a fluorescent reporter gene that allows visualization of CK distribution *in planta*. However, neither knock-out mutants, reporter assays, nor transient expression in isolated plant cells (protoplasts) and *Nicotiana bethamiana* leaves have overcome the impossibility of studying single signalling elements´ contribution to CK responses in plants. An alternative to tackle this problem is the recombination of the building blocks comprising CK perception and signalling in a genuine unrelated (orthogonal) system.

Bacteria and yeast have historically been chosen as chassis for signalling and metabolic pathway reconstruction for their sequenced genome, cheap maintenance and easy handling. These partial reconstructions have also been applied to the study of auxin and CK pathways. However, there are two main constraints when analysing CK signalling in an evolutionary unrelated organism. First, the alien environment of a prokaryote membrane can lead to incorrect folding and function of the AHKs. Secondly, these organisms have several endogenous TCS networks. The high homology between the components of *A. thaliana* CK pathway and the *Saccharomyces cerevisiae* TCS mediated by the synthetic lethal of N-rule 1 (SLN1) HK, was fundamental for deciphering the role of AHKs and AHPs. However, this component analogy demands a careful interpretation of the results when studying single components, as their effect may be enhanced or masked by endogenous proteins.

Mammalian cells have recently gained impulse as chassis for plant signalling pathway studies. The evolutive proximity to plant cells is evidenced in the conserved post-translational modifications and similar membrane architecture, while no TCS has yet been characterized. Further, a plethora of approaches is now available for successful heterologous reconstruction and posterior quantitative output of the observed phenomena. As a milestone, partial reconstruction in Human embryonic kidney (HEK) cells of the gibberellins perception components has recently elucidated the importance of their protein-protein interactions (PPIs) in downstream signalling.

In this study, we pursued the design and implementation of an experimental platform for the study of the CK signalling pathway, by reconstructing the full *Arabidopsis thaliana* CK pathway in Chinese hamster ovary (CHO) cells. From the AHK selectivity to different hormone derivates down to ARR1 and ARR10 differential transactivation, our reporter system will allow

us to quantitatively evidence the role of individual components to the CK responses. Moreover, we will systematically use mammalian-x-hybrid approaches to interrogate several PPIs, and competition among the TCS elements. Lastly, we will interrogate the role of the conserved aspartate (D) residue of the RR both in the transactivation of the reporter, and PPIs.

Results

Reconstruction of the complete CK signalling pathway in mammalian cells

Partial reconstruction in heterologous organisms has been instrumental for the identification of key events comprising CK signal responses. The hormone binding to the receptors, and the phosphor-transfer between these and the AHPs are two examples[61–63]. To overcome the limitations of working in bacteria and yeast, while reducing the inherent complexity of studies *in planta*, we reconstructed the full CK perception and signalling network in the mammalian (orthogonal) model CHO cells (**Fig. 1A - B**). To this aim we engineered constructs harbouring the full cDNA of selected members of the AHK3, the AHP2, and the ARR10 (a B-ARR), downstream the simian virus 40 early promoter (P_{SV40}), controlling their expression in mammalian cells. To evidence CK responses, we engineered a promotor-reporter system by placing repetitions of the core sequence for B-ARRs´ DNA binding in proximity to a minimal human cytomegalovirus early promoter (P_{CMVmin}) controlling the expression of the Secreted embryonic alkaline phosphatase, SEAP (henceforth, TCSm) (**Fig. 1C**). In plants, AHK perception of the hormone will trigger a Histidine-to-Aspartate phospho-relay. The phosphoryl group will then be transferred to the AHPs, and later to the B-ARR. Phosphorylation of the B-ARRs at their conserved aspartate is believed to induce a conformational change that will expose these RRs DNA binding domain, enhancing their transcriptional activators activity[139,140]We thus expect to observe SEAP expression in cells co-transfected will all CK network components only after hormone treatment. To evidence the hormone treatment effect on the cell's growth and survival, a normalization module harbouring the reporter gene Gaussia luciferase (GLuc) under the control of the SV40 promotor was routinely co-transfected. An example of GLuc expression can be found in **Supplementary Fig. 1**.

Next, to establish the experimental set-up for the upcoming assays, we tested our system's responsiveness after 3-, 6-, 12-, 24-, and 48 h of exposure to 6-bencilaminopurine (BA) (**Fig. 1D**). Vectors containing either AHK3, AHP2, ARR10 and the TCSm were co-transfected in equimolar concentration. Significant activation of the system was observed after 12-, 24-, and 48 h treatment. For the 12 h treatment an approximated 16-fold increase in the activation of the

TCSm was observed in comparison with the mock cells (treated with water) at concentration ≥ 10 nM BA, independently of the hormone concentration. For the lack of dynamic range of this condition, we decided to dismiss it. On the other hand, the 24- and 48 h treatments showed a good dynamic range between the system responses to 1 nM, 10 nm, and 100 nM. Further additions of BA up to 10 µM did not increased the TCSm activation. Remarkably, our system sensitivity is equivalent to the CK concentrations found in plants[52]

Due to a slight increase in the background signal in the mock cells after 48 h of BA exposure, the fold increase in this condition was not remarkably higher than for the 24 h treatment. Comparing these two conditions, the systems showed a 5- and 4-fold increase for a 1nM concentration BA; 14- and 16-fold increase for 10 nM BA, and 21-, and 25-fold for concentrations ≥ 100 nM after 24 h and 48 h treatment, respectively. In addition, both treatments showed a similar GLuc expression level. These results evidence that an additional 24 h treatment, after the first 24 h does not affect the rate of cell growth/death. Altogether, extending the exposure time over 24 h presented no quantitative advantage for which we selected a 24 h treatment with BA for the following experiments. Next, we decided to induce the system with either water (also referred to as "0 nM BA"), or BA in a 10 nM BA or 100 n M concentration. We dismissed the 1 nM concentration for in later experiments the TCSm activation at this hormone concentration was less significant.

Next, to investigate a similar promotor-reporter system activation in *Arabidopsis* protoplasts, we engineered constructs harboring the full-length cDNA of AHP2 and ARR10 under the control of the cauliflower mosaic virus 35S promoter (P35S). The plasmids were co-transformed together with a promotor-reporter system were repetitions of the B-ARRs DNA binding region were cloned upstream a P35S minimal promotor (P35Smin), controlling the expression of the Firefly luciferase (FLuc) reporter gene. Our results showed that the activation of CK responses in protoplasts required the addition of a concentration of 10 nM BA, observe for our mammalian circuit (**Supplementary Fig. S2**).

Finally, we explored the possibility of our system activation being influenced by mammalian endogenous proteins. To this aim, we co-transfected each component of our reconstructed pathway either alone, or in every possible combination with the others, always in the presence of the TCSm. Our results showed that activation of the system is only possible when the full CK pathway has been reconstructed (**Fig. 1E**).

Individual contribution of specific TCS components to CK response

To explore the contribution of individual components to CK signalling we next analysed the activation of the TCSm in responses mediated by the each of the members of the AHP family, acting downstream AHK3, and AHK4 receptor. In addition, we explored the change in the reporter expression in ARR1-, and ARR10-mediated responses, again, downstream both receptors. For this purpose, we designed new constructs for the expression in mammalian cells of AHP1, AHP3 to 6, ARR1, and AHK4.

The AHK4-mediated responses led to a remarkably stronger TCSm activation in every tested combination. However, it required a higher concentration of BA, in comparison with AHK3-mediated activation. The approximate sensitivity of AHK4 for BA was previously investigated in our work showing that the AHK4-mediated TCSm activation requires the addition of 20 nM BA (**Fig. 2; Supplementary Fig. S3)**.

Further, unlike ARR10, ARR1 was able to activate CK responses acting downstream AHK4, after addition of BA in a 10 nM concentration (**Fig. 2B-C**). In addition, co-transfection of both RRs in cells expressing the same receptor significantly increased TCSm activation. At 100 nM concentrations of BA this seems to be the summary of ARR1 and ARR10 individual responses (**Fig. 2C)**. However, an addition of ARR1, and ARR10 responses does not explained the remarkably high activation of the TCSm observed at concentrations of 10 nM BA and, particularly, in the mock cells.

Next, we investigated the different AHP-mediated activation of the TCSm. Notably, the profile of activation was conserved regardless the AHK co-transfected, with the exception of AHP5, which lead to no activation downstream of AHK3 (**Fig. 1C-D**). The observed activation pattern was AHP1~AHP2>AHP3>AHP4, for AHK3, and AHP1~AHP2>AHP3>AHP4>AHP5 for AHK4. Not surprisingly, AHP6 showed no activation of the system, accordingly with its pseudo-HP activity.

AHKs´ sensitivity and selectivity to different CK forms, and their TCSm activation.

Up-to-date, most studies of the sensitivity and selectivity of the AHKs were performed in isolated system. In comparison with bacteria-based systems[109,110], plant-membranes based assays[52] presented the advantage of providing a native-like environment for the receptor[112,113].

Next, we aimed to explore our eukaryotic platform suitability to perform fast, quantitative, and (notably) *in vivo* screening of the selectivity and sensitivity of AHK3, and AHK4 for different

CK forms. For this, we co-transfected CHO cells with AHK3 (or AHK4) together with ARR10, and AHP2, to fully reconstruct CK canonical circuit, and treated the cells for 24 h with 10 adenine derivates. Among the 32 CK forms isolated up-to-date from plants´ biological samples[114], we selected for this study 7 of the most abundant forms in plants, the isoprenoid derivates, including: isopentenyladenine (iP), the 2-Methylthio-N^6-isopentenyladenine (2MeSiP); cis-, and trans-Zeatin (cZ and tZ), Dihydrozeatin (DZ), the tZ-riboside (tZR), and the nucleotide trans-Zeatin riboside-5´-monophosphate sodium salt (tZRMP). As representative of the aromatic CK we selected Kinetin (KIN), in addition to BA, and the diphenylurea Tidiazuron (TDZ), a synthetic CK extensively used as herbicide and plant growth regulator[266]. Considering that the samples will only differ in the expressed AHK, we interpretated the requirement of a lower hormone concentration for the TCSm activation, as a higher sensitivity of the receptor for the CK form. Later, the quantified SEAP expression will give us information regarding the differential activation of CK responses attributed to specific AHK-CK combinations.

Our results showed that lower concentrations of most CK forms were necessary for the AHK3-mediated activation of the TCSm, in comparison with AHK4 (**Fig. 3B-E**). This higher sensitivity of the AHK3 promotor was previously evidenced in our work for BA.The AHKs selectivity and sensitivity for the 10 derivates can be summarized as following, from higher to lower sensitivity (thus, 1nM>10nM>100nM>1µM>10µM):

1. AHK3: tZR = tZ = TDZ > DZ = iP = BA > cZ = KIN > 2MeSiP > tZMP; and
2. AHK4: 2MeSiP > tZ = TDZ > cZ = iP = K = BA > DZ > tZMP.

Interestingly, cZ and KIN were perceived at 100 nM by both receptors, showing as well a similar activation of the TCSm. The nucleotide form tZMP, as well perceived by both receptor with an equal sensitivity (10 µM concentration) showed instead stronger TCSm activation downstream AHK3 (**Fig. 3B and D**). On the other hand, the riboside tZR only activated AHK3-mediated responses in a 1 nM, 10 nM, 100 nM and 1 µM concentration (**Fig. 3B**). For this derivate, an increase in the concentration did not affect the mediated TCSm activation.

A notable exception to AHK3 higher sensitivity was with 2MeSiP. This derivate was perceived at a 1 µM concentration by AHK3, while the sensitivity for AHK4 was as low as 1nM (**Fig. 3C and E**). Moreover, posterior AHK4-mediated activation was significantly higher, and was unmodified by subsequent 2MeSiP addition. Lastly, AHK4-mediated activation of the TCSm after treatment with TDZ and BA resulted in the strongest responses observed for either HK,

in combination with all CK forms (**Fig. 3C and E**). Moreover, for both derivates, the reporter signal steadily increased with higher hormone concentrations, not reaching a saturation in the tested conditions.

Our results showed a higher sensitivity of AHK3 for most adenine derivates, in comparison to AHK4 (**Fig. 3B-E**). Exceptions were cZ, KIN and tZRMP, perceived at equal concentrations by both receptors (100 nM for cZ and KIN, and 10 μM for tZRMP). Interestingly, while cZ is believe to generate weaker responses in plants it displayed similar TCSm activation compared with KIN. On the other hand, AHK4 showed higher sensitivity only for the 2-Methylthio-N^6-isopentenyladenine (2MeSiP), while the tZR was instead perceived solely by AHK3, at a concentration of 1nM. Posterior 10-fold increase in tZR concentrations did not affected the TCSm activation. Moreover, the proposed higher activation of Ck responses of AHK4[109] was only observed in 3 of the 10 adenine derivates tested: BA, TDZ and 2MeSiP. As these CK forms are not representative of the CK composition in plants (BA is only found in fewer species, TDZ is a synthetic CK[72]and 2MeSiP is present in low concentrations[249]this observation may not pose biological significance. Regardless, AHK4 increased response after binding of these atypical CK forms propose a broader range of ligands for this receptor that could be further exploited for the design of new CK analogous (or antagonists) taking advantage of our tool sensitivity and high signal-to-noise ratio.

Role of the conserved aspartate of the B-ARRs in their responses and PPI.

It has been observed that substitution of the conserved aspartate of the B-ARRs by the phosphomimic residue glutamate [ARR1(D94E)[142], ARR2(D80E)[16], and ARR18(D70E)[143]], or deletion of the entire receiver (REC) domain[139,140] leads to increased CK responses. These results conducted to a hypothesis that up-to-date defines the canonical TCS activation. It is believed that in the absence of CK the REC domain may mask the DNA binding domain of these RRs. After CK perception, phosphorylation in the conserved D of the B-ARRs will expose their DNA binding region, realising them form the inhibition, and activating CK responses. enhancing these RRs activity[139,140]. However, this theory does not necessarily explains the unaffected ability to generate CK responses observed for the constitutive non-phosphorylated forms of these B-ARRs where the D was replaced by asparagine[16,143,169].

To further interrogate the phosphate-independent transactivation of CK responsive genes by the non-phosphorylated B-ARRs we substituted the conserved D of ARR1 and ARR10 for alanine, and studied their ability to activate the TCSm promoter. In addition, MxH approaches

were implemented to interrogate the effect of the conserved D in each B-ARR PPI with AHP2 as describe in[267]. Briefly, the two candidates for PPI were fused either to the tetracycline repressor (TetR) or the transcriptional activation domain of the Herpes simplex virus (VP16). For the reporter module the operator motif of tetR (tetO) was cloned upstream the P_{CMVmin}, controlling the expression of SEAP. It is expected that our candidate's interaction will bring the VP16 into the proximity of the P_{CMVmin}, activating SEAP expression. We will refer to as "M3H" for the analysis of two proteins interaction in the presence of a third factor, the CK; and M4H when a fourth element, such as a competitor, is included. Plasmids were described in **Methods**, and a schematic representation of the MxH system under analysis was opportunely included in the corresponding figures.

1. Role of the D69 residue in ARR10-mediated responses

Our results show that a mutation in the conserved residue D69 of ARR10 leads both to a complete depletion of its activity (**Fig. 4A**), and the disruption of its interaction with AHP2 (**Fig 4C**). Interestingly, co-expression of the wild-type (WT) ARR10 with increasing concentration of the "non active" ARR10(D69A) mutant in 1:0,3, 1:0,6, or 1:1 ratio, resulted in a significantly higher TCSm expression either at 100nM (for a 1:0,3), or both at 10nM and 100nM (for 1:0,6 and 1:1 ratio) (**Fig 4C**). This observation suggested the possibility of an active WT: mutant heterodimer. Further analysis showed that AHP6 can interact with ARR10 while no AHP2-AHP6 heterodimer was observed (**Fig. 4C**). Thus, we hypothesize that ARR10 homodimerization could mediate the reassembly of the tetR-AHP2 + AHP6-VP16 split TF. Our results show that, effectively, addition of ARR10 increased significantly TCSm expression, reinforcing the previous observations. In agreement, the ability to activate transcription as dimers was previously evidenced for ARR18[143], and for the heterodimer ARR1-ARR12[155].

2. Role of the D89, and D94 in ARR1-mediated responses

In a previous work, overexpression of ARR1(D94E) showed constitutive CK responses at molecular, physiological and developmental levels, suggesting an important role for the residue D94 in CK signalling[142]. Therefore, to explore the effect of the non-phosphorytable ARR1 mutant on the activation of the TCSm, we introduced a point mutation in the same residue D94 to generate the ARR1(D94A) variant. In comparison with ARR1WT, the ARR1(D94A) show

a higher activation of the TCSm both in cell treated with water (mock) and after addition of 10nM BA, increasing the reporter expression 2-, and 13-fold, respectively. Contrary, mutation in the D94 reduced a 6-fold the CK-dependent response at higher hormone concentration (100 nM) (**Fig. 5A**).

Unaltered activation of promotor-reporter systems by non-phosphorytable forms of ARR2(D80N) and ARR18(D70N) was previously evidenced; raising the suggestion that overexpression of the variants may bypass an negative regulation of these B-ARRs[16,143,169]. These observations and our results suggest that ARR1 may have the ability to activate CK responses, in the absence of the signal. To test this hypothesis, we co-transfected CHO cells with AHK3, AHP2, ARR1, either alone or in every possible combination, always in the presence of the TCSm, as it was assayed initially for ARR10. Our results show a strong TCSm activation in cells expressing only ARR1, or ARR1 and the AHK3, in samples treated with a concentration of 10 nM and 100 nM BA, but also in cells that received no hormonal treatment. (**Fig. 5C**). While full reconstruction of the pathway, as previously observed displayed the canonical of increasing TCSm activation in response to addition of higher hormone concentrations, cells co-transfected with only AHP2 and ARR1 showed no activation.

To continue exploring this newly proposed regulatory mechanism we decided to investigate the role of the phosphorylation, and thus the conserved D in. For this, in addition to the ARR(D94A) mutant we generated two new variants. Sequence alignment between the B-ARRs (**Supplementary Fig. S4**) shows the D89 residue as the conserved D of ARR1; equivalent to the D69 in ARR10, D80 in ARR2[61], and D70 in ARR18[143]. Therefore, we included to our analysis both the ARR1(D89A) variant, and the double mutant. We then transfected our three mutants either alone, with AHP2, or with AHP2 + AHK3 (full reconstruction). Notably, all mutants conserved the ability to activate the TCSm in every tested condition (**Fig. 6B**). Contrary to the ARR1 WT, co-transfection of AHP2, depleted the signal, proposing an important role of the mutated residues in AHP2 regulation. Further, after full reconstruction of the pathway, the fold increase between the activation of the WT and the mutants after treatment with water (mock) or a concentration of 10 nM BA was (approximately) 8-, and 2-fold. At higher hormone concentration, the difference was only slightly significative.

Finally, we investigated the role of the D89 and D94 in ARR1-AHP2 interaction, using a mammalian-3-hybrid approach. Our results showed a conserve ability to interact with AHP2 of the ARR1(D89A) mutant, as well as the double mutant (**Fig. 6C**), while the ARR1(D94A)-

AHP2 interaction was not visualized with our system. Remarkably, contrary to ARR10-AHP2 interaction, the ARR1 WT interaction with the HP was significantly reduced with increasing hormone concentrations.

Mode of action of three known negative regulators of CK pathway

As a final proof-of-principle application of our orthogonal platform predictive power we decided to investigate the molecular mechanisms behind the three known negative regulators of CK signalling; the A-ARRs(ref), the C-ARR(), and AHP6(). As a representative member of the A-ARR and the C-ARR families we selected for our study ARR7 and ARR22, respectively. The following results show the effect of these RRs in the TCSm activation after reconstruction of the pathway with AHK3, AHP2, and both B-ARRs. Analysis of AHK4-AHP2-ARR10 mediated responses were as well performed leading to similar results, and are included in **Supplementary Fig. S6D**.

1. ARR7 inhibition of CK signalling depends on the B-ARR present, and the HP nature

Our results show that of ARR7 blocked TCSm activation in ARR10-mediated CK responses, while it only reduced CK signalling in ARR1-expressing cells (**Fig. 7C**). Interestingly, we observed that replacing AHP2 by the yeast homologous YPD1, ARR10-mediated response, while still reduced by ARR7, are no longer blocked (**Supplementary Fig. S6C**). These results suggest a strong influence of the B-ARR and HP present in ARR7 function.

Previously it was proposed that phosphorylated A-ARRs could form an inactive heterodimer with the phosphorylated B-ARRs through receiver domains[136], suggesting the phosphorylation of ARR7 as a requirement for its function. Thus, we next explored a possible hormone-dependent PPI between the ARR7 and both B-ARRs. Using the M3H assay, no interaction was observed with either of the B-ARRs, or with AHP2 independently (**Fig. 7D**). However, our M4H approach showed that ARR7 was able to stabilize the complex between the B-ARR and AHP2, independently of the hormone concentration. These observations are compatible with the previous ones, yet rather suggest that the inhibitory complex may include as well AHP2.

2. ARR 22 blocks CK signalling in mammalian cells

The molecular mechanism driving ARR22 regulation of CK signalling has been previously analysed. *In vitro* studies showed a rapid dephosphorylation of some AHPs later attributed to

ARR22 higher autophosphorylation rate, suggesting their function as a phospho-histidine phosphatase[67,160,161]. Furthermore, ARR22 overexpression in protoplast and *in planta* resulted in the reduction of CK responsive gene expression[66,67,162]. This effect was abolished by replacing a conserved D74 for: A (non-phosphorylatable), E (phosphomimic), or after deletion of the receiver domain[161]. Therefore, we next aimed to prove our platform suitability to validate the previous observations, and to investigate the effect of ARR22 on the B-ARRs interaction with AHP2.

Unlike ARR7, ARR22 blocked CK responses independently of the B-ARR (**Fig. 7E**), and replacement of AHP2 for YPD1 did not lessened the inhibition (**Supplementary Fig. S6C**). Further, while there is no previous evidenced of and B-ARR-ARR22 interaction, ARR22-AHP2 interaction was formerly reporter using Y2H[66]. Thus, we next assayed the same interactions using our M3H assay. No interaction was observed between ARR22 and ARR1, ARR10, or AHP2; still, ARR22 slightly reduced the B-ARRs-AHP2 interaction (**Fig. 7F**). The impossibility of visualizing the ARR22-AHP2 heterodimer may reflect the transient nature of this complex. However, we will not have then expected to be observable neither by Y2H. Therefore, we suggest that the ARR22-VP16 fusion used for the M3H assay may interfere with the AHP2-ARR22 complex formation.

3. AHP6 reduces the TCSm activation by interacting with the B-ARRs

Previous observations led to the suggestion that AHP6 interference with the phospho-relay involves PPI with one or more CK signalling components[94-68]. Therefore, we next investigated AHP6 influence in the TCSm activation and its effect on the B-ARRs and AHP2 interactions. In our studies, AHP6 was able to diminish CK signalling independently of the B-ARR mediating the response (**Fig. 7G**). Opposite to what was observed for ARR7, replacing AHP2 by YPD1 resulted in a stronger depletion of CK responses (**Supplementary Fig. S6C**). Next, M4H assays showed that addition of AHP6 drastically depleted the interaction between B-ARRs and AHP2 (**Fig. 7H**). As there was no evidence of an AHP2-AHP6 heterodimerization in our studies (or else), the depletion of these PPIs suggests a competition of both AHPs for the RRs. To further address this, in a competition assay we tested the effect of adding AHP2 to the ARR10-AHP6 split TF, resulting in a much weaker depletion of the signal (**Supplementary Fig. S6E**). In the same assay, we also evidenced that unlike AHP2, AHP6 can still form heterodimers with the ARR10(D69A) mutant. Altogether, the results displayed suggest that the

molecular mechanism behind the regulation of CK responses by AHP6 involves the formation of an inhibitory complex with the B-ARRs. This complex will be preventing their activation by phosphorylation (for ARR10), or blocking permanently their constitutive activation (for ARR1).

Discussion

Partial reconstruction of plant signalling pathway in mammalian cells have contributed to deepener our understanding of the molecular mechanism behind these sophisticated networks. By providing a "complexity-free" environment these platforms allow the quantitative answer questions impossible to address in plants, such as investigating the role of single components. In this work, we pursuit the full reconstructed of CK perception and signalling network from *Arabidopsis thaliana* in CHO cells, introducing a new experimental platform for the study of CK responses. The implementation of quantitative approaches such as M3H and promotor-reporter activation, allowed us to evaluated, from CK perception to the transcriptional activation, the role of each molecule involved in CK signalling. Our system response to physiological concentration of the hormone, and the conserve lipid composition of mammalian and plant membranes permitted to investigate the CK receptors sensitivity and selectivity for 10 adenine derivates. In comparison with AHK4, AHK3 displayed higher sensitivity for most of the assayed CK forms, including tZ and tZR which are transported via the xylem into the shoot, where this receptor is most abundant, as previously suggested in bacteria-, and plant membrane-based assays (**Fig. 3B-C**). Whether or not the tZR form has genuine CK activity[52,107,114] has long been debate. The binding of these derivates to the AHKs has only been previously evidenced in bacteria-based systems[110]. Therefore, it was strongly argued if the nature of the prokaryote membrane[112], or a possible conversion into the free active form was the reason for such observations. However, if an interconversion of tZR to the active form is having place in our model, we would expect to have evidenced TCSm activation as well downstream AHK4. Nevertheless, the possibility of this (or any other) adenine derivate being metabolised has not been dismissed, and should be further investigated.

Another accepted observation when studying CK binding to the AHKs was the stronger AHK4-mediated activation of the reporter gene, in comparison with AHK3 responses. In *E. coli* this was suggested to be, once more, an effect of the bacteria environment, however, it was later confirmed in transient expression assays *in planta*[169]. Here, a stronger AHK4-mediated response was observed as well when assaying different combinations of downstream elements,

AHPs or ARRs, after BA induction (**Fig. 2**). Nevertheless, when exploring the effect of different CK forms this was only true for BA, TDZ and 2MeSiP (**Fig. 3 D-E**). These three derivates are not representative of the CK composition in plants. BA has been only found in abundance in fewer plant species[36], while TDZ is a synthetic CK used as herbicide[20]and the 2MeSiP is normally found in small concentration[249]. Still, these results suggest AHK4´ broader range of substrates.

In this work, we have extensively and quantitively showed how combination of particular signalling elements contribute to the fine tuning of CK responses. An example is the distinguishable activation observed for each AHP regardless of the AHK mediating the signal transduction (**Fig. 2D-E**). We suggests that, despite their structural homology and similar distribution in plants[122], the control of the level of expression of these AHPs may be fundamental for the regulation of CK responses. AHP4 is predominantly expressed in shoots, thus co-localizing with AHK3, and showing a poor activation of the TCSm in agreement with previous observations *in planta*[122,126].

ARR1 and ARR10, together with ARR12, regulate the majority of genes involved in typical CK responses and their function has been mostly analysed in *arr1*, *arr10*, *arr12* triple mutants[147,148,150]. Even more, they are similarly expressed in roots, hypocotyl, and cotyledons, and localized in the cell's nucleus[149]. Here we showed that despite their similarities the B-ARRs also mediate different CK responses. In our study, ARR1 transactivation was consistently stronger than the mediated by ARR10 (**Fig. 2B-C**). Surprisingly, only ARR10 checked every box from the "expected behaviour" of a RR belonging to the CK canonical circuit. Knowingly, the canonical activation of the B-ARRs requires the exposure of the DNA binding domain, normally masked by the REC domain, which occurs after the conformational change triggered by the phosphorylation. Therefore, it is accepted for mutants where the REC domain is removed or phosphomimic (replacement of D for E) variants to exhibit constitutive activation of CK responses[137,139,142,149]. Based on our observations, we believe this to be true for ARR10. This RR transactivation of the TCSm was only observed after hormone induction; its conserved D69 residue was essential for its transactivity, as its replacement for A depleted the signal; and, the ARR10(D69A) mutant was no longer able to interact with AHP2 (**Fig. 4**). Even more, preliminary results suggest the ARR10 homodimer activation of the TCSm as it was observed for ARR18 homodimer activation of ARR6 promoter[154] and, ARR1-ARR12 transactivation of TRYPTOPHAN AMINOTRANSFERASE OF ARABIDOPSIS 1

(TAA1)[155]. In our work, however, this dimerization was evidenced indirectly. First, we showed that increasing concentration of the non-active ARR10(D69A) variant to ARR10WT-containing samples raised the TCSm expression significantly (**Fig. 4A**). Later, addition of ARR10WT to the non-interacting split TF, tetR-AHP2 + AHP6-VP16, was sufficient to recover the system activation (**Fig. 4C**). Thus, further studies using our M2H approach for direct visualization ARR10-ARR10 interaction will be performed in the future to support our preliminary observations.

Contrasting with ARR10 canonical behaviour, our results evidence the ability of ARR1 to constitutively activate CK responses. ARR1 basal activation was further inhibited by the presence of AHP2, until hormone treatment restored the classic CK-dependent response (**Fig. 5**). Although these results may seem counter-intuitive, we strongly believe that evidence of ARR1 (and other B-ARRs) non-canonical behaviour has been already presented, but lacked validation due to the drawbacks of the models of study. A strong example is the conserved ability to generate CK responses of the non-phosphorylated (replacement of D for N) forms of the ARR2 and ARR18[16,143,169]. Pertinently, we showed that ARR1 non-phosphorytable variants: ARR1(D89A), ARR1(D94A), and the double mutant were also able to generate CK response. However, the basal activation at each hormone concentration, including the mock cell, was higher reducing the dynamic range (**Fig. 6**). Notably, these observations suggest the existence of a third phosphor-acceptor residue. Thus, we wonder, if this multiple-residue regulation of ARR1 transactivation it is also extended to other members of the family. We further suggest that the loss of AHP2 downregulatory effect observe in the WT is due to a reformulation of the classic ARR1-AHP2 interaction, not necessarily a depletion, as this effect was only observed for the D94 mutant (**Fig. 6C**). Altogether these remarkable results suggest a novel dual role of AHP2, acting both as an activator of the RR in its phosphorylated state, while inhibiting ARR1 constitutive activation of the target genes, in the absence of a phospho-relay. To further validate our observations, we propose *in silico* prediction of ARR1 mutant structure to visualize the proposed change in ARR1-AHP2 interaction, followed by a mass spectroscopy analysis of the double mutant to visualize the proposed existence of a third phosphorytable D.

ARR1 and ARR10 also responded differently to ARR7 inhibition. This RR completely depleted the signal in ARR10-mediated responses, while the signal was only diminished in the presence of ARR1 (**Fig. 7**). Analysis by M2H suggested that ARR7 may form an inhibitory

complex with both the B-ARRs and the AHP2, as addition of ARR7 increased ARR10-AHP2 interaction, while it was not able to form a stable dimer with either of these proteins independently. This type of inactive complex formation was previously suggested between the phosphorylated form of ARR7 and the B-ARRs[136]. However, the increase of the B-ARR-AHP2 PPI after addition of ARR7 was independent of the hormone. The ARR7-AHP2 interaction was, however, previously assayed in yeast and plant models. This could suggest that the stability of the interactions is not sufficient to be evidenced by our M2H system. or that the endogenous RRs present in yeast or plants, are inconspicuously facilitating the complex formation. As PPI seems to be essential for this inhibitor function, the difference observed between ARR1 and ARR10 could be founded in the different strength of this RR interaction. The importance of the protein's identity for ARR7 function was further evidenced as replacement of AHP2 for its yeast homologous YPD1 partially reduced this RR inhibition of ARR10-mediated responses (**Supplementary Fig. S6C**).

Our quantitative measurements of the PPIs were also instrumental to start unravelling AHP6 inhibitory molecular mechanism. Our M2H analysis showed a strong depletion of AHP2-ARR10 interaction in the presence of AHP6, which correlated with a strong interaction between AHP6 and the B-ARRs (**Fig. 7G-H**). Importantly, addition of AHP2 to the ARR10-AHP6 interacting pair, did not show the same effect, proposing that AHP6 forms a more stable complex with the B-ARRs. Moreover, mutation in the D69 of ARR10 was not sufficient to deplete the ARR10-AHP6 interaction, reinforcing the above-mentioned. Our results thus provide experimental evidence to the previous hypothesis of the AHP6 interfering with the phosphor-relay by participating in PPI with other signalling elements[94]. Here we show that AHP6 can physically interact with the pathway RRs preventing their activation by the functional HPs.

Lastly, we observed the conserved histidine phosphatase activity of ARR22 in mammalian cells, that led to the complete depletion of CK responses in every tested condition (**Fig. 7E-F**), as it was previously observed in *Arabidopsis* protoplasts[66,161]. This was as well extended to the YPD1 suggesting that ARR22 phosphatase activity is also conserved among kingdoms.

Through the selection of key proof-of-principle applications we have here provided robust experimental evidence of the predictive power of our synthetic platform. We further propose that it could be implemented for the investigation of new CK derivates (or antagonists), as well as for the study of newly discovered (or synthetic) CK responsive promoter. For this, we could

profit of the superior dynamic range between AHK4-YPD1-ARR1 strong signal, and its posterior depletion by addition of either AHP6, or ARR22. Moreover, our tool could be used as an experimental model for the study of homologous pathways from agronomically relevant plant species. Altogether we strongly believe that our orthogonal platform will be instrumental for the rapid advance of our understanding of plant signalling pathways.

Methods

Plasmid construction. A detailed description of the plasmid construction can be found in Supplementary Table 1. DNA fragments were either amplified from cDNA or released from previous vectors by PCR with primers provided by Sigma Aldrich (Supplementary Table S2), using Q5 High-Fidelity DNA Polymerase (New England Biolabs). Gel extractions were performed using NucleoSpin® Gel and PCR Clean-up kit (Macherey-Nagel). All plasmids in this work were assembled using the AQUA cloning method [210] prior to the transformation into chemically competent Escherichia coli strain 10-beta (NEB). The plasmids were purified using Wizard® Plus SV Minipreps DNA Purification Systems (Promega), NucleoBond® Xtra Midi kit (Macherey-Nagel). All preparations were tested by restriction enzyme digests and sequencing (GATC-biotech/SeqLab). All restriction enzymes were purchased from New England Biolabs. The promoter-reporter construct use to evidence CK-responsiveness of the system was inspired in the previously describe TCS:LUC[131,169], with a sequence modification. Our TCSm consist in five direct repeats of AAAATCTACAA-AATCTTTTTGGATTTTGTGGATTTTCTAGC (core for B-type DNA binding pentamers is underlined), followed for a minimal promoter, and a reporter gene. The P_{CMVmin} and SEAP were cloned downstream the TCSm. For PPIs analysis using MxH, the proteins of interest were fused either at the tetracycline repressor (TetR), or the transcriptional activation domain of the Herpes simplex virus (VP16). The reporter plasmid included the operator motif of tetR (tetO) upstream the P_{CMVmin}, which controls the expression of SEAP.

Mammalian cell culture and transfection. Chinese hamster ovary cells (CHO-K1) were cultivated in HAM´s F12 medium (PAN, cat. no. P04-14500) supplemented with 10% fetal calf serum (FCS, PAN, cat. no. P30- 3602) and 1% penicillin/streptomycin (PAN, cat. no. P06-07100) in a 5% CO2 atmosphere at 37°C. Mammalian cells were routinely transfected as described in[260]. Briefly, 50,000 CHO-K1 cells/well were seeded in 500µl HAM cell culture medium 24h prior to transfection in 24 well plates (Corning). 0.75µg DNA per well were diluted in 50µL OptiMEM (Invitrogen, Thermo Fisher Scientific) and mixed with a

polyethyleneimine (PEI)/OptiMEM mix [2.5µL PEI solution (1 mg/ml, Polysciences Europe GmbH cat. no. 23966-1) in 50µL OptiMEM]. After 20 min incubation at RT, 100µl of the transfection mixes were added to each well in a dropwise manner. The medium was exchanged 4h post transfection. In co-transfections, all plasmids were transfected in equal amounts (weight-based), unless stated differently in the text.

CK treatment. All CK derivates were purchased from OlChemim Ltd and prepared as 10mM stock solution in DMSO. When needed, the hormones were further diluted in miliQ water, with exception of 2-MeSiP that proved only soluble in DMSO. In mammalian-based assays 24h post transfection the cultured media was exchanged for 480µl of fresh HAMs medium and 20µl of the corresponding CK dilution for a final concentration per well of 10nM, 20nM, 100nM, 1µM, or 10µM, according to the specific assay. In protoplast-based measurements, 20µl of the different hormone's dilution was applied directly into the protoplast's suspension. 20µl of sterile miliQ water was used as control for both assays (0nM CK).

SEAP reporter assay. The reporter 472 SEAP was quantified using a colorimetric assay as described previously[261]. In detail, 24h after hormone induction 200µl of the supernatant of the transfected cells was transferred into 96-well round-bottom (Costar) and incubated at 68°C for 1h, to inactivate endogenous phosphatases. Afterwards, 80µL of the heated samples were transferred into 96-well flat-bottom plates (Costar) together with 100µL of SEAP buffer (20mM homoarginine, 1mM MgCl2, 21% (v/v) diethanolamine), and 20µL of 120mM para-Nitrophenylphosphate (pNPP, Sigma-Aldrich). The absorbance of four technical replicates was measured at 405nm for 1h using a BMG Labtech CLARIOstar multimode plate reader (Berthold Technologies, Bad Wildbad, Germany). Determination of SEAP activity [U/L] was calculated as the slope of the absorbance values [OD/min] using Lambert-Beers´s-law:

$$\frac{U}{L} = \frac{E}{\varepsilon \times d} \cdot 10^6 \cdot \frac{200}{80}$$

E= increase in optical density/para-nitrophenolate per minute; ε=18,600 M^{-1} cm^{-1}, d = length of the light path (cm), 0,6 cm; 200/80= amount of SEAP-containing supernatant (sample dilution factor).

Statistical analysis and reproducibility. Statistical analysis was performed by using one-, or two-way ANOVA with GraphPad Prism 7.0. Outlier were determined and excluded in all experiments as described in[263]. Data are reported as mean ± SEM of n ≥ 3 biologically

independent replicates. Corresponding *P* values are indicated in the figure captions. All experiments could be reproduced with similar results.

Software. Benchling [Biology Software] (2020) was implemented for cloning, GraphPad Prism 7.0 for graphs and statistical analysis, and BioRender.com was selected for graphical design.

Acknowledgements

Authors contribution

E.P. designed and cloned the constructs, conducted all experiments, analysed the data, and wrote the initial manuscript with input from all authors. E.P., M.D.Z. and T.V. designed the experiments, discussed the results and contributed with the editing and read the final version of the manuscript. M.D.Z and T.V. supervised the research, planned and directed the project.

Competing interest

The authors declared no competing interest

Additional information

Supplementary information is available

Figures

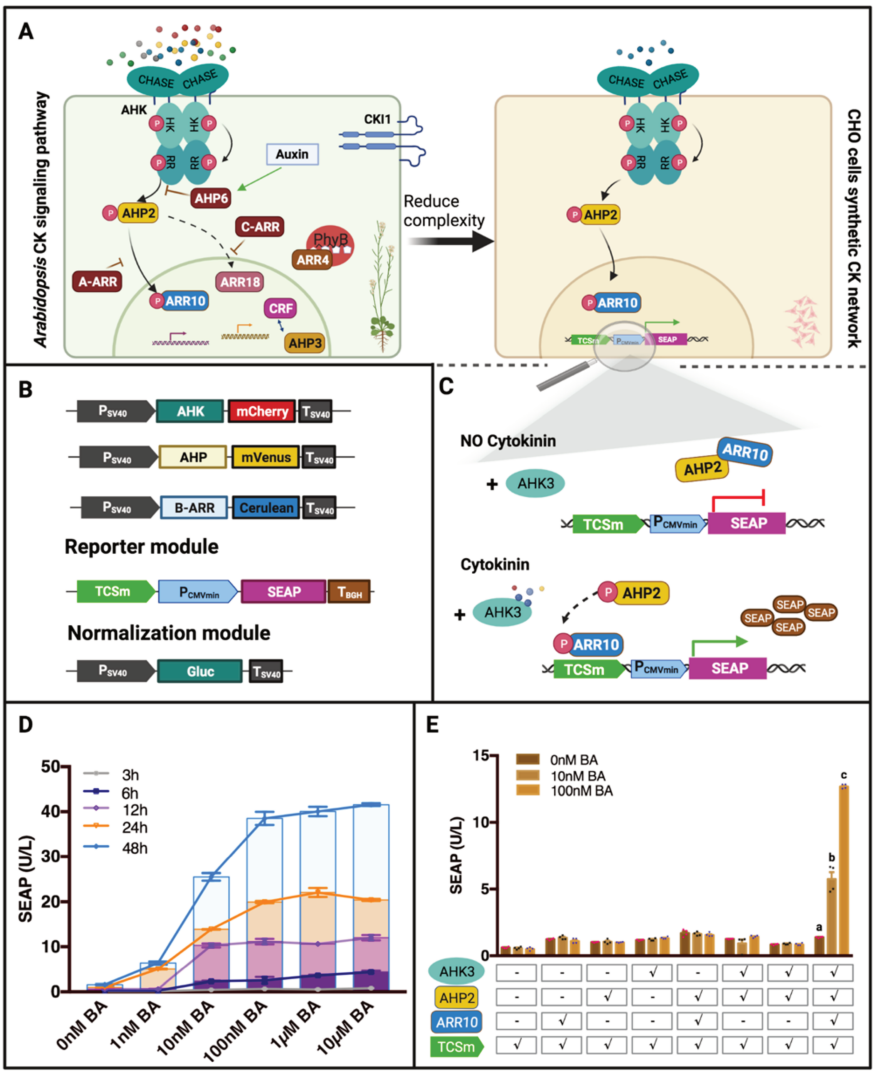

Figure 1. Synthetic reconstruction of CK pathway in CHO cells. A. Representation of the principle of heterologous expression in orthogonal systems. B. Representation of the different modules engineered for the analysis of CK responses in mammalian cells. C. Schematic representation of CK-responsive promotor-reporter assay used in figure D and E. It is expected that after hormone perception the B-ARRs will bind the TCSm promotor and activate the reporter, SEAP, expression. D. Analysis of the CK-responsiveness of the TCSm reporter in cells co-transfected with the system described in panel B, 3-, 6-, 12-, 24- or 48-h after hormone treatment E. Study of system leakiness and possible interactions with mammalian proteins after co-transfection of the indicated proteins. In D and E SEAP expression of samples treated with the indicated BA concentrations is expressed in units per litre. Data are representative of three independent experiments. Mean and S.E.M. are plotted for n= 4 mammalian samples. The statistical significance was determined using a two-way ANOVA analysis (P value < 0.0001) and is indicated with bold letters. AHK, Arabidopsis histidine kinase; A-, B-, C-ARR, Arabidopsis response regulator type A, B or C; AHP, Arabidopsis histidine-containing phosphotransferase; BA, 6-bencilaminopurine; CRF, Cytokinin response factor; CHASE, Cyclase/histidine kinases associated sensor extracellular; CKI1, Cytokinin independent 1; m-Cherry, mVenus and Cerulean, fluorescent proteins; Gluc, Gaussia luciferase; P, phosphate; PCMVmin, minimal cytomegalovirus promotor; PhyB, Phytochrome B; PSV40, Simian virus 40 early promoter; SEAP, Secreted embryonic alkaline phosphatase; TCSm, CK-responsive synthetic promoter designed for this work; TBGH, Bovine growth hormone polyadenylation signal terminator; TSV40 SV40 virus terminator.

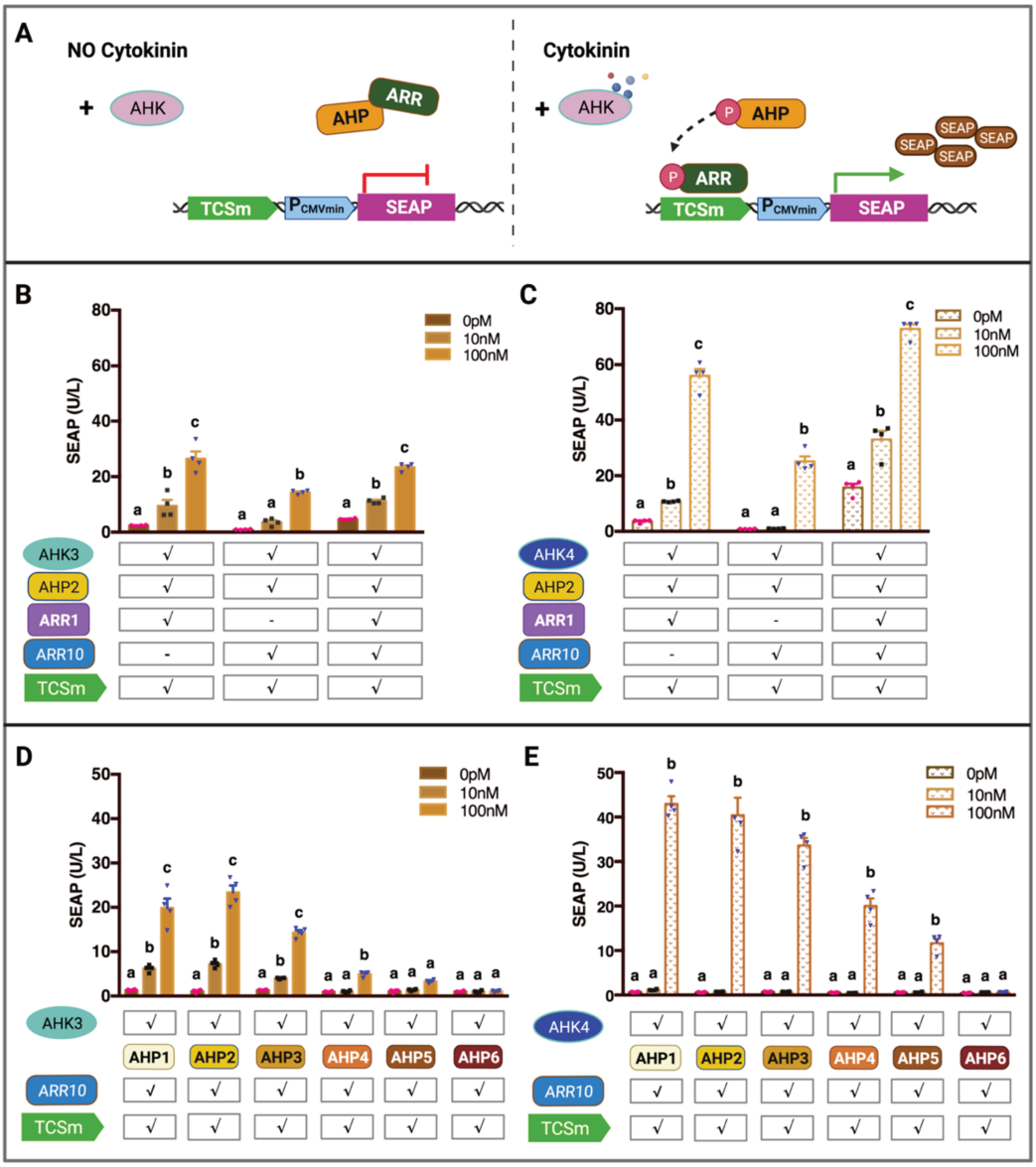

Figure 2. Contribution of specific signalling elements to CK response. A. Schematic representation of CK-responsive promotor-reporter assay used in figures B-E. It is expected that after hormone perception the B-ARRs will bind the TCSm promotor and activate the reporter, SEAP, expression. B-C. ARR1-, and ARR10-mediated activation of the TCSm promotor. D-E. AHP1 to 6 mediated activation of the TCSm promotor. In B-E SEAP expression of samples treated with the indicated BA concentrations is expressed in units per litre. Data are representative of three independent experiments. Mean and S.E.M. are plotted for n= 4 mammalian samples. The statistical significance was determined using a two-way ANOVA analysis (P value < 0.001) and is indicated with bold letters. Filled bars represent AHK3-mediated responses and pattern bars. P value AHK, Arabidopsis histidine kinase; ARR, Arabidopsis response regulator; AHP, Arabidopsis histidine-containing phosphotransferase; BA, 6-bencilaminopurine; PCMVmin, minimal cytomegalovirus promotor; SEAP, Secreted embryonic alkaline phosphatase; TCSm, CK-responsive synthetic promoter designed for this work.

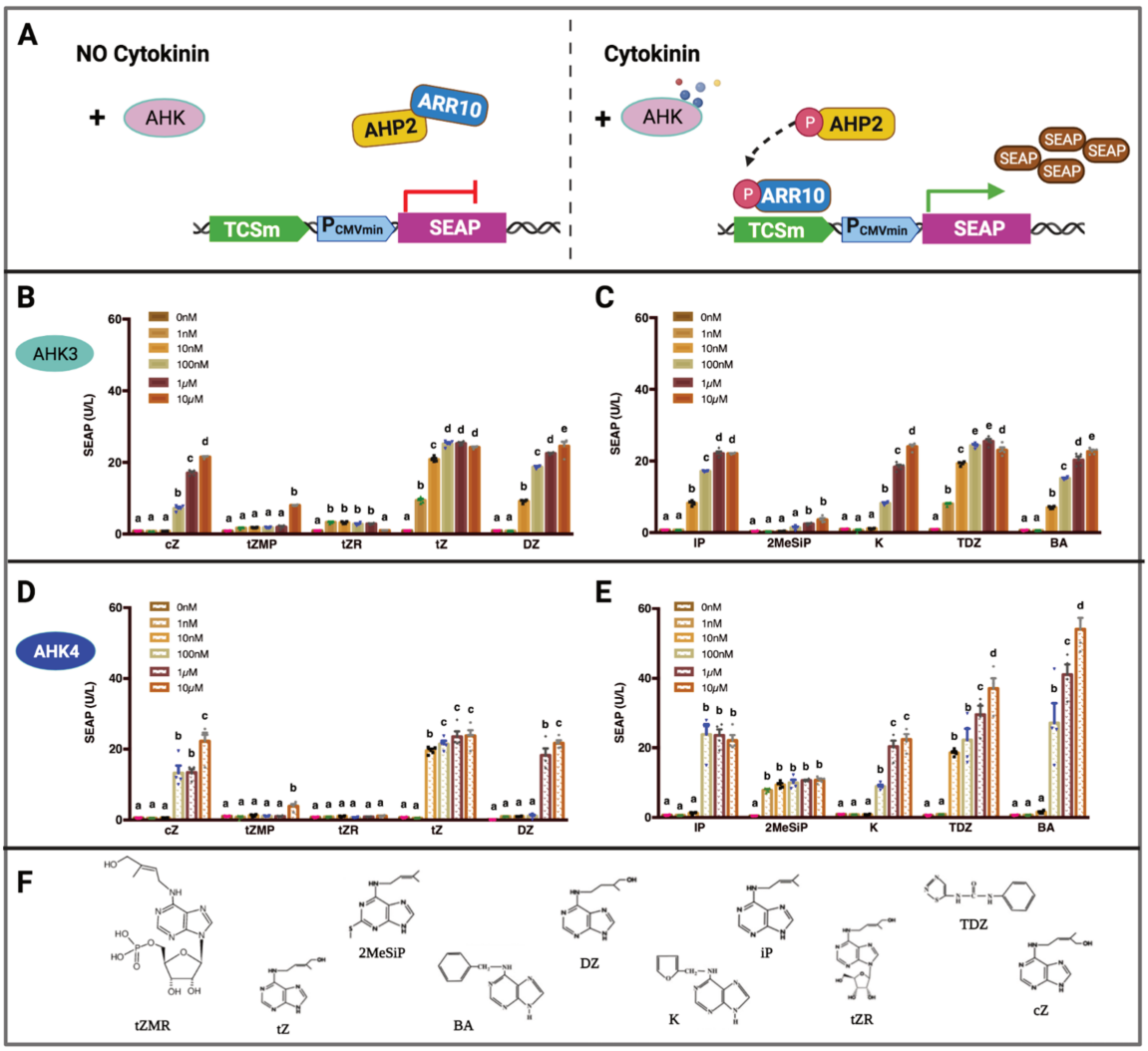

Figure 3. AHKs sensitivity and selectivity for different adenine derivates, and their downstream activation. A. Schematic representation of CK-responsive promotor-reporter assay used in figures B-E. It is expected that after hormone perception the B-ARRs will bind the TCSm promotor and activate the reporter, SEAP, expression. B-C. AK3-mediated activation of the TCSm promotor in response to the indicated adenine derivates at different hormones concentration. D-E. AHK4-mediated activation of the TCSm promotor in response to the indicated adenine derivates at different hormones concentration. F. Representation of the chemical structure of the different adenine derivates use in this study. In B-E SEAP expression of samples treated with the indicated concentration of each hormone is expressed in units per litre. Data are representative of three independent experiments. Mean and S.E.M. are plotted for n= 4 mammalian samples. The statistical significance was determined using a two-way ANOVA analysis (P value < 0.001) and is indicated with bold letters. Filled bars represent AHK3-mediated responses and pattern bars AHK4-mediated responses. AHK, Arabidopsis histidine kinase; ARR, Arabidopsis response regulator; AHP, Arabidopsis histidine-containing phosphotransferase; BA, 6-bencilaminopurine; cZ, cis-Zeatin; DHZ, Dihydrozeatin; iP, isopentiladenine; K, Kinetin; PCMVmin, minimal cytomegalovirus promotor; SEAP, Secreted embryonic alkaline phosphatase; TCSm, CK-responsive synthetic promoter designed for this work; TDZ, Tidiazuron; tZ, trans-Zeatin; tZR, trans-Zeatin riboside; tZRMP, trans-Zeatin riboside-5´-monophosphate sodium salt; 2MeSiP, 2-Methylthio-N^6-isopentenyladenine.

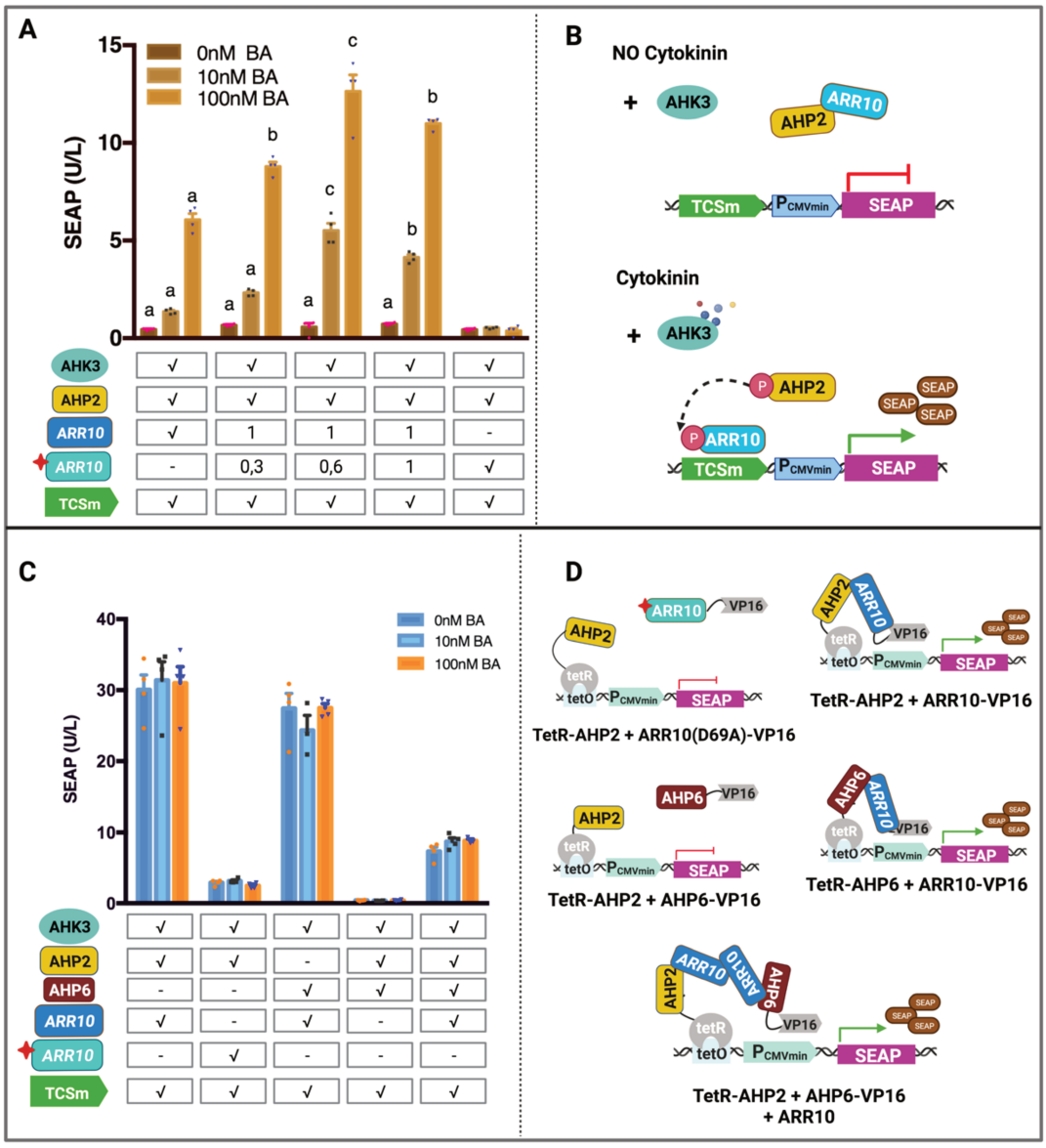

Figure 4. Role of the conserve D in ARR10 transactivation and PPIs. A. Analysis of the ARR10(D69A) non-phosphorytable mutant transactivation activity when transfected alone, or in increasing concentrations with the ARR10 WT. **B**. Schematic representation of CK-responsive promotor-reporter assay used in figure A. It is expected that after hormone perception the B-ARRs will bind the TCSm promotor and activate the reporter, SEAP, expression. **C**. Analysis of the effect of the D69A replacement in ARR10 PPIs, and study of ARR10 dimerization. **D.** Schematic representation of the M3H and M4H assays used in figure C. tetR and VP16 conform a split transcription factor wich reconstitution after interaction of their fused proteins will lead to the promotor activation. In A and C, the star represents a mutation in the conserve D69. SEAP expression of samples treated with the indicated BA concentrations is expressed in units per litre. The co-transfected proteins are indicated in below the corresponding graph. Data are representative of three independent experiments. Mean and S.E.M. are plotted for n= 4 mammalian samples. The statistical significance was determined using a two-way ANOVA analysis (P value < 0.001) and is indicated with bold letters. AHK, Arabidopsis histidine kinase; ARR, Arabidopsis response regulator; AHP, Arabidopsis histidine-containing phosphotransferase; BA, 6-bencilaminopurine; PCMVmin, minimal cytomegalovirus promotor; SEAP, Secreted embryonic alkaline phosphatase; TCSm, CK-responsive synthetic promoter designed for this work; tetO, operator motif for the repressor; tetR, tetracycline repressor; VP16, transcriptional activation domain of the Herpes simplex virus.

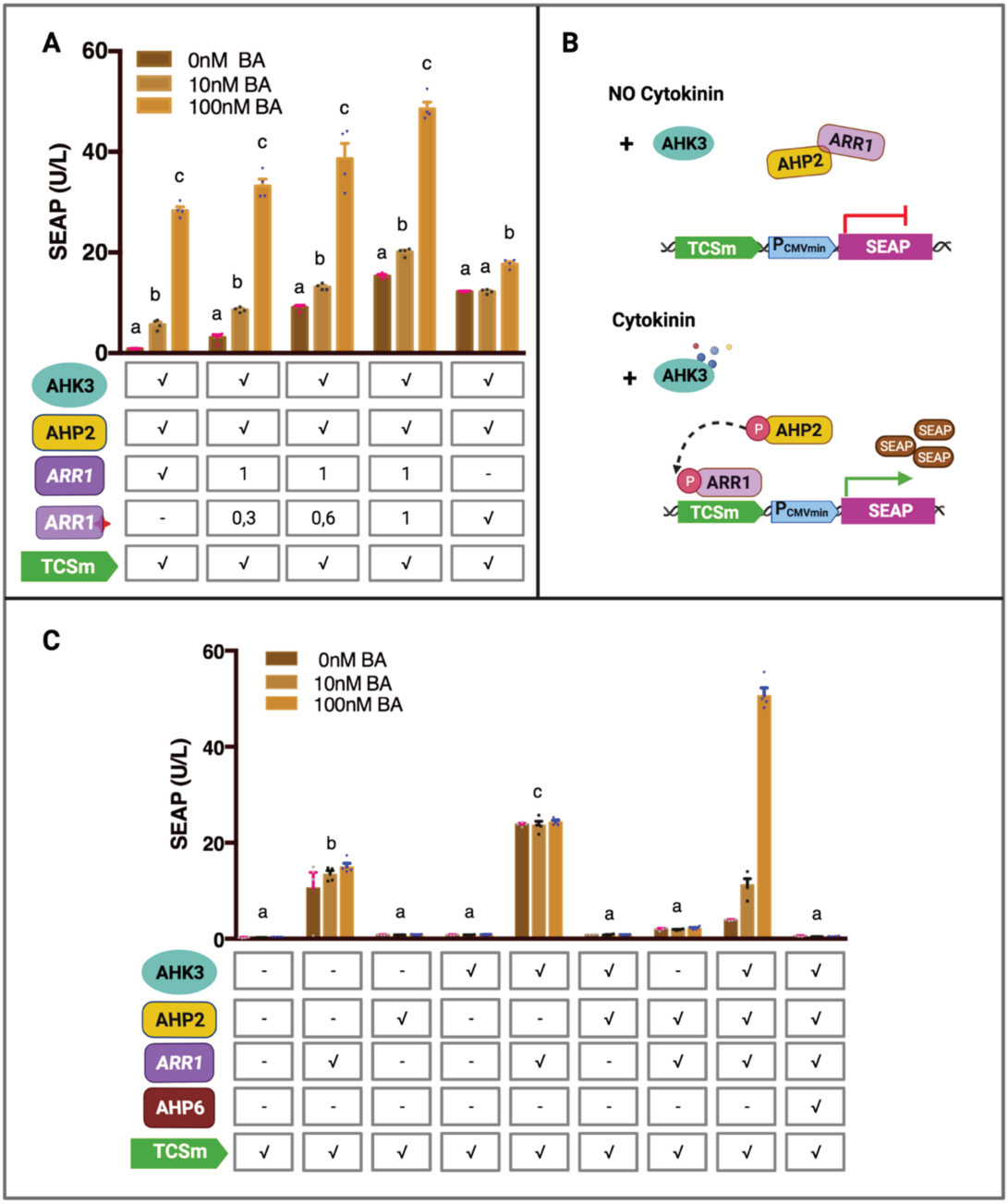

Figure 5. Study of ARR1 constitutive activation of the TCSm, and role of its D94 residue. A. Analysis of the ARR1(D94A) non-phosphorytable mutant transactivation activity when transfected alone, or in increasing concentrations with the ARR1 WT. The star represents a mutation in the conserve D94. The letters indicate statistical significance of different BA concentrations within the same sample. B. Schematic representation of CK-responsive promotor-reporter assay used in figures A and C. It is expected that after hormone perception the B-ARRs will bind the TCSm promotor and activate the reporter, SEAP, expression. C. Study of the ARR1 constitutive transactivation of the TCSm. Letter indicate statistical significance of the level of TCSm activation between different samples. In A and C, SEAP expression of samples treated with the indicated BA concentrations is expressed in units per litre. The co-transfected proteins are indicated in below the corresponding graph. Data are representative of three independent experiments. Mean and S.E.M. are plotted for n= 4 mammalian samples. The statistical significance was determined using a two-way ANOVA analysis (P value < 0.001) and is indicated with bold letters. AHK, Arabidopsis histidine kinase; ARR, Arabidopsis response regulator; AHP, Arabidopsis histidine-containing phosphotransferase; BA, 6-bencilaminopurine; PCMVmin, minimal cytomegalovirus promotor; SEAP, Secreted embryonic alkaline phosphatase; TCSm, CK-responsive synthetic promoter designed for this work; tetO, operator motif for the repressor; tetR, tetracycline repressor; VP16, transcriptional activation domain of the Herpes simplex virus.

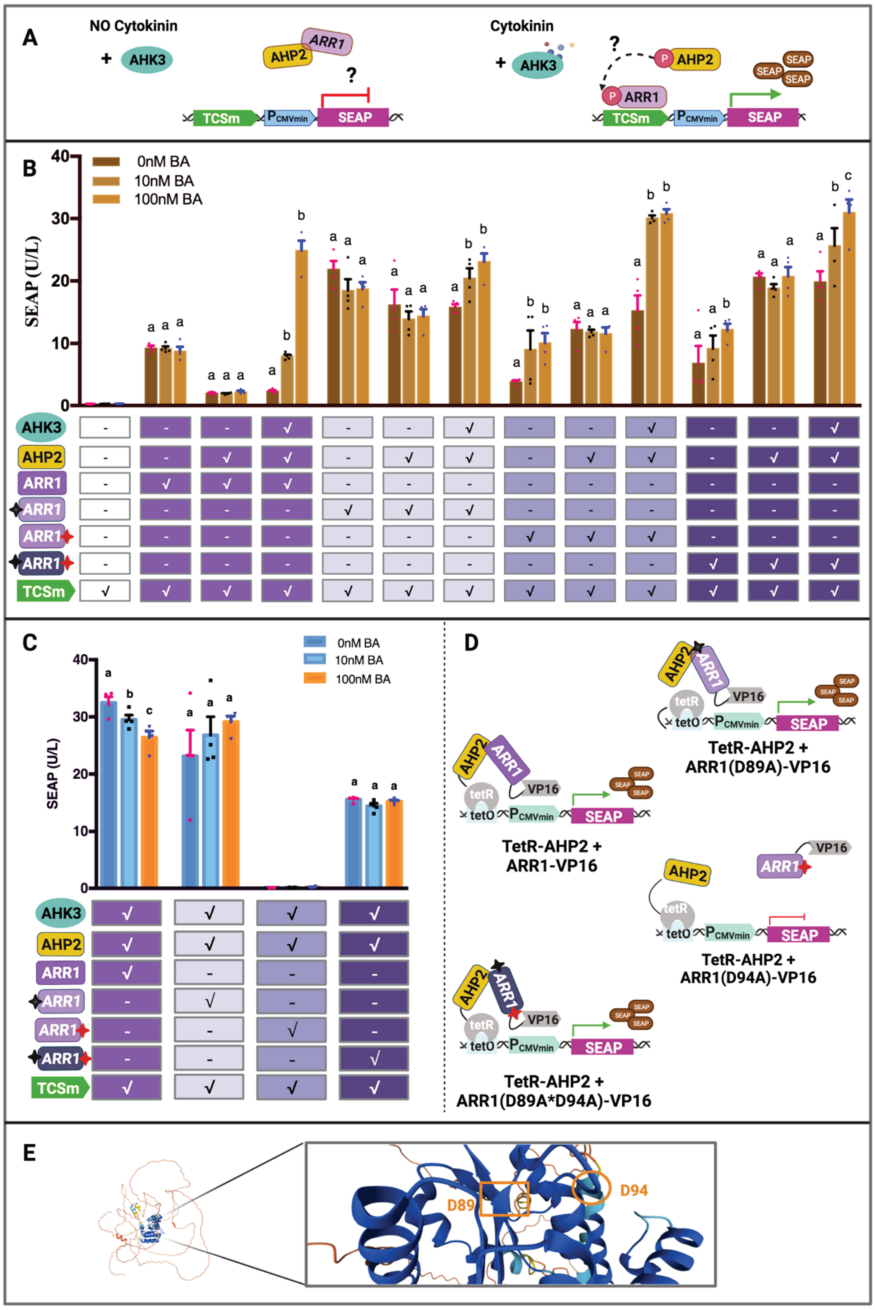

Figure 6. Comparison of the constitutive activation of CK responses and PPIs between ARR1WT and three mutants. A. Schematic representation of the CK-responsive promotor-reporter assay used in figure B. It is expected that after hormone perception the B-ARRs will bind the TCSm promotor and activate the reporter, SEAP, expression. B. Analysis of the transactivation activity of ARR1WT and non-phosphorytable mutants ARR1(D89), ARR1(D94A) and ARR1(D89A*D94A) when transfected alone, with AHP2, or AHP2 and AHK3. C. Analysis of AHP2 interaction with either ARR1 WT and mutants. D. Schematic representation of the M3H assay used in figure C. tetR and VP16 conform a split transcription factor which reconstitution after interaction of their fused proteins will lead to the promotor activation. E. Ribbon representation of a section of ARR1 REC domain. The D89 and D94 residues are indicated either by a square, or a circle, respectively. In B and C, one black star (to the left), a single red star (o the right), or two stars (left and right) represents the D89A, D94A, and double mutant, respectively. SEAP expression of samples treated with the indicated BA concentrations is expressed in units per litre. The co-transfected proteins are indicated in below the corresponding graph. Data are representative of three independent experiments. Mean and S.E.M. are plotted for n= 4 mammalian samples. The statistical significance was determined using a two-way ANOVA analysis (P value < 0.001) and is indicated with bold letters.. AHK, Arabidopsis histidine kinase; ARR, Arabidopsis response regulator; AHP, Arabidopsis histidine-containing phosphotransferase; BA, 6-bencilaminopurine; PCMVmin, minimal cytomegalovirus promotor; SEAP, Secreted embryonic alkaline phosphatase; TCSm, CK-responsive synthetic promoter designed for this work; tetO, operator motif for the repressor; tetR, tetracycline repressor; VP16, transcriptional activation domain of the Herpes simplex virus.

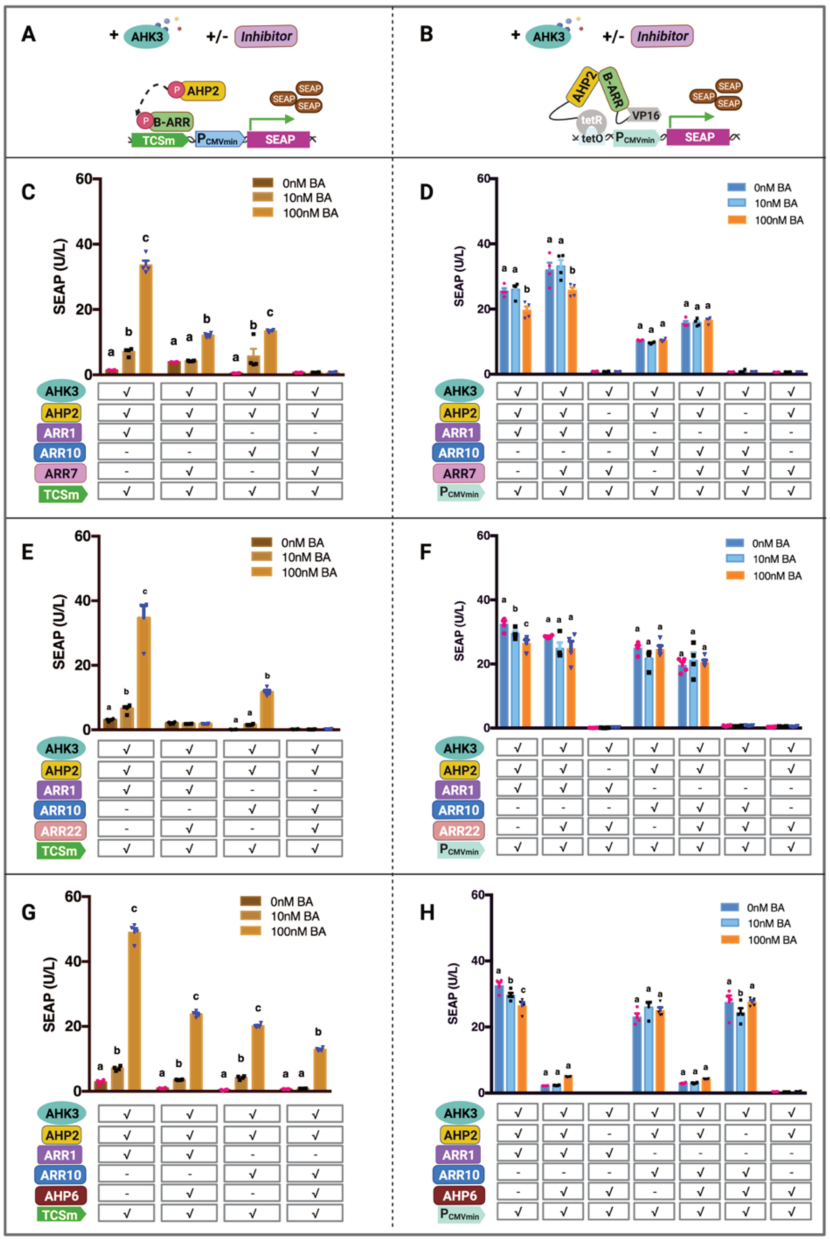

Figure 7. Analysis of the mode of action of the negative RR: ARR7, ARR22 and AHP6. A. Schematic representation of the CK-responsive promotor-reporter assay used in figures C, E and G. It is expected that after hormone perception the B-ARRs will bind the TCSm promotor and activate the reporter, SEAP, expression. B. Schematic representation of the M3H and M4H assays used in figures D, F and H. tetR and VP16 conform a split transcription factor which reconstitution after interaction of their fused proteins will lead to the promotor activation. C-D. Analysis of ARR7 effect in the TCSm activation, or B-ARRs- AHP2 interactions, respectively. Interaction between ARR7 and AHP2, or the B-ARRs were also assayed. E-F. ARR22 effect in the TCSm activation, or B-ARRs-AHP2 interactions, respectively. Interaction between ARR22 and AHP2, or the B-ARRs were also tested. G-H. Study of AHP6 effect in the TCSm activation or the interaction between B-ARRs and AHP2, respectively. Interaction of AHP6 with AHP2 and the B-ARRs was well represented. C-H. SEAP expression of samples treated with the indicated BA concentrations is expressed in units per litre. The co-transfected proteins are indicated in below the corresponding graph. Data are representative of three independent experiments. Mean and S.E.M. are plotted for n= 4 mammalian samples. The statistical significance was determined using a two-way ANOVA analysis (P value < 0.001) and is indicated with bold letters. AHK, Arabidopsis histidine kinase; ARR, Arabidopsis response regulator; AHP, Arabidopsis histidine-containing phosphotransferase; BA, 6-bencilaminopurine; PCMVmin, minimal cytomegalovirus promotor; SEAP, Secreted embryonic alkaline phosphatase; TCSm, CK-responsive synthetic promoter designed for this work; tetO, operator motif for the repressor; tetR, tetracycline repressor; VP16, transcriptional activation domain of the Herpes simplex virus.

SUPPLEMENTARY INFORMATION

Full reconstruction of *Arabidopsis* CK signalling in mammalian cells reveals new regulatory mechanisms

Estefania Pavesi[1,2], (nn), Teva Vernoux[1*], Matias Zurbriggen[2,3*]

1 Laboratoire de Reproduction et Développement des Plantes, Université de Lyon, ENS de Lyon, Lyon, France
2 Institute of Synthetic Biology, Heinrich-Heine Universität of Düsseldorf, Düsseldorf, Germany.
3 CEPLAS - Cluster of Excellence on Plant Sciences, Düsseldorf, Germany.

*Corresponding authors:
Matias Zurbriggen, Institute of Synthetic Biology, Heinrich-Heine Universität of Düsseldorf, and, CEPLAS - Cluster of Excellence on Plant Sciences, Düsseldorf, Germany.
E-mail: matias.zurbriggen@uni-duesseldorf.de
Teva Vernoux, Laboratoire de Reproduction et Développement des Plantes, CNRS, INRA, ENS Lyon, UCBL, Université de Lyon, Lyon, France.
E-mail: teva.vernoux@ens-lyon.fr

Supplementary Figures

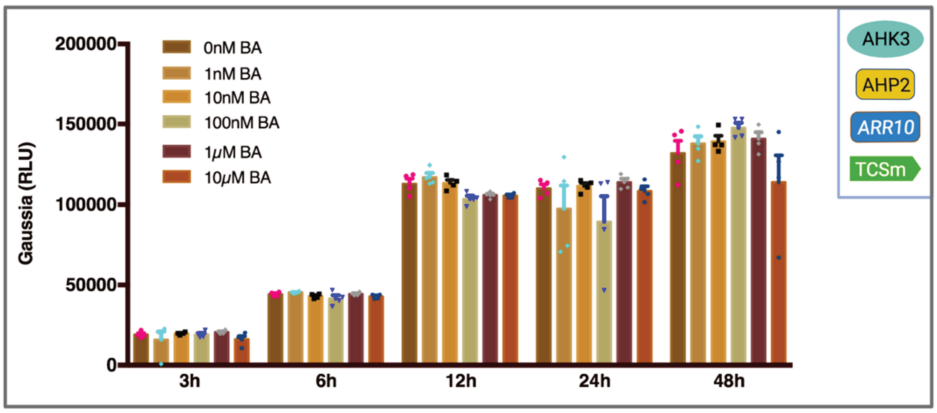

Supplementary Figure S1. Gaussia luciferase (Gluc) expression assay corresponding to figure 1D. Gluc activity was quantified in cells expressing AHK3, AHP2, ARR10 and the TCSm, 3-, 6-, 12-, 24-, or 48 h after induction with BA in the indicated concentrations. No significant differences were observed in the survival of cells expose to CK treatment in comparison with the mock, at any time point. Gluc expression is represented in relative luminescence units (RLU). Mean and S.E.M. are plotted for n= 4 mammalian samples. Detailed description can be found in Supplementary methods. AHK, Arabidopsis histidine kinase; ARR, Arabidopsis response regulator; AHP, Arabidopsis histidine-containing phosphotransferase; BA, 6-bencilaminopurine; TCSm, CK-responsive synthetic promoter designed for this work.

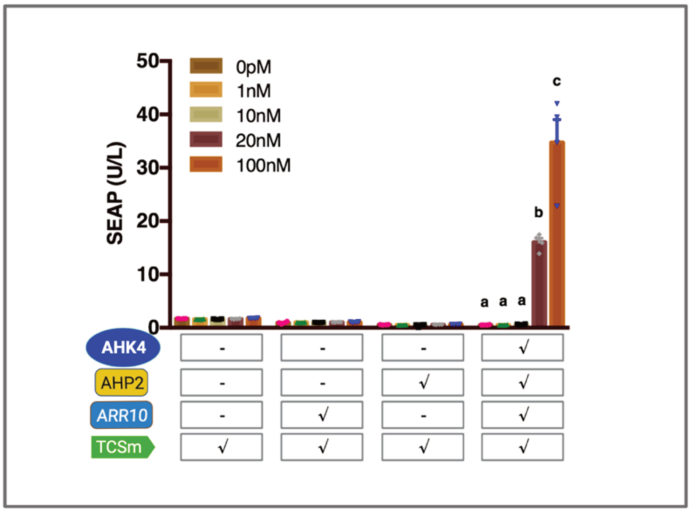

Supplementary Figure S2. AHK4-mediated activation of the TCSm in mammalian cells. Co-transfection of AHK4, AHP2 and ARR10 into CHO cells resulted in a hormone-dependent activation of the TCSm for concentrations ≥ 20nM. SEAP expression of samples treated with the indicated BA concentrations is expressed in units per litre. Mean and S.E.M. are plotted for n= 4 mammalian samples. The statistical significance was determined using a two-way ANOVA analysis (P value < 0.0001) and is indicated with bold letters. AHK, Arabidopsis histidine kinase; ARR, Arabidopsis response regulator; AHP, Arabidopsis histidine-containing phosphotransferase; BA, 6-bencilaminopurine; CHO, Chinese hamster ovary; SEAP, Secreted embryonic alkaline phosphatase; TCSm, CK-responsive synthetic promoter designed for this work.

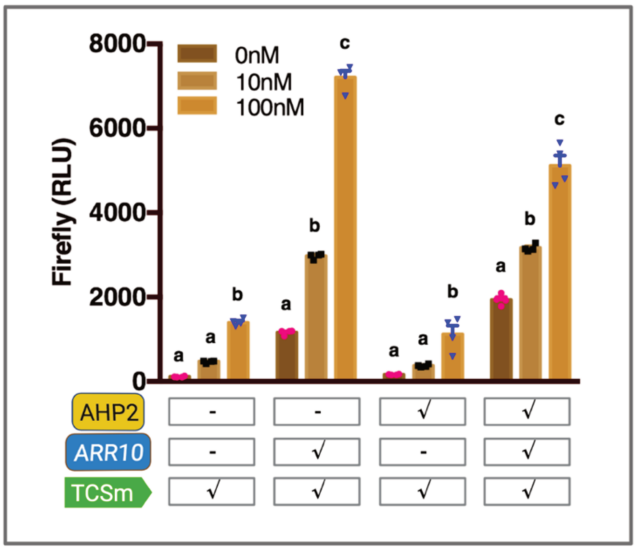

Supplementary Figure S3. TCSm:Fluc transactivation in *Arabidopsis* leaf mesophyll protoplasts. Protoplast were transfected with either the TCSm reporter alone, or in combination with ARR10, AHP2, or both to visualize TCSm expression after addition of BA in the indicated concentrations. Our results evidence a sensitivity of 10nM after addition of ARR10, as observed in mammalian cells. Full reconstruction resulted as well in an increase mock cells expression attributed to the influence of endogenous CK elements. Firefly luciferase (Fluc) expression is represented in relative luminescence units (RLU). Mean and S.E.M. are plotted for n= 4 mammalian samples. The statistical significance was determined using a two-way ANOVA analysis (P value < 0.0001) and is indicated with bold letters. Detailed description can be found in Supplementary methods. ARR, Arabidopsis response regulator; AHP, Arabidopsis histidine-containing phosphotransferase; BA, 6-bencilaminopurine; TCSm, CK-responsive synthetic promoter designed for this work.

```
ARR19      MLVGKISG-YEDNTRSLERETSEI--TSLLSQ-------FP-GNTNVLVVDTNFTTLLNM 49
ARR20      --MSVFSNILDENSRNLRNEIPCD--DGIASPINDDDEEFLTKSNRVLLVG--ADSNSSL 54
ARR21      --MSVFSNILDENSRNLRNEIPCD--DGIASPINDDDEEFLTKSNRVLLVG--ADSNSSL 54
ARR13      -------------------------MAFAQ--SVYNQSSV-LKINVMVVDDNRVFLDIW 31
ARR18      -------------------------MEFGSTEDGRHDKFP-VGMRVLAVDDNPTCLRKL 33
ARR10      -------------------------MTMEQEIEVLDQFP-VGMRVLAVDDDQTCLRIL 32
ARR12      -------------------------MTVEQNLEALDQFP-VGMRVLAVDDDQTCLKIL 32
ARR1       -MMN------PSHGRGLGSAGGSSSGRNQGGGGETVVEMFP-SGLRVLVVDDDPTCLMIL 52
ARR14      -------------------------------MPINDQFP-SGLRILVVDDDTSCLFIL 26
                                                    .:: *.

ARR19      KQIMKQYAYQVSI---ETDAEKALAFLTSCKHEINIVIWDFHMPGIDGLQALKSITS-KL 105
ARR20      KNLMTQYSYQVTK---YESGEEAMAFLMKNKHEIDLVIWDFHMPDINGLDALNIIGK-QM 110
ARR21      KNLMTQYSYQVTK---YESGEEAMAFLMKNKHEIDLVIWDFHMPDINGLDALNIIGK-QM 110
ARR13      SRMLEKSKYREITVIAVDYPKKALSTLKNQRDNIDLIITDYYMPGMNGLQLKKQITQEFG 91
ARR18      EELLLRCKYHVTK---TMESRKALEMLRENSNMFDLVISDVEMPDTDGFKLLE-IGL-EM 88
ARR10      QTLLQRCQYHVTT---TNQAQTALELLRENKNKFDLVISDVDMPDMDGFKLLELVGL-EM 88
ARR12      ESLLRHCQYHVTT---TNQAQKALELLRENKNKFDLVISDVDMPDMDGFKLLELVGL-EM 88
ARR1       ERMLRTCLYEVTK---CNRAEMALSLLRKNKHGFDIVISDVHMPDMDGFKLLEHVGL-EM 108
ARR14      EKMLLRLMYQVTI---CSQADVALTILRERKDSFDLVLSDVHMPGMNGYNLLQQVGLLEM 83
           . ::    *.           *:  * .  . ::::: *  **. :* .  : :
```

Supplementary Figure S4. Section of a full sequence alignment among the 9 members of the B-ARR family. Alignment of the full coding region of 9 representative members of the B-ARR family revealed that the D89, is the most conserve aspartate residue of ARR1. The black arrow indicates the position of the D89, coincident with the D69 of ARR10, protein also used in this work. The alignment was performed with Clustal O version 1.2.3, and the results can be visualized in https://www.ebi.ac.uk/Tools/services/rest/clustalo/result/clustalo-I20220715-121128-0749-36603109-p1m/out

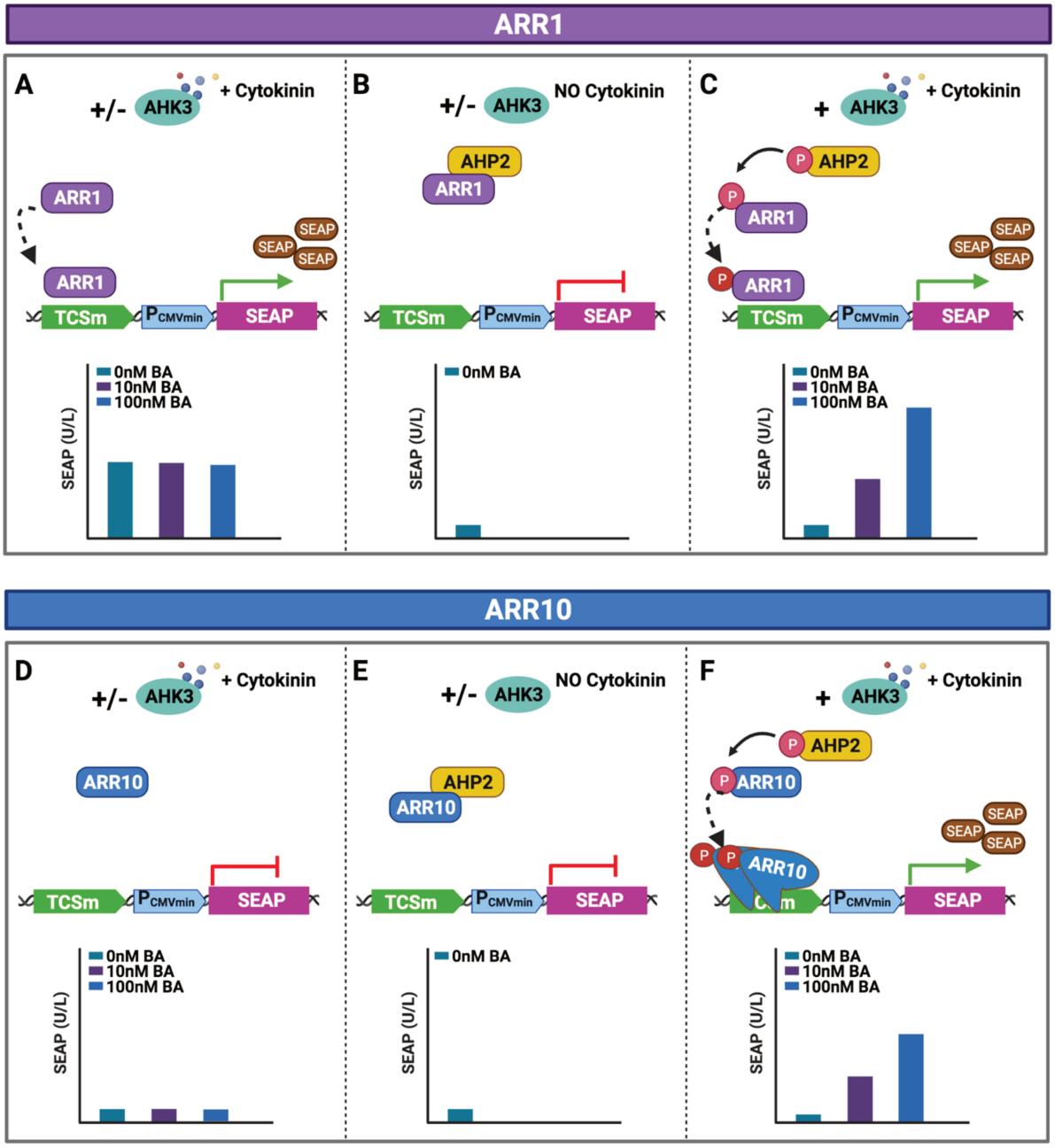

Supplementary Figure S5. Schematic representation of the proposed mechanism behind ARR1- and ARR10-CK responses. ARR1 constitutively binds and activates the expression of its target genes (represented here by the TCSm)(A). In the presence of AHP2, ARR1 activation of the TCSm is complete repressed, probably (but not only) as a result of their PPI (B), until hormone perception (C). The phosphorelay triggered by CK will release ARR1 from its inhibition probably by inducing a conformational change, in a hormone dependent manner. On the other hand, ARR10 does not show constitutive activation of the TCSm (D-E), and can only transactivate the CK-responsive genes after hormone perception, possibly binding as homodimers (F). AHK, Arabidopsis histidine kinase; ARR, Arabidopsis response regulator; AHP, Arabidopsis histidine-containing phosphotransferase; BA, 6-bencilaminopurine; SEAP, Secreted embryonic alkaline phosphatase; TCSm, CK-responsive synthetic promoter designed for this work. The bar charts are only a representation of the expected SEAP activity in each situation, they do not show experimental data.

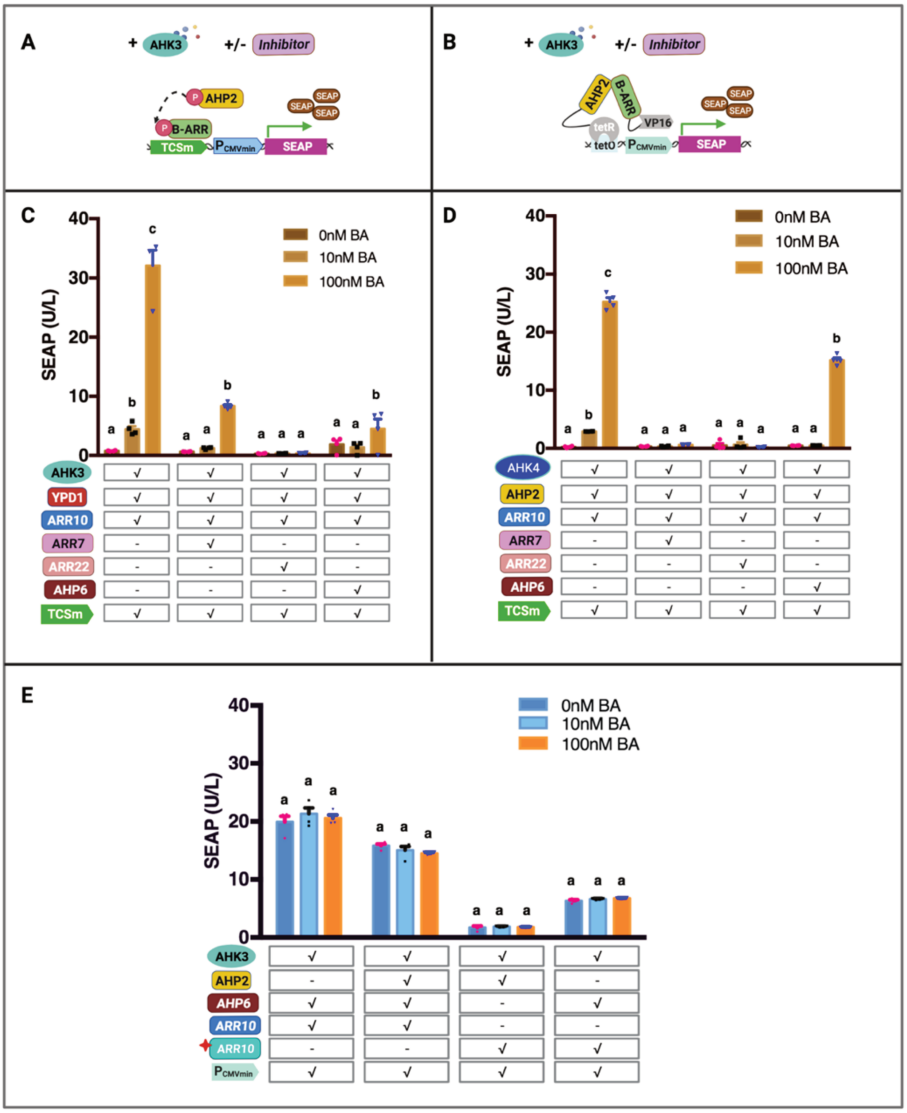

Supplementary Figure S6. Analysis of the mode of action of the negative RR: ARR7, ARR22 and AHP6. A. Schematic representation of system analysed in figures C and D. B. Schematic representation of the M3H and M4H assays used in figure E. tetR and VP16 conform a split transcription factor which reconstitution after interaction of their fused proteins will lead to the promotor activation. C. Analysis of the effect of the three negative RR in YPD1-mediates responses. AS observed for AHP2-mediated responses, ARR22 completely depleted the signal. Differently, replacement of AHP2 by YPD1 increased the inhibitory effect of AHP6, while buffered ARR7 inhibitory role. D. Effect of the three RR in AHK4-mediated responses showed similar results as for AHK3-mediated responses. Complete depletion was observed in ARR10-mediated responses after addition of either ARR7, or ARR22; while AHP6 only reduced the signal. E. Analysis of AHP6 PPIs. AHP6 interaction with ARR10 was significantly, but weakly reduced by addition of AHP2. In comparison with this functional HP, AHP6 was still able to interact with the ARR10 mutant. The red star indicated the mutant variant. In C-E. SEAP expression of samples treated with the indicated BA concentrations is expressed in units per litre. The co-transfected proteins are indicated in below the corresponding graph. Mean and S.E.M. are plotted for n= 4 mammalian samples. The statistical significance was determined using a two-way ANOVA analysis (P value < 0.001) and is indicated with bold letters. AHK, Arabidopsis histidine kinase; ARR, Arabidopsis response regulator; AHP, Arabidopsis histidine-containing phosphotransferase; BA, 6-bencilaminopurine; PCMVmin, minimal cytomegalovirus promotor; SEAP, Secreted embryonic alkaline phosphatase; TCSm, CK-responsive synthetic promoter designed for this work; tetO, operator motif for the repressor; tetR, tetracycline repressor; VP16, transcriptional activation domain of the Herpes simplex virus; YPD1, *Saccharomyces cerevisiae* HP.

Supplementary methods

Protoplast reporter construction. A detailed description of the plasmid construction can be found in Supplementary Table 1. Briefly, for protoplast transformations, the 35S minimal promoter (P_{35S}) and FLuc were cloned downstream the TCSm, using AQUA cloning has detailed in the Methods section of the main text.

***Arabidopsis* leaf mesophyll protoplasts isolation and transformation.** Plants were grown for two weeks on 12 cm square plates containing SCA medium (0.32% (wt./vol) Gamborg's B5 basal salt powder with vitamins (bioWORLD), 4 mM MgSO4 $7H_2O$, 43.8 mM sucrose and 0.8% (wt./vol) phytoagar in H_2O, pH 5.8, autoclaved, 0.1 % (vol/vol) Gamborg's B5 Vitamin Mix (bioWORLD)) a 23 °C, with a 16 h light/ 8 h dark photoperiod. Protoplast were isolated from the plantlet leaves and transformed as described in[262]. Briefly, *Arabidopsis* leaf material was sliced with a scalpel and incubated in MMC solution (10 mM MES, 40 mM $CaCl_2 \cdot H_2O$, 467 mM mannitol, pH 5.8, sterile filtered) containing 0.5% cellulase Onozuka R10 and macerozyme R10 (SERVA Electrophoresis) and kept in darkness overnight at 23 °C. Protoplast were then isolated by pipetting, and the suspension was transferred to a MSC solution (10 mM MES, 0.4 M sucrose, 20 mM $MgCl_2 \cdot 6H_2O$, 467 mM mannitol, pH 5.8, sterile filtered) and overlaid with MMM solution (15 mM $MgCl_2$, 5 mM MES, 467 mM mannitol, pH 5.8, sterile filtered). The interphase containing the protoplasts was collected and kept in W5 solution (2 mM MES, 154 mM NaCl, 125 mM $CaCl_2 \cdot 2H_2O$, 5 mM KCl, 5 mM glucose, pH 5.8, sterile filtered), until transformation. Meanwhile, plasmids were pre-mixed distributed in a total amount of 30 µg, and used to transform 500,000 protoplasts by dropwise addition of a polyethylene glycol (PEG) solution (4 g PEG_{4000}, 2.5 ml of 800 mM mannitol, 1 ml of 1 M $CaCl_2$ and 3 ml H_2O). The protoplasts concentration was calculated using the Rosenthal counting chamber. After 8 min incubation, 120 µl MMM and 1,240 µl PCA (0.32% (wt./vol) Gamborg's B5 basal salt powder with vitamins (bioWorld), 2 mM $MgSO_4 \cdot 7H_2O$, 3.4 mM $CaCl_2 \cdot 2H_2O$, 5 mM MES, 0.342 mM l-glutamine, 58.4 mM sucrose, 444 mM glucose, 8.4 µM calcium pantothenate, 2% (vol/vol) biotin from a biotin solution 0.02% (wt./vol) 0.1% (vol/vol) in H_2O, pH 5.8, sterile filtered, 0.1% (vol/vol) Gamborg's B5 Vitamin Mix, 64.52 µg μl^{-1} ampicillin) were added. After transformation, protoplasts were divided in 24-well plates in 800 µl aliquots (250,000 protoplasts/well).

Luciferase assay. The reporter gene, FLuc, and the normalization protein RLuc were quantified as detailed previously[262]. Briefly, four replicates of 80 µl protoplast suspention,

containing aproximately 25000 protoplast, were transferred into 2 separated 96-well white flat-bottom plates (Costar) for simultaneous adquisition. 20 µl of either FLuc substrate (0.47 mM d-luciferin (Biosynth AG), 20 mM tricine, 2.67 mM $MgSO_4 \cdot 7H_2O$, 0.1 mM $EDTA \cdot 2H_2O$,33.3 mM dithiothreitol, 0.52 mM adenosine 5′-triphosphate, 0.27 mM acetyl– coenzyme A, 5 mM NaOH, 264 µM $MgCO_3 \cdot 5H_2O$, in H_2O, pH 8) or RLuc substrate (0.472 mM coelenterazine stock solution in methanol, diluted directly before use, 1:15 in PBS) were added into each well. A 20 min measurement was performed, with integration time of 0,1 s, with either a BertholdTriStar2 S LB 942 multimode plate reader, for RLuc, or with a Berthold Centro XS3 LB 960 microplate luminometer, for FLuc.

Normalization assay in mammalian cells. Gaussia luciferase (Gluc) activity was quantified to visualize the effect of the hormone treatment in the mammalian cell model, as previously described[262]. Four technical replicates of 80µL of the supernatant of the mammalian cells were transferred into a 96-well white flat-bottom plates (Costar). After addition of 20µL coelenterazine (472mM stock solution in methanol, diluted 1:1,500 in PBS; Carl Roth, Karlsruhe, Germany, no. 4094.4), the luminescence was measured for 20 min using TriStar2 LB 941 multimode plate readers (Golonka *et al*., 2019).

Supplementary tables

Table 1. Plasmid designed and used in this study. All pEP plasmids were assemble using AQUA cloning[210]

Plasmid				
ID	**Description**	**Backbone**	**Insert**	**Cloning procedure**
pEP037	Psv40::mCherry::Tsv40	pLH002	mCherry	Insert was amplified from plasmid pEP096. Backbone was digested with NotI and XbaI.
pEP038	Psv40::AHP1-mCherry::Tsv40	pEP037	AHP1	Insert was amplified from TAIR clone U09679 with oligos oEP084 and oEP085. Backbone was digested with NotI and CIP
pEP039	Psv40::AHP2-mCherry::Tsv40	pEP037	AHP2	Insert was amplified from TAIR clone U21117 with oligos oEP086 and oEP087. Backbone was digested with NotI and CIP.
pEP041	Psv40::AHP3-mCherry::Tsv40	pEP037	AHP3	Insert was amplified from TAIR clone U11235 with oligos oEP090 and oEP091. Backbone was digested with NotI and CIP.
pEP042	Psv40::AHP4-mCherry::Tsv40	pEP037	AHP4	Insert was amplified from wt *A. thaliana* COL1 cDNA with oligos oEP092 and oEP093. Backbone was digested with NotI and CIP.
pEP043	Psv40::AHP5-mCherry::Tsv40	pEP037	AHP5	Insert was amplified from TAIR clone U89383 with oligos oEP094 and oEP095. Backbone was digested with NotI and CIP
pEP044	Psv40::AHP6-mCherry::Tsv40	pEP037	AHP6	Insert was amplified from wt A. thaliana COL1 cDNA with oligos oEP096 and oEP097. Backbone was digested with NotI and CIP.
pEP046	Psv40::AHK3-mCherry::Tsv40	pEP037	AHK3	Insert was amplified from wt A. thaliana COL1 cDNA with oligos oEP078 and oEP079. Backbone was digested with NotI and CIP.
pEP053	P35s::AHP2-mCherry::Tnos	PGEN016	AHP2	Insert was amplified from pEP039 with oligos oEP188 and oEP193. Backbone was

				digested with AfeI and BamHI.
pEP350	Psv40::YPD1-mVenus::Tsv40	pLH002	YPD1	Insert was amplified from *Saccharomyces cerevisiae* strain ATCC 204508 / S288c genomic DNA with oligos oEP274 and oEP275. mvenus was amplified from pRD093 with oligos oEP288 and oEP289. Backbone was digested with NotI and XbaI.
pEP379	Psv40::AHP2-VP16-NLS(SV40)-IRES(PV)-TetR-AHP6-NLS(SV40)::Tsv40	pEP179	AHP6	Insert was amplified from pEP044 with oligos oEP239 and oEP248. Backbone was digested with BsrGI and AscI.
pEP602	P35s::RLUC::Tnos || (etr)8::Pcmvmin::FLUC::Tsv40	pROF052	P35s::RLUC::Tnos	Insert was amplified from GB109 with oligos oEP368 and oEP369. Backbone was digested first digested and religated with XhoI. And the resulting plasmid was digested with SspI + CIP.
pEP727	Psv40::mCherry-AHK4::Tsv40	pEP037	AHK4	Insert was amplified fron pEP047.2 with oligos oEP497 and oEP498. Backbone was digested with BsrGI + CIP
pEP730	(TCS)5-Pcmvmin::SEAP::Tsv40	pPF034	(TCS)5	Insert was amplified from pJA176 with oligos oEP502 and oEP503. Backbone was digested with SspI and NheI.
pEP732	Psv40::AHP2-mVenus::Tsv40	pLH002	AHP2	Insert was amplified from pEP039 with oligos oEP086 and oEP505. mVenus was amplified from pRD093 with oligos oEP506 and oEP289. Backbone was digested with NotI and XbaI.
pEP733	Psv40::ARR10-Cerulean::Tsv40	pEP351	ARR10	Insert was amplified from pEP103 with oligos oEP507 and oEP508. Backbone was digested with NotI and EcoRI
pEP734	P35s::ARR10-VP16::Tnos	pEP708	ARR10	Insert was amplified from pEP103 with oligos oEP511 and oEP512. Backbone was digested with AgeI and EcoRI.
pEP754	Psv40::ARR10-VP16-NLS(SV40)-IRES(PV)-	pEP387	AHP2	Insert was amplified from pEP733 with oligos oEP551

	TetR-AHP2-NLS(SV40)::Tsv40			and oEP552. Backbone was digested withSpeI and EcoRV.
pEP755	Psv40::ARR10-VP16-NLS(SV40)-IRES(PV)-TetR-AHP6-NLS(SV40)::Tsv40	pEP754	AHP6	Insert was amplified from pEP044 with oligos oEP239 and oEP248. Backbone was digested withBsrGI and AscI.
pEP756	Psv40::ARR7-mCherry::Tsv40	pEP039	ARR7	Insert was amplified from pEP724 with oligos oEP579 and oEP580. Backbone was digested with NotI and EcoRI
pEP757	Psv40::ARR1-Cerulean::Tsv40	pEP733	ARR1	Insert was amplified from the TAIR clone TOPO-U19-A06 with oligos oEP581 and oEP582. Backbone was digested with NotI and EcoRI
pEP758	Psv40::ARR22-mCherry::Tsv40	pEP039	ARR22	Insert was amplified from TAIR clone TOPO-U11-H11 with oligos oEP583 and oEP584. Backbone was digested with NotI and EcoRI
pEP765	Psv40::ARR10(D69A)-Cerulean::Tsv40	pEP733	ARR10(D69A)	Baackbone was amplified with oligos oEP593 and oEP594
pEP767	Psv40::ARR1(D94A)-Cerulean::Tsv40	pEP757	ARR1(D94A)	Baackbone was amplified with oligos oEP597 and oEP598 (Tm 72°C)
pEP768	Psv40::ARR1(D89A)-Cerulean::Tsv40	pEP757	ARR1(D89A)	Baackbone was amplified with oligos oEP599 and oEP600 (Tm 72°C) and imner primers for backbone, oEP611 and oROF439
pEP769	Psv40::ARR1(D89A*D94A)-Cerulean::Tsv40	pEP768	ARR1(D89A*D94A)	Baackbone was amplified with oligos oEP630 and oEP631, with inner primers for backbone, oEP611 and oROF439
pEP770	Psv40::ARR10(D69A)-VP16-NLS(SV40)-IRES(PV)-TetR-AHP2-NLS(SV40)::Tsv40	pEP387	AHP2	Insert was amplified from pEP765 with oligos oEP551 and oEP552. Backbone was digested withSpeI and EcoRV.
pEP772	Psv40::ARR10-VP16-NLS(SV40)-IRES(PV)-TetR-ARR7-NLS(SV40)::Tsv40	pEP754	ARR7	Insert was amplified from pEP756 with oligos oEP613 and oEP614. Backbone was digested with BsrGI and AscI.
pEP773	Psv40::ARR10-VP16-NLS(SV40)-IRES(PV)-	pEP754	ARR22	Insert was amplified from pEP758 with oligos oEP615

	TetR-ARR22-NLS(SV40)::Tsv40			and oEP616. Backbone was digested with BsrGI and AscI.
pEP775	Psv40::ARR10(D69A)-VP16-NLS(SV40)-IRES(PV)-TetR-AHP6-NLS(SV40)::Tsv40	pEP774	AHP6	Insert was amplified from pEP044 with oligos oEP239 and oEP248. Backbone was digested withBsrGI and AscI.
pEP776	Psv40::ARR1-VP16-NLS(SV40)-IRES(PV)-TetR-AHP2-NLS(SV40)::Tsv40	pEP387	ARR1	Insert was amplified from pEP757 with oligos oEP617 and oEP618. Backbone was digested withSpeI and EcoRV.
pEP777	Psv40::ARR10(D89A)-VP16-NLS(SV40)-IRES(PV)-TetR-AHP2-NLS(SV40)::Tsv40	pEP387	ARR1(D89A)	Insert was amplified from pEP768 with oligos oEP617 and oEP618. Backbone was digested withSpeI and EcoRV.
pEP778	Psv40::ARR10(D94A)-VP16-NLS(SV40)-IRES(PV)-TetR-AHP2-NLS(SV40)::Tsv40	pEP387	ARR1(D94A)	Insert was amplified from pEP767 with oligos oEP617 and oEP618. Backbone was digested withSpeI and EcoRV.
pEP779	Psv40::ARR10(D89A*D94A)-VP16-NLS(SV40)-IRES(PV)-TetR-AHP2-NLS(SV40)::Tsv40	pEP387	ARR1(D89A*D94A)	Insert wsa amplified from pEP769 with oligos oEO617 and oEP618. Backbone was digested withSpeI and EcoRV.
pEP781	Psv40::ARR1-VP16-NLS(SV40)-IRES(PV)-TetR-ARR7-NLS(SV40)::Tsv40	pEP776	ARR7	Insert was amplified from pEP756 with oligos oEP613 and oEP614. Backbone was digested with BsrGI and AscI.
pEP782	Psv40::ARR7-VP16-NLS(SV40)-IRES(PV)-TetR-AHP2-NLS(SV40)::Tsv40	pEP387	ARR7	Insert was amplified from pEP756 with oligos oEP622 and oEP623. Backbone was digested withSpeI and EcoRV.
pEP784	Psv40::ARR22-VP16-NLS(SV40)-IRES(PV)-TetR-AHP2-NLS(SV40)::Tsv40	pEP387	ARR7	Insert was amplified from pEP756 with oligos oEP622 and oEP623. Backbone was digested withSpeI and EcoRV.
pEP788	Psv40::ARR1-VP16-NLS(SV40)-IRES(PV)-TetR-ARR2-NLS(SV40)::Tsv40	pEP776	ARR22	Insert was amplified from pEP758 with oligos oEP615 and oEP616. Backbone was digested with BsrGI and AscI.
pEP793	Psv40::ARR1-VP16-NLS(SV40)-IRES(PV)-TetR-AHP6-NLS(SV40)::Tsv40	pEP776	AHP6	Insert was amplified from pEP044 with oligos oEP239 and oEP248. Backbone was digested withBsrGI and AscI.
pGEN016				
pJA176	(TCS)5-P35s::FLUC::Tnos	pROF206	(TCS)5	Insert was amplified with oJA393 and oJA394. Backbone was amplified with oJA395 and oJA396.

pPF034	(tetO)13-Pcmvmin::SEAP::Tbgh||Psv40::GLUC::Tsv40pA	pPF002	GLUC	Insert was amplified with oligos oPF047 and oPF048 from pKM083. Backbone was digested with EcoRV and NotI.

Supplementary Table 2. Oligonucleotides used in this work. Lowercase corresponds to annealing part and uppercase corresponds to overhangs

Oligonucleotide ID	Sequence 5´-> 3´
oEP001	ttcaggtcccggatcggaattgcgcggccgcATGGTGAGCAAGGGC
oEP002	gaagcttgggctgcaggtcgacttctagattaAGCCTTGTACAGCTCG
oEP078	tttatttcaggtcccggatcggaattgcgcATGAGTCTGTTCCATGTGC
oEP079	gctcaccatactgccactgccggcgaattcTGATTCTGTATCTGAAGGCG
pEP084	tttcaggtcccggatcggaattgcgcggccgcATGGATTTGGTTCAGAAGCAG
pEP085	gccatgttatcctcctcgcccttgctcaccatactgccactgccggcgaattcAAATCCGAG TTCGACGG
oEP086	tttcaggtcccggatcggaattgcgcggccgcATGGACGCTCTCATTGC
oEP087	gccatgttatcctcctcgcccttgctcaccatactgccactgccggcgaattcGTTAATATC CACTTGAGGAACTATAC
oEP090	tttcaggtcccggatcggaattgcgcggccgcATGGACACACTCATTGCTC
oEP091	gccatgttatcctcctcgcccttgctcaccatactgccactgccggcgaattcTATATCCAC TTGAGGGATTCTACC
oEP092	tttcaggtcccggatcggaattgcgcggccgcATGCAGAGGCAAGTGG
oEP093	gccatgttatcctcctcgcccttgctcaccatactgccactgccggcgaattcCTTGGGCCT ACGTGC
oEP094	tttcaggtcccggatcggaattgcgcggccgcATGAACACCATCGTCGTTG
oEP095	gccatgttatcctcctcgcccttgctcaccatactgccactgccggcgaattcATTTATATC CACTTGAGGAATTGTACC
oEP096	tttcaggtcccggatcggaattgcgcggccgcATGTTGGGGTTGGGTG
oEP097	gccatgttatcctcctcgcccttgctcaccatactgccactgccggcgaattcCATTGGATA TCTGACTCCTGC
oEP188	tttggagagaacacggggactctagcgctaATGGACGCTCTCATTGC
oEP193	gggaaattcgcctcgagatcagttatctAGTTAAGCCTTGTACAGCTCG
oEP 239	ggaagtggtggcggaggtagcgattgtacaATGTTGGGGTTGGGTG
oEP248	atcatgtctggatcgaagcttttaggcgcgccttacaccttccgctttttcttgggCATTGGA TATCTGACTCCT
oEP274	tttcaggtcccggatcggaattgcgcggccgcATGTCTACTATTCCCTCAGAAATC

oEp275	ggtgaacagctcctcgcccttgctcaccatactgccactgccggcgaattcTAGGTTTGTG TTGTAATATTTAGATAACTC
oEP289	cgaagcttgggctgcaggtcgacttctAGATTACTTGTACAGCTCGTCC
oEP368	gttgaatactcatactattaatttttcaatattCGAGTCGGTCCCATTATTG
oEP369	gacaataaccctgataaatgcttcaataatACCGGTACTAGAGCCAAGCTGATCT C
oEP497	ccgccactccaccggcggcatggacgagctgtacaaggctggatccagtggcagtggcagtg gcagtggcATGAACTGGGCACTCAAC
oEP498	gcaggtcgacttctagattaagccttgtacTTACGACGAAGGTGAGATAGGATTA G
oEP502	gttgaatactcatactcttccttttttcaatattGCTAGCAAAATCTACAAAATCTTTTT G
oEP503	cactaaacgagctctgcttatatagggctagcgGTCTTGGCTAGAAAATCCAC
oEP505	tgctcaccatactgccactgccggcgaattcGTTAATATCCACTTGAGGAACTATA C
oEP506	attaaccgaattcgccggcagTGGCAGTATGGTGAGCAAGGGC
oEP507	tttatttcaggtcccggatcggaattgcgcggccgcATGACTATGGAGCAAGAAATT GAAG
oEP508	tgctcaccatactgccactgccggcgaattcAGCTGACAAAGAAAAGGGAAAATG
oEP511	tttggagagaacacggggactctagcgctaTGTACAATGACTATGGAGCAAGAA ATTGAAG
oEP512	tgtacgcggaactgccactgccggcgaattgGACGTCAGCTGACAAAGAAAAGG GAAAATG
oEP551	cttttatttcaggtcccggatcggaattgactagtcccaccATGACTATGGAGCAAGA AATTGAAG
oEP552	accagcactaccagcactatcgaattcgatatcAGCTGACAAAGAAAAGGGAAAA TG
oEP567	gtcgtgaaaactaccccaagctggcctctgaggccATGAACTGGGCACTCAAC
oEP568	ctctagagaattgatccccaagcttggcctgacaggccTTACGACGAAGGTGAGATA GG

oEP579	tttatttcaggtcccggatcggaattgcgcggccgcATGGCGGTTGGTGAG
oEP580	cccttgctcaccatactgccactgccggcgaattcAAGTAGAGAAAAAAGGTTTTCAGATTCTG
oEP581	tttatttcaggtcccggatcggaattgcgcggccgcATGATGAATCCGAGTCACG
oEP582	tgctcaccatactgccactgccggcgaattcAACCGGAATGTTATCGATGG
oEP583	tttatttcaggtcccggatcggaattgcgcggccgcATGGCAACAAAATCCACC
oEP584	cccttgctcaccatactgccactgccggcgaattcAGCATCGAAGAGGTGG
oEP593	GTTTGATCTTGTTATTAGCGCTGTCGACATGCCAGACATG
oEP594	CATGTCTGGCATGTCGACAGCGCTAATAACAAGATCAAAC
oEP597	GTTCATATGCCTGCCATGGACGGTTTC
oEP598	GAAACCGTCCATGGCAGGCATATGAAC
oEP599	CGATATAGTAATCAGTGCTGTTCATATGCCTGAC
oEP600	GTCAGGCATATGAACAGCACTGATTACTATATCG
oEP613	gcggtggaagtggtggcggaggtagcgattgtacaATGGCGGTTGGTGAG
oEP614	gtctggatcgaagcttttaggcgcgccttaAAGTAGAGAAAAAAGGTTTTCAGATTCTG
oEP615	gcggtggaagtggtggcggaggtagcgattgtacaATGGCAACAAAATCCACC
oEP616	atcatgtctggatcgaagcttttaggcgcgccttaAGCATCGAAGAGGTGG
oEP617	cttttatttcaggtcccggatcggaattgactagtcccaccATGATGAATCCGAGTCACG
oEP618	agcactaccagcactatcgaattcgatatcAACCGGAATGTTATCGATGG
oEP630	GCTCTTGAGCATGTTGCCCTAGAGATGGACTTAC
oEP631	GTAAGTCCATCTCTAGGGCAACATGCTCAAGAGC